Australian Government
Department of the Environment
Supervising Scientist

internal report 631

A summary and review of ***eriss'*** groundwater chemistry data at Ranger uranium mine

Andreas Bollhöfer, Peter Medley & Sarah Marshall

February 2015

Release status – unrestricted

Project number – MON-1996-001

This page has been left blank intentionally.

A summary and review of *eriss*' groundwater chemistry data at Ranger uranium mine

Andreas Bollhöfer, Peter Medley & Sarah Marshall

Supervising Scientist
GPO Box 461, Darwin NT 0801

February 2015

(Release status – unrestricted)

Australian Government
Department of the Environment
Supervising Scientist

How to cite this report:

Bollhöfer A, Medley P & Marshall S 2015. A summary and review of ***eriss***' groundwater chemistry data at Ranger uranium mine. Internal Report 631, February, Supervising Scientist, Darwin.

Project number: MON-1996-001

Authors of this report:

Andreas Bollhöfer – Environmental Research Institute of the Supervising Scientist, GPO Box 461, Darwin NT 0801, Australia

Peter Medley – Environmental Research Institute of the Supervising Scientist, GPO Box 461, Darwin NT 0801, Australia

Sarah Marshall – Office of the Supervising Scientist, GPO Box 461, Darwin NT 0801, Australia

The Supervising Scientist is a branch of the Australian Government Department of the Environment.

Supervising Scientist
Department of the Environment
GPO Box 461, Darwin NT 0801 Australia

environment.gov.au/science/supervising-scientist/publications

Disclaimer

Printed and bound in Darwin NT by Supervising Scientist.

Contents

1 Background

Groundwater samples from bores around the Ranger uranium mine have been collected by the Environmental Research Institute of the Supervising Scientist (***eriss***), Energy Resources of Australia Ltd (ERA) and the Northern Territory Government Department of Mines and Energy (DME) for more than 30 years. These groundwater samples were primarily collected to monitor seepage of contaminants from the tailings storage facility (TSF) and the land application areas (LAAs) into the surrounding environment.

Mining of pit 1 started in 1981 and ceased in 1996, mining of pit 3 started in 1998 and continued through to the end of December 2012. The two pits have been acting as groundwater sinks while being mined, and have been of less interest during this period from a groundwater monitoring perspective. However, pit 1 has now been filled with tailings, wicks have been installed for de-watering, and tailings are being covered with waste rock to create a final landform above the pit. Pit 3 is also being being prepared to accept brines from the brine concentrator and tailings from the tailings storage facility from 2015 onwards. Consequently, more attention has been given to pits 1 and 3, including both monitoring groundwater quality and groundwater movement, and modelling groundwater behaviour in the vicinity of the two pits.

Groundwater quality parameters routinely measured include **major ions** (ERA/DME), **heavy metals** (ERA/DME/***eriss***) and **radionuclides** (ERA/***eriss***) (e.g. Martin & Akber 1994, 1999; Klessa 2001; ERA 2012). ERA is collecting groundwater samples from four statutory and a large number of operational monitoring bores on a quarterly or biannually basis (ERA 2013), for the purpose of analysing major cations and anions, metals and radium (for some of the bores).

Between 1996 and 2003, a number of bores were routinely sampled annually and analysed by ***eriss***. However, due to operational reasons, in 2003 the decision was made that radionuclides and metals would be analysed in aliquots of bore waters sampled by DME (biannually) and, consequently, groundwater collection by ***eriss*** was discontinued. Since 2004, ***eriss*** has received aliquots of samples collected by DME at the end of the dry season (September/ October) around the Ranger mine site. DME analyses these samples routinely for metals and major ions. Results of ERA's comprehensive groundwater monitoring program are published regularly in their annual *Ranger Wet Season Groundwater Report* (e.g. ERA 2012).

A review of the ***eriss*** research program and groundwater related research in 1989 emphasised that dispersion of contaminants via the groundwater pathway occurs on a long time scale and is likely to reach its most significant impact after rehabilitation (OSS 1989). Consequently, it is important that these long time scales are acknowledged in any groundwater quality monitoring program. At its 12th meeting in April 2003, the Alligator Rivers Region Technical Committee (ARRTC) identified that further research on groundwater pathways was needed. The following two key areas were identified in a review by Johnston & Milnes (2007) and subsequently supported by ARRTC:

1) To investigate options for the management of seepage, in particular from the TSF, to ensure that there are no detrimental impacts to downstream water quality at Ranger uranium mine; and

2) to study the behaviour of the groundwater mound under the TSF following de-commissioning and rehabilitation of the mine.

ARRTC has also identified groundwater dispersion as one of the Key Knowledge Needs that need to be addressed from a monitoring perspective. Monitoring of groundwater should target the TSF, pit 1 and pit 3, where tailings are stored at present and will be stored following rehabilitation, and will have to continue during and following rehabilitation for a timeframe suitable to assess the success of rehabilitation and the integrity of the pits as tailings repositories in the long term.

ARRTC also recommended that a whole-of-footprint solute transport model based on a fractured rock simulation should be developed. The hydrogeological modelling is performed by ERA and consultants, mainly the Commonwealth Scientific and Industrial Research Organisation (CSIRO) and INTERA, a geosciences and engineering consulting firm based in Austin, Texas. Whereas previous model development and application has focussed on the TSF (e.g. Puhalovich et al 2012a,b), pit 1 (Kalf & Associates 2004; Anderson & Timms, 2009) and pit 3 (Salama et al 1998a-c; 1999) in isolation, INTERA has developed a groundwater model for ERA including both, pits 1 and 3. Such modelling will, ultimately, need to integrate groundwater seepage and surface water runoff from the whole rehabilitated landform.

The focus of ***eriss***' groundwater monitoring and research projects has been the measurement of groundwater radionuclide activity concentrations in various bores around the mine, with some time records going back to the early 1980s. Whereas radium isotopes and radium activity ratios were used as a process tracer and provided information about adsorption and desorption mechanisms of radium in groundwater (Martin & Akber 1996, 1999), uranium and uranium activity ratios are often used as a source tracer to investigate the potential sources of uranium in groundwater (Ivanovich & Harmon, 1994; Zielinski et al 1997; Iles et al 2002). However, longer time series are needed to detect any changes in those parameters, which were not available in 2003 (Johnston & Milnes 2007). Consequently, it was decided that ***eriss*** would continue the groundwater monitoring program around Ranger and focus on the measurement of ^{226}Ra and ^{238}U activity concentrations, and the ^{234}U/^{238}U activity ratio in bore waters. Uranium and radium activity concentrations have also been investigated at the rehabilitated Nabarlek uranium mine and results of these investigations have been published in Ryan & Bollhöfer (2007) and Ryan et al (2007).

In their conceptual pollution model for the operational phase of Ranger, Bartolo et al (2013) identified the transport of inorganic toxicants and radionuclides via the 'seepage to groundwater to surface water pathway' as a pathway of medium importance, with a medium scientific knowledge base. Although significant progress has been made with regards to groundwater modelling and tailings characterisation, some of the information is still not used to its full extent, due to a disconnect between the various programs involved in groundwater monitoring at Ranger. Groundwater quality data are currently stored in various individual databases and formats. A meeting led by groundwater experts from ERA was held in November 2011 to discuss a joint organisational approach, as part of an effort to improve the Ranger groundwater knowledge base, facilitate a more coordinated approach to the acquisition and storage of groundwater data and to progress the development of closure criteria for Ranger. As an outcome of the meeting, ***eriss*** radionuclide data from bores sampled by DME up to 2009 were sent to ERA for inclusion in their comprehensive groundwater GIS.

All groundwater data available to ***eriss*** up to the end of December 2013, which include ^{226}Ra and uranium isotopes and metals, have now been quality checked and verified and imported into a single groundwater quality spreadsheet. The data have also been migrated into the new ***eriss*** *EnviroSys* database. A summary of this ***eriss*** data is provided in this report.

1.1 Aquifers at Ranger

Two aquifers exist at Ranger: an unconfined shallow aquifer varying in thickness from 2 m to 20 m and associated with the soil profile and underlying laterite layer, and a confined to semi-confined deep aquifer underlying weathered and fresh bedrock (Martin & Akber 1996). A layer of low permeability sandy silty clay is commonly found between the laterite and the weathered bedrock. Where it occurs, this layer forms a semi-confining upper boundary to the deep aquifer. Ahmad and Green (1986) have divided the aquifers in the Ranger region into three main types (rather than into a shallow and deep aquifer only): **type A** is groundwater in the loose sand and gravels with high permeabilities, **type B** is groundwater in the weathered profile with relatively low permeabilities and **type C** groundwater occurs in the relatively fresh fractured rocks in the deep aquifer. This has subsequently been modified by Salama & Foley (1997) who proposed a system that recognises zonal influences and host lithologies. The aquifers are classified in their work as alluvial (shallow) (aquifer 1a), weathered rock (upper: aquifer 1b; intermediate: aquifer 2) and deep fractured rock (aquifer 3) (Klessa 2001). The aquifers have been characterised chemically by Salama and Foley (1997), and their classification is reproduced in Table 1.

Table 1 Cation facies, anion facies, pH and EC (µS·cm^{-1}) in the three aquifer classes (Klessa 2001).

	Major cations	**Major anions**	**pH**	**EC**
Superficial deposits and alluvium (aquifer1a)	Ca-Na	HCO3-Cl	5.5	<50
Weathered Nanambu complex (aquifers 1b & 2)	Na-Ca-Mg	HCO3-Cl	6-6.5	<200
Fractured Nanambu complex (aquifer 3)	Ca-Na	HCO3 and HCO3-Cl-SO4	6.6-7.1	180-310

Figure 12 in ERA (2013) show groundwater monitoring sites and aquifer zones, together with the specific aquifers (1a, 1b, 2 and 3) that are being intersected by some of their groundwater monitoring bores.

1.2 Groundwater contaminants

1.2.1 Sources of groundwater contaminants

Figure 1 shows an aerial photograph of the site with the main sources of groundwater contamination highlighted.

The main sources of radionuclides in groundwater on the minesite at present are the tailings in pit 1 and the TSF, application of radionuclides via land irrigation and the waste rock and low grade ore stockpiles (Bartolo et al 2013). The TSF has historically been a focus of groundwater investigations and, following a hydrogeological review of the area surrounding the Ranger TSF, a groundwater monitoring program specifically focussed on the TSF was developed and implemented by ERA in 2010. Results of ERA's groundwater monitoring program are routinely reported in ERA's groundwater monitoring reports (e.g. ERA 2012).

Tailings are also stored in pit 1. The RL0 level in pit 1 is at the base of the weathered profile (and approximately 20 m below the lowest point at the edge of the pit) with permeabilities of approximately 10^{-7} m/s (Haylen, 1981). This base acts like a barrier between the deep aquifer, with relatively widespread groundwater occurrences, and the shallow aquifer. The shallow aquifer has much higher permeabilities and can easily connect to the surface water system (Mudd 2002). The MBL-aquifer (mine bore L) to the south-east of pit 1 for example is highly permeable with permeabilities of around 10^{-4} m/s (Haylen 1981; Anderson & Timms, 2009) and connects to the Corridor Creek system. A barrier has been put in place at the south-eastern wall of the pit (permeability 10^{-7}-10^{-8} m/s) to prevent seepage into that layer and allow storage of tailings above RL0 (for which final approval is yet to be given). A large number of monitoring bores have been installed in this area (ERA 2013).

Figure 1 Principal potential sources of contamination at Ranger

Mining in pit 3 ceased in December 2012 and backfilling of the pit with waste rock started in 2013. Pit 3 is currently being prepared to accept tailings that will be dredged from the TSF and deposited in the pit from 2015. Consequently, pit 3 is another area to be targeted in any future groundwater monitoring programme, in particular the area between the northern pit wall and Magela Creek, due to the existence of an extensive shallow sand lens in that area that has been shown to be the major pathway for groundwater from pit 3 into Magela Creek.

The land application areas (LAAs) within the Ranger lease are another potential source of groundwater contamination. Since 1985, water stored in RP2 has been disposed of on-site using land application methods during the dry season. RP2 receives seepage from all stockpiles including ore and waste rock. The Magela LAA was the first to be established using the spray irrigation method, and additional LAAs followed as the amount of water to be disposed of increased over time as a result of the increasing area occupied by waste rock and stockpiles. Starting in 1995, the RP1 and Djalkmara wetland filters were used to polish RP2 water before being applied to the RP1 and the Djalkmara East and West LAAs. Additional LAAs have been established in the Corridor Creek catchment and at Jabiru East. From 2006 onwards, increasing volumes of pond water have been treated by MF/RO water treatment plant with the clean permeate being discharged along the Corridor Creek catchment line (Akber et al 2011a).

Land application to dispose of water is utilised because radionuclides bind strongly to the surface horizons of soil profiles (Akber & Marten 1992; Willett & Bond 1992; Hollingsworth et al 2005) and have limited impact on groundwater. A recently completed project initiated by ERA has characterised the Ranger LAAs in the context of their radiological status (Akber et al 2011 a,b,c). More conservative constituents, such as Mg and SO_4, however, may seep into the ground and influence groundwater quality downgradient of the LAAs. This has, for example, been observed at the rehabilitated Nabarlek uranium mine that exhibited deviations from baseline nitrate, ammonium, aluminium, cobalt and cadmium due to transport of contaminated groundwater associated with irrigation at the forest irrigation area (Parker 2001).

1.2.2 Species of contaminants

The relevant substances that may contaminate groundwater at Ranger can be divided into three subgroups:

- inorganic contaminants
- organic contaminants
- radionuclides

1.2.2.1 Inorganic contaminants

Noller (1991) identified nine inorganic elements in Ranger ore body 1 minerals with an enrichment factor above 9.5 relative to typical Alligator Rivers Region rock. The most important elements identified are **gold**, **uranium**, **lead**, **copper**, **cadmium**, **silver** and **mercury** (in this context it should be noted that the ARR rocks themselves are enriched relative to the crustal average in a variety of other elements). The milling process introduces a number of additional other elements, mainly **sulphur**, **magnesium** and **manganese**, into the process that may be present in groundwater in significant quantities as well.

The Fox Inquiry (RUEI, 1975) predicted a number of contaminants that may influence the Gulungul catchment, due to runoff from the waste rock used to construct the TSF wall or via seepage from the TSF. The inorganic species specifically mentioned were

arsenic, **cadmium**, **copper**, **lead**, **manganese**, **mercury**, **zinc** and **sulfate**. Sulfate moves freely in groundwater and is often used as an indicator for conservative mine derived contaminants. leGras et al (1991, 1993) for instance found that tailings are the main source of sulphur to groundwater in bores north of the TSF, where various faults exist (Salama & Foley 1997), using sulphur isotope ratios.

Some typical concentrations of inorganic contaminants in tailings pore water for the above mentioned elements are listed in leGras (1992) and reproduced in Table 2. Also shown are data for runoff from waste rock and retention pond 2 water (Noller, 1991), which has been used for irrigation of the various land application areas, and concentrations in RP1 from a recent study by Turner & Jones (2010). Treated RP2 water is spray and flood irrigated at various application areas around the mine site and might add contaminants into the groundwater system by recharging the shallow and deep aquifers. This recharge may occur along fractures with only a limited cover of material of low permeability.

Table 2 Concentrations [$\mu g \cdot L^{-1}$] of some inorganic contaminants in various mine waters (data from leGras, 1992; B. Noller, 1991, Ahmad and Green; 1986; Turner & Jones, 2010).

Analyte	Tailings pore water	Waste rock runoff	RP2	RP1	Groundwater
SO_4	47,000	N/A	N/A	223	1000-21000
Mg	8750	N/A	N/A	58.8	2000-33000
NH_4	2880	N/A	N/A	N/A	N/A
Mn	880	0.07	0.007	N/A	N/A
Na	368	N/A	N/A	N/A	1000-31000
Ca	560	N/A	N/A	N/A	2000-40000
K	313	N/A	N/A	N/A	1000-20000
Fe	~ 0.5	8	N/A	213	100-25000
Cu	~ 0.05	0.005	0.006	1.32	0.01 – 5.2
Zn	~ 0.05	0.023	0.023	N/A	0.1 – 60
Sr	~ 0.01	0.02	0.04	N/A	N/A

1.2.2.2 Radionuclides

Taking into account half-lives only, the following is the list of uranium and actinium-series radionuclides in groundwater that may be of interest:

^{238}U, ^{234}U, ^{230}Th, ^{226}Ra, ^{210}Pb, and ^{227}Ac.

As thorium and lead are particle reactive and readily adsorbed and removed from solution, it is not expected that either of these elements will migrate significant distances through the groundwater aquifer. This is also assumed to be the case for actinium. Consequently, the reduced list for radionuclides potentially contaminating the groundwater is:

^{238}U, ^{234}U and ^{226}Ra.

1.2.2.3 Stable isotope ratios of contaminants

LeGras et al (1991) used sulphur isotope ratios ($^{34}S/^{32}S$) to identify seepage from the TSF and to discriminate between TSF and surface runoff water samples. Although $\partial^{34}S$ can be obscured by reduction processes (because sulphur is a relatively light element) of SO_4, the difference in stable isotope ratios of sulphur prill ($\partial^{34}S = 18.4$) samples and metal sulphides from stockpiles ($\partial^{34}S = 2.2$) that may release SO_4 into runoff water after oxidation is large enough to discriminate between the two sources. Sulfate is a conservative contaminant and the sulphur isotope ratios provided a useful source tracer, based on an existing difference between the sources of sulphur.

Furthermore, lead isotope ratios have also been used as a source tracer. Large variations are found between lead isotope ratios in natural waters and TSF pore water for instance (Gulson et al. 1996). Lead concentrations in bore waters are expected to be quite low, as lead is readily adsorbed by particles in the groundwater. However, typical detection limit for the measurement of lead via ICPMS is 0.02 ppb (parts per billion) or 20 ng per litre, which is at least one order of magnitude lower than levels measured by Martin and Akber (1999) or Gulson et al (1996).

1.2.2.4 Organic contaminants

Noller (1990) additionally listed the following potential organic contaminants:

- alamine 336
- iso-decanol
- kerosene
- diesel fuel
- lubricants and greases
- detergents
- pesticides and herbicides.

In the context of groundwater at Ranger, these contaminants are relatively insignificant compared to inorganic and radiological contaminants.

1.3 Solute transport

1.3.1 Groundwater flow at Ranger

Haylen (1981) provided a description of the groundwater flows around the TSF and pit 1. The general direction of the groundwater flow in the region is towards the north along the Ranger (Coonjimba) fault line. There are various other smaller fault lines in the general Ranger area. One is in a north-easterly direction in the area of pit 3, and another couple of fault lines dip towards the south-west near pit 1. Figure 2 highlights fault lines in the vicinity of the Ranger TSF as shown in Verma & Salama (1986).

The possibility of rapid groundwater movement along fractures and cherts in the deep aquifer, in particular in the vicinity of the TSF and RP1 area, was highlighted by Klessa (2001). Changes in the surface topography at Ranger as a result of mining operations have also resulted in significant changes to the characteristics of local hydrogeological systems, primarily groundwater quality and flow patterns (Johnston & Milnes 2007). Seepage has resulted in the development of groundwater mounds under the TSF and other water bodies on the mine site and the waste rock and ore stockpiles. Leakage is controlled by fault zones which act as conduits, potentially transmitting contaminants to downstream areas. However, most leakage from the TSF occurs along the fault-controlled alignment of Coonjimba Creek and is likely to be contained within the existing retention pond system (Puhalovich et al 2012a,b).

Recharge of the groundwater system is through infiltration of rainfall and through infiltration from (natural and man made) water bodies, although substantial amounts of early rainfall are lost due to evaporation (Ahmad and Green, 1986). The water from the shallow aquifer percolates through the shallow and deep groundwater aquifer along the higher permeability zones into the fractured rock aquifer. Haylen (1981) has also highlighted the critical role of permeable carbonate units around Ranger mine in the deep aquifer, present downstream of Magela Creek, and of fracture zones and carbonate horizons in particular in the vicinity of pits 1 and 3. These fracture zones have variable permeabilities, and can be orders of magnitude more permeable than the surrounding bedrock.

1.3.1.1 Pit 1

Above the RL0 level, groundwater connects to a more permeable surface aquifer, which connects with surface water bodies in the Corridor Creek catchment.

Mine bore L (MBL; Figure 3), just to the south east of the pit wall is pumping the so-called MBL aquifer to the east of pit 1, a highly permeable zone that connects with the Corridor Creek system. During mining of the pit, the net flow from this aquifer was towards pit 1, and MBL was pumping to reduce or stop this flow. Modelling investigations have shown that storage of tailings above RL0, plus a waste rock capping to about RL22 (22 m above RL0) without a seepage barrier would likely result in a substantial plume and increased expression of saline waters and groundwater quality deterioration within approximately 50 years (Kalf, 2004). Consequently, a barrier has been put in place at the south-eastern wall of the pit (permeability 10^{-7}–10^{-8} m/s) to greatly reduce seepage into that layer and allow storage of tailings above RL0.

1.3.1.2 Tailings storage facility (TSF)

Placement of tailings into the TSF will continue until 2015. Once the bottom of pit 3 has been prepared to accept tailings and concentrated brines, brines will be injected and tailings will be dredged from the TSF and placed into pit 3.

Investigations have shown that, at present, solutes move away from the TSF due to the height of the groundwater pressure head. There is an east-west fault line underneath the TSF (Figure 2), however, it is not clear whether or not there is a connection with surface water, for example within the Gulungul system. The primary fault line is a major east-north-east thrust fault north of the north wall of the TSF, and there are a series of secondary north-east trending normal faults under the north wall. A north trending normal fault is located beneath Coonjimba Creek, and a similar fault exists east of the TSF (Salama & Foley 1997; Klessa 2001; Puhalovich et al 2012a,b).

Modelling and groundwater monitoring data (e.g. Martin & Akber 1994) showed that groundwater quality changes have been most significant to the north of the TSF along this major fault and may extend up to 800 m north of the TSF wall (Puhalovich et al 2012a,b). The south-west corner of the TSF shows impacts from the base of the TSF wall, however bores more than 200 m away from the wall do not show any evidence of seepage (ERA 2012).

1.3.1.3 Pit 3

Three hydrogeological units are intercepted by pit 3. Significant seepage is occurring from the southern wall of pit 3 and isotopic studies have shown that approximately 80% of the inflow into pit 3 is originating from RP2. This is due to a more permeable carbonate unit existing between the two site features, which connects RP2 and the pit.

The western and northern walls of pit 3 are mainly chlorite schists, with almost no groundwater flow and very low permeabilities. It is not expected that significant seepage of contaminated material will occur through the west wall. Investigations focus on the southern wall and specifically the north eastern wall of the pit, due to its proximity to the Magela system in that area of the pit and a sand lense that exists between pit 3 and Magela Creek (ERA 2012).

Figure 2 Fault lines around the TSF, from Verma & Salama (1986)

1.3.2 Storage and reaction processes

There are two distinctively different sources of groundwater solutes: primary and secondary sources. Primary sources, for example, are radionuclides or more conservative solutes such as SO_4 originating directly from tailings, spray- or flood irrigation, and runoff from on-site structures or seepage from tailings. Secondary sources could be solutes remobilised due to groundwater- rock interaction caused by pH and redox reactions, desorption and ion-exchange processes and dissolution of minerals. These secondary processes may have a significant effect on solute concentrations in groundwater.

Martin and Akber (1999), for example, showed that competition for cation adsorption sites is the primary driver of elevated Ra-226 concentrations in bores around the TSF. This is caused by an increase in salinity, rather than from direct transport of radium from the tailings. Overall, they concluded that remobilisation rather than direct transport is the most important factor controlling radium concentration in ground waters. Kalf & Dudgeon (1999) estimated that retardation factors for uranium are 5–10 times lower than for radium in the Kombolgie and Cahill formations. Therefore, it can be expected that uranium concentrations may be less influenced by storage processes than radium.

Contaminants can also be stored in various ‘compartments’. Akber and Marten (1992), Willet and Bond (1992) and Akber et al (2011a,b) showed that uranium, radium and lead applied to the land application areas are readily adsorbed in the first few centimetres of the soil profile, and that remobilisation of these elements is small. In contrast, most soils have a limited capacity to retain major ions such as magnesium and sulfate, and also nitrate after oxidation of ammonia in the aerobic zone of soils (McBride 1992). Based on these considerations, land application can most likely be excluded as a significant source of radionuclides and most heavy metals, but it can play a major role in adding more conservative ions to the groundwater aquifer. This has, for instance, been shown at Nabarlek where spray irrigation has led to a significant impact on sulfate concentration measured in groundwater bores around the site (Mudd 2002).

2 Methods

2.1 Bore locations

Figure 3 shows the location of bores in the Ranger area and the Site ID and associated RN numbers are listed in Table 3. This only represents those bores for which ***eriss*** has analysed radionuclides. A large number of additional bores are monitored routinely by ERA, but these are not included in this report.

Many bores have been investigated in the past by ***eriss*** for radionuclides using various alpha and gamma spectrometry techniques and heavy metals using ICPMS from about 2000 onwards. Table 3 gives a summary of bore information including the location of the bores. Information on the time period that individual bores were sampled for and screening depths are given in the subsequent tables. It is obvious from the number of bores investigated that the focus has been on bores in the vicinity of the TSF.

With mining in pit 3 now finalised and deposition of tailings into the pit expected to start in 2015, the focus has shifted towards monitoring groundwater bores in the vicinity of pit 3, between the northern pit wall and Magela Creek, without neglecting important bores in the vicinity of the TSF. ERA has four statutory monitoring bores: 21030 Deep, 23931 Deep, 83/1 Deep and OB 27, which are routinely sampled on a quarterly basis. Furthermore, there are 22 groundwater monitoring bores that are sampled in their operational monitoring program, quarterly and monthly, respectively (ERA 2012).

The Northern Territory DME is also routinely collecting bore waters around the Ranger mine site. It typically samples 10 bores around May and September each year, and sub-samples are provided to the Environmental Radioactivity group of ***eriss*** for radioanalyses. Statutory bores 23931 Deep, 83/1 Deep and OB 27 are included in DME's sampling, and continuous time series exist for various other bores.

Based on their location, bores were grouped into 9 groups in this report:

- Coonjimba catchment and RP1
- TSF north
- TSF north-west and Gulungul area
- TSF south and south-west wall
- TSF south
- Pit 1
- Corridor Creek and Georgetown area
- RP2 and Pit 3, and
- Djalkmarra and Magela Creek.

Figure 3 Bores at Ranger uranium investigated by ***eriss***, 1988-2012.

Table 3 Information on the bores sampled and analysed by ***eriss*** between 1988 and 2012.

SiteID	RN number	Easting	Northing	Site name
23931_DEEP	RN023931	272415	8599496	Coonjimba
R.P. 79/ 1 Ranger	RN020090	273803	8597674	RP2
R.P. 79/ 2 Ranger	RN020091	273797	8597466	RP2
79/6	RN022901	274302	8597908	Djalkmarra Ck
79/9	RN020098	274240	8598223	Djalkmarra Ck
83_1	RN023010	274414	8598255	Magela/Pit 3
B11	RN007243	272126	8599051	Coonjimba
C12		274930	8596518	Corridor Creek area
C1SHALLOW		272729	8595219	TSF South
Magela Ck 11/80	RN020369	274886	8598810	Magela Creek
MBH	RN023721	274151	8596111	Pit 1 Area
MBL	RN023725	273933	8595935	Pit 1 Area
MC24	RN025466	274516	8597943	Magela/Pit 3
MC27	RN025469	275153	8597990	Magela Creek
OB10A	RN022920	272822	8596651	TSF North Area
OB11A	RN022922	272538	8596823	TSF North Area
OB12A	RN022923	271857	8596869	TSF North Area
OB13A	RN022924	272233	8596813	TSF North Area
OB15	RN022926	272320	8596972	TSF North Area
OB16	RN022927	272292	8596818	TSF North Area
OB112_DEEP	OB112_DEEP	271143	8595656	TSF Gulungul Area
OB116_DEEP	OB116_DEEP	271459	8595355	TSF Gulungul Area
OB116_SHALLOW		271460	8595349	TSF Gulungul Area
OB17A	RN026588	271745	8596882	TSF North Area
OB19A	RN026589	271812	8595640	TSF South Area
OB1A	RN022902	271561	8596865	TSF Gulungul Area
OB20	RN022934	271822	8595161	TSF South Area
OB21A	RN022935	272484	8595180	TSF South Area
OB23	RN022937	271844	8597241	TSF North Area
OB24	RN022938	272040	8597220	TSF North Area
OB26		272409	8597134	TSF North Area
OB27	RN022930	275523	8597063	Georgetown Area
OB28	RN023939	275473	8597067	Magela LAA
OB29	RN022940	274115	8597457	RP2 Area
OB2A	RN022904	271017	8596684	TSF Gulungul Area
OB30	RN022941	273923	8595706	Corridor Creek area
OB44	RN026593	272399	8597199	TSF North Area
OB6	RN022911	272413	8595569	TSF South Area
OB6A	RN022912	272410	8595566	TSF South Area
OB7A	RN022914	272707	8595639	TSF South Area
OB9A	RN022918	272738	8596373	TSF North Area
RN22211	RN022211	274683	8598647	Magela Ck
RN23551	RN023551	272435	8597838	RP 1 Area
RN23556	RN023556	271473	8597040	TSF North Area
RN23562	RN023562	274404	8598253	Magela Creek
RN23566	RN023566	270911	8596382	TSF Gulungul Area
RN23568	RN023568	272121	8595210	TSF South Area
RN8708	RN8708	273262	8595136	Corridor Creek Tails Corridor Area (DME)
79/2 RANGER	RN009329	270863	8596371	Gulungul
RP1N1	RN026625	272337	8597379	RP1 headwaters
RP1N2	RN026626	272338	8597378	RP1 headwaters
OB4A	RN22908	271686	8595767	TSF South Area
OB22		272950	8596271	

2.1.1 Bores in the Coonjimba and RP1 catchment

Figure 4 shows a close up of the bores in the Coonjimba catchment and RP1 area. Table 4 shows the site ID and RN numbers, the depths of the screen and some other comments regarding the bores.

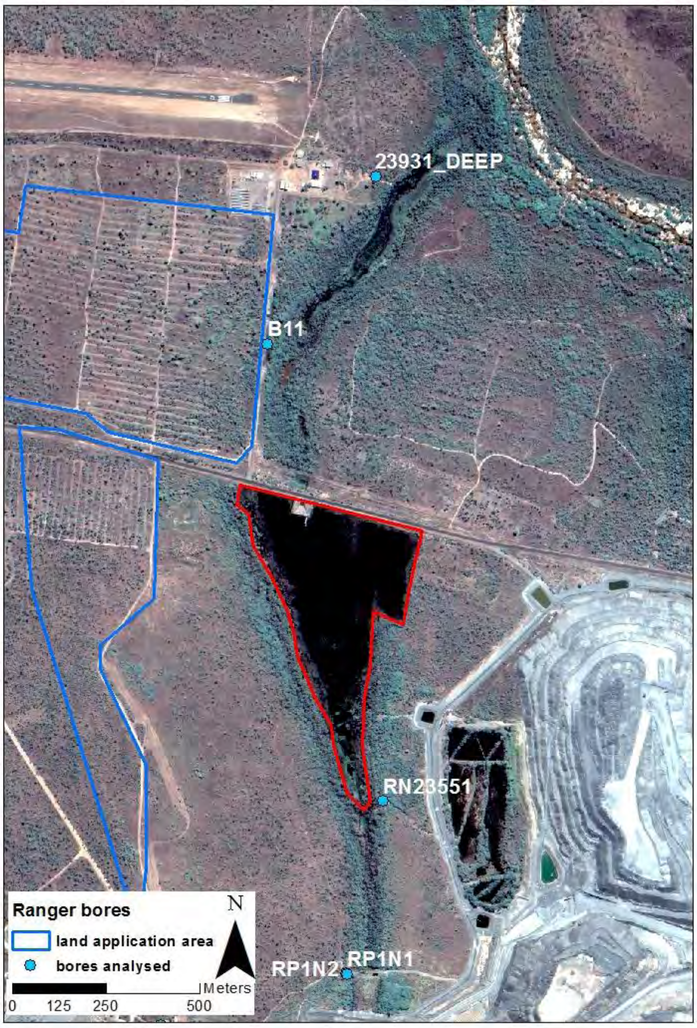

Figure 4 Bores in the Coonjimba catchment and RP1 area

Table 4 Site IDs, RN numbers, time period of data available and screen depths of bores in the Coonjimba catchment and RP1 area.

SiteID	RN number	Data from-to	Top of screen (m)	Bottom of screen (m)	comments
23931_DEEP	RN023931	9/11-9/12	29.2	37.0	active*
B11	RN007243	9/06-9/09	0.0	13.0	active
RN23551	RN023551	9/04-9/12	4.0	4.5	active
RP1N1	RN026625	5/03	1.5	8.9	1 sample only
RP1N2	RN026626	5/03	11.0	20.0	1 sample only

*: active means that the bore is still being sampled by either ERA or DME.

2.1.2 Bores in the TSF north area

Figure 5 shows a close up of the bores in the TSF north area. Table 5 shows the site ID and RN numbers, the fitted screen depths and some other comments regarding the bores. Bore OB44 was drilled in July 1988 as a substitute for OB26 (Martin & Akber 1996).

Figure 5 Bores in the TSF north area.

Table 5 Site IDs, RN numbers, time period of data available and screen depths of bores north of TSF.

SiteID	RN number	Data from-to	Top of screen (m)	Bottom of screen (m)	comments
OB23	RN022937	11/89-9/12	36.0	51.0	active
OB24	RN022938	11/89-5/02	21.5	36.2	active
OB44	RN026593	11/89-5/02	11.0	16.0	
OB17A	RN026588	1/89-5/02	23.0	41.0	buried*
OB12A	RN022923	11/89-5/96	16.0	31.0	buried
OB15	RN022926	11/88-5/97	10.0	25.0	buried
OB16	RN022927	9/88-5/97	10.0	20.0	buried
OB13A	RN022924	9/88-5/98	10.0	30.0	buried
OB11A	RN022922	9/88-5/97	11.0	23.0	buried
OB9A	RN022918	11/88-3/99	12.0	30.0	probably buried
OB10A	RN022920	5/89-5/02	12.0	30.0	buried
OB26		7/88-1/89		61.0	buried

*: buried means that the bore has been buried by infrastructure on site and no longer exists

2.1.3 Bores to the north-west of TSF and the Gulungul catchment

Figure 6 shows a close up of the bores to the north-west of TSF and the Gulungul catchment. Table 6 shows the site ID and RN numbers and the fitted screen depths and some other comments regarding the bores.

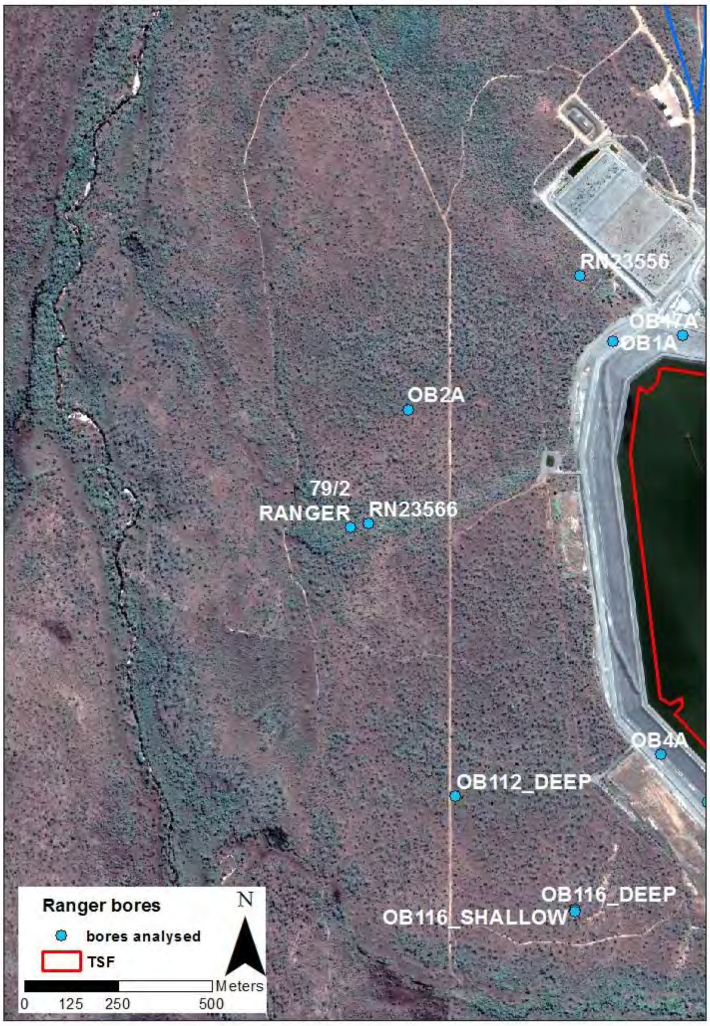

Figure 6 Bores to the north-west of TSF and the Gulungul catchment.

Table 6 Site IDs, RN numbers, time period of data available and screen depths of bores to the north-west of TSF and the Gulungul catchment.

SiteID	RN number	Data from-to	Top of screen [m]	Bottom of screen [m]	comments
RN23556	RN023556	3/12	4.1	5.1	active
OB1A	RN022902	11/89-9/12	16.0	31.0	buried
OB2A	RN022904	11/89-5/02	15.0	30.0	
RN23566	RN023566	10/10-3/12	4.0	5.5	active
79/2 Ranger	RN009329	9/03-9/12	17.1	19.0	active
OB112_Deep	OB112_DEEP	3/12	14.0	20.0	active
OB116_Deep	OB116_DEEP	10/10-3/12	14.0	19.9	active
OB116_Shallow		3/12	0.0	5.0	active

2.1.4 Bores on the south and south-west wall of TSF

Figure 7 shows a close up of the bores located close to the south and south-west wall of the TSF. All of these bores are now buried. Table 7 shows the site ID and RN numbers, the fitted screen depths and some other comments regarding the bore.

Figure 7 Bores on the south and south-west wall of TSF.

Table 7 Site IDs, RN numbers, time period of data available and screen depths of bores on the south and south-west wall of TSF.

SiteID	RN number	Data from-to	Top of screen [m]	Bottom of screen [m]	comments
OB4A	RN22908	7/88-5/01	22.0	37.0	buried
OB19A	RN026589	11/90-5/02	33.0	51.0	buried
OB6	RN022911	5/00			buried
OB6A	RN022912	9/88-5/02	14.0	26.0	buried
OB7A	RN022914	11/89-5/02	15.0	30.0	buried

2.1.5 Bores to the south of TSF

Figure 8 shows a close up of the bores to the south of the TSF. Table 8 shows the site ID and RN numbers, the fitted screen depths and some other comments regarding the bore.

Figure 8 Bores to the south of the TSF.

Table 8 Site IDs, RN numbers, time period of data available and screen depths of bores to the south of the TSF.

SiteID	RN number	Data from-to	Top of screen [m]	Bottom of screen [m]	comments
OB20	RN022934	11/89-9/12	21.0	36.0	active
RN23568	RN023568	3/12	3.3	4.3	active
OB21A	RN022935	11/89-9/12	31.0	43.0	active
C1SHALLOW		5/03	2.5	8.4	

2.1.6 Bores in the vicinity of Pit 1

Figure 9 shows a close up of the bores in this area. Table 9 shows the site ID and RN numbers, the fitted screen depths and some other comments regarding the bore.

Figure 9 Bores in the vicinity of Pit 1

Table 9 Site IDs, RN numbers, time period of data available and screen depths of bores in the vicinity of Pit 1.

SiteID	RN number	Data from-to	Top of screen [m]	Bottom of screen [m]	comments
MBH	RN023721	5/03	44.0	50.0	Pit 1 Area
MBL	RN023725	5/03		50.0	Pit 1 Area

2.1.7 Bores in the Corridor Creek - Georgetown Creek Area

Figure 10 shows a close up of the bores in the Corridor and Georgetown Creek area. Table 10 shows the site ID and RN numbers, the fitted screen depths and some other comments regarding the bores.

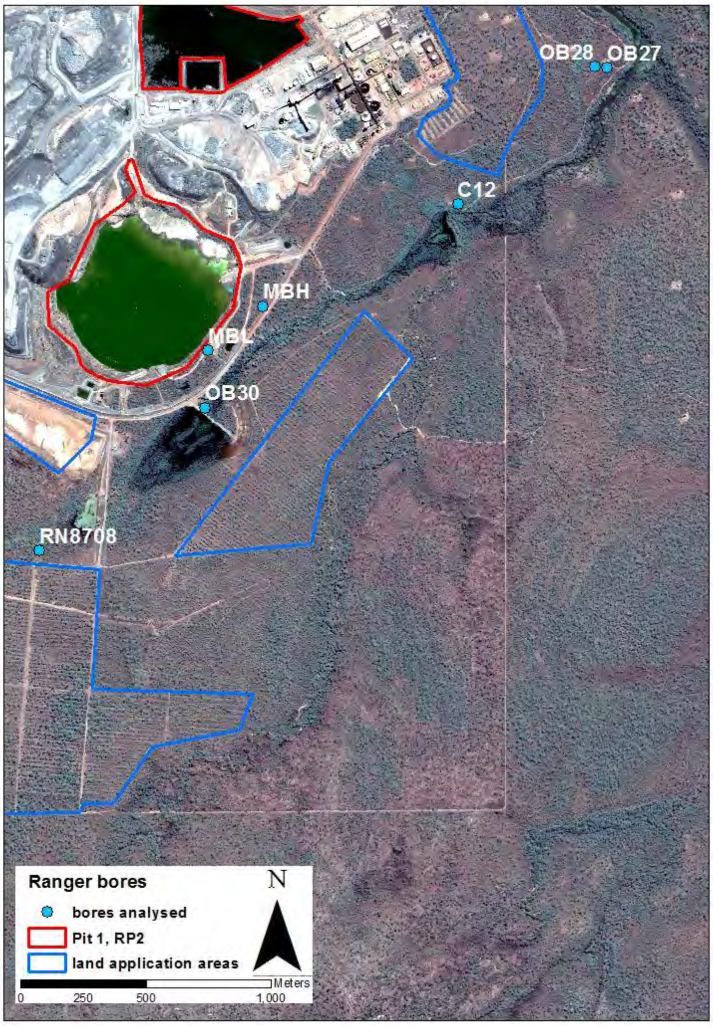

Figure 10 Bores in the Corridor and Georgetown Creek area.

Table 10 Site IDs, RN numbers, time period of data available and screen depths of bores in the Corridor and Georgetown Creek area.

SiteID	RN number	Data from-to	Top of screen [m]	Bottom of screen [m]	comments
RN8708		9/09-9/12			Corridor Creek Area
OB30	RN022941	11/89-9/12	20.0	35.0	active
C12		9/11	7.0	13.0	active
OB27	RN022930	9/03-9/12	15.0	40.0	active
OB28	RN023939	11/89-5/00	31.0	46.0	

2.1.8 Bores in the RP2/Pit 3 Area

Figure 11 shows a close up of the bores in the RP2/Pit 3 area. Table 11 shows the site ID and RN numbers, the fitted screen depths and some other comments regarding the bore.

Figure 11 Bores in the RP2/Pit 3 area.

Table 11 Site IDs, RN numbers, time period of data available and screen depths of bores in the RP2/Pit 3 area.

SiteID	RN number	Data from-to	Top of screen [m]	Bottom of screen [m]	comments
R.P. 79/ 1 Ranger	RN020090	7/88-5/96	21.0	23.0	buried
R.P. 79/ 2 Ranger	RN020091	1/89			active
OB29	RN022940	1/89-5/02	35.0	50.0	buried

2.1.9 Bores in the Djalkmarra and Magela Creek area

Figure 12 shows a close up of the bores in the Djalkmarra and Magela Creek area. Table 12 shows the site ID and RN numbers, the fitted screen depths and some other comments regarding the bore.

Figure 12 Bores in the Djalkmarra and Magela Creek area.

Table 12 Site IDs, RN numbers, time period of data available and screen depths of bores in the Djalkmarra and Magela Creek area.

SiteID	RN number	Data from-to	Top of screen [m]	Bottom of screen [m]	comments
MC24	RN025466	9/03			1 sample only
MC27	RN025469	9/03-9/04	1.0	3.0	
83_1	RN023010	5/03-9/12	0.0	90.0	active
79/6	RN022901	11/89-5/92			buried
79/9	RN020098	11/89-5/96	20.0	70.0	
RN23562	RN023562	9/07-9/11	4.4	5.4	active
RN22211	RN022211	9/07-9/09			not active
Magela Ck 11/80	RN020369	9/07			1 sample only, active

2.2 Analytical methods

2.2.1 Measurement of radioisotopes

Measurement of radioisotopes was done at Supervising Scientist using methods developed in-house (Martin & Hancock, 2004; Medley et al 2005).

Uranium isotope activity concentrations (and hence activity ratios) were determined by alpha spectrometry after radiochemical separation of uranium from a bulk sample. This involved iron hydroxide co-precipitation for sample pre-concentration followed by chemical separation. Chemical separation was performed in two stages, first a tributyl phosphate (TBP) solvent extraction, then an anion exchange to ensure complete separation of thorium (in particular ^{230}Th which can interfere with ^{226}Ra on the final source). Chemical separation is followed by electro deposition of uranium onto a stainless steel planchet for alpha counting. Uranium-232 was used as a source tracer for chemical recovery determination (Martin and Hancock 2004).

Some earlier groundwater samples were analysed for radionuclides using gamma spectrometry techniques. Radionuclides were co-precipitated in a 20 litre pail with manganese dioxide. This first precipitation was followed by a second precipitation using ferric hydroxide. After separation of the precipitate from the supernatant, the precipitate and filter were ashed, then cast in a mould using a polyester resin before counting on a high purity germanium (HPGe) gamma-ray spectrometer (Martin & Akber 1996). Casting and analysis techniques have been described in detail in Murray et al (1987).

Radium-226 activity concentrations were determined by alpha spectrometry after radiochemical separation of radium from a bulk sample. For samples analysed prior to 2001 a method developed by Martin and Hancock (2004) was used. This involved co-precipitation of radium with $Ba/PbSO_4$, anion and cation exchange separations followed by electro deposition of radium onto a stainless steel planchet. Radium-225 was used as a source tracer for chemical recovery determination in this technique and high resolution of the source allowed measurement of all four naturally occurring radium isotopes. Since 2001 a new technique (Medley et al 2005) involving a dual co-precipitation of radium with $Ba/PbSO_4$ followed by micro-filtration of the colloidal precipitate for source preparation. Due to the poorer resolution of this source, alpha spectrometric measurement only allows determination of ^{226}Ra on these sources. Barium-133 was used as a source tracer in these measurements and typical chemical recoveries should be above 85% to be confident that the assumption of similar chemical behaviour of barium and radium in the chemical separation process is valid.

In cases where expected radium and/or uranium activity concentrations are close to the detection limits for alpha spectrometric analysis (i.e. – less than 4 mBq/L), consecutive analysis of radium and uranium was undertaken. This involved iron hydroxide co-precipitation and TBP extraction. The aqueous waste solution from this solvent extraction was heated with concentrated nitric acid to remove traces of solvent then used for ^{226}Ra determination using the micro-filtration technique.

Where consecutive analysis was undertaken chemical recoveries usually were lower than for samples undergoing co-precipitation of radium with $Ba/PbSO_4$ only. It is believed that this can be explained by massic losses during the iron hydroxide and TBP extraction steps and that the accuracy of chemical recovery determination using the ^{133}Ba tracer is not adversely affected by this consecutive analysis process.

2.2.2 Measurement of metal concentrations

Elemental and major anion analysis of filtered groundwater samples was undertaken by a variety of isotope dilution, Inductively Coupled Plasma (ICP) spectrometry techniques. These include ICP-Atomic emission spectrometry (ICPAES), ICP-Mass spectrometry (ICPMS) and ICP-Optical emission spectrometry (ICPOES).

The particular suite of analytes that were measured in each batch of samples varied over the period of sample collections, and the technique used for each element was determined by the expected concentration of the analyte and the accuracy and precision of the measurement technique (with ICPMS being the most sensitive method). ICP analyses were performed at three different laboratories during the period of sample collection; Charles Darwin University (formerly Northern Territory University) from 1999 to 2001 and 2004 to 2005, the Northern Territory Environmental Laboratories (*NTEL*) from 2002 to 2003 and 2006 to 2011, and *EnviroLabs* in Sydney from 2012 onwards.

Samples were prepared for analysis by filtration through 0.45 µm cellulose acetate or nitrocellulose filter papers. Samples were filtered in the ***eriss*** laboratories until 2003, at which point filtration was undertaken in the field by DME.

Acidification of samples was done for sample preservation using either 2% concentrated nitric acid or 0.5% concentrated hydrochloric acid (on a volume:volume basis). Typical detection limits varied by analyte, sample volume and the technique used for analysis. The range of detection limits for ICP analysis is shown in Table 13.

Table 13 Typical upper and lower range of detection limits for various ICP analytical techniques used for elemental and major anion analysis

Analyte	As	Ba	Ca	Cd	Cl	Cr	Cu	Fe	K	Li	Mg
Lowest Detection Limit (µg.L^{-1})	0.1	0.01	0.1	0.01	1000	0.1	0.02	1	0.1	0.05	0.1
Highest Detection Limit (mg.L^{-1})	0.1	0.02	300	0.01	1000	0.1	0.02	20	100	0.05	100
Analyte	Na	Pb	Rb	S	SO$_4$	Se	Sr	Th	U	V	Zn
Lowest Detection Limit (µg.L^{-1})	0.1	0.01	0	200	1000	0.2	0.01	0.01	0.001	0.05	0.04
Highest Detection Limit (mg.L^{-1})	100	0.07	0	200	1000	100	0.02	0.01	0.01	10	0.1

2.2.3 Comparison of uranium concentrations measured via ICPMS and alpha spectrometry

As uranium concentrations have been measured in some of the bore water samples by both alpha spectrometry and ICPMS an independent quality assurance check of the measured uranium concentration data was possible.

Figure 13 shows a comparison of uranium concentration results measured via ICPMS and ^{238}U activity concentration measurements via alpha spectrometry in the same sample, for bore waters investigated in this study. The concentration range of these measurements span four orders of magnitude.

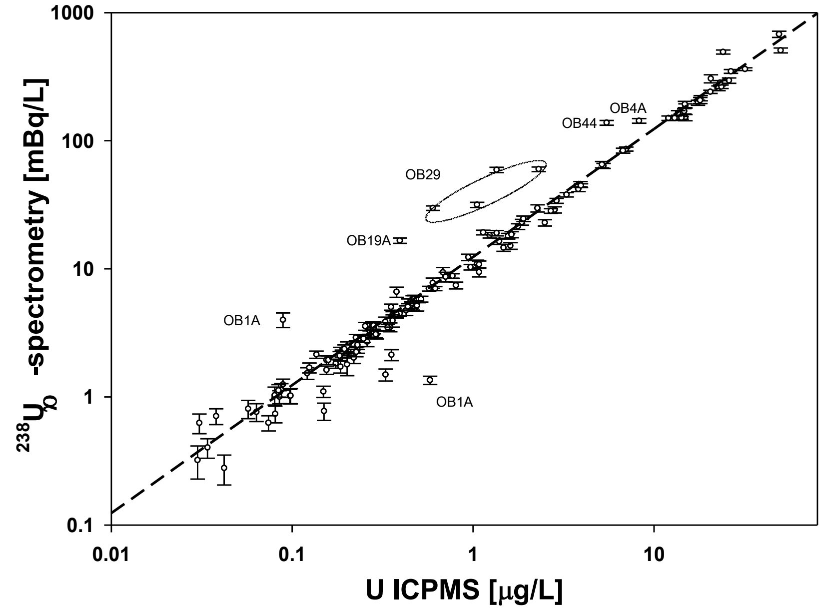

Figure 13 Comparison of uranium measurements via ICPMS and alpha spectrometry.

The dashed line in Figure 13 indicates the expected ^{238}U activity concentration, using the conversion factor of 1 Bq ^{238}U ≡ 80.962 µg of natural uranium. Figure 13 shows generally a good agreement between ICPMS and alpha-spectrometry results over four orders of magnitude. A number of samples however showed ^{238}U activity concentrations different to those expected from U measurements via ICPMS, in particular for samples collected between 1999 and 2001. The bores affected were bores OB1A, OB19A, OB44 and OB29. The reason for the discrepancy in these samples is unknown, but could be due to sample storage times and acidification of the aliquots after sample collection.

2.2.4 The use of the ^{234}U/^{238}U activity ratio for source apportionment

In a plot of the ^{234}U/^{238}U activity ratios against the inverse of the ^{238}U activity concentration, the intercept of the regression line with the y-axis gives an indication of the ^{234}U/^{238}U activity ratio of a single contaminating uranium source (the 'contaminating end-member') in a system that has a constant background ^{238}U activity concentration.

Due to the recoil effect of ^{234}U and its preferential leaching over the ^{238}U isotope in natural ground waters most natural ground waters have a ^{234}U/^{238}U activity ratio greater than 1 (see Osmond & Cowart 1982). In contrast, it is generally assumed that uranium in liquid waste generated by the processing of uranium ore (with ^{234}U in secular equilibrium with ^{238}U) shows ^{234}U/^{238}U activity ratios of ~1, as the strong acid used in the processing of ores will effectively dissolve all of the uranium without preferentially leaching one of the isotopes (Zielinski et al 1997).

Figure 14 is a conceptualisation of the inverse concentration approach. If natural groundwater with a ^{234}U/^{238}U activity ratio greater than 1 and low ^{238}U activity concentrations mixes with low pH water from the TSF, high in U and with a ^{234}U/^{238}U activity ratio that equals 1, then a mixing line similar to the line indicated by AB, with an intercept around 1 can be expected. If the source of uranium is leached from relatively uranium rich mine material by rainwater percolating though the material, ^{234}U would preferentially leach over the ^{238}U isotope, and a mixing line similar to the line indicated by CD, with an intercept greater than 1 can be expected. If the source of uranium does not change but changes in bore water chemistry affect the uranium concentration in the groundwater, the ^{234}U/^{238}U activity ratio should remain constant, as indicated by EF. More than one contaminating end member will result in uncorrelated data.

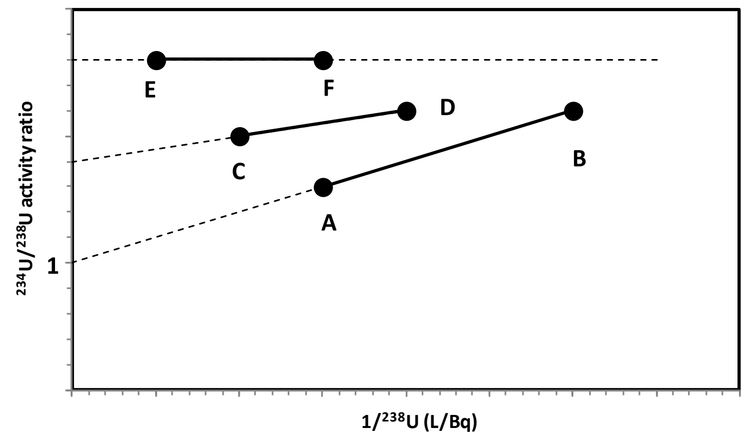

Figure 14 Conceptualisation of the inverse activity concentration approach

2.2.4 Statistical multivariate analysis (PCA)

Groundwater quality data are summarised for the various catchments around the Ranger mine site using Principal Components Analysis (PCA).

PCA is an eigenvector-based multivariate analysis for identifying a smaller number of uncorrelated variables, called principal components, from a larger set of data. The general goal of principal components analysis is to simplify a data set and explain the maximum amount of variance with the fewest number of principal components (Jolliffe 2002; Minitab 2015). In groundwaters, electrical conductivity (EC) or redox conditions often are the driving factors of variability in water quality (e.g. Chen et al 2007).

Three plots are usually displayed to visualise the results of a PCA. These are the so-called scree, loading and score plots. The scree plot displays the eigenvalues associated with each factor from the PCA and can be used to assess the importance of each factor in explaining the variability of the original data. The loading plot displays to what degree a factor determined from the PCA explains the variability of a certain measured variable and whether metal concentrations are positively or negatively correlated with the principal components. PCA scores are calculated for each variable within a sample and are plotted to investigate similarities between samples or sampling sites.

Minitab 16 is used for multivariate statistical analysis. Bores are grouped into various catchments and the correlation matrix was used. Each variable is normalised to unit variance and thus contributes equally to the PCA.

3 Results

3.1 Bores in the Coonjimba catchment and RP1

3.1.1 Major constituents

Figure 15 shows the results of measurements of major constituents (cations Ca, Na, Mg, K; anions: SO$_4$) in ground waters sampled from bores in the Coonjimba catchment and in the vicinity of RP1.

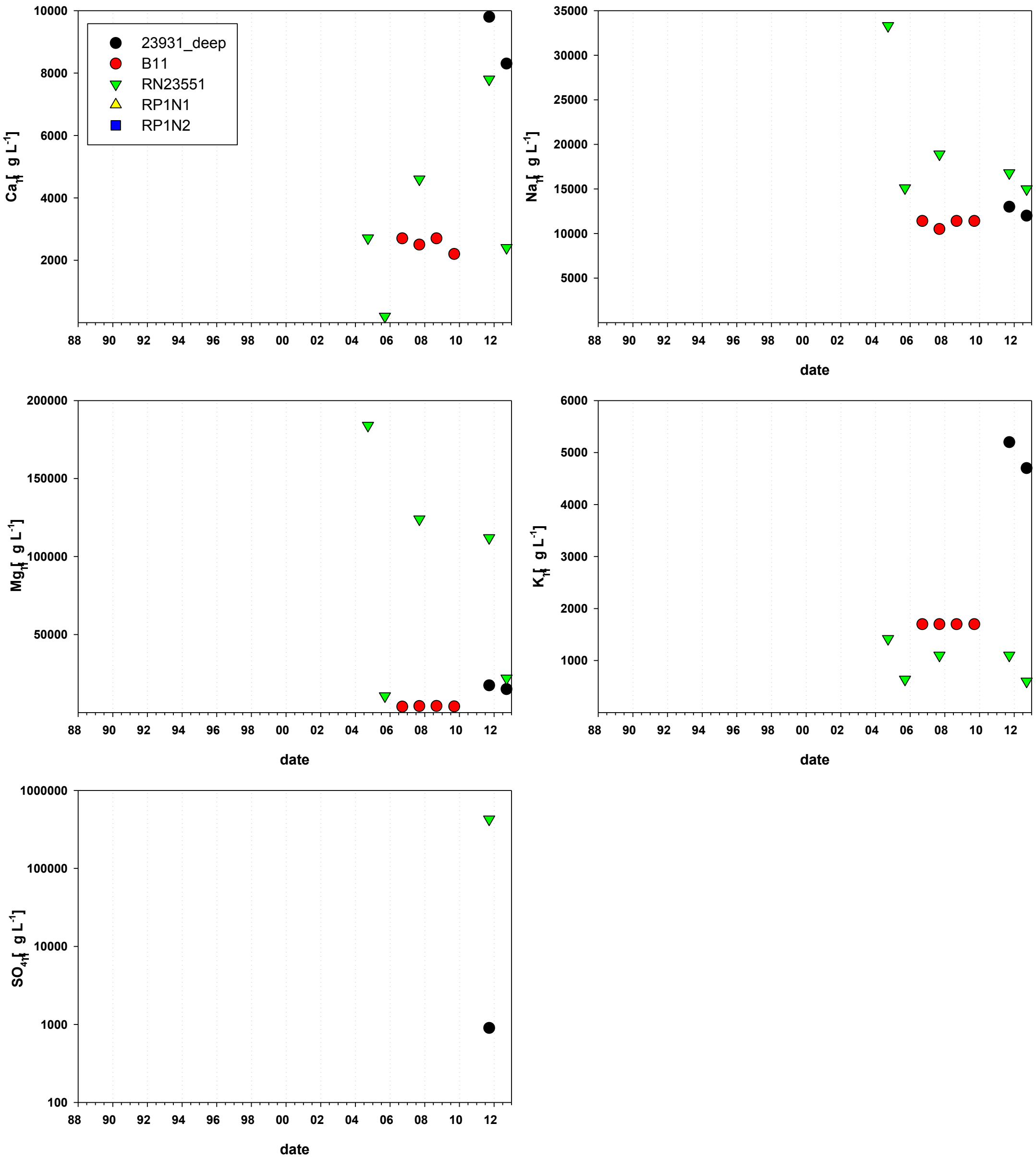

Figure 15 Major constituent concentrations plotted against sampling date in bores 23931_deep, B11 and RN23551.

Figure 15 shows that shallow bore RN23551, located at the southern margin of RP1, is dominated by Mg with a maximum concentration of 180 mg L^{-1} measured in September 2004. Na was highest in 2004 as well at 33 mg L^{-1}, maximum Ca concentration was measured in September 2011 at about 8 mg L^{-1}. Generally, major cation concentrations in bore RN23551 show a very large variability, which is also reflected in the data for bore

RN23551 measured by ERA (ERA 2012). Sulfate in bore RN23551 was more than 400 mg L^{-1} in 2011.

Bore B11 is located between Coonjimba Billabong and the Jabiru East irrigation area. Major cation concentrations show little variability, with Ca concentrations of about 2.5 mg L^{-1}, Na about 10 mg L^{-1}, Mg about 4 mg L^{-1} and K about 1.7 mg L^{-1}.

The deep groundwater monitoring bore 23931_deep, located further downgradient of Coonjimba Billabong, is a statutory monitoring bore of ERA. A comparison with data from ERA shows that Ca concentrations (8-10 mg L^{-1}) are similar to end of the dry season measurements made by ERA, with wet season concentrations being lower at about 5 mg L^{-1} (ERA 2012). Bore 23931_deep is dominated by Ca and Na, typical for bores located in the fractured Nanambu complex (Klessa 2001).

3.1.2 Metals

Figure 16 shows the available results of bore water metal (Fe, Mn, Ba, Sr, U) concentrations in bores RN23551, B11 and 23931_deep. Bores were sampled at the end of the dry season and results are available from 2004 onwards. Metal concentrations were generally well above detection limits.

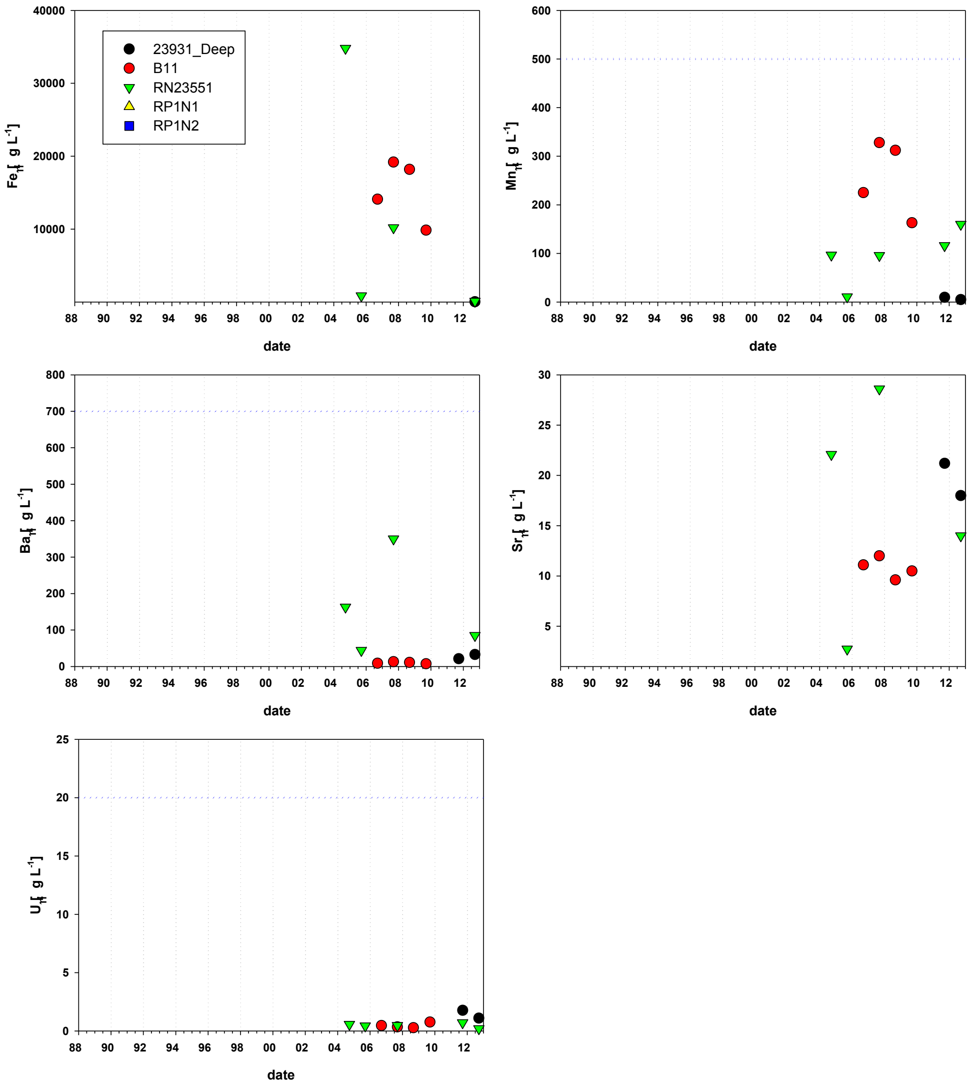

Figure 16 Metal concentrations plotted against sampling date in bores RN23551, B11 and 23931_deep. The blue dotted lines indicate the Australian drinking water quality guidelines (NHMRC 2011).

Bore RN23551 shows quite variable concentrations of Fe, Mn, Ba and Sr. Concentration minima coincide with minima in major cations measured in this bore. Concentrations of Fe vary by more than 2 orders of magnitude from 0.1 mg L^{-1} to 35 mg L^{-1}. Concentrations of Ba and Sr in RN23551 vary by one order of magnitude from 40 to 350 and from 2.7 to 29 µg L^{-1}, respectively. The variability of U is much smaller, with uranium concentration between 0.2 and 0.7 µg L^{-1}, similar to concentrations for this bore reported by ERA (2012).

Bore B11 shows similar Fe but slightly higher Mn concentrations compared to RN23551. Ba concentrations are much lower, whereas U is similar again to RN23551. There is some variability in Fe and Mn that cannot be seen in major cation concentrations measured in this bore. However, Mn and Fe appears to be negatively correlated to U.

Bore 23931_deep has generally low Fe, Mn, Ba and Sr concentrations. Concentrations of U are also low, but higher than concentrations measured in bores B11 and RN23551.

3.1.3 Radionuclides

Figure 17 shows the results of radionuclide activity concentration measurements, and the $^{234}U/^{238}U$ activity ratios measured in bores 23931_deep, B11, RN23551, RP1N1 and RP1N2.

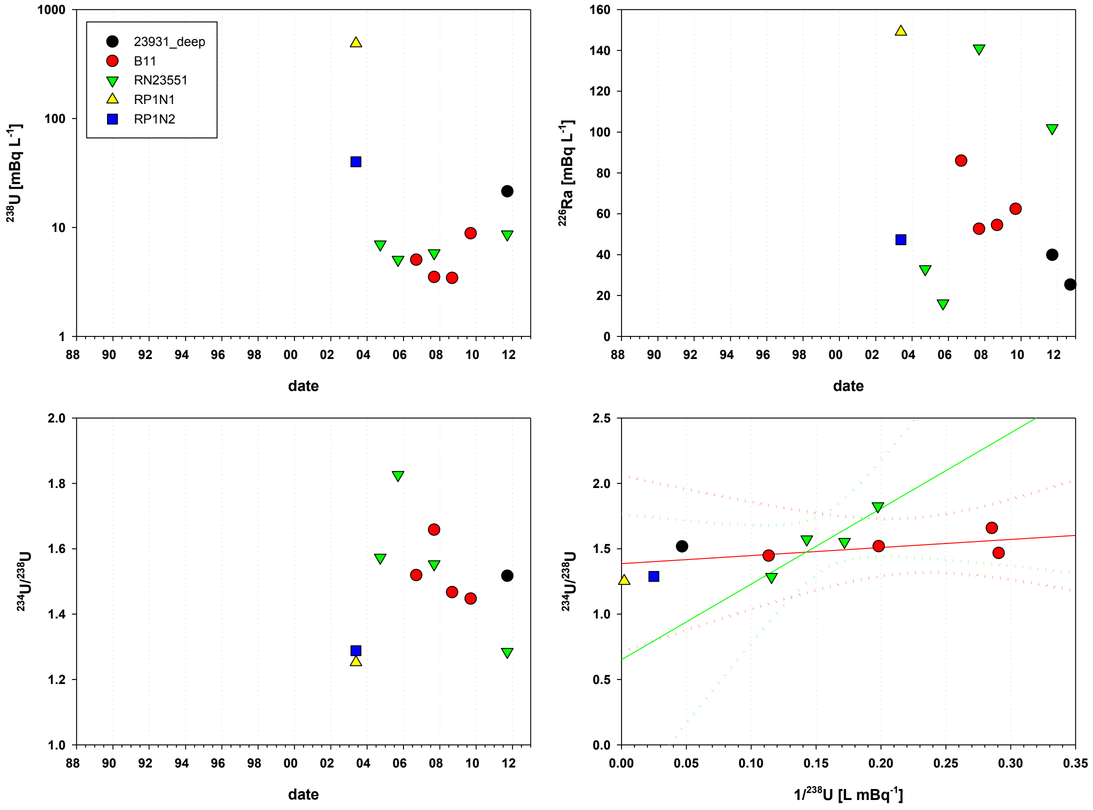

Figure 17 ^{238}U and ^{226}Ra activity concentrations plotted against sampling date, and the $^{234}U/^{238}U$ activity ratio plotted against sampling date and inverse ^{238}U activity concentration, respectively. Data for bores RN23551, B11, 23931_deep, RP1N1 and RP1N2 are shown. Linear fits to the $^{234}U/^{238}U$ activity ratio (bores RN23551 and B11) in the inverse concentration plots and associated 95% confidence intervals are shown as well.

Activity concentrations of ^{238}U are highest in bores RP1N1 (487 mBq·L^{-1}) and RP1N2 (40 mBq·L^{-1}), located in the headwaters of RP1. Samples are available from one collection only and these bores were sampled at the end of the wet season 2004/05 (21

May 2005). According to ERA (2012), bores RP1N1 and RP1N2 do not exhibit major variability with time of year.

Activity concentrations of ^{238}U in bore RN23551 are low and in agreement with U concentrations measured via ICPMS. There appears to be an increase of ^{238}U between 2005 and 2011, associated with a decrease in ^{234}U/^{238}U activity ratios. The range of ^{238}U activity concentration in this bore however is small and thus the intercept determined from an inverse concentration plot (^{234}U/^{238}U activity plotted versus the inverse ^{238}U activity concentration) is associated with a very large error (0.65±1.11). The p-value for the slope is 0.07, whereas the intercept has a p-value of 0.13.

Activity concentrations of ^{238}U in shallow bore B11 are also low and in agreement with U concentrations measured via ICPMS. They are slightly higher than concentrations measured by ERA during and at the end of the wet season (ERA 2012). Similar to RN23551, the intercept determined from an inverse concentration plot is associated with a large error (1.39±0.68) and the correlation between the ^{234}U/^{238}U activity ratios and inverse of the uranium concentration is not statistically significant ($p = 0.45$).

The variability of ^{226}Ra activity concentration in bore RN23551 is larger than in bore B11, and similar to the variability observed in Mg, Fe, Ba, Sr and major cations. High Mn and Fe coincide with lower ^{238}U in bore B11.

3.2 Bores in the TSF north area

3.2.1 Major constituents

Figure 18 shows the results of measurements of major constituents (cations Ca, Na, Mg and K; anions: SO_4) in ground waters collected from bores north of the TSF.

Many of the bores that were investigated in this area were decommissioned in the early 2000s. Bores OB17A, OB12A, OB16, OB13A, OB11A and OB15 are buried either under the TSF lift or the construction of RP6. OB10A is buried under the ore stockpile, the status of OB9A is unknown, but it is likely that this bore is buried as well. Bore OB44 was drilled in July 1988 as a substitute for OB26, but sampling of bore OB44 ceased in 2002. OB23 and OB24 are the only observation bores still active in this area.

Deep bores OB10A, OB44, OB15 and OB16 were dominated by Mg with concentrations ranging from 120 to 580 mg L^{-1}. Bores OB44, OB15 and OB16 were located within the old Conjimba Creek line. SulfateSulfate concentrations measured in these bores were high, in agreement with Martin & Akber (1999) who have shown that sulfate concentration in OB44 has been increasing from January 1989, and OB9A and OB10A have shown increases in sulfate concentrations since 1986. It is thus likely that these bores were affected by seepage from the TSF before they were buried under new mine infrastructure, as these bores are located along a major fault line north of the TSF wall.

Observation bore OB23 is the only bore for which time series extends to 2012. OB23 is a deep bore approximately 400 m north of the TSF wall, dominated by Ca and Na, typical for bores in the fractured Nanambu complex (Klessa 2001).

The variability of major cation and sulfate concentration in bore waters from OB23 is relatively small and there is no evidence of an increase in the major constituents in this bore over time, apart from an increase in Ca between 1999 and 2004.

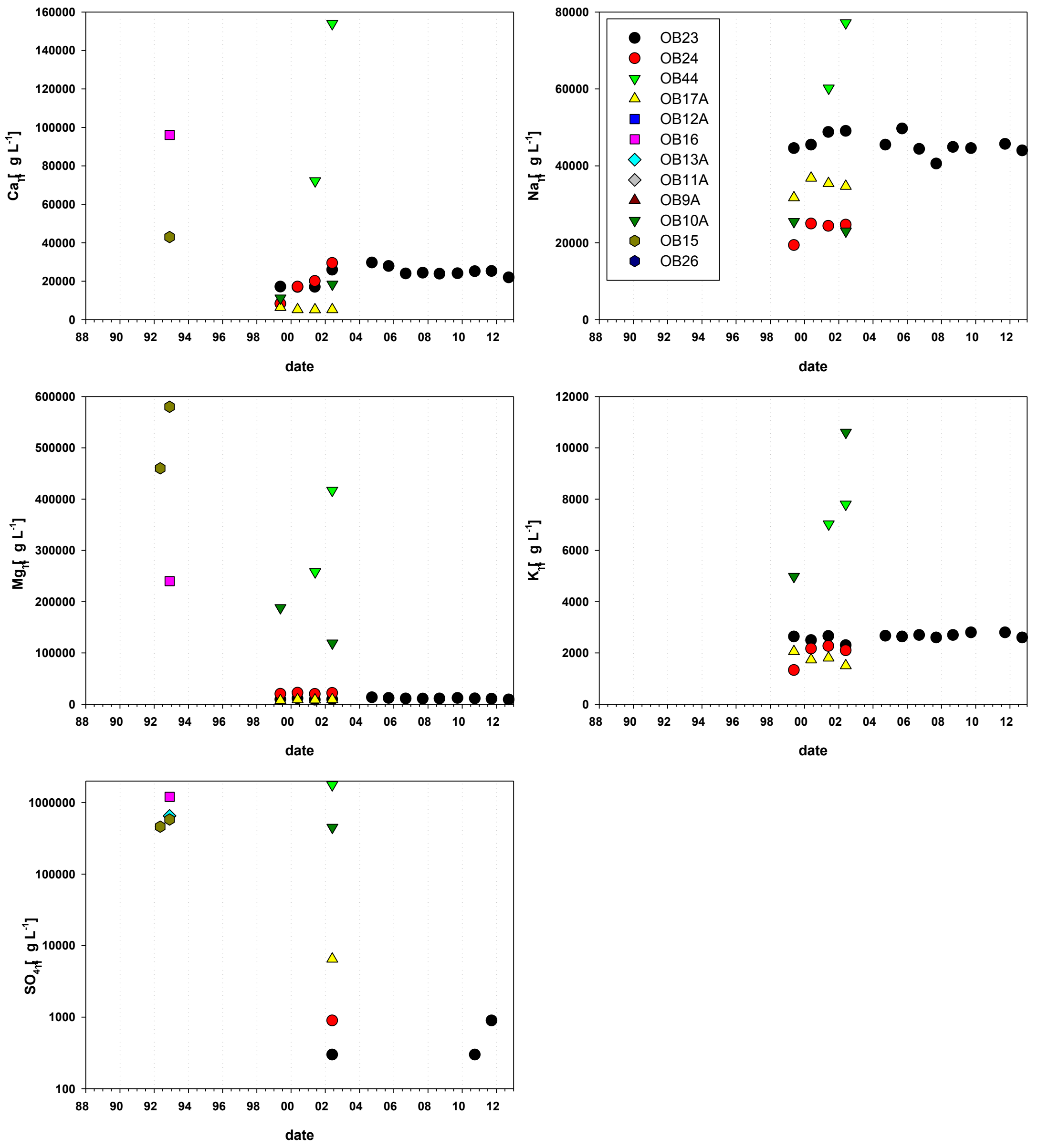

Figure 18 Major constituent concentrations plotted against sampling date in bores OB23, OB24, OB44, OB17A, OB16, OB13A, OB10A and OB15.

3.2.2 Metals

Figure 19 shows the results of metal (Fe, Mn, Ba, Sr, U) concentration measurements via ICPMS from 1999 onwards.

Observation bores OB24, OB44, OB17A and OB10A were analysed between 1999 and 2002, when they were buried under a TSF lift or various stockpiles. Concentrations of Fe were highest in OB10A, Sr and U were highest in OB44.

Bore OB24 showed an increase in Fe, Ba and Mn between 1999 and 2001. Manganese concentrations measured in this bore in 2010 (ERA, 2012) are similar to concentrations measured in 2001. The reason for the increase in Fe and Mn between 1999 and 2001 is unknown and does not coincide with a similar increase in U.

Metal concentrations in OB23 show some variability, in particular for Mn and Fe, with minima for those two metals observed in September 2000 and September 2001, respectively. Concentrations of Ba and Sr are relatively constant. Uranium concentration is low, with maxima around 3.5 µg L^{-1} measured in 2001 (and 2011). There is a good agreement between uranium concentrations measured via ICPMS and ^{238}U activity concentrations measured using alpha spectrometry.

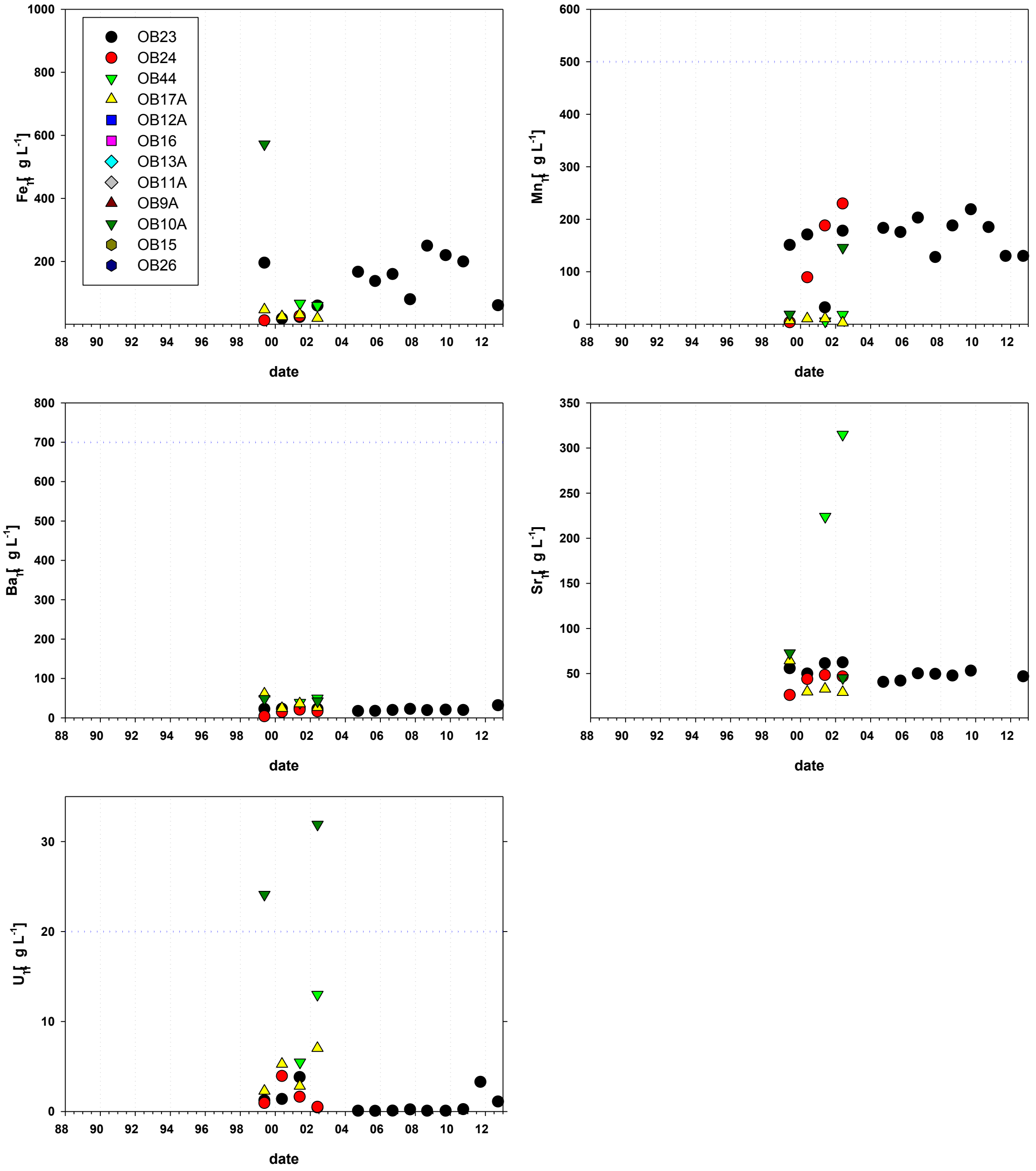

Figure 19 Metal concentrations plotted against sampling date in bores OB23, OB24, OB44, OB17A and OB10A. The blue dotted lines indicate the Australian drinking water quality guidelines (NHMRC 2011).

3.2.3 Radionuclides

Figure 20 shows the results of radionuclide activity concentration measurements, and the ^{234}U/^{238}U activity ratios measured in bores OB23, OB24, OB44, OB17A, OB12A, OB16, OB13A, OB11A, OB9A, OB10A, OB15 and OB26, from the start of sampling in 1988 onwards.

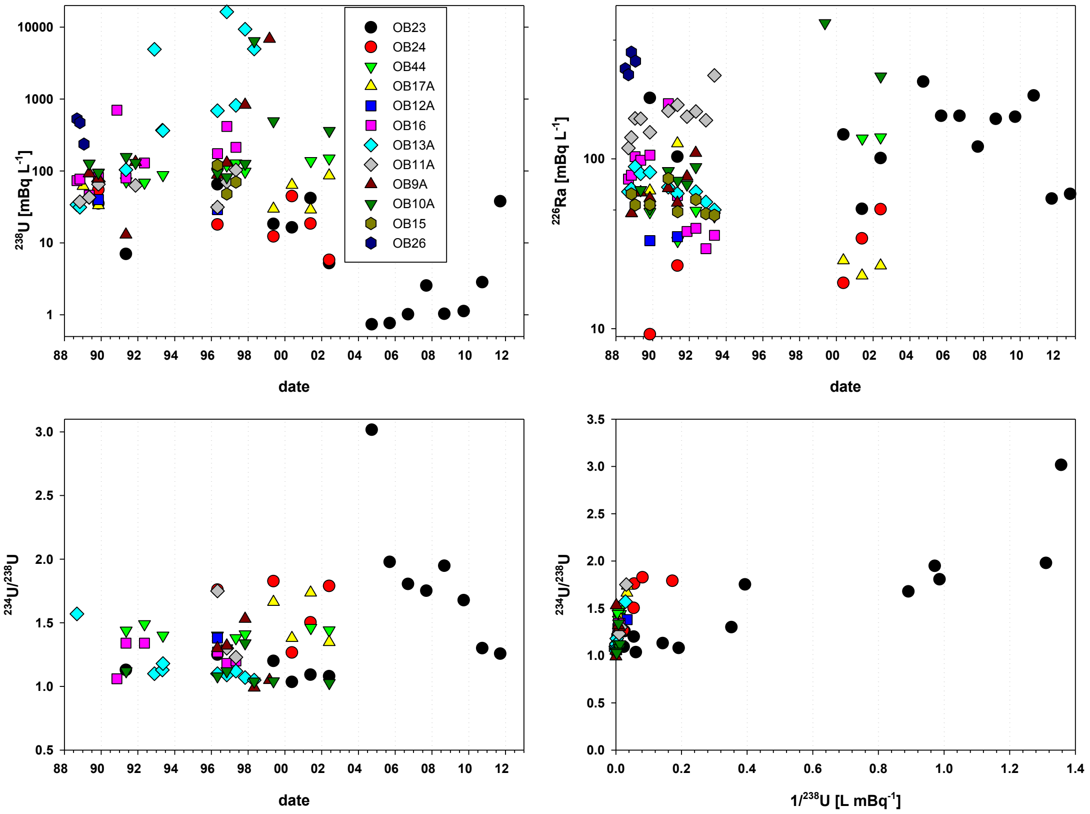

Figure 20 ^{238}U and ^{226}Ra activity concentrations plotted against sampling date, and the ^{234}U/^{238}U activity ratio plotted against sampling date and inverse ^{238}U activity concentration, respectively, in bores OB23, OB24, OB44, OB17A, OB12A, OB16, OB13A, OB11A, OB9A, OB10A, OB15 and OB26. Linear fits to the inverse concentration data are shown in Figure 20a and 20b.

Activity concentrations of ^{238}U in the 1990s were highest in bores OB9A, OB10A and OB13A. Bores OB9A and OB10A were located between the TSF and pit 1. Martin & Akber (1999) hypothesised that changes in the hydrological conditions, as the TSF was raised and pit 1 deepened, influenced the sulfate concentrations in these two bores, and that the two bores were affected by uranium seeping from the TSF. The ^{234}U/^{238}U activity ratio in bore OB10A is low at 1.12, but is somewhat higher in OB9A (up to 1.53). Figure 20a however shows that there is no correlation between ^{234}U/^{238}U activity ratios and the inverse uranium concentration in these two bores (OB9A: $p = 0.54$; OB10A: $p = 0.32$). Consequently, more than 1 contaminating end-member may have been responsible for elevated uranium concentrations measured in these two bores but seepage from the TSF, in particular in bore OB9A, cannot be excluded. Investigations showed that both, OB9A and OB10A, were influenced by earthworks between 1997 and 1999, leading to high ^{238}U activity concentrations measured in 1998 (Iles et al 2002). Monitoring was discontinued, bores OB9A and OB10A are now buried under the stockpile.

Activity concentration of ^{238}U in bore OB13A has increased substantially between the late 1980s and late 1990s, in agreement with ERA monitoring data. Iles et al (2002) report an increase of ^{238}U activity concentrations of 3 orders of magnitude between the early 1980s and late 1990s. This bore was likely influenced by uranium seeping from the TSF or leaching of uranium from construction materials used in the raising of the TSF wall (Martin & Akber 1996). The high sulfate concentrations measured in 1992 are indicative of seepage. Figure 21a (and Figure A-18 in the Appendix) shows that a significant correlation exists between ^{234}U/^{238}U activity ratios and the inverse uranium concentration in this bore ($p << 0.005$), with a contaminating end-member ^{234}U/^{238}U activity ratio of (1.08 ± 0.02).

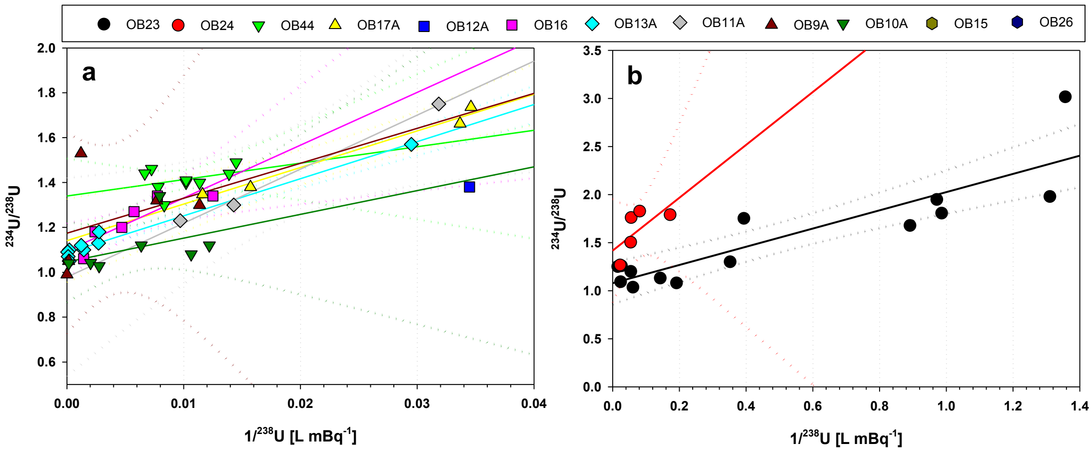

Figure 21 a,b Inverse concentration plots for bores OB44, OB17A, OB16, OB13A, OB11A, OB9A, OB10A, OB15, OB26, OB23 and OB24. Linear fits to the ^{234}U/^{238}U activity ratio in the inverse concentration plots and associated 95% confidence intervals are shown as well.

Samples from bores OB24, OB44 and OB17A have been analysed for radionuclides up until 2002. OB24 and OB44 are approximately 500 m north of the TSF and separated by less than 400 m. Uranium-238 activity concentration has increased by a factor of two in OB44 between 1989 and 2002. During the same time period the U concentration has decreased in OB24. The inverse concentration plots show that neither OB24 ($p = 0.23$) nor OB44 ($p = 0.32$) exhibit a significant correlation between the ^{234}U/^{238}U activity ratios and the inverse uranium concentration, indicating that there are multiple sources of uranium responsible for the variability observed in these two bores. Activity ratios of ^{234}U/^{238}U measured in OB24 and OB44 are generally >1.3 (see Figure 21a) which makes seepage from the TSF as a source of uranium measured in these bores unlikely. In contrast OB17A shows a significant correlation between the ^{234}U/^{238}U activity ratios and the inverse uranium concentration ($p = 0.01$) and the contaminating end member ^{234}U/^{238}U activity ratio is (1.14±0.19).

The only still active bore in this area investigated by ***eriss*** with existing time series up until September 2012 is deep bore OB23. Analysis of samples from this bore via alpha spectrometry has started in 1989. The bore shows variable ^{238}U activity concentrations between 1989 and 2012, with generally low activity concentrations between 2002 and 2010, an increase in 2011 followed by a decrease in 2012 (see Figures 19 and 20). The variability in uranium concentration is accompanied by a variability of the ^{234}U/^{238}U activity ratio. The inverse U concentration plot shows a statistically significant decrease of the ^{234}U/^{238}U activity ratio ($p<<0.05$) with an end member ratio of (1.08±0.10) (see Figure 21b).

Radium-226 activity concentrations were highest in OB26 in the late 1980s and the early 1990s. Activity concentration of ^{226}Ra in OB11A increased by a factor of approximately 3 between 1988 and 1993, associated with a large increase in sulfate concentrations. This increase has previously been associated with influence of seepage from the TSF leading to desorption reactions in the aquifer and an increase in ^{226}Ra (Martin & Akber 1996, 1999).

Although bore OB44 was drilled in July 1988 as a substitute for OB26 (Martin & Akber 1996), ^{226}Ra (and ^{238}U) activity concentrations in OB44 were significantly lower than in OB26. However, the ^{226}Ra activity concentration in OB44 has increased by 2002 and was above 100 mBq L^{-1}. Sulfate and Mg concentrations are high in OB44, indicating that ^{226}Ra may have been mobilised by secondary processes and consequently this bore may also be affected by seepage from the TSF. The activity concentration of ^{226}Ra is lower in OB24 than in OB26, but has also increased between 1990 and 2002. During the same time period ^{226}Ra activity concentration has decreased in OB17A.

Bore OB23 shows ^{226}Ra activity concentrations between 58 and 285 mBq L^{-1}. The variability of ^{226}Ra activity concentration is similar to the variability in Mn and Fe, whereas U concentration behaves in the opposite way. It is possible that reduction and dissolution processes for Mn and Fe influence the ^{226}Ra activity concentration measured in the bore, due to the high affinity of ^{226}Ra with oxides of those two elements.

3.3 Bores to the north-west of the TSF and in the Gulungul catchment

3.3.1 Major constituents

Figure 22 shows the results of measurements of major constituents (cations Ca, Na, Mg and K; anion: SO_4) in bore waters collected north-west and west of the TSF and in the Gulungul catchment.

Major cation concentrations for deep bores OB1A, OB2A, RN9329 and OB116 are less than 5 mg L^{-1} for K, less than 10 mg L^{-1} for Ca and 10 to 20 mg L^{-1} for Na and Mg. Bore RN23566 shows higher Mg concentrations up to 100 mg L^{-1}. Major cation concentrations are much lower in the shallow bores OB112 and OB116 compared to their deep counterparts and other bores in the area.

Sulfate concentrations are highest in bore RN23566, up to 470 mg L^{-1}. This bore is close to bore RN9329, but the screen depth of this bore is only 4 to 5.5 m. The sulfate concentrations measured in bore RN23566 are similar to those measured in surface water in the Gulungul catchment in 2004-05 (Mellor, 2005). At those shallow depths it is possible that groundwater quality is affected by the high sulfate concentrations in acid sulfate soils commonly observed in the area (Klessa 2002).

3.3.2 Metals

Figure 23 shows the result of metal measurements via ICPMS in bore waters collected in the Gulungul catchment, north-west and west of the TSF.

Metal concentrations for bore OB1A at the north-west corner of the TSF are highest with concentrations of Fe of about 10 to 20 mg L^{-1}, Mn about 1 mg L^{-1} and Ba between 0.1 and 0.2 mg L^{-1}. The variability of U concentrations in this bore is large, with concentrations between 0.03 and 1.08 μg L^{-1}, but concentrations are generally low from 2003 onwards.

Fe and Mn concentrations in OB2A are significantly lower but the U concentration is similar to the concentration measured in bore water from OB1A. RN9329 to the west of the TSF shows Fe and Mn concentrations about half the concentrations measured in OB1A, and U concentrations are similar to those measured in OB1A.

The high Fe and Mn results for bore OB1A has been highlighted before by Martin & Akber (1996). They emphasised the possibility that iron and/or manganese oxide colloids are present in the waters from OB1A that may influence trace metal and radionuclide concentrations. The large variability of Ba and Sr, and in particular U in this bore may be a result of these iron and/or manganese oxide colloids.

The highest U concentrations are measured in bore OB116 deep. This bore is located to the south-west of the TSF, and samples groundwater from a depth of 14 m to 20 m. Concentrations of uranium and major cations in deep bore OB112 are quite similar to concentrations measured in OB116 deep.

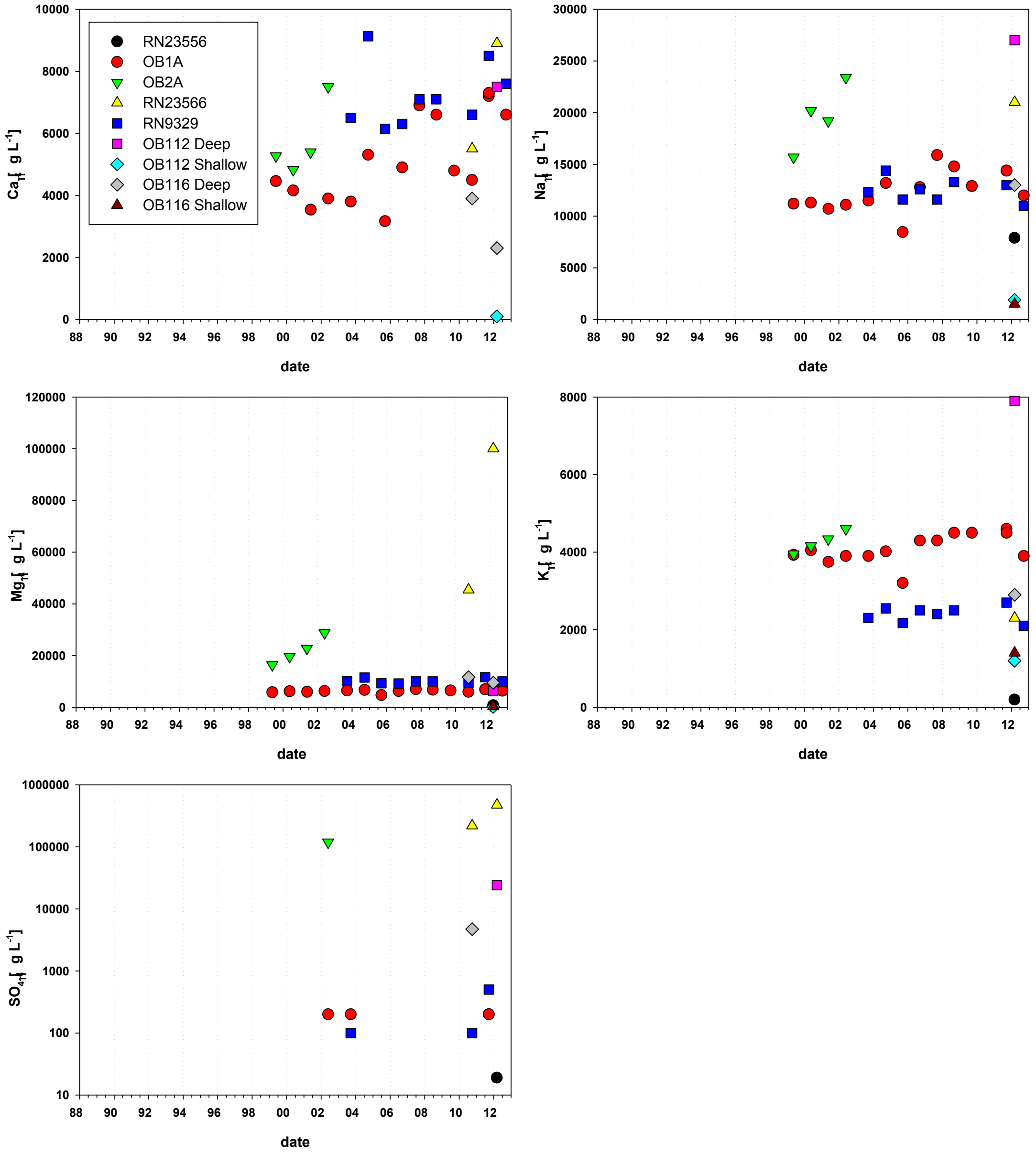

Figure 22 Major constituent concentrations plotted against sampling date in bores RN23556, OB1A, OB2A, RN23566, RN9329, OB112 deep and shallow, and OB116 deep and shallow.

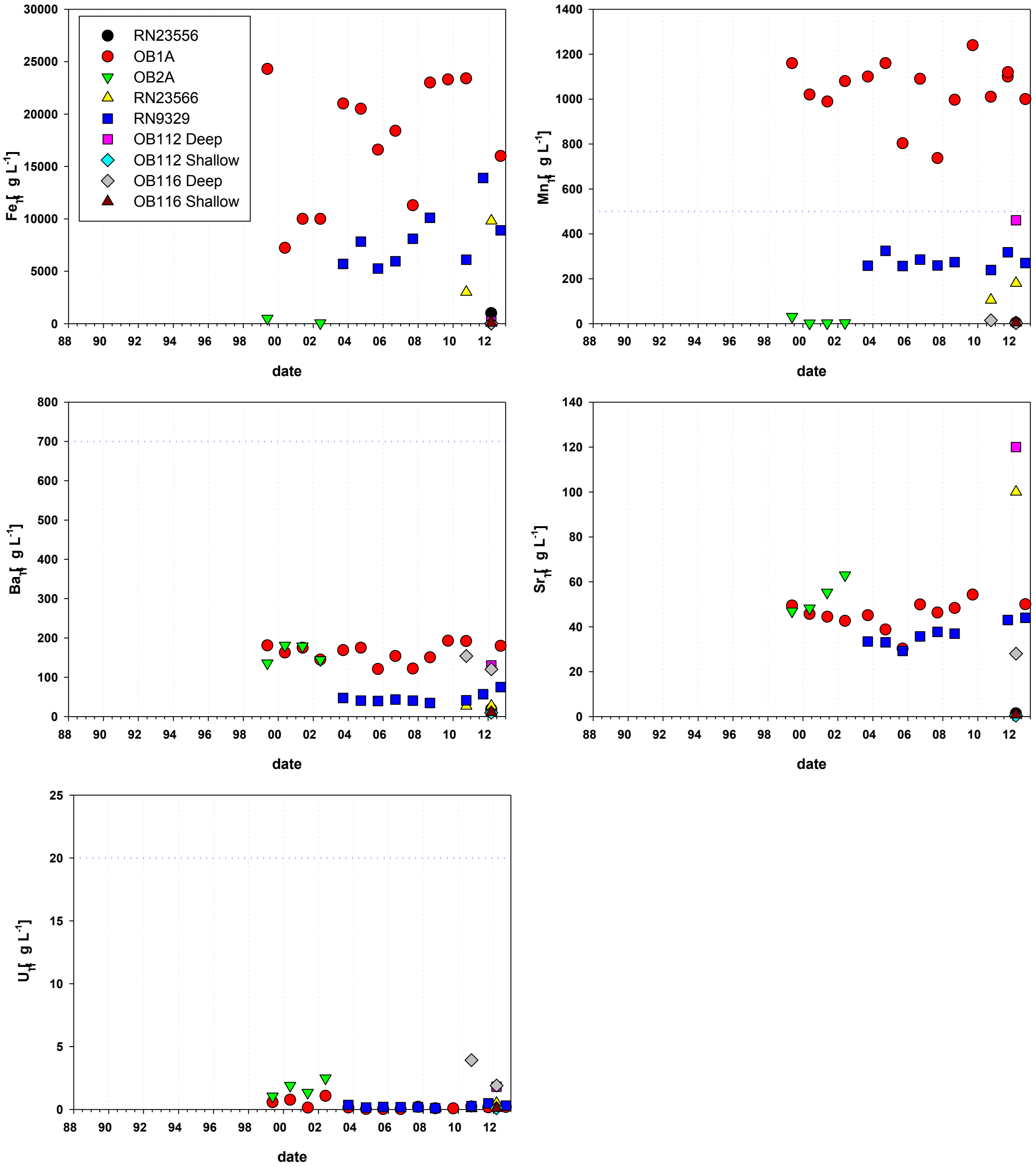

Figure 23 Metal concentrations plotted against sampling date in bores OB1A, OB2A, RN9329, RN23556, RN23566, and OB112 and OB116, deep and shallow. The blue dotted lines indicate the Australian drinking water quality guidelines (NHMRC 2011).

3.2.3 Radionuclides

Figure 24 shows the results of radionuclide activity concentration measurements, and the ^{234}U/^{238}U activity ratios measured in bores OB1A, OB2A, RN9329, RN23566, OB116, from 1989 onwards. Uranium activity concentrations are generally in agreement with U concentrations measured via ICPMS.

There is no statistically significant trend of the ^{234}U/^{238}U activity ratio with time. There is also no statistically significant trend of the ^{234}U/^{238}U activity ratio with the inverse of the U concentrations in bores OB1A ($p = 0.15$), OB2A ($p = 0.85$) or RN9329 ($p = 0.37$), although both, ^{238}U activity concentration and ^{234}U/^{238}U activity ratio are very variable in OB1A. RN9329 exhibits generally higher ^{234}U/^{238}U activity ratios than bores OB1A and OB2A.

Activity concentrations of ^{226}Ra are highest and most variable in bore OB1A. This bore is closest to the TSF wall, and shows a maximum of 179 mBq L^{-1} ^{226}Ra measured in 2001. Bore RN9329 had a maximum ^{226}Ra activity concentration of about 30 mBq L^{-1} measured in 2011. None of the bores investigated shows an increase of the ^{226}Ra activity concentration over time.

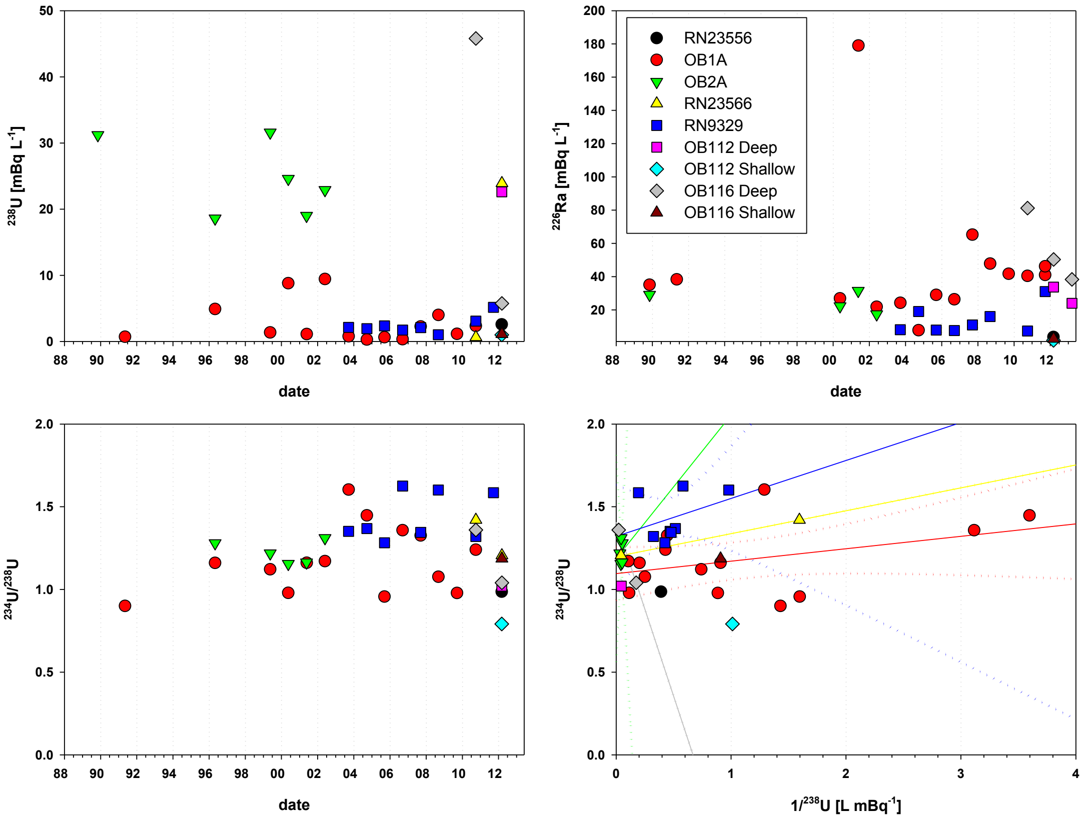

Figure 24 ^{238}U and ^{226}Ra activity concentrations plotted against sampling date, and the ^{234}U/^{238}U activity ratio plotted against sampling date and inverse ^{238}U activity concentration in bores OB1A, OB2A, RN9329, RN23566, and OB116 deep. Linear fits to the ^{234}U/^{238}U activity ratio in the inverse concentration plots and associated 95% confidence intervals are shown as well.

3.4 Bores close to the south and south-west wall of the TSF

The five deep monitoring bores that are part of this group have been buried under the TSF wall lift, and monitoring data are only available up to 2002.

3.4.1 Major constituents

Figure 25 shows the results of measurements of major constituents (cations Ca, Na, Mg and K; anion: SO_4) in bores close to the south and south-west wall of the TSF.

Bore OB4A was dominated by Ca and Mg, with concentrations of about 200 mg L^{-1} (Ca) and 250-400 mg L^{-1} (Mg), respectively. This area along the TSF wall where OB4A was located has previously been identified as an area exhibiting high sulfate concentrations of up to 37 g L^{-1} (ERA 2012). It appears that bore OB4A on the south-western wall of the TSF was clearly affected by seepage from the TSF.

Major cation concentrations in bore OB6A of about 100 mg L^{-1} (Ca) and about 150 mg L^{-1} (Mg) are high as well and Na concentration is higher than in OB4A. Klessa (2001) has shown that both, OB4A and OB6A have shown increasing Mn, Mg and SO_4

concentrations between 1980 and 2000. This increase, and the high concentrations measured in OB4A and OB6A are indicative of a breakthrough of $MgSO_4$ and other conservative elements from the TSF.

In contrast, bores OB19A and OB7A show much lower Ca and Mg concentrations and appear less affected by seepage, in agreement with bore water sulfate concentration results shown in ERA (2012). However, Klessa (2001) suggested that there is evidence to suggest that some sulfate enrichment of groundwater at bores OB7A and OB19A was starting to take place from 2000 onwards.

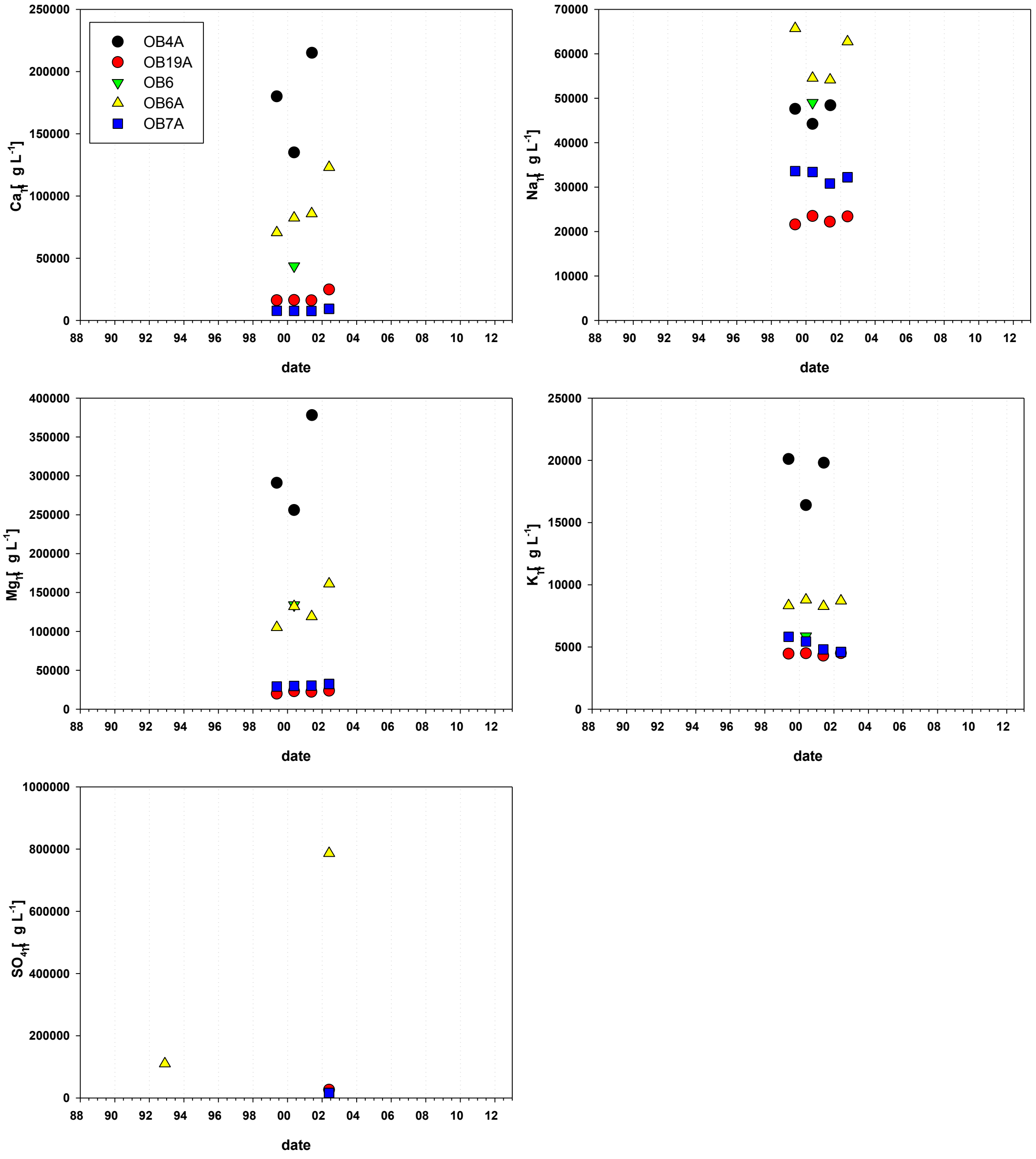

Figure 25 Major constituent concentrations plotted against sampling date in bores OB4A, OB19A, OB6, OB6A and OB7A.

3.4.2 Metals

Metal concentrations are shown in Figure 26. Iron and Mn are highest in OB4A, whereas U concentrations are highest in bore OB6A on the TSF south wall. While OB6A is affected by seepage from the TSF (Klessa 2001), OB7A exhibits much smaller Mg and sulfate concentrations, and generally lower U concentrations (with the exception of the U concentration measured in 2000). This is indicative of lesser influence of seepage from the TSF in bore OB7A.

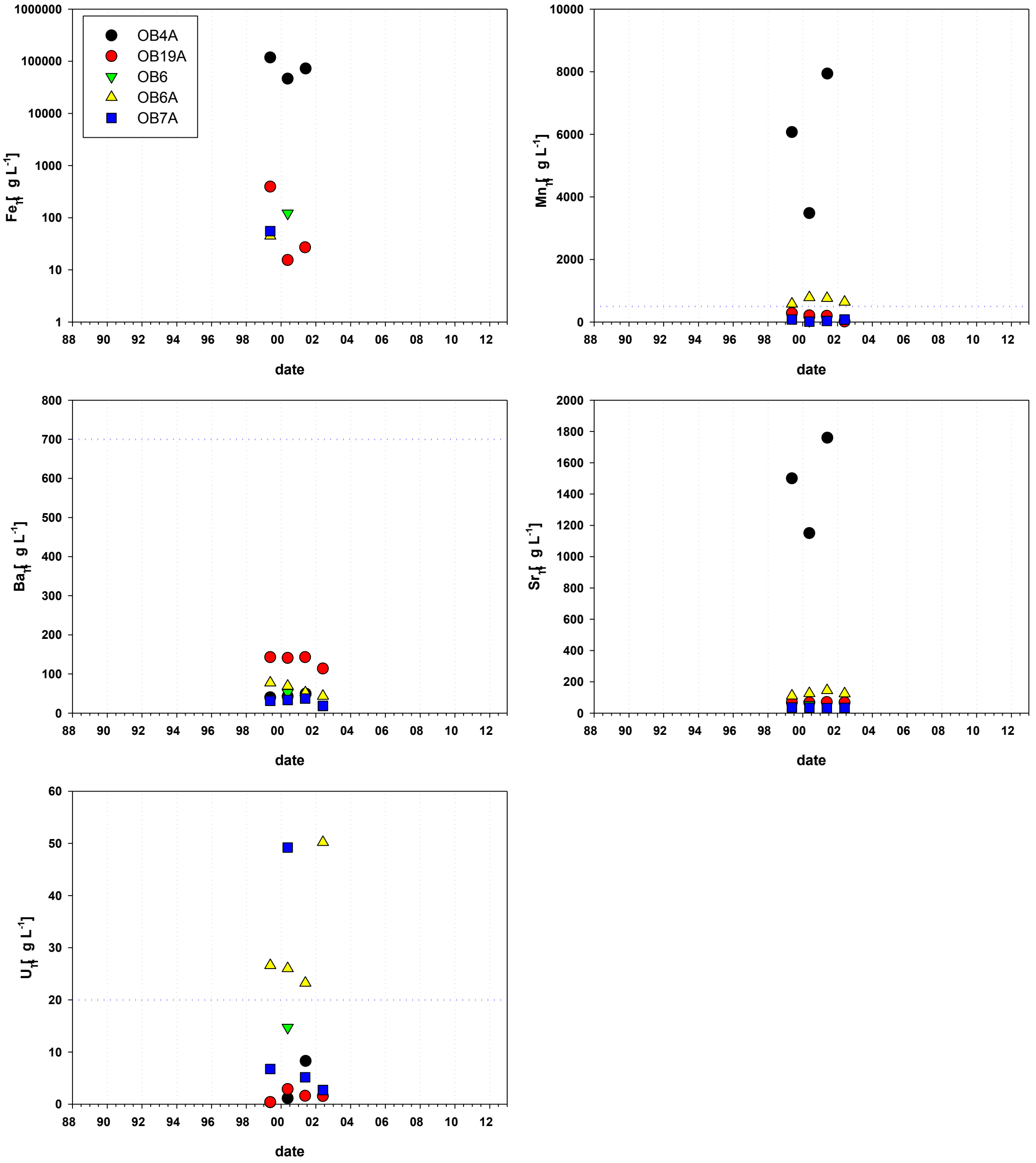

Figure 26 Metal concentrations plotted against sampling date in bores OB4A, OB19, OB6, OB6A and OB7A. The blue dotted lines indicate the Australian drinking water quality guidelines (NHMRC 2011).

3.4.3 Radionuclides

Radionuclide activity concentrations and ^{234}U/^{238}U activity ratios are available from 1988, when investigations of bore water from bores OB4A and OB6A began (Figure 27).

Bores OB4A, OB6A and OB7A showed maximum U activity concentrations in 1998 followed by a sharp drop in U activity concentrations in 1999. The increase in the U activity concentrations are associated with a decline in the ^{234}U/^{238}U activity ratios in those bores, with ratios of about 1.07 to 1.26. The reason for the increase in U activity concentration during that time is unknown, but may be due to major works conducted at the TSF, when tailings were transferred from the TSF to pit 1 in 1997 – 98.

The $^{234}U/^{238}U$ activity ratios in OB4A were generally around 1, with the exception of activity ratios measured in 1988 and 1997 (~1.5). There is no discernible trend in $^{234}U/^{238}U$ activity ratios plotted against time of sampling or inverse U concentration in these bores, except for bore OB7A. This bore exhibits a statistically significant decrease of the $^{234}U/^{238}U$ activity ratio when plotted against the inverse U activity concentration ($p = 0.01$), with a y-intercept for the $^{234}U/^{238}U$ activity ratio of 1.13±0.12.

The activity concentration of ^{226}Ra was highest in bore OB6A with a value of above 1 Bq L^{-1} measured in May 2001. A ^{226}Ra maximum was also observed in OB4A during that time (0.2 Bq L^{-1}) but none of the other analytes showed a maximum.

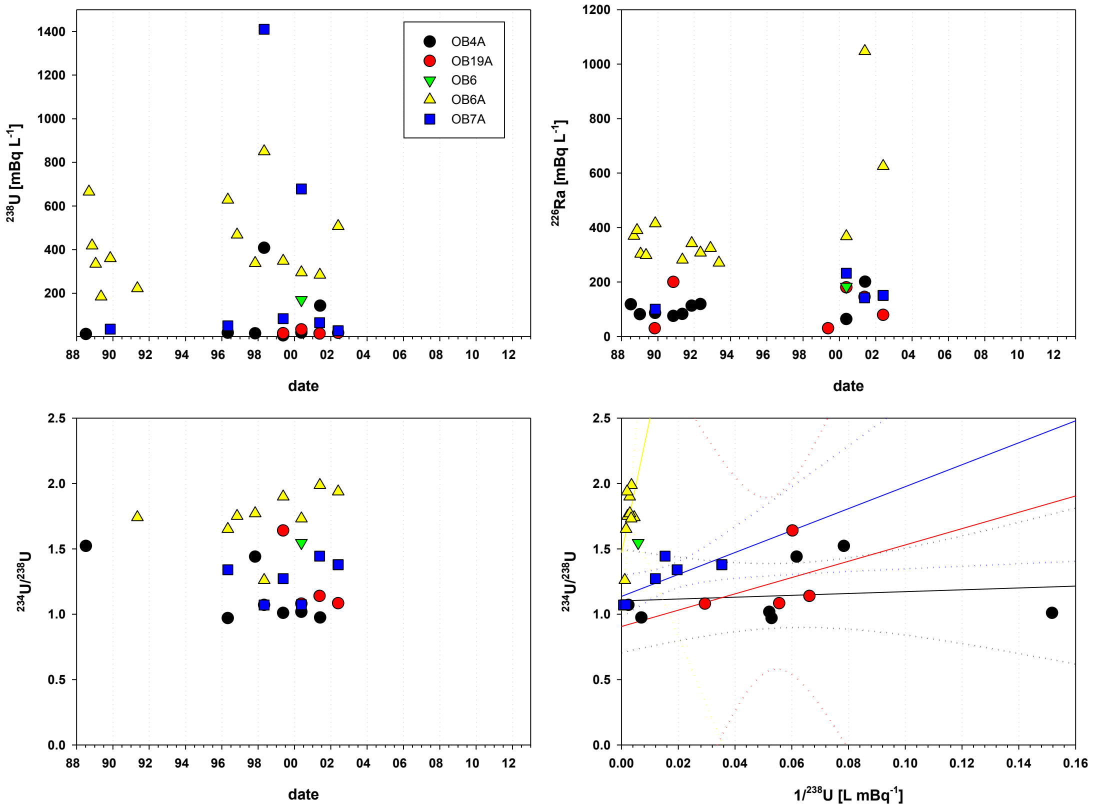

Figure 27 ^{238}U and ^{226}Ra activity concentrations plotted against sampling date, and the $^{234}U/^{238}U$ activity ratio plotted against sampling date and inverse ^{238}U activity concentration in bores OB4A, OB19, OB6, OB6A and OB7A. Linear fits to the $^{234}U/^{238}U$ activity ratio in the inverse concentration plots and associated 95% confidence intervals are shown as well.

3.5 Bores south of the TSF

Bores OB20, OB21A, RN23568 and C1_shallow are located approximately 400 m to the south of the TSF wall.

3.5.1 Major constituents

Figure 28 shows the results of measurements of major constituents (cations Ca, Na, Mg and K; anion: SO_4) in bore waters sampled from bores located south of the TSF.

Concentrations of Ca are typically about 10 mg L^{-1} in OB20 and 20 mg L^{-1} in OB21A. Sodium and Mg concentrations are between 10-20 mg L^{-1} in these two bores. The concentrations of K are about 1 mg L^{-1} (OB20) and 2 mg L^{-1} (OB21A). The two bores exhibit similar trends with time, with maxima measured in 2004, followed by a decline in concentrations and a minimum measured in 2007-2008. Sulfate concentrations are generally low in OB20 and OB21A with concentrations measured below 3 mg L^{-1}.

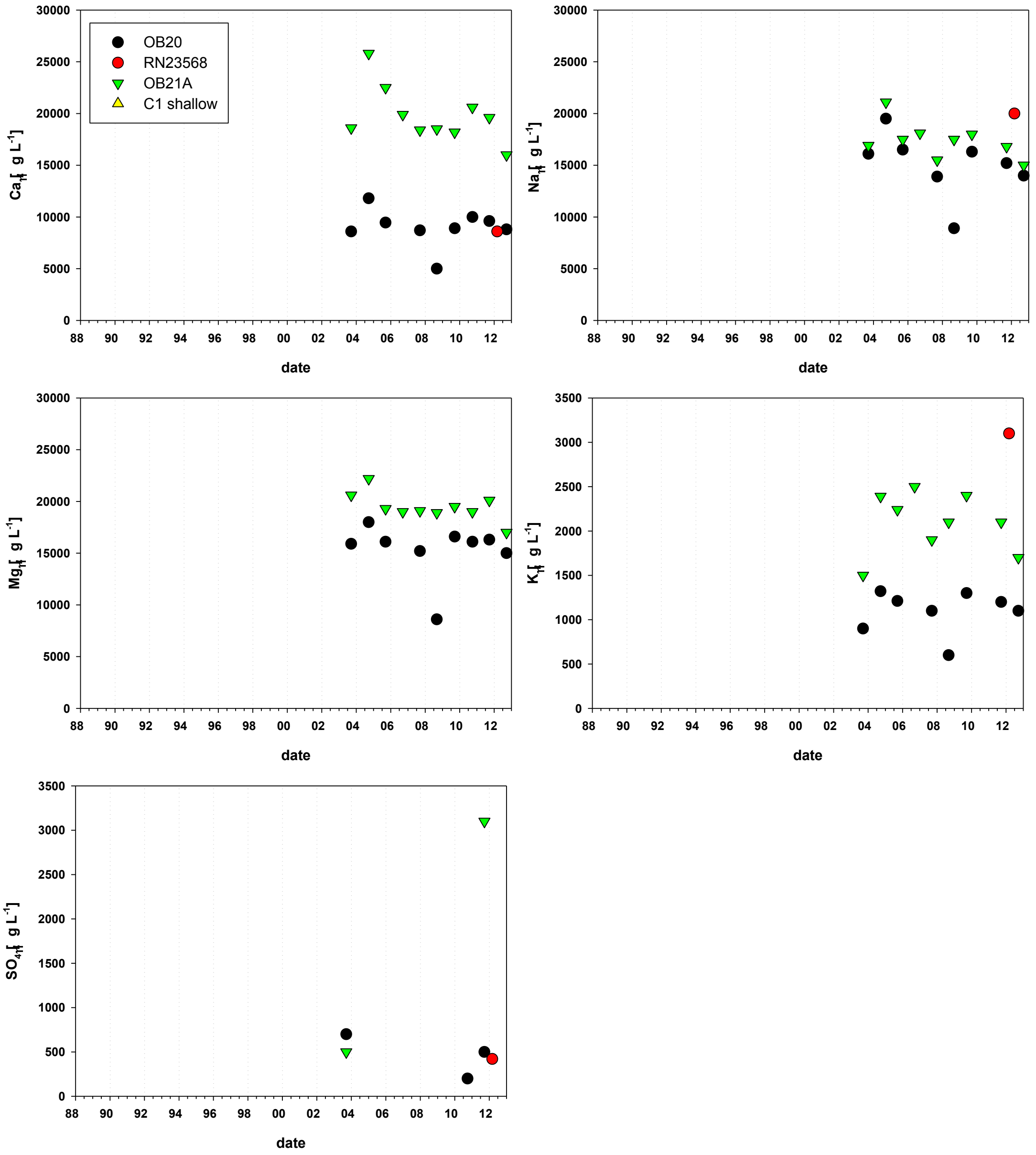

Figure 28 Major constituent concentrations plotted against sampling date in bores OB20, OB21A, RN23568 and C1_shallow.

3.5.2 Metals

Metal concentrations for bores OB20, OB21A, RN23568 and C1_shallow are shown in Figure 29. Concentrations of Fe in bores OB20 and OB21A exhibit similar trends, with OB21A following the trend observed in OB20. Klessa (2001) has reported an increasing Mn concentration in OB21A between 1983 and 2000, when the concentration increased from less than 150 µg L^{-1} to more than 400 µg L^{-1}. Our data show that Mn concentrations in OB21A have declined again since 2003 to levels around 300 µg L^{-1}. The concentrations of Mn are generally lower in OB20 but appear to be slightly increasing since 2008 when Fe concentration was lowest.

U concentrations are low and show the same trend in the two bores, with OB21A following the trend observed in OB20. Maximum U concentrations of 0.6 µg L^{-1} (OB20) and 1.3 µg L^{-1} (OB21A) were measured in samples collected in September 2012.

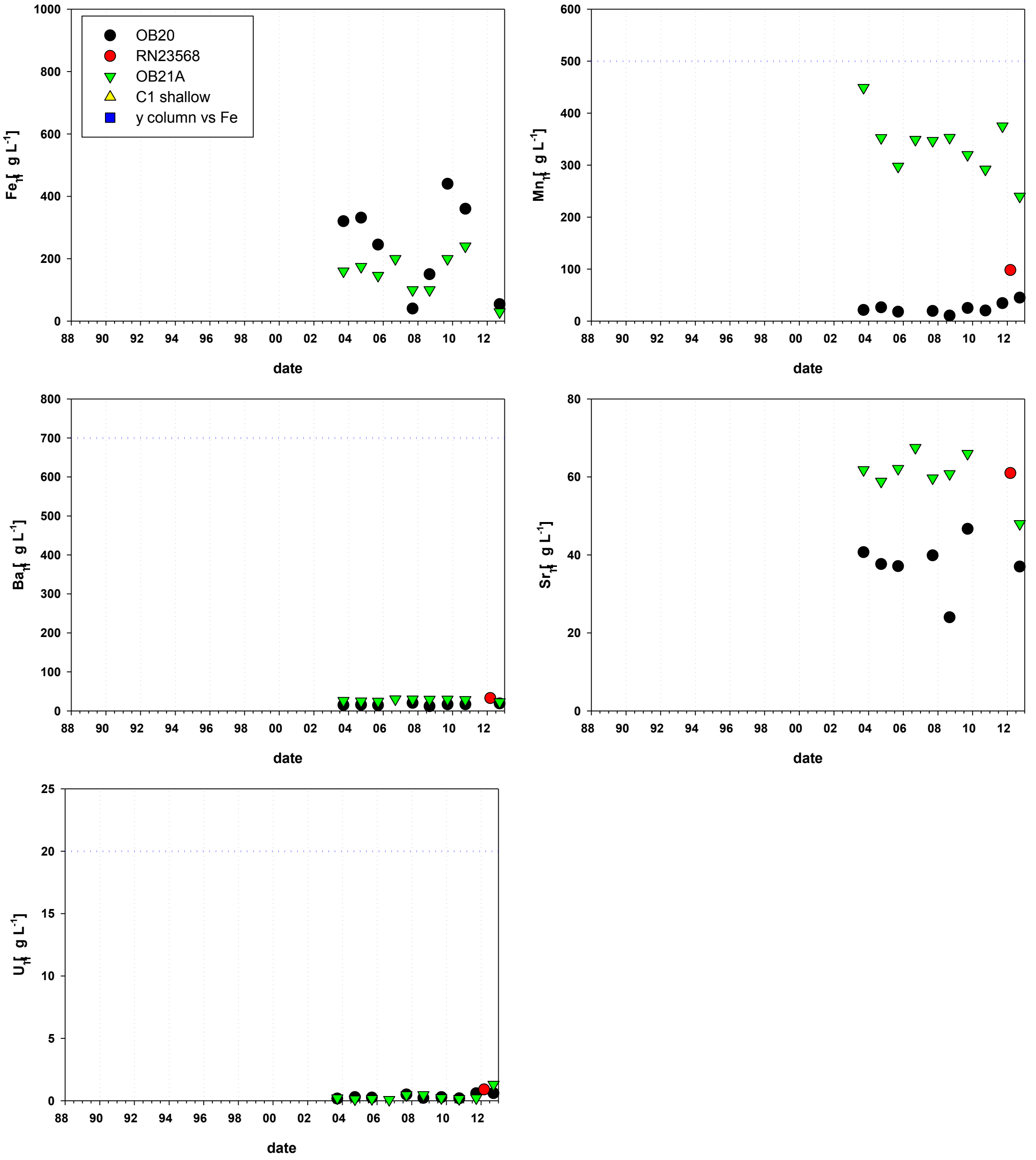

Figure 29 Metal concentrations plotted against sampling date in bores OB20, OB21A, RN23568 and C1_shallow. The blue dotted lines indicate the Australian drinking water quality guidelines (NHMRC 2011).

3.5.3 Radionuclides

Figure 30 shows the results of the ^{238}U activity ^{226}Ra concentrations measured in bores OB20, OB21A and C1_shallow, and the $^{234}U/^{238}U$ activity ratio plotted against date of sampling and the inverse ^{238}U activity concentration, respectively.

U activity concentrations in OB20 and OB21A are similar, and activity ratios generally >1 in the two bores. The inverse concentration plots do not show a significant correlation between the measured $^{234}U/^{238}U$ activity ratios and the inverse of the ^{238}U activity concentration measured in the bores.

The activity concentrations of ^{226}Ra are quite variable and are highest in bore OB21A, with activity concentrations of almost 400 mBq L^{-1} measured in 2004. Minimum activity concentrations measured in this bore are just below 100 mBq L^{-1}. Activity concentrations of ^{226}Ra in bore OB20 are between 8 and 40 mBq L^{-1}.

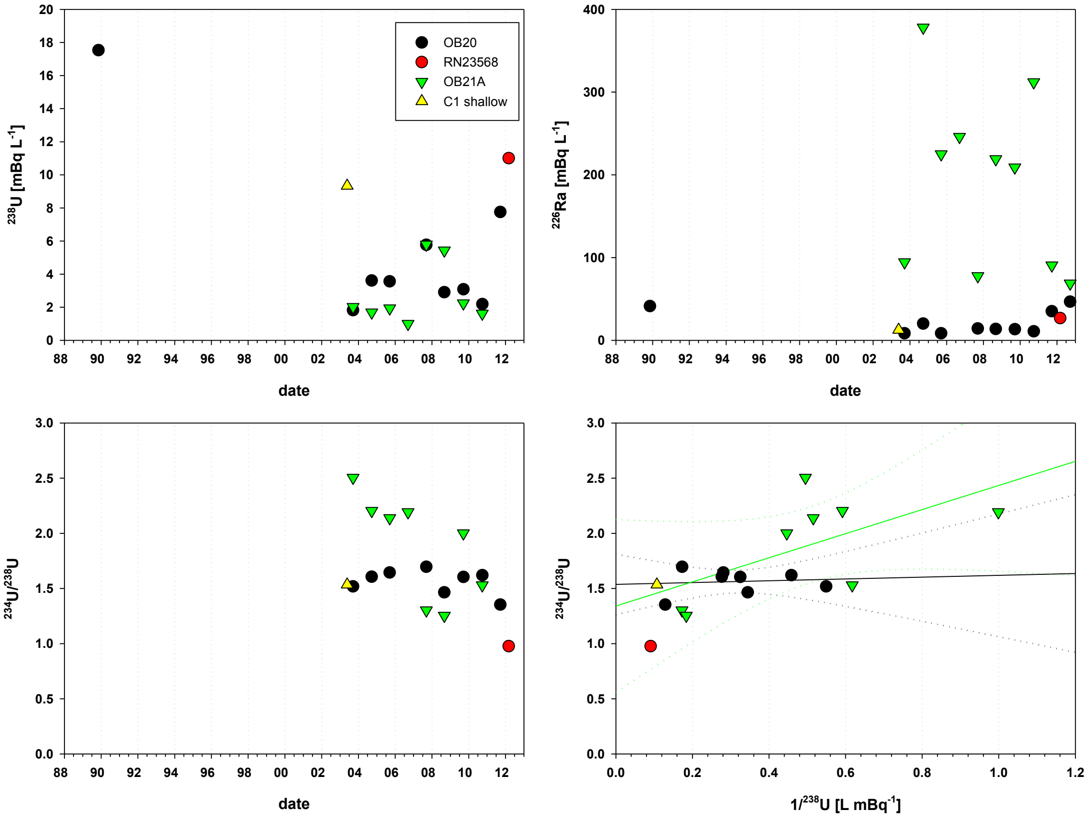

Figure 30 ^{238}U and ^{226}Ra activity concentrations plotted against sampling date, and the ^{234}U/^{238}U activity ratio plotted against sampling date and inverse ^{238}U activity concentration in bores OB20, OB21A, RN23568 and C1_shallow. Linear fits to the ^{234}U/^{238}U activity ratio in the inverse concentration plots and associated 95% confidence intervals are shown as well.

3.6 Bores in the vicinity of Pit 1 and in the Corridor and Georgetown Creek catchments

3.6.1 Major constituents

Figure 31 shows the results of measurements of major constituents (cations: Ca, Na, Mg and K; anion: SO_4) in bore waters from bores situated in the vicinity of pit 1, and within the Corridor and Georgetown Creek catchments.

Time series starting in 1999 exist for two bores, OB30, south-east of pit 1 and next to the Corridor Creek wetland filter, and OB27, close to the Corridor Creek–Georgetown Creek confluence at Georgetown Billabong.

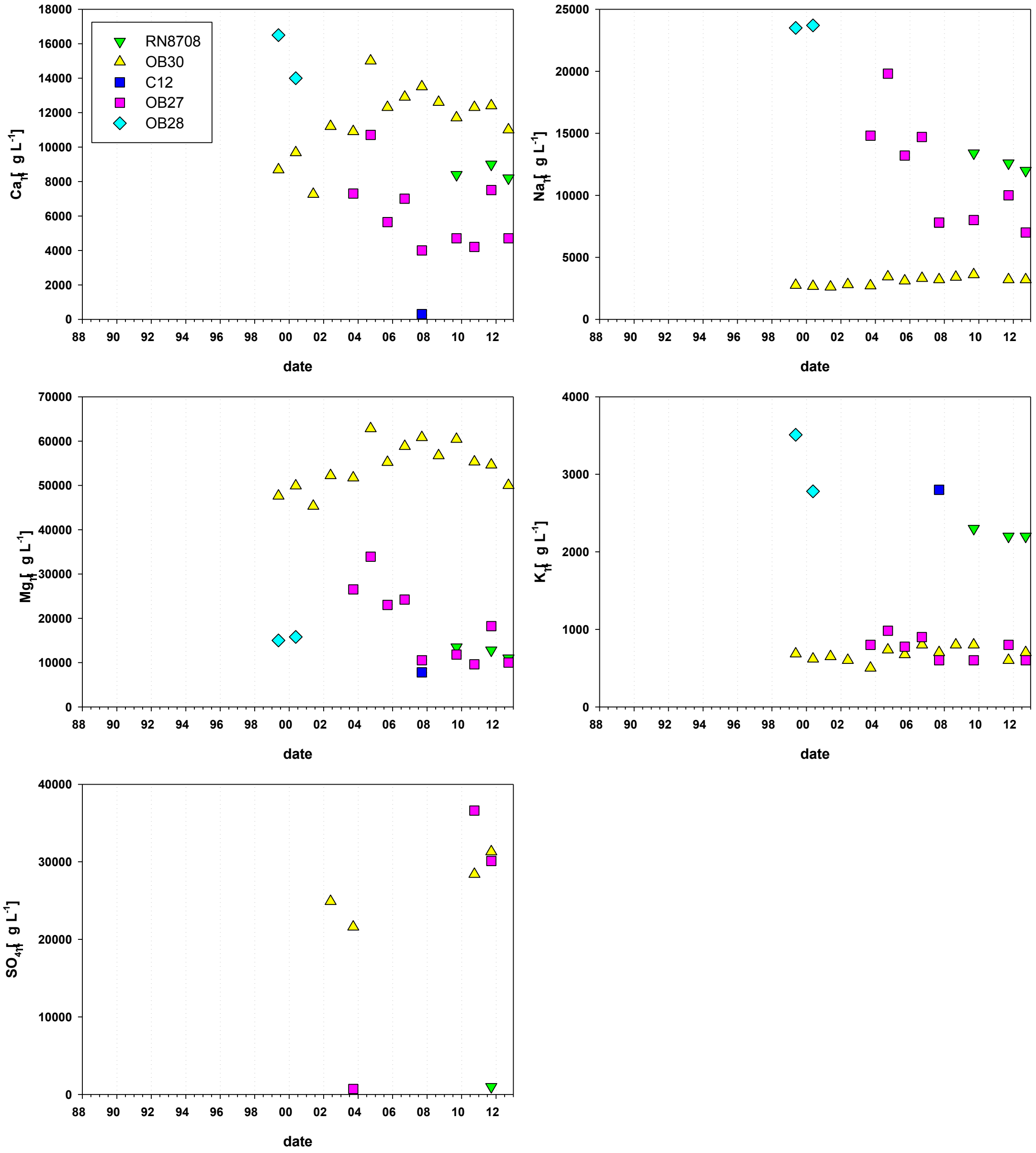

Figure 31 Major constituent concentrations plotted against sampling date in bores OB30, OB28, OB27, RN8708 and C12.

Deep bore OB30 is dominated by Mg and Ca, with concentrations above 10 mg L^{-1} of Ca and above 50 mg L^{-1} for Mg. Concentrations of Na are generally below 5 mg L^{-1} in OB30 and K is below 1 mg L^{-1}. Deep bore OB27 shows about 3-4 times lower Ca and Mg concentrations but Na is typically higher (up to 20 mg L^{-1}) than in OB30. Calcium, Na and Mg appear to have decreased over the past decade in OB27.

Sulfate concentration in bore OB27 has increased from 0.7 mg L^{-1} in 2003 to above 30 mg L^{-1} in 2010-11, concentrations which are similar to the sulfate concentrations in bore OB30. None of the major cations exhibited a similar increase during that period.

Magnesium and Ca have increased in bore OB30 between 1999 and 2004. Tailings deposition in pit 1 has started in 1996. The increase of the concentrations of these two conservative elements could potentially be due to the deposition of tailings into the mined out pit.

Bore OB28 in the vicinity of OB27 shows major cation concentrations similar to OB27, although K concentrations are higher.

Bore RN8708 is a deep bore located in the head waters of Corridor Creek. Concentrations of Mg in this bore are similar to OB27, but sulfate concentrations are much lower. Calcium and Na concentrations are 8-9 mg L^{-1} (Ca) and 12-13 mg L^{-1} (Na), respectively. Potassium is higher than in OB27 at about 2 mg L^{-1}.

3.6.2 Metals

Concentrations of Fe, Mn, Ba and Sr are generally higher in OB27 than in OB30 (Figure 32). Iron, Mn, Ba and Sr concentrations have shown a decrease since 2004 in OB27 similar to the decrease in major cations, whereas OB30 shows an increase in Mn concentration but steady Ba and Sr concentrations.

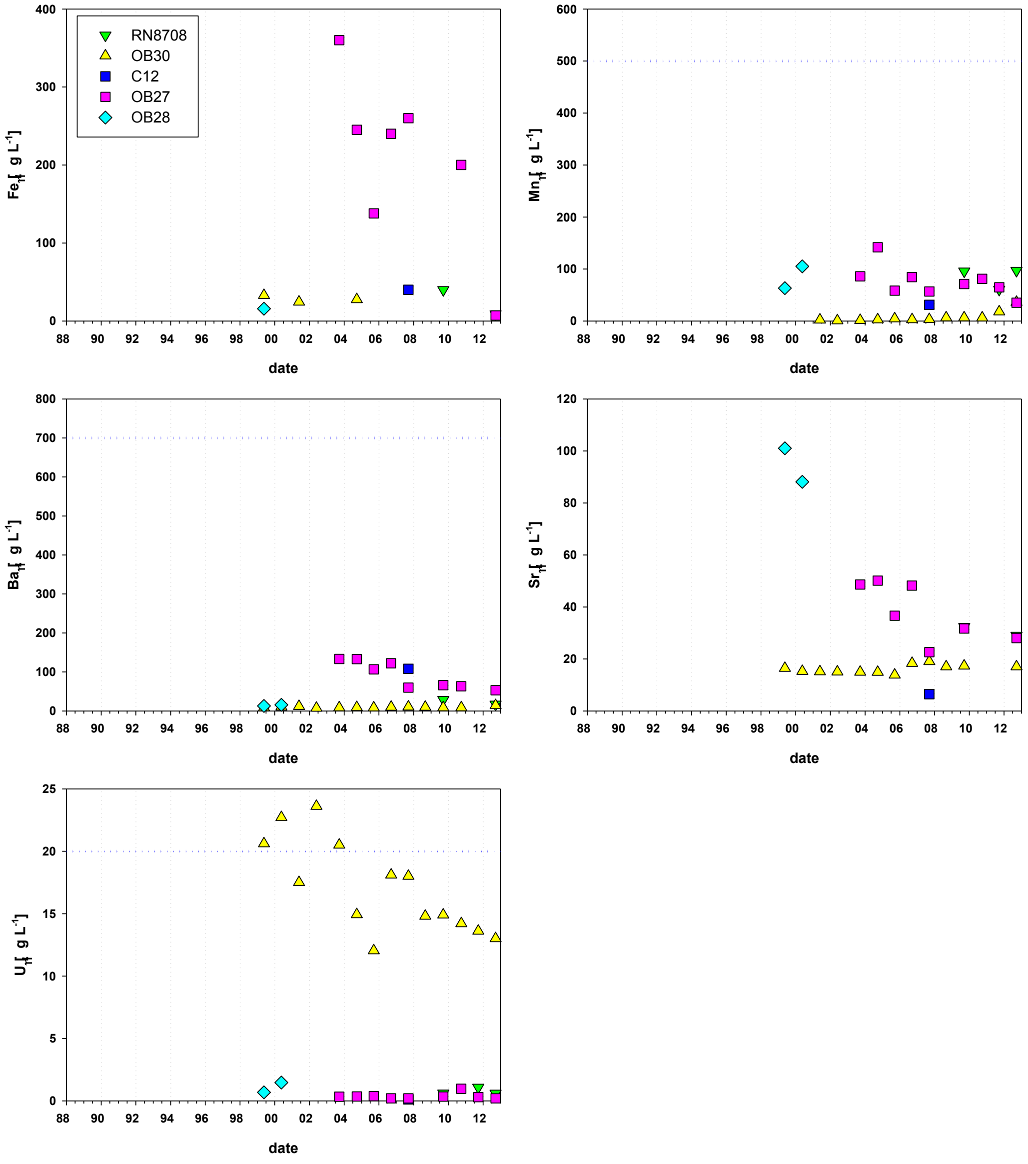

Figure 32 Metal concentrations plotted against sampling date in bores OB30, OB28, OB27, RN8708 and C12. The blue dotted lines indicate the Australian drinking water quality guidelines (NHMRC 2011).

The concentration of U has decreased slightly in OB30 over the past decade from about 20-25 µg L^{-1} to values less than 15 µg L^{-1} in 2012. Uranium concentration in OB27 is much lower compared to OB30, with a maximum of 1 µg L^{-1} measured in 2010, similar to U concentrations measured in bore RN8708.

3.6.3 Radionuclides

Figure 33 shows the ^{238}U activity ^{226}Ra concentrations and the ^{234}U/^{238}U activity ratio measured in bore waters from this catchment.

Uranium activity concentration is highest in pit dewatering bore MBL. An activity concentration of almost 2 Bq L^{-1} was measured in this bore in 2003 indicative of seepage from tailings stored in the pit (data not shown in Figure 29). The next highest ^{238}U activity concentration was measured in bore OB30 but ^{238}U activity concentration has decreased from 1999 onwards. OB30 exhibits little variability in ^{234}U/^{238}U activity ratios, which is close to 1 (1.08 on average) and there is no statistically significant correlation between ^{234}U/^{238}U activity ratios and the inverse of the ^{238}U activity concentration in either OB30 or OB27.

Activity concentrations of ^{238}U in bore OB27 are below 10 mBq L^{-1}. ^{226}Ra activity concentrations in this bore are higher than in OB30, highlighting the different geochemical characteristics of the uranium and radium radioisotopes in groundwater.

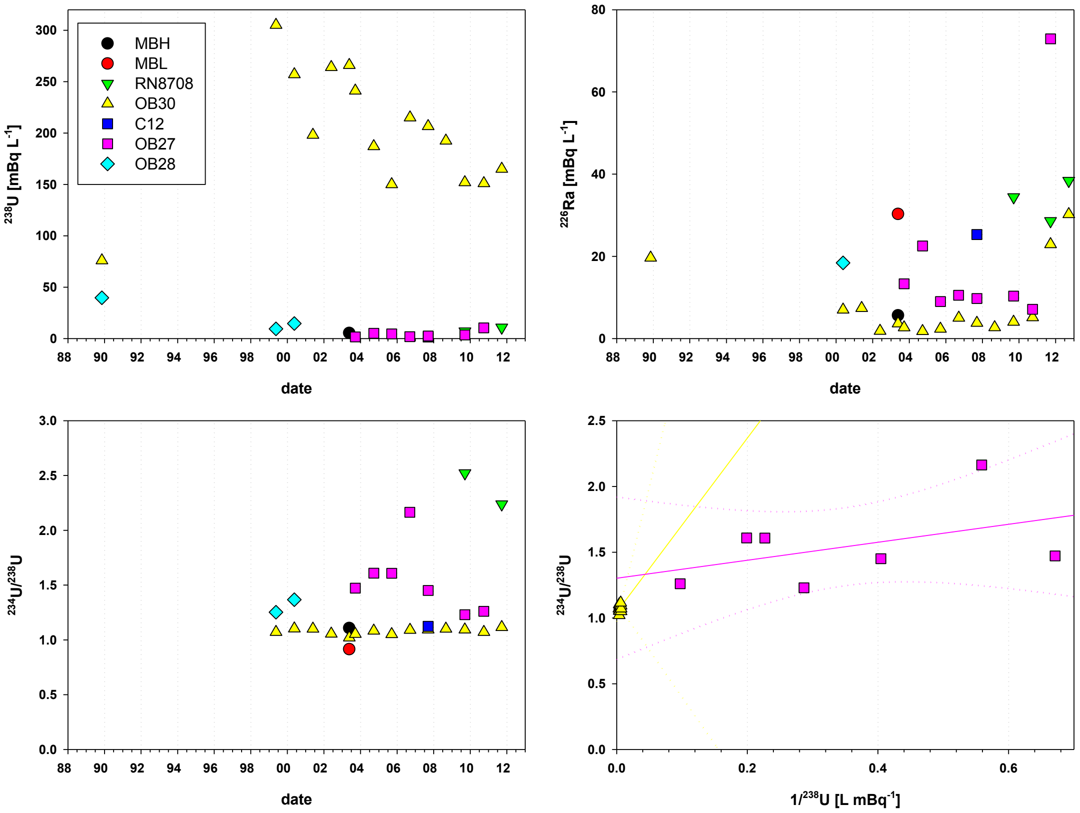

Figure 33 ^{238}U and ^{226}Ra activity concentrations plotted against sampling date, and the ^{234}U/^{238}U activity ratio plotted against sampling date and inverse ^{238}U activity concentration in bores MBH, MBL OB30, OB28, OB27, RN8708 and C12. Linear fits to the ^{234}U/^{238}U activity ratio in the inverse concentration plots and associated 95% confidence intervals are shown as well.

3.7 Bores in the RP2 and Pit 3 area

Three bores were investigated over the years from this area. Only bore OB29 has metal and major ion data available. Some radionuclide data exist for R.P. 79/1 and R.P 79/2, which were investigated by ***eriss*** in the late 80s to mid 90s. Whereas bore 79/2 in the RP2 area is still active, bore 79/1 is most likely buried. OB29 is no longer sampled.

3.7.1 Major constituents

Figure 34 shows the results of measurements of major constituents (cations Ca, Na, Mg and K; anion: SO_4) in water from bore OB29 situated to the north of RP2.

Bore OB29 is dominated by Mg, with concentrations of 90-100 mg·L^{-1}. The concentrations of Na and Mg are 6-10 mg·L^{-1}, K concentrations are generally below 5 mg·L^{-1}. Sulfate concentrations in 2002 were high at 47 mg·L^{-1}.

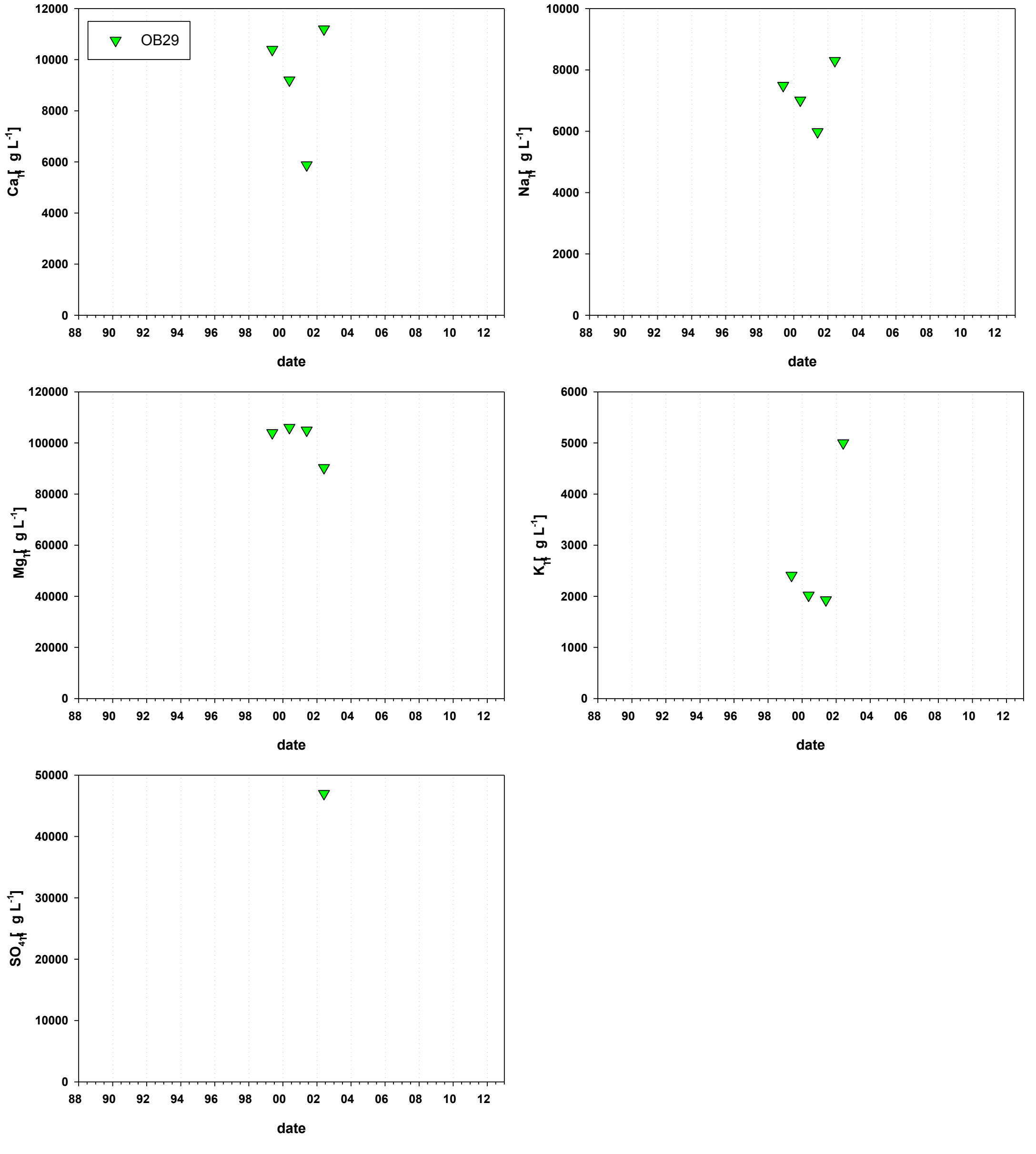

Figure 34 Major constituent concentrations plotted against sampling date in bore OB29.

3.7.2 Metals

Concentrations of Fe, Mn, Ba, Sr and U in bore OB29 are shown in Figure 35. There is a distinct increase of Fe, Mn and U concentrations in OB29 observed in 2002. ERA reported that the groundwater level in this bore has dropped significantly between 1999 and 2001. Reasons for this drop in the groundwater level were developments of pit 3 further to the south and east that took place during that period (ERA 2001). It is likely that the increase in Fe, Mn and U in this bore is associated with an increase in seepage of water from RP2 in this bore associated with observed flow of groundwater into pit 3. This is also indicated by the high sulfate concentrations measured in 2002.

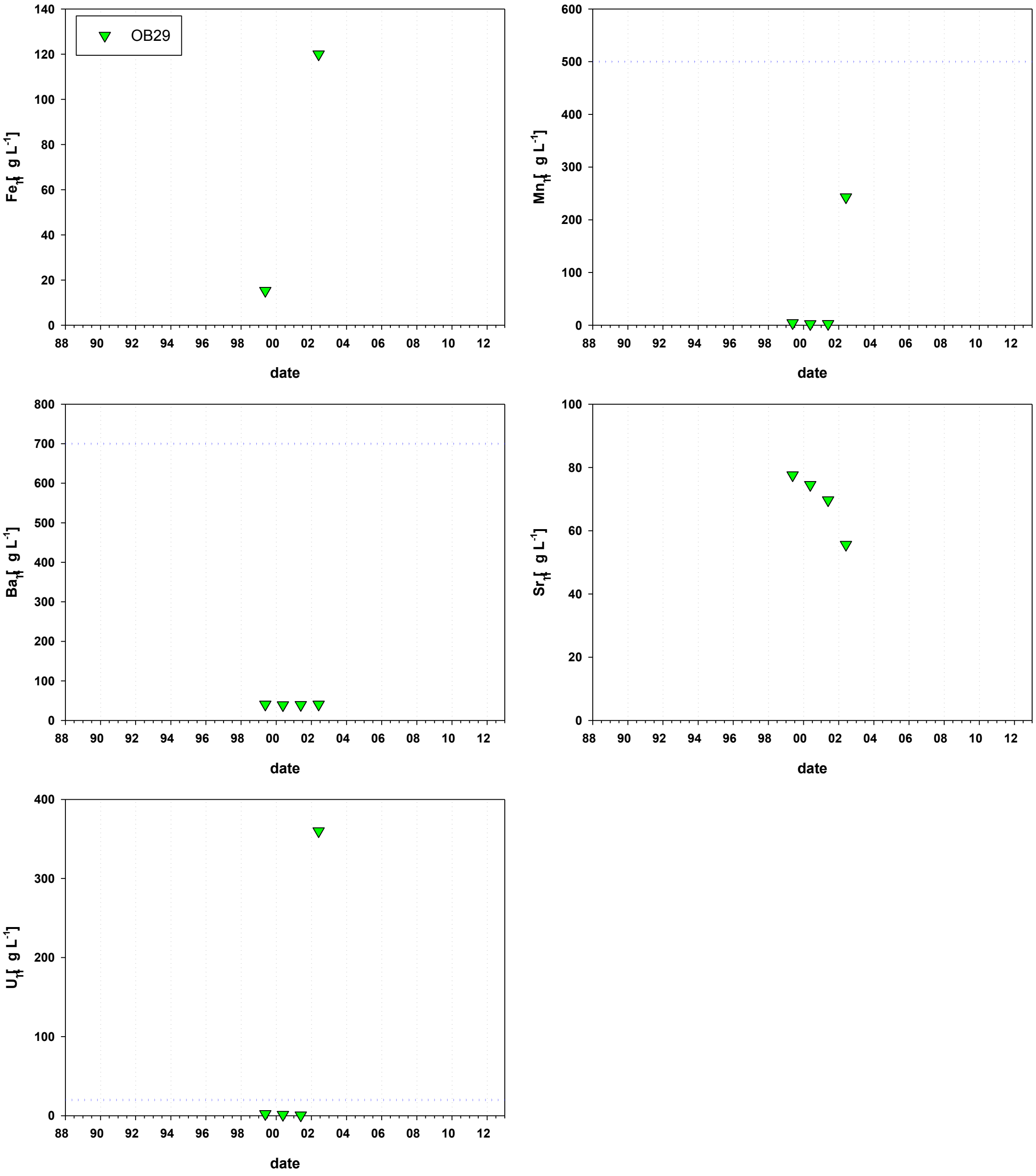

Figure 35 Metal concentrations plotted against sampling date in bores OB29. The blue dotted lines indicate the Australian drinking water quality guidelines (NHMRC 2011).

3.7.3 Radionuclides

Results of radionuclide analyses are shown in Figure 36. Activity concentrations of ^{238}U measured via alpha spectrometry agree well with measurements performed using ICPMS. The activity concentrations of ^{238}U in bores OB29 and RP 79/1 between 1989 and 2001 ranged from 30 to about 180 mBq·L^{-1}. In 2002, the ^{238}U activity concentration increased. This increase coincides with an increase in the activity concentration of ^{226}Ra. At the same time a decrease in the ^{234}U/^{238}U activity ratio to a value of 1.11 can be seen.

Although there is a linear correlation of the ^{234}U/^{238}U activity ratio with the inverse of the ^{238}U activity concentration in bore OB29, the decrease is not statistically significant (p = 0.11). Nonetheless it is likely that this bore has been affected by seepage of water from RP2, due to further developments of Pit 3 to the south and east during that time. Bore OB29 is no longer sampled.

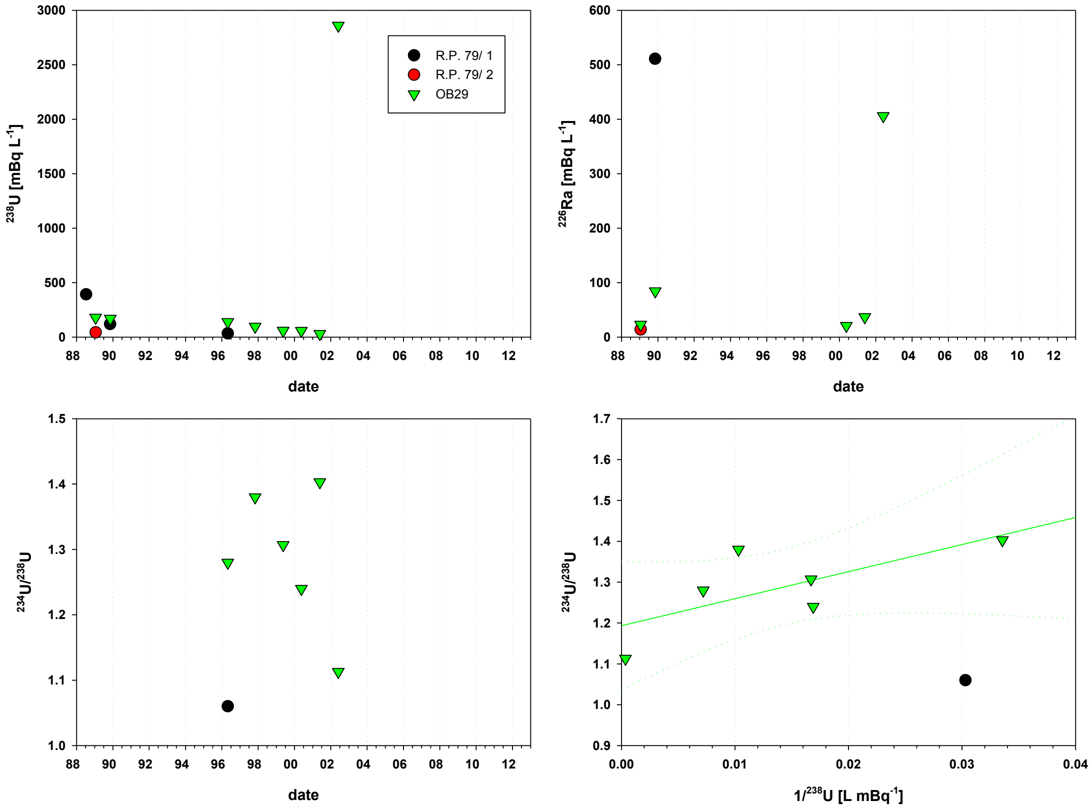

Figure 36 ^{238}U and ^{226}Ra activity concentrations plotted against sampling date, and the ^{234}U/^{238}U activity ratio plotted against sampling date and inverse ^{238}U activity concentration in bores OB29, R.P.79/1 and R.P.79/2. A linear fit to the ^{234}U/^{238}U activity ratio in the inverse concentration plot for OB29 and the associated 95% confidence interval is shown as well.

3.8 Bores in the Djalkmarra Billabong and Magela Creek area

3.8.1 Major constituents

Figure 37 shows the results of measurements of major constituents (cations: Ca, Na, Mg and K; anion: SO$_4$) in bore water collected from bores situated in the Djalkmarra Billabong and Magela Creek area.

Only bore 83_1 has a time series that extends over the past 10 years. Results from other bores are sporadic, bores RN23562 and RN22211 (which is no longer active) have data available from the last 5 years, starting in 2008.

Bore 83_1 is a deep (0-90 m) statutory bore of ERA and is located at the edge of the Magela Land Application Area. It shows seasonal variability in major ion concentrations, with lower concentrations generally measured during and at the end of the wet season. The concentrations measured by ***eriss*** in samples collected at the end of the dry season are in good agreement with those reported by ERA (ERA 2012).

Bore 83_1 is dominated by Na, Ca and Mg, with concentrations around 4-10 mg·L^{-1}. The concentrations of K are around 1 mg·L^{-1}. Cation concentrations are generally lower in bores RN23562 and RN22211.

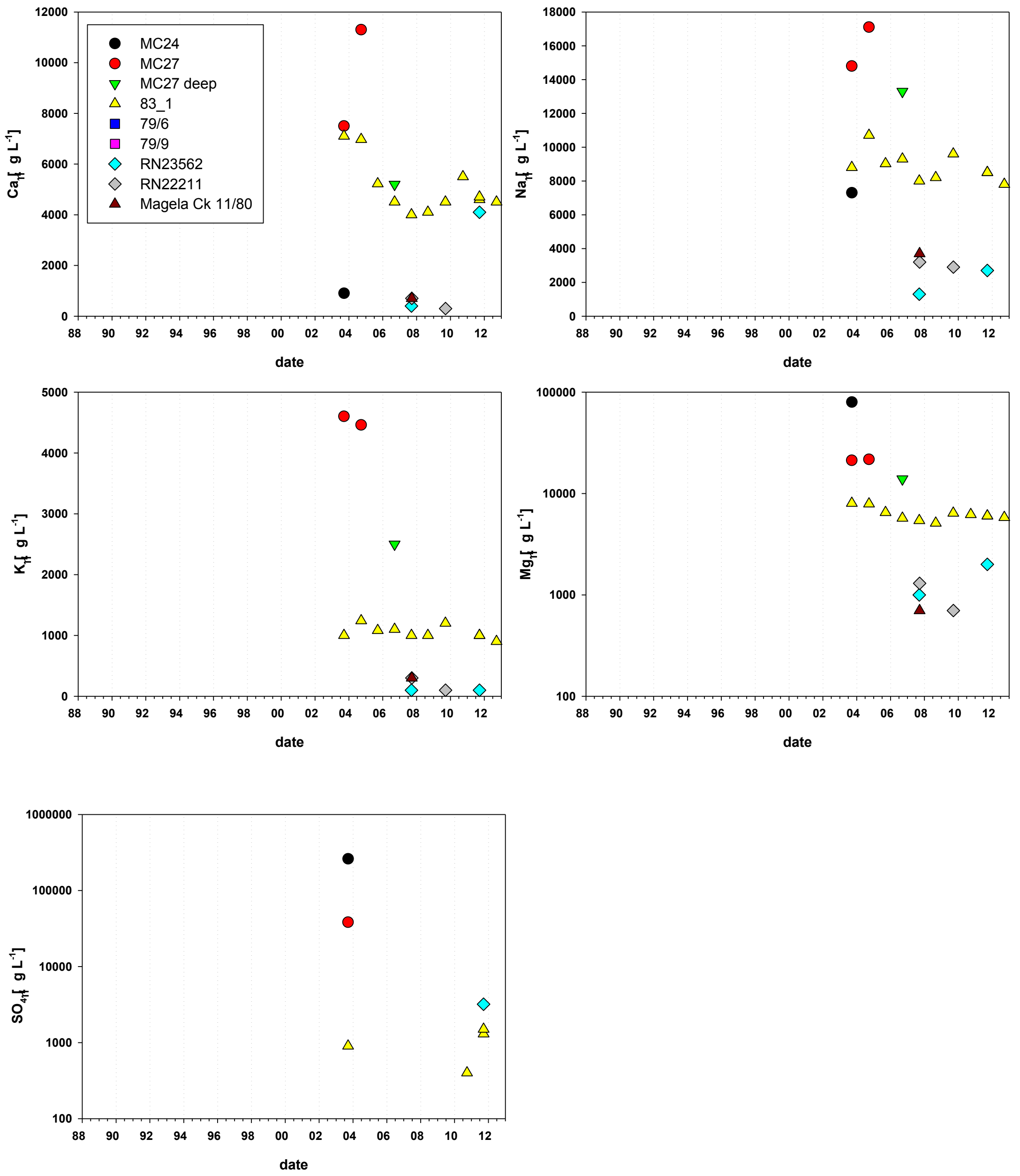

Figure 37 Major constituent concentrations plotted against sampling date in bores MC24, MC27, 83_1, RN23566, RN22211 and Magela Ck 11/80.

3.8.2 Metals

Results of metal analyses are shown in figure 38.The levels of Mn and U in bore 83_1 are in good agreement with those reported by ERA for this bore (ERA 2012). Uranium concentrations were highest in 2003 but seem to have decreased since. In 2010 U shows another maximum, in agreement with the levels published in ERA (2012) for this period.

Bore RN23562 shows concentrations of Mn and U comparable to concentrations in bore 83_1. In contrast, Mn concentration is higher in bore RN22211, whereas U concentration is much lower.

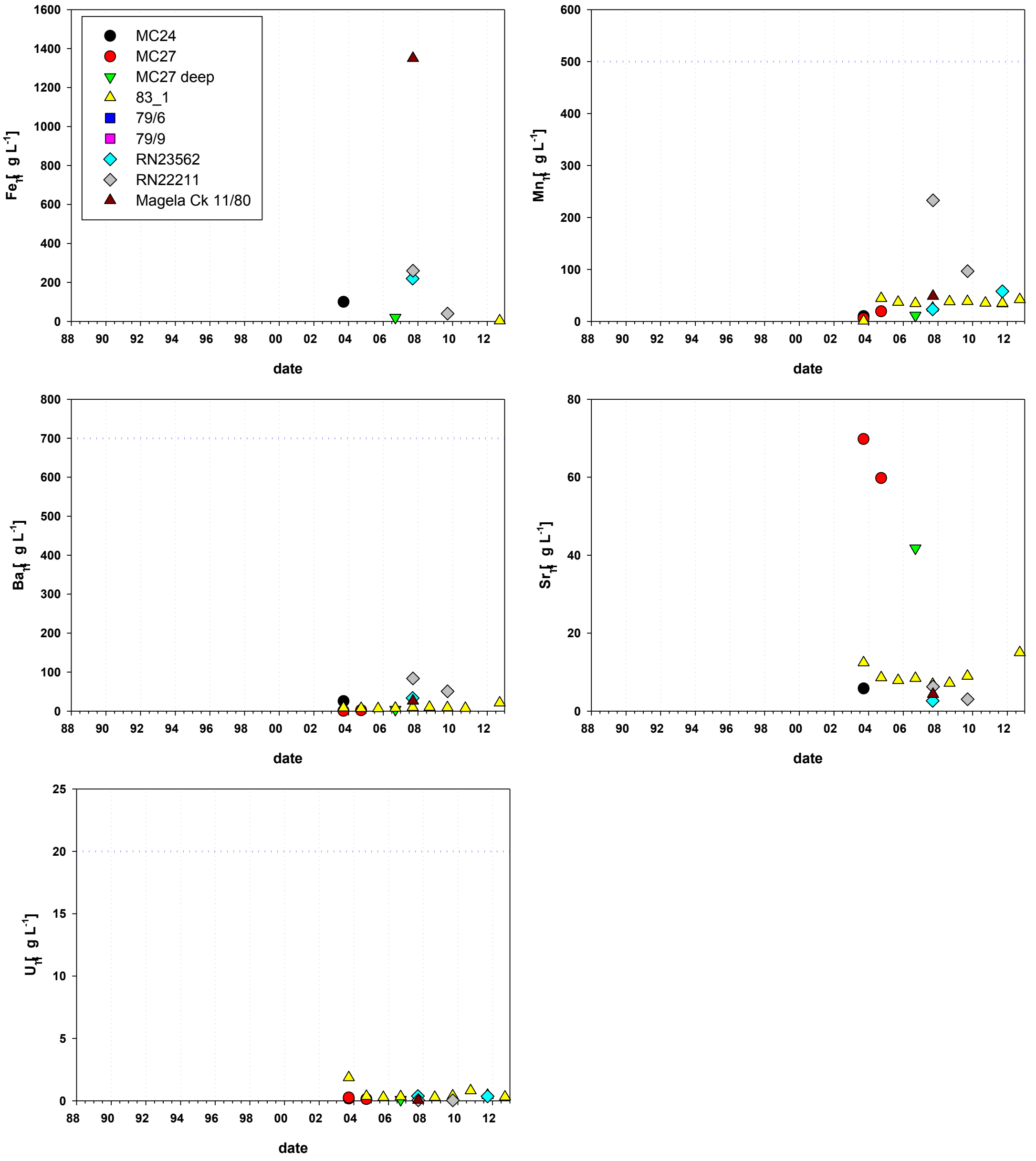

Figure 38 Metal concentrations plotted against sampling date in bores MC24, MC27, 83_1, RN23566, RN22211 and Magela Ck 11/80. The blue dotted lines indicate the Australian drinking water quality guidelines (NHMRC 2011).

3.8.3 Radionuclides

Activity concentrations of ^{238}U and ^{226}Ra and the ^{234}U/^{238}U activity ratios are shown in Figure 39. Generally, ^{238}U activity concentrations measured via alpha spectrometry agree well with measurements performed using ICPMS.

The activity concentration of ^{238}U in bore 83_1 is low, with a maximum of 23 mBq·L^{-1} measured in 2003, and values between 3-7 mBq·L^{-1} since 2004. It appears that higher ^{238}U activity concentrations are associated with lower ^{234}U/^{238}U activity ratios in bore 83_1. However, the regression of the inverse concentration plot is not statistically significant ($p = 0.13$).

^{226}Ra activity concentrations are between 2 and 12 mBq·L^{-1} in bore 83_1. ^{226}Ra activity concentrations were highest in bores 79/6 and 79/9 in the early 1990s when these bores were most likely influenced by seepage from RP2. Bore 79/6 is now buried on the walls of Pit 3 and bore 79/9 is destroyed.

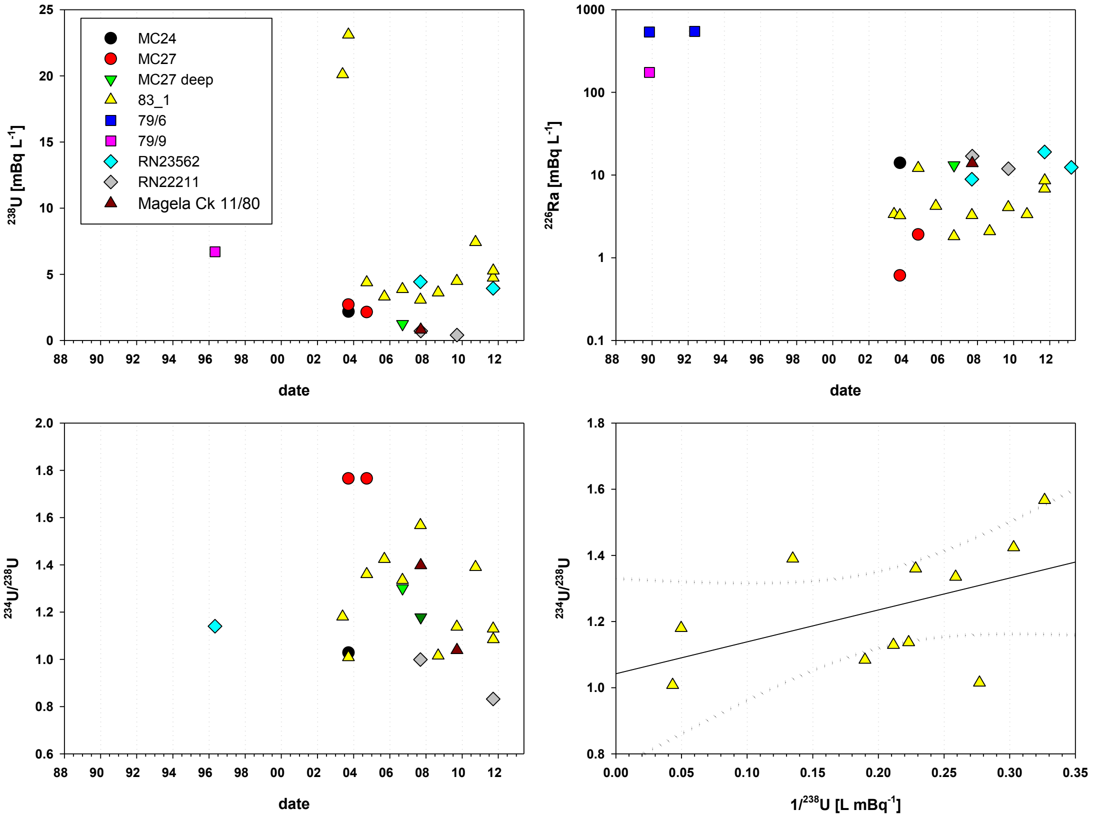

Figure 39 ^{238}U and ^{226}Ra activity concentrations plotted against sampling date, and the ^{234}U/^{238}U activity ratio plotted against sampling date and inverse ^{238}U activity concentration in bores MC24, MC27, 79/6, 79/9, 83_1, RN23566, RN22211 and Magela Ck 11/80. A linear fit to the ^{234}U/^{238}U activity ratio in the inverse concentration plot for 83_1 and associated 95% confidence interval is shown as well.

4 Discussion

In this section, concentrations and time series will be discussed of samples from groundwater monitoring bores that are still active and for which data is available up until 2010 and beyond.

Figure 40 shows an aerial photograph of the Ranger mine and those longer time series (> 7 years) Ranger monitoring bores (note: not all of the bores were sampled every year). The bores show a good spatial distribution around the site, with an obvious focus on monitoring bores around the TSF. Figure 41 shows the same map with soil classification overlaid.

Figure 40 Groundwater monitoring bores around Ranger uranium mine and analysed by ***eriss*** for radionuclides and metals with time series > 7 years up to 2012/13.

Id, MAP_UNIT, SOIL_DESC

🟪 0, G, Deep yellowish gradational sandy loams to clay loams with gravels at depth.
🟩 0, W, Djalkmara Billabong
🟧 0, H, Deep greyish to yellowish brown gradational clay loams to mottled medium-heavy c
🟦 0, A, Shallow yellow uniform sands with gravels throughout.
🟥 0, D, Moderately deep yellowish brown uniform sand and earthy sands over gravel pan.
🟨 0, W, Georgetown Billabong
🟩 0, F, Moderately deep yellow gradational sands to looms over gravel pan.
🟦 0, W, Coonjimba Billabong
🟪 0, B, Shallow red or brown uniform sands with gravels throughout.
🟪 0, C, Shallow greyish or yellowish brown uniform sands with very minor gravels.
🟥 0, E, Moderately deep greyish brown uniform sands over matted clay.
🟨 0, O, Very rare shallow sands mainly rock outcrops.

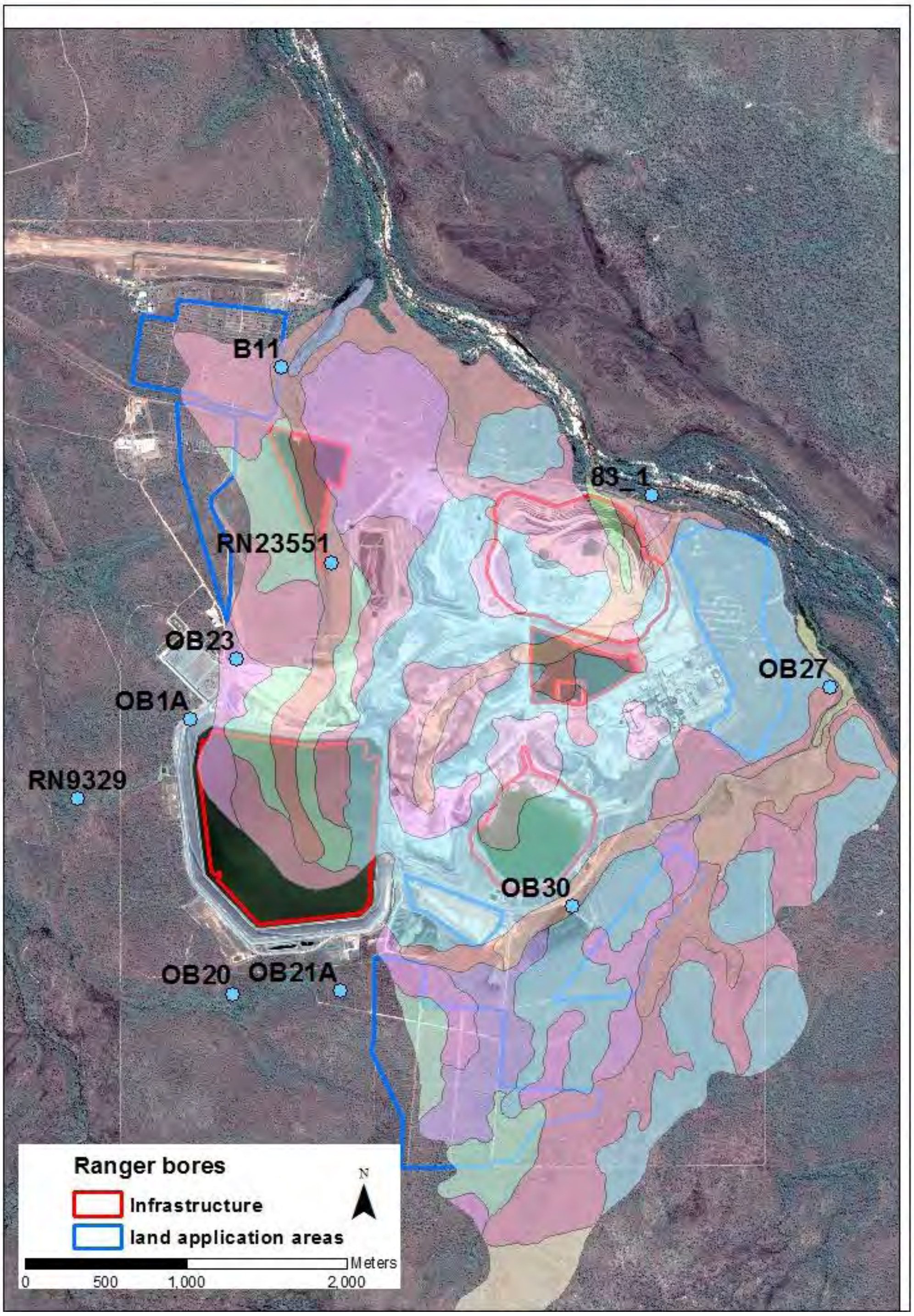

Figure 41 Groundwater monitoring bores around Ranger uranium mine and analysed by ***eriss*** for radionuclides and metals with time series > 5 years up to 2012/13 with a soil map overlaid.

Figure 42 shows a ternary plot of the major cation concentrations (in per cent) measured in the ten bores shown in Figure 41. Due to the lack of anion concentrations measured in the bores a piper diagram is not provided.

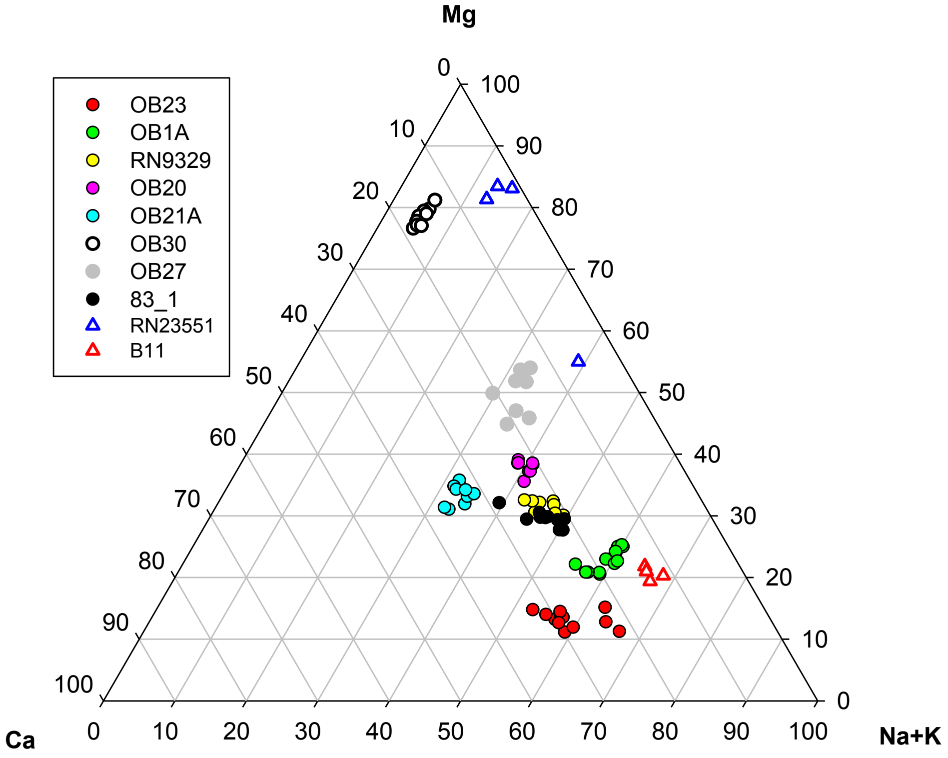

Figure 42 Ternary diagram of major cation concentrations in long time series bores.

4.1 Bores around the TSF

Bores OB23 (RN22937), OB1A (RN22902), RN9329, OB20 (RN22934) and OB21A (RN22935) are deep bores located around the TSF. They sample aquifers 2 or 3, with screen depths of 36-51 m (OB23), 16-31 m (OB1A), 17-19 m (RN9329), 21-36 m (OB20) and 31-43m (OB21A). Element and radionuclide activity concentrations for the individual bores are shown in Appendices A26, A27, A28, A30 and A57.

4.1.1 Major cations

The ternary plot (Figure 42) shows that OB23 and OB1A to the north of the TSF are dominated by 50-70% (Na+K) with 10-30% of both, Mg and Ca. Bore OB23 is located in the vicinity of fault 1, north of the TSF (Salama & Foley 1997) and exhibits high Na concentrations, typical for bores in the fractured Nanambu complex (Klessa 2001). Calcium, Na and Mg concentrations in OB1A are lower than in OB23, whereas K is higher (Figure 42).

Separated in the ternary plot from bores OB23 and OB1A are bores RN9392, OB21A and OB20. These bores are situated to the west and south of the TSF and are located more than 400 m away from the TSF wall.

Bores OB20, OB21A and RN9329 show a similar temporal variability in their cation concentrations. RN9329 and OB20 are dominated by 40-50% (Na+K), but major cation concentrations in bore RN9329 are lower than in OB20, except for K (Figure 43). In contrast, OB21A shows about equal contribution from (Na+K), Mg and Ca in the water, and the bore exhibits the highest Mg concentrations of the bores in the TSF area.

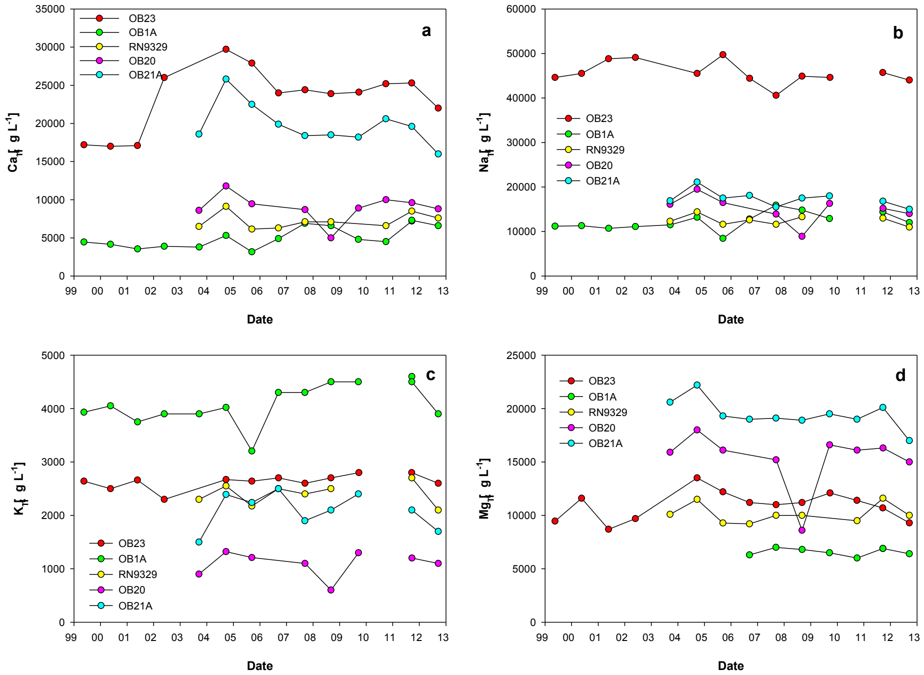

Figure 43 Major cation concentrations in bores around the TSF.

4.1.2 Metals and radionuclides

Figure 44 shows the concentrations of metals and activity concentrations of radionuclides, and the $^{234}U/^{238}U$ activity ratios in the five bores around the TSF, plotted against sampling date.

Fe, Mn and Ba concentrations are highest in bore OB1A immediately north-west of the TSF, followed by RN9329. The variation of the Fe concentration are similar in bores OB23, OB20 and OB21A (and to a lesser extent OB1A), with low concentrations measured in 2007 and 2012. Uranium concentrations in the bores have generally been low throughout the last decade ($< 1\ \mu g\ L^{-1}$), but higher U concentrations were measured in OB21A and OB23 in 2011 and 2012, respectively.

Klessa (2001) observed an increase in Mn from ~150 to ~400 $mg \cdot L^{-1}$ in OB21A in 1998-2001, believed to be an effect of a succession of wetter than normal years that increased groundwater level height leading to Mn reduction in the shallow aquifer and its migration into the fractured aquifer. Mn concentration has remained relatively stable at 400 $mg \cdot L^{-1}$ in OB21A for the last decade, suggesting that the increase was not due to seasonal changes and has persisted due to lasting wetter than normal years.

The similar variability in Fe concentration (and major cation concentrations in some bores) is likely due to the time of sampling, dilution and seasonal effects (such as the length and intensity of the preceding wet-season) and potentially associated changes in seasonal redox conditions. These changing conditions also appear to influence the U concentration in bores OB23, OB20 and OB21A, which exhibits a trend opposite to Fe concentrations: high U concentrations were measured in OB23 in 2001 and 2011 and these high concentrations are associated with low Fe. Generally, the five bores show activity concentrations of ^{226}Ra larger than ^{238}U. Radium-226 and ^{238}U activity concentrations in the bores are in agreement with levels reported by ERA for bores in the general areas (ERA 2012).

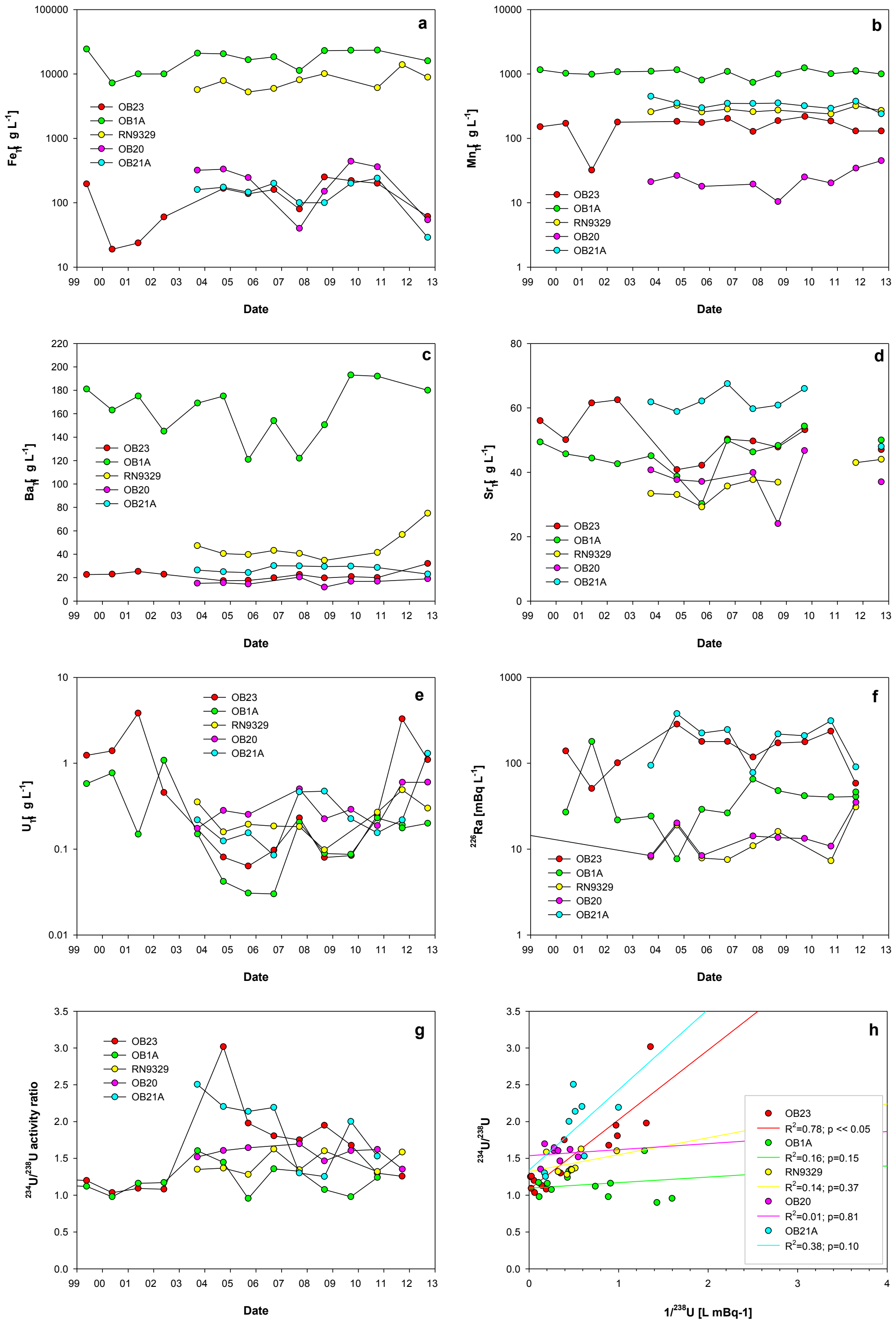

Figure 44 Metal and radionuclide activity concentrations and ratios in bores around the TSF.

OB23 to the north of the TSF has the highest U concentration and shows a statistically significant ($p<0.05$) decrease of the $^{234}U/^{238}U$ activity ratio when plotted against the inverse of the ^{238}U activity, with a contaminating end-member $^{234}U/^{238}U$ activity ratio of 1.08±0.10, i.e. high U concentrations in this bore are characterised by $^{234}U/^{238}U$ activity ratios close to 1.0. This is indicative of seepage from the TSF. However, the large variability of ^{238}U and ^{226}Ra activity concentrations may have also been caused by extensive earthworks in the area from 2005 onwards, with several TSF wall lifts and the construction of the trial landform in late 2008 and early 2009 in the immediate vicinity of bore OB23.

OB1A to the north-west of the TSF wall shows essentially no trend in either ^{226}Ra or ^{238}U activity concentrations until 2005 but there has been an increase in ^{226}Ra and ^{238}U activity concentrations in 2007. The contaminating end-member ^{234}U/^{238}U activity ratio is close to 1 (1.10±0.07), but the correlation between the ^{234}U/^{238}U activity ratio and the inverse of the ^{238}U activity concentration is not significant ($p=0.15$).

RN9329 in the Gulungul catchment shows a y-intercept of 1.32±0.13, and a slight decrease of the ^{234}U/^{238}U activity ratio with increasing uranium activity concentrations but the correlation is not statistically significant ($p=0.37$).

OB20 and OB21A are located to the south of the TSF and exhibited maximum ^{226}Ra activity concentrations in September 2004, whereas uranium peaked in 2012. OB21A ^{226}Ra activity concentrations are higher than in OB20, in agreement with levels reported in ERA (2012).

There is no statistically significant correlation between the ^{234}U/^{238}U activity ratio and the inverse of the ^{238}U activity concentration for OB20 ($p=0.81$) and the intercept with the y-axis is significantly different from 1 (1.54±0.11). The ^{234}U/^{238}U activity ratio in OB21A decreases with increasing uranium concentration although the correlation is not statistically significant ($p=0.11$). It is thus unlikely that this OB21A is impacted by seepage from the TSF. Based on the considerations above, the one bore potentially influenced by seepage from the TSF is OB23, located close to one of the major fault zones north of the TSF area (Figure 2).

4.1.3 Principal components analysis (PCA)

Table 14 summarises the results of the PCA for the deep bores (OB1A, OB23, RN9329, OB20 and OB21A) around the TSF, including the loadings and eigenvalues of the first three principal components.

Electric Conductivity (EC) and pH values measured in the bores at or around the time of sample collection were acquired from the Northern Territory DME and are included in the PCA. EC and pH values in these bores are given in Appendix A62. Concentration values below detection limits have been included in the PCA and a value corresponding to half of the detection limit of that element has been assigned to the sample. In our study, only factors with eigenvalues greater than 1 were taken into account.

The first three factors explain 88% of the total variance observed. Figure 45 shows the scree, loading and score plots for bores OB1A, OB23, RN9329, OB20 and OB21A.

Table 14 Principal component loadings of bores around the TSF

Variable	PC1	PC2	PC3
Ba	-0.32	0.37	0.18
Ca	0.37	0.22	-0.11
Fe	-0.35	0.29	0.10
Mg	0.31	-0.19	0.39
Mn	-0.27	0.44	0.27
Na+K	0.25	0.31	-0.47
Sr	0.22	0.34	0.53
U	0.09	-0.38	0.43
Ra-226	0.31	0.32	0.07
EC	0.36	0.21	-0.08
pH	0.37	0.06	0.16
Eigenvalue	6.00	2.31	1.35
Proportion	0.55	0.21	0.12
Cumulative	0.55	0.76	0.88

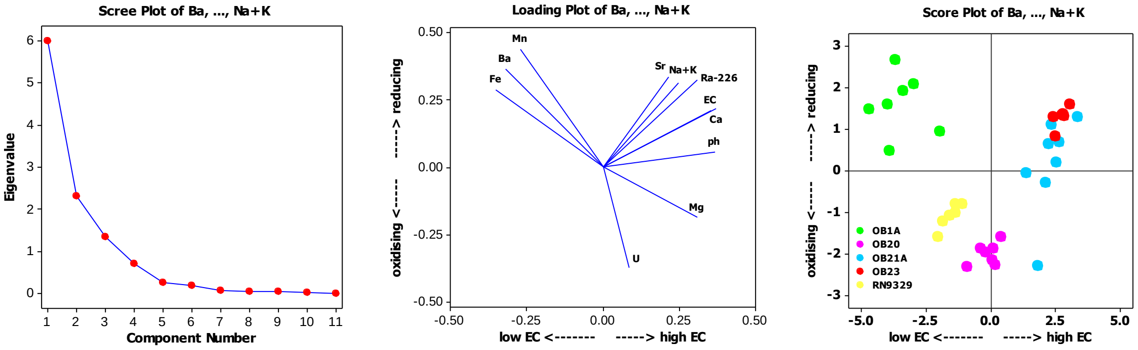

Figure 45 Principal components analysis for bores OB1A, OB23, RN9329 OB20 and OB21A.

EC, Ca, Mg and Na+K are positively correlated to the 1st eigenvector, whereas variations in Mn, U and Ba are dominated by variations in the 2nd eigenvector of the PCA. Mn and Ba are negatively correlated to the 1st eigenvector and U is negatively correlated to the 2nd eigenvector. The score plot demonstrates that bores group according to the first two principal components. OB1A is dominated by the variance in the 1st eigenvector. Bores OB23 and OB21A have similar scores for the first two eigenvectors, but OB21A appears to be influenced by larger variations in the 2nd eigenvector. OB20 and RN9329 are negatively correlated to the 2nd eigenvector.

The PCA can be interpreted such that changes in EC (and thus Ca, Mg, Na+K) lead to an increase in ^{226}Ra and Sr associated with desorption reactions in the aquifer, similar to the increases observed in bores close to the TSF by Martin & Akber (1999). Martin & Akber (1999) also observed that increases in Sr in bores in the vicinity of the TSF were not associated with increases in Ba in agreement with the PCA.

On the other hand, oxygen depleted ground waters lead to higher concentrations in the redox sensitive elements, Fe, Mn and Ba (see for example Chen et al 2007), described by the 2nd eigenvector. In contrast, oxygen rich groundwater leads to higher concentrations of U and Mg. Consequently, the variability of the U concentrations in bores OB20 and OB21A appears to be mainly driven by changes in the redox conditions, whereas OB1A appears to be influenced to a greater extent by variations in electric conductivity (EC).

Monitoring of bores OB1A and OB23 to the north of the TSF should continue, to be able to detect long term changes of groundwater quality. Bore OB23 is of particular importance as it is located in the vicinity of major fault 1 (Figure 2), north of the TSF, which shows higher permeabilities. Bores to the west of the TSF (RN9329) and the south (OB20, OB21A) should also continue to be monitored, to detect potential changes associated with the remediation works at the TSF and anticipated changes in the groundwater heads, to make sure that any long term changes in groundwater quality are detected and quantified to the south of the TSF.

4.2 Bores in the Corridor Creek catchment

Figure 46 shows major cations, Figure 48 shows the metal concentrations measured in bores OB30 (RN22941) with a screen depth of 20-35 m, and OB27 (RN22930) with a screen depth of 15-40 m.

4.2.1 Major cations

OB30 is located close to pit 1 and the Corridor Creek Wetland Filter and is dominated by Mg (75-85%). It is a tertiary ERA bore located in downstream locations from pit 1 and the seepage limiting barrier, and it is used to determine whether seepage has reached the MBL aquifer (ERA 2012).

Bore OB27 is situated on the western side of the confluence of Corridor Creek and Georgetown Creek, and is also dominated by Mg (~ 50%), with 10-20% Ca and 30-40% (Na+K) (Figure 39).

Ca and Mg are higher in OB30, whereas Na is highest in OB27. Major cation concentrations have decreased over the past decade in OB 27 (Figure 46).

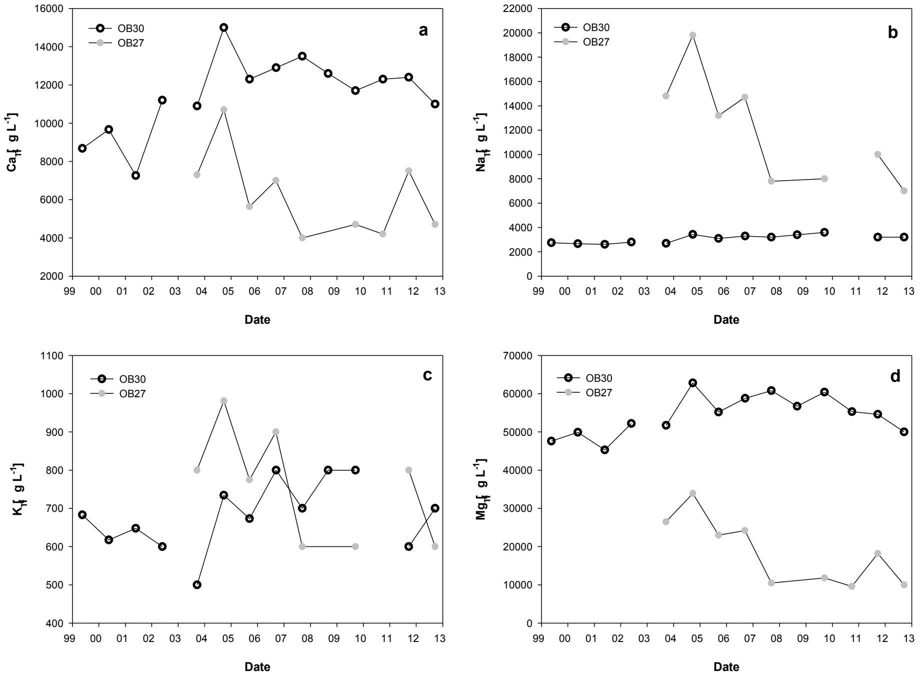

Figure 46 Major cations in OB27 and OB30 in the Corridor Creek catchment.

4.2.2 Metals and radionuclides

Figure 47 show the metal and radionuclide activity concentrations in the two bores plotted against sampling date. Iron, Mn, Ba, Sr and U concentrations have decreased in OB27, close to the confluence of Corridor and Georgetown Creeks, over the past decade. This decline coincides with a gradual decline of the pH in this bore over the past 10 years (ERA 2012).

Ba and Sr levels in OB30 have been relatively constant over the past decade, whereas U concentration has decreased from 1999. Increases of Mn and ^{226}Ra in bore OB30 occurred in 2011 and 2012. OB27 showed an increase in ^{226}Ra activity concentration in 2011, but Mn concentration decreased.

The ^{234}U/^{238}U activity ratio plots shown in Figures 46 g and 46 h, indicate that there is no significant correlation between ^{234}U/^{238}U activity ratios and the inverse of the uranium concentration in either of the two bores. However, U concentrations in OB30 are generally high, and average ^{234}U/^{238}U activity ratio measured over the past 13 years in OB30 was around 1.08±0.03. Compared to 1989, the ^{238}U activity concentration in OB30 has increased 4-fold by 1999 (Figure 32) but is currently decreasing. The increase observed in the late 1990s may indicate an influence of uranium originating from tailings deposition in pit 1.

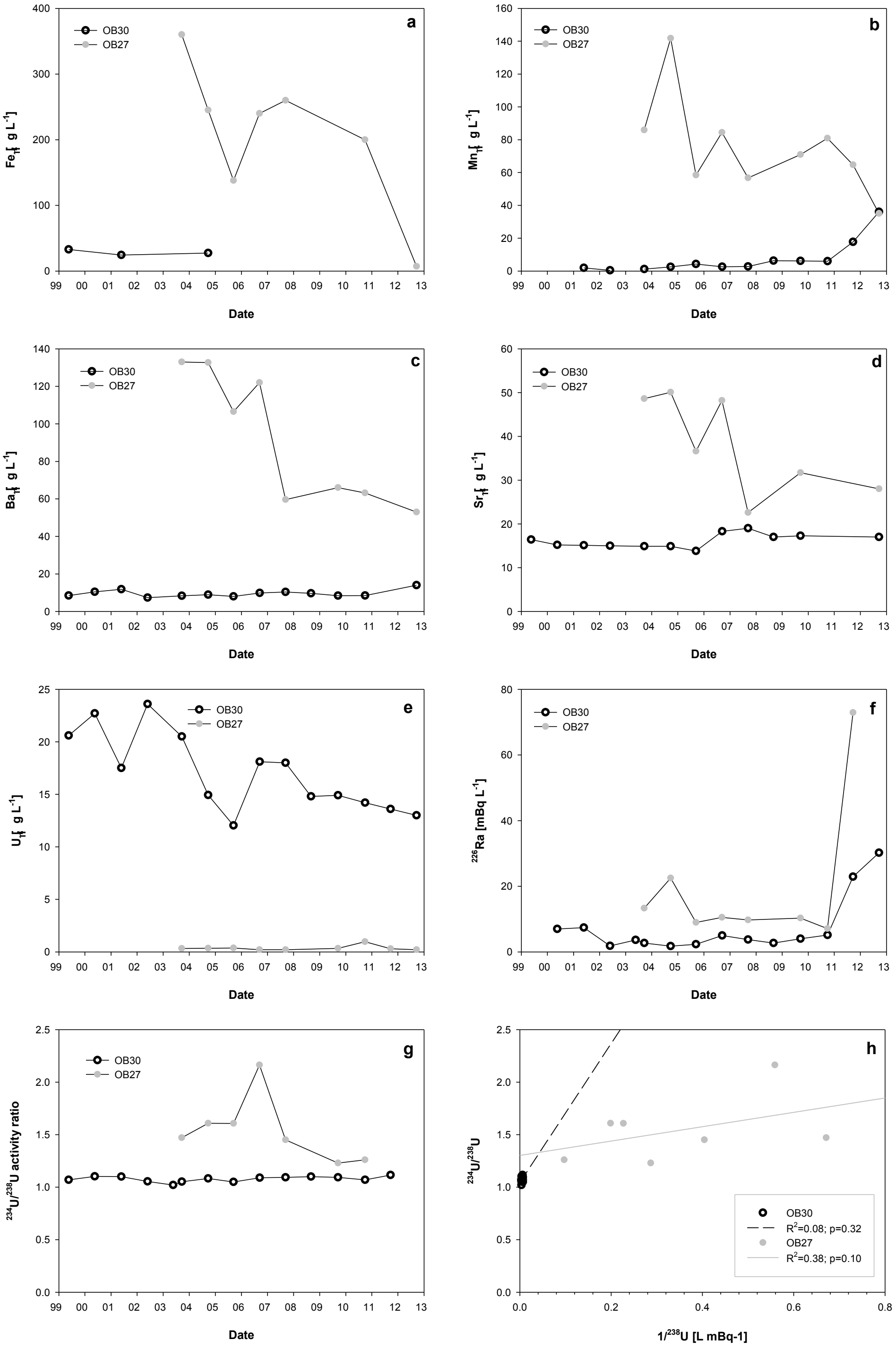

Figure 47 Metal and radionuclide activity concentrations and ratios in bores OB30 and OB27.

4.2.3 Principal components analysis (PCA)

Figure 48 summarises the results of the PCA for bores OB30 and OB27, including the loadings and eigenvalues of the first two principal component. More than 90% of the variability in the two bores is explained by the first two factors, Table 15 shows the results of the PCA.

Table 15 Principal component loadings of bores OB30 and OB27

Variable	PC1	PC2
Ba	0.33	-0.18
Ca	-0.25	-0.54
Fe	0.28	-0.18
Mg	-0.30	-0.39
Mn	0.32	-0.20
Na+K	0.32	-0.30
Sr	0.31	-0.28
U	-0.32	-0.07
Ra-226	0.30	-0.24
EC	-0.28	-0.46
pH	-0.29	-0.09
Eigenvalue	8.64	1.34
Proportion	0.79	0.12
Cumulative	0.79	0.91

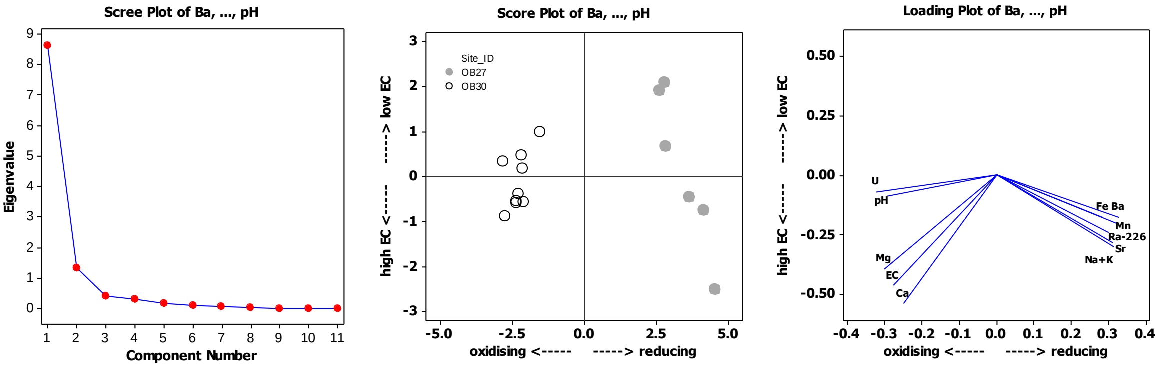

Figure 48 Principal components analysis for bores OB30 and OB27.

The first eigenvector of the PCA dominates Ba, Mn, Fe, Sr and ^{226}Ra activity concentrations and is negatively correlated to uranium. Similar to the interpretation of the bores around the TSF, this factor may be best described by the existing redox conditions in the bores, with oxygen rich ground waters favouring high uranium and low Mn and Fe concentrations, and oxygen depletion favouring low uranium and high Mn, Fe and Ba concentrations. The second factor is dominating variations in Mg, Ca and Na+K, and thus EC, in groundwater.

OB27 shows high positive scores with the first eigenvector, consequently this bore appears to be characterised by a more reducing environment than OB30. Associated with the low oxygen are low dissolved U concentrations in the groundwater collected from this bore. In contrast OB30 scores are negatively correlated with the first factor, meaning ground water is more oxygenated and U concentration in this bores is higher. To assess the performance of the seepage limiting barrier in pit 1, groundwater quality monitoring of OB30 should continue.

OB27 is located along the Corridor Creek catchment, which is one of the major pathways of contaminants leaving the site. Long-term monitoring of this bore should continue and focus on detecting changes in groundwater quality associated with the rehabilitation of Ranger mine, and in particular with the storage of tailings in pit 1.

4.3 Magela LAA Bore 83_1 in the Djalkmara Creek catchment

Bore 83_1 (RN23010) is a statutory monitoring bore of ERA and is dominated by (Na+K) (Figure 42) with about equal contributions of between 20-30% Ca and Mg, similar to bores RN9392, OB21A and OB20 in the TSF area. The bore is located at the edge of the Magela Land Application area, close to Magela Creek and has a screen depth of 0 – 90 m, targeting aquifers 1B, 2 and 3. It is located in a sand lens between pit 1 and Magela Creek (ERA, 2012).

Appendix A6 shows the time series of major cations, SO_4, metals and radionuclides. Radium-226 und ^{238}U activity concentrations are similar and there is no significant correlation between the $^{234}U/^{238}U$ activity ratio and the inverse uranium concentration in this bore.

4.3.1 Principal components analysis (PCA)

Table 16 shows the results of the PCA for the first 3 principal components. Almost 80% of the variability in this bore is explained by the first two factors. Due to most measurements of Fe being below the minimum detection levels in water from this bore, Fe has not been included in the PCA. Figure 49 shows the loading plot for bore 83_1.

Table 16 Principal component loadings of bore 83_1

Variable	PC1	PC2	PC3
Ba	-0.28	-0.21	-0.43
Ca	0.44	-0.13	0.08
Mg	0.45	-0.11	0.08
Mn	-0.08	0.53	0.00
Na+K	0.36	0.32	-0.15
Sr	0.32	-0.38	-0.09
U	0.23	-0.48	-0.05
Ra-226	0.33	0.28	0.00
EC	0.37	0.29	-0.15
pH	0.05	0.05	-0.86
Ba	-0.28	-0.21	-0.43
Eigenvalue	4.64	3.24	1.25
Proportion	0.46	0.32	0.13
Cumulative	0.46	0.79	0.91

The first principal component is described by Ca, Mg, Na+K and EC. Loading for Ca and Mg are high, and this is interpreted as major cation concentration (i.e. EC) being the dominating factor influencing metal and radionuclide activity concentrations in this bore. Due to the vicinity of bore 83_1 to the Magela LAA, this bore is potentially still influenced by elements from past application of mine waters, despite the fact that land application in the area has ceased in 2008.

^{226}Ra and EC in this bore are closely correlated but Ba is negatively correlated to EC. This is most likely due to adsorption/desorption mechanisms in the groundwater aquifer and potential barite formation in the groundwater with increasing salinity, as reported by Martin & Akber (1996, 1999) for bores north of the TSF. Uranium levels in bore 83_1 are influenced by the redox conditions and are higher when more oxidising conditions persist.

Due to its strategically important location as along an exit line from Ranger mine along the Djalkmara Creek aquifer, monitoring of this bore should continue.

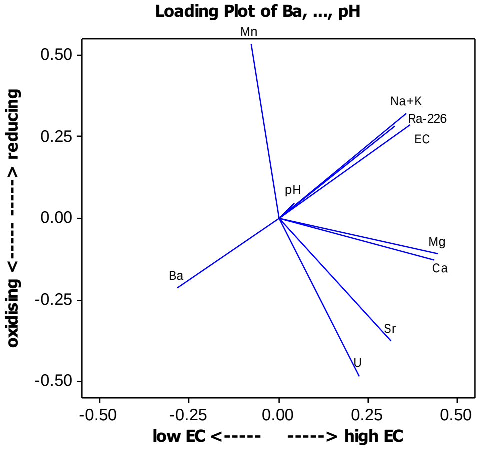

Figure 49 Loading plot for the first two eigenvectors of the PCA for bore 83_1.

4.4 Bores RN23551 and B11 in the Coonjimba Creek catchment

Bores RN23551 and B11 (RN7243) both sample the shallow aquifer immediately to the North of the TSF along the Coonjimba line. RN23551 is located in the headwaters of RP1 in the vicinity of major fault line 2a and within an area of very high permeabilities (Salama & Foley 1997).

4.4.1 Major cations

The ternary plot (Figure 41) shows a large separation of these two bores. RN23551 is dominated by Mg, whereas B11 is dominated by Na. Potassium concentrations are low in both bores.

Figure 50 shows major ion concentrations measured in RN23551 and B11. It is obvious that bore RN23551 in the headwaters of RP1 is a lot more variable in its major cation concentrations, in particular Ca and Mg. In contrast, B11 major cation concentrations have been constant between 2006 and 2010. The variability in major cation concentrations in RN23551 is similar to the variability reported in Klessa (2001) and ERA (2012).

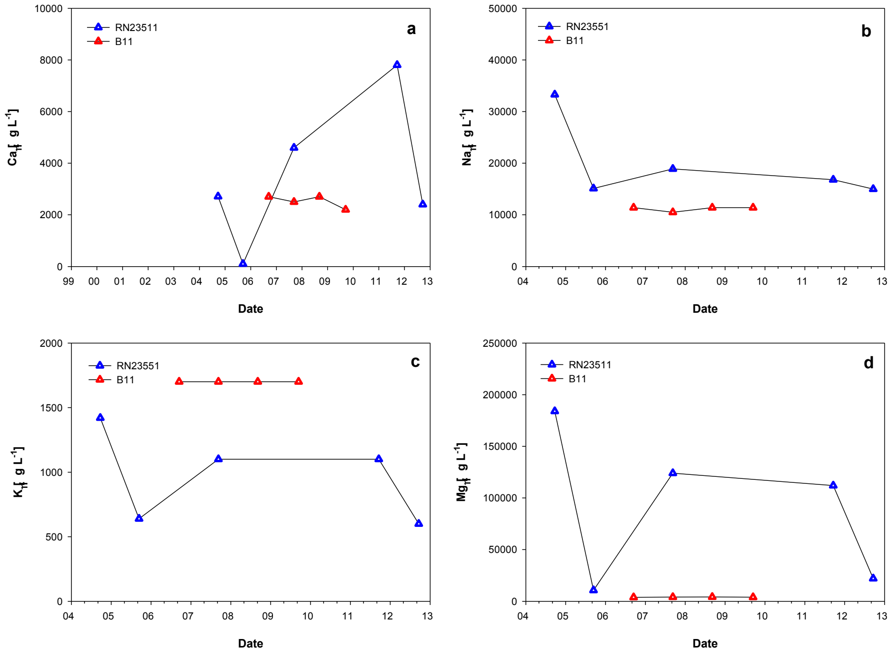

Figure 50 Major cations in RN23551 and B11 in the Coonjimba Creek catchment.

4.4.2 Metals and radionuclides

Figure 51 shows the metal and radionuclide activity concentrations in bores RN23551 and B11 plotted against sampling date.

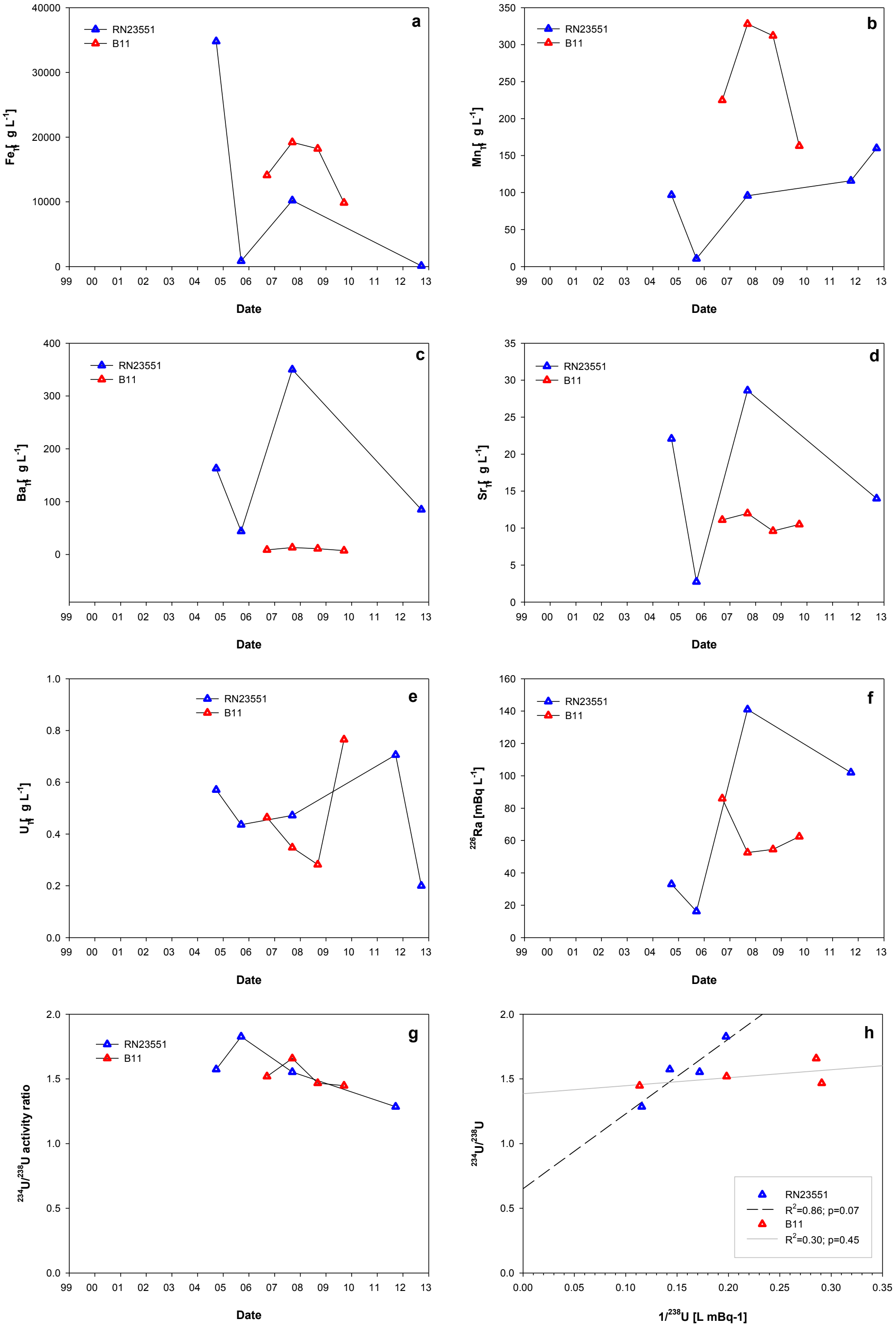

Figure 51 Metal and radionuclide activity concentrations and ratios in bores RN23511 and B11.

The variability of metal concentrations (Fe, Mn, Ba, Sr, U and ^{226}Ra) in bore RN23551 is large, whereas variations in bore B11 are large only for the redox sensitive elements Fe, Mn and U. Manganese concentrations (Figure 50b) are generally higher in bore B11, but U concentrations are comparable.

Four years of ^{234}U/^{238}U activity ratio data from RN23551 indicate that the decrease of the ^{234}U/^{238}U activity ratio with increasing uranium concentration in this bore might be statistically significant. However, the intercept (0.65±0.26) is not statistically significant ($p=0.13$) and more data is needed to reduce the uncertainties in the fit.

4.4.3 Principal Component Analysis

Table 17 shows the results of the PCA for the first three principal components in bores RN23551 and B11. 75% of the variability in the two bores is explained by the first two factors. Figure 52 shows the loading plot for bores RN23551 and B11.

Table 17 Principal component loadings of bores RN23551 and B11

Variable	**PC1**	**PC2**	**PC3**
Ba	0.38	0.15	-0.26
Ca	0.21	0.52	-0.03
Fe	0.18	0.14	0.68
Mg	0.42	0.00	0.17
Mn	-0.26	0.40	0.34
Na+K	0.38	-0.15	0.33
Sr	0.37	0.31	-0.01
U	0.12	-0.13	-0.12
Ra-226	0.15	0.45	-0.41
EC	0.32	-0.32	-0.20
pH	-0.34	0.29	-0.05
Eigenvalue	5.24	2.80	1.70
Proportion	0.48	0.25	0.16
Cumulative	0.48	0.73	0.89

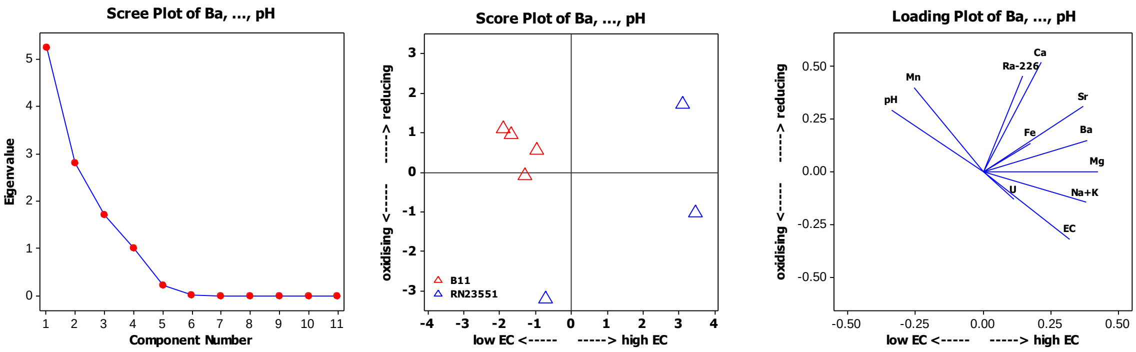

Figure 52 Principal components analysis for bores RN23551 and B11.

The variability of metal concentration in bore RN23551 appears to be due to both EC and redox conditions in the bore, but EC appears to be the dominating factor. The 2nd principal component is characterised by Ca, ^{226}Ra and Mn but loadings for Fe and U are quite small, indicating that the redox conditions might be additionally characterised by a 3rd principal component, which shows a high loading for Fe and Mn and describes about 16% of the variability in metal concentrations.

It is concluded that EC is the major influence on metal concentrations in these two bores. Measurements of groundwater quality in these two bores should continue to monitor long term impacts on groundwater along the Coonjimba Creek aquifer, associated with decommissioning of the TSF and rehabilitation of Ranger mine.

5 Conclusions and recommendations

Groundwater chemistry and radiochemistry data measured by ***eriss*** over the past three decades are summarised in this report. The report highlights the sparseness of data for some bores, whereas other bores have time series extending over decades. Most of the bores investigated exhibited Ba, Mn and U levels below the Australian Drinking Water Guidelines, with only a few bores, noticeably those located in the immediate vicinity of the TSF, showing levels at or above the guideline values.

Ten bores have been identified that have metal and radionuclide time series data (with monitoring records > 7 years) extending to September 2012 and beyond, that are distributed around site at strategically important locations. More data have become available since commencing work on this report, but have not been included. The ten long time series bores are located in various groundwater catchments around the site.

Bores RN9329, OB20 (RN22934) and OB21A (RN22935) are located south and west of the TSF in the Gulungul groundwater catchment and sample aquifers 2 and/or 3. They are characterised by equal Ca, Mg and Na+K, whereas OB1A (RN22902) and in particular OB23 (RN22937, which according to ERA (2013) is located at the border of the Coonjimba and Gulungul groundwater catchments and samples deep aquifer 3) are dominated by Na+K and Ca (Figure 42). The PCA (Figure 45) shows that groundwater chemistry in the five bores around the TSF is dominated by variations in EC, and bores OB1A and OB23 generally exhibit more reducing conditions compared to the other three bores. Using the uranium activity ratio ($^{234}U/^{238}U$) (Figure 21b), bore OB23, located close to one of the major fault zones north of the TSF area, has been identified as potentially influenced by seepage from the TSF or by other activities on site, such as the construction of the trial landform and several TSF lifts.

Bores RN23551 and B11 are located in the Coonjimba groundwater catchment immediately to the North of the TSF along the Coonjimba line. RN23551 samples aquifer 2 and is dominated by Mg, whereas B11 samples aquifers 1a and 1b and is dominated by Na+K (Figure 52). Variability in EC appears to be the dominating factor for metal and radionuclide activity concentrations in the two bores (Figure 3b), but there is no trend of increasing metal or radionuclide activity concentrations in our data.

Bore 83_1 is located in the Djalkmara groundwater catchment close to the Magela LAA, and samples all three aquifers. It is characterised by equal Ca, Mg and Na+K (Figure 42). The bore is located within a sand lens that was previously identified between pit 3 and Magela Creek (ERA 2012). The dominating factor influencing metal and radionuclide activity concentrations in this bore appears to be the EC (Table 16). ^{226}Ra and EC in this bore are closely correlated but Ba is negatively correlated to EC (Figure 49). This is potentially due to adsorption/desorption mechanisms in the groundwater aquifer and potential barite formation in the groundwater with increasing salinity, as reported by Martin & Akber (1996, 1999) for bores north of the TSF. Redox conditions also have a great influence in particular on U and Mn levels in bore 83_1, and U is generally higher when more oxidising conditions persist

Groundwater samples from two bores have been collected over an extended period of time within the Corridor groundwater catchment. Bore OB30 (RN22941) targets aquifer 3 close to pit 1 and is dominated by Mg, OB27 (RN22930) targets aquifer 2 and 3 on the western side of the confluence of Corridor Creek and Georgetown Creek and is dominated by Mg and Na+K (Figure 42). Metal and radionuclide activity concentrations in these two bores are governed by redox chemistry, which explained almost 80% of the metal variability observed in the two bores (Table 15, Figure 48). No increases of metal or radionuclide activity concentrations over time were observed in these two bores. Uranium concentration however has declined in OB30 over the past decade.

This report provides information about data availability and data type, as well as general correlations and characteristics of the bores sampled by ***eriss***. It describes only one small existing dataset, with additional datasets existing from ERA's and DME's respective groundwater monitoring programmes. ERA and DME sample a large number of bores quarterly and biannually, respectively. The datasets from the three organisations should be combined and investigated in a GIS, comparing the results obtained by the various organisations taking into account QA/QC procedures in place for populating the various databases. As a first step, the ***eriss*** data are provided in this report.

There is also the need to compare the results for the bores to the distribution of faults (Figure 2), hydraulic conductivities, the aquifers sampled (Figure 12 in ERA 2013), lithology, soil type (Figure 41), distance from potential seepage locations etc. It is recommended to include variables such as sampled aquifer, groundwater catchment and lithology in a PCA of all available data, to strengthen outputs and information that can be gleaned from the groundwater monitoring results. This information can then be used to test hydrodynamic models, and thus assist in forward modelling of long-term closure impacts on groundwater quality. Understanding the connectivity between pit 1 and Corridor Creek (and the effectiveness of the barrier), and characterising the existing sand lens between pit 3 and Magela Creek are important in any forward modelling of groundwater quality after closure.

Whereas ***eriss*** has analysed bore water as they were received from DME in the past ten years, it is now recommended that the long time series bores identified in this report are sampled strategically, by ERA or DME, with samples provided to ***eriss*** for analysis on an annual basis. Samples received from other bores will be stored by ***eriss*** for a period of up to a maximum of two years and then disposed off, following procedures and recommendations outlined in Medley (2009).

References

Ahmad M and Green DC 1986. Groundwater Regimes and isotopic studies, Ranger mine area; Northern Territory, *Australian Journal of Earth Sciences* 33, 391 -399.

Akber R, Lu P & Bollhöfer A 2011a. Distribution of radioactivity in the land application areas assessed via direct measurement. Energy Resources of Australia Ltd, Darwin.

Akber R, Lu P, Bollhöfer A 2011b. External radiation dose in the land application areas. Energy Resources of Australia Ltd, Darwin.

Akber R, Lu P, Bollhöfer A 2011c. 222Rn in the land application areas. Energy Resources of Australia Ltd, Darwin.

Akber R & Marten R 1991. Remobilisation of radionuclides from the land application area at Ranger. Internal report 31, Supervising Scientist for the Alligator Rivers Region, Canberra. Unpublished paper.

Akber R & Marten R 1992. Fate of radionuclides applied to soil in the Ranger Uranium Mine land application area – Proceedings of Workshop on Land Application of Effluent Water from Uranium Mines in the Alligator Rivers Region: Supervising Scientist for the Alligators Rivers Region, AGPS Canberra pp 139-165.

Anderson D & Timms W 2009. Modelling of Ranger mine pit #1. Flow model: Progress Report. Water Research Laboratory of the University of New South Wales Report to EWL Sciences. Presented at ARRTC meeting #22, 2009.

Bartolo R, Parker S, van Dam R, Bollhöfer A, Kai-Nielsen K, Erskine W, Humphrey C & Jones D 2013. Conceptual models of stressor pathways for the operational phase of Ranger Uranium Mine. Internal Report 612, January, Supervising Scientist, Darwin.

Chen K, Jiao JJ, Huang J & Huang R 2007. Multivariate statistical evaluation of trace elements in groundwater in a coastal area in Shenzhen, China. *Environmental Pollution* 147, 771-780.

ERA 2012. 2011-12 Ranger Wet Season Groundwater Report. Energy Resources of Australia Ltd. Darwin NT.

ERA 2013. ERA Ranger Water Management Plan. RWMP001. Energy Resources of Australia Ltd. Darwin NT.

Gulson BL, Mizon KJ, Korsch MJ, Carr GR, Eames J & Akber RA (1992). Lead isotope results for waters and particulates as seepage indicators around the Ranger tailings dam: A comparison with the 1984 results. Open file record 95, Supervising Scientist for the Alligator Rivers Region, Canberra.

Haylen ME 1981. Uranium Tailings Disposal Ranger Project – A Rationale. M.Env.Stud Thesis, Macquarie University, North Ryde, NSW.

Iles M, Martin P, Ryan B & leGras C 2002. Long-term study of groundwater dispersion of uranium at Ranger Mine. In Environmental Research Institute of the Supervising Scientist research summary 1995–2000. Supervising Scientist Report 166, Supervising Scientist, Darwin NT, 7–12.

Hollingsworth I, Overall R & Puhalovich A 2005. Status of the Ranger Irrigation Areas – Final Report, EWL Sciences Pty Ltd, Darwin.

Ivanovich M & Harmon RS 1994. Uranium Series Disequilibrium. Applications to Environmental Problems. Clarendon Press, Oxford.

Johnston A & Milnes AR 2007. Review of mine-related research in the Alligator Rivers Region 1978–2002: Prepared for ARRTC9 meeting, 25–27 February 2002. Supervising Scientist Report 186, Supervising Scientist, Darwin NT.

Jolliffe IT 2002. *Principal Component Analysis*. 2nd Edition. Springer Verlag New York.

Kalf FRP & Dudgeon CR 1999. Analysis of long-term groundwater dispersal of contaminants from proposed Jabiluka Mine tailings repositories. Supervising Scientist Report 143, Supervising Scientist, Canberra.

Kalf & Associates Pty Ltd, 2004. Ranger Pit No. 1 Closure, Three-Dimensional Regional Numerical Flow and Solute Transport, Model Analysis. Volume 1 (Executive Summary and Phases 1, 2, 3 and 4 Report) & Volume 2 (Report Figures). 30 November 2004.

Klessa DA 2001. A review of groundwater chemistry monitoring data at Ranger. Internal Report 363, Supervising Scientist, Darwin. Unpublished paper.

leGras C 1992. Vertical gradients in the chemical and sulfur-isotope composition of Ranger tailings pore water. Part 1: Gradients in non-radioactive chemical species. Internal report 70, Supervising Scientist for the Alligator Rivers Region, Canberra. Unpublished paper.

leGras C, Akber RA & Andrew A 1993. The sulfur-isotope composition of pore water, seepage and infiltration samples from the tailings dam, Ranger Uranium Mine, Northern Territory. Internal report 126, Supervising Scientist for the Alligator Rivers Region, Canberra. Unpublished paper.

leGras CAA, Akber RA & Andrew A 1991. The sulfur-isotope composition of mineral, surface and groundwater samples from the Ranger uranium mine, Northern Territory. Internal report 44, Supervising Scientist for the Alligator Rivers Region, Canberra. Unpublished paper.

Martin P & Akber RA 1994. Radium isotopes as seepage indicators in the vicinity of a uranium tailings dam. in: Techniques for the analysis of radionuclides in the environment and their application: Part 1. Technical memorandum 47, Supervising Scientist for the Alligator Rivers Region, AGPS, Canberra.

Martin P & Akber RA 1996. Groundwater seepage from the Ranger uranium mine tailings dam: Radioisotopes of radium, thorium and actinium. Supervising Scientist Report 106, Supervising Scientist, Canberra.

Martin P & Akber RA 1999. Radium isotopes as indicators of adsorption-desorption interactions and barite formation in groundwater. *Journal of Environmental Radioactivity* 46, 271–286.

Martin P & Hancock GJ 2004. Routine analysis of naturally occurring radionuclides in environmental samples by alpha-particle spectrometry. Supervising Scientist Report 180, Supervising Scientist, Darwin NT.

McBride TP 1992. Fate of solutes applied to land application areas. In: Proceedings of the Workshop on Land Application of Effluent Water from Uranium Mines in the Alligator Rivers Region. Supervising Scientist for the Alligators Rivers Region, AGPS Canberra pp 181-186.

Medley P, Bollhöfer A, Iles M, Ryan B & Martin P 2005. Barium sulfate method for radium-226 analysis by alpha spectrometry. Internal Report 501, June, Supervising Scientist, Darwin. Unpublished paper.

Medley P 2009. A review of chemical storage and handling protocols in the Environmental Radioactivity laboratories of ***eriss***. Internal Report 548, September, Supervising Scientist, Darwin. Unpublished Paper

Mudd G 2002. Uranium mill tailings in the Pine Creek Geosyncline, northern Australia: past, present and future hydrogeological impacts. In: Uranium in the Aquatic Environment. Proceedings of the International Conference uranium Mining and Hydrogeology III, Merkel BJ, Planer-Friedrich B, Wolkersdorfer C (Eds), 831-840.

NHMRC 2011. Council Australian Drinking Water Quality Guidelines 6. National Health and Medical Research/National Resource Management Ministerial Council.

Noller, B. N. 1991, 'Non-radiological contaminants from uranium mining and milling at Ranger, Jabiru, Northern Territory, Australia, Environmental Monitoring and Assessment 19, pp 383-400.

The Office of the Supervising Scientist 1989. Submission to Review of the Office of the Supervising Scientist for the Alligator Rivers Region. Vol 2. Alligator Rivers Region Research Institute Review of Research 1978–1989.

Osmond JK and Cowart JB 1982. Ground water. in: *Uranium series disequilibrium: Applications to environmental problems*. ed. M. Ivanovich and R.S. Harmon. Clarendon Press, Oxford.

Parker G 2001. Nabarlek chemistry issues. In Proceedings of Workshop, Darwin NT, Australia, 18 –19 April 2000, ed D Klessa, Supervising Scientist Report 160, Supervising Scientist, Darwin, 53–75.

Puhalovich A, Mundle K, Pol R & Toll N 2012b. One- and three-dimensional sub-surface solute transport processes in the region of Ranger uranium mine's tailings storage facility, Northern Territory, Australia. In: McCullough, Lund & Wyse (Ed). Proceedings of the International Mine Water Symposium, Bunburry, Australia 2012. 107-112.

Puhalovich A, Thomas A, Toll N, Puig P & O'Neill A 2012a. Characterisation of hydrogeological conditions and solute transport pathways in the region of the Ranger uranium mine tailings storage facility, Northern Territory, Australia. In: McCullough, Lund & Wyse (Ed). Proceedings of the International Mine Water Symposium, Bunburry, Australia 2012. 101-105.

Ranger Uranium Environmental Inquiry (RUEI) 1977. 2nd report. Canberra, Australian Government Publishing Service.

Ryan B & Bollhöfer A 2007. A summary of radionuclide activity and dissolved metal concentrations in Nabarlek borewaters from 1996 to 2005. Internal Report 530, September, Supervising Scientist, Darwin. Unpublished paper.

Ryan B, Bollhöfer A & Martin P 2007. Uranium in groundwater at a rehabilitated Uranium mine in Western Arnhem Land, Australia. International Atomic Energy Agency (IAEA) conference, Environmental Radioactivity: From measurement and Assessment to Regulation. 23–27 April 2007, Vienna, Austria.

Salama R & Foley GA 1997. Ranger regional hydrology conceptual model. CSIRO Land & Water, October 1997.

Salama R, Kin P & Pollock DW 1999. Assessment of potential solutes migration from Pit #3 under different capping and treatment scenarios. Consultancy report for ERA Ranger Mine. CSIRO Land and Water Consultancy Report no 99/57, October 1999.

Salama R, Pollock D & Foley G 1998a. The impacts of final landform scenarios on the groundwater systems of Ranger Minesite: A GIS-Hydrogeomorphic approach. CSIRO Land and Water report no 98/17, May 1998.

Salama R, Kin P, Foley GA, Pollock D & Ellerbroek D 1998b. Groundwater interaction with Magela Creek. CSIRO Land and Water Report no 98/18, April 1998.

Salama R, Kin P, Pollock D & Foley GA 1998c. Assessment of final tailings repositories in Ranger minesite, tailings dam and Pit #3. Report for ERA Ranger Mine. CSIRO Land & Water Report no 98/19, May 1998.

Timms W, Wasko C, Pells S & Miller B 2010. Ranger Pit No.1 - Groundwater Flow Modelling of Post-Closure Conditions. Water Research Laboratory, University of New South Wales, Report 2010/15.

Turner K & Jones D 2010. Review of solute selection for water quality and bioaccumulation monitoring. In ***eriss*** research summary 2008–2009, eds Jones DR & Webb A, Supervising Scientist Report 201, Supervising Scientist, Darwin NT, 66-72.

Verma M & Salama R (1986) Preliminary Groundwater Studies in the Ranger Area. Northern Territory. Department of Mines and Energy. Report31/1986.

Willett IR, Akber R & Bond WJ 1991. The fate of water and solutes following irrigation with Retention Pond 2 water at the Ranger Uranium Mine: Summary of the final report. Internal report 26, Supervising Scientist for the Alligator Rivers Region, Canberra. Unpublished paper.

Willett IR & Bond WJ 1992. Adsorption properties of the soils of the Ranger Uranium Mine land application area for solutes in water from Retention Pond 2. In: Proceedings of the Workshop on Land Application of Effluent Water from Uranium Mines in the Alligator Rivers Region. Supervising Scientist for the Alligators Rivers Region, AGPS Canberra pp 113-138.

Zielinski RA, Chafin DT, Banta ER & Szabo BJ 1997. Use of 234U and 238U isotopes to evaluate contamination of near-surface groundwater with uranium-mill effluent: a case study in south-central Colorado, U.S.A. Environmental Geology, 32, 2, 124–136.

Appendix 1

Individual bore chemistry and radiochemistry data

Bore ID - RN23931

BORE ID - RN23931

Data - Calcium, Potassium, Magnesium, Sodium and Sulfate

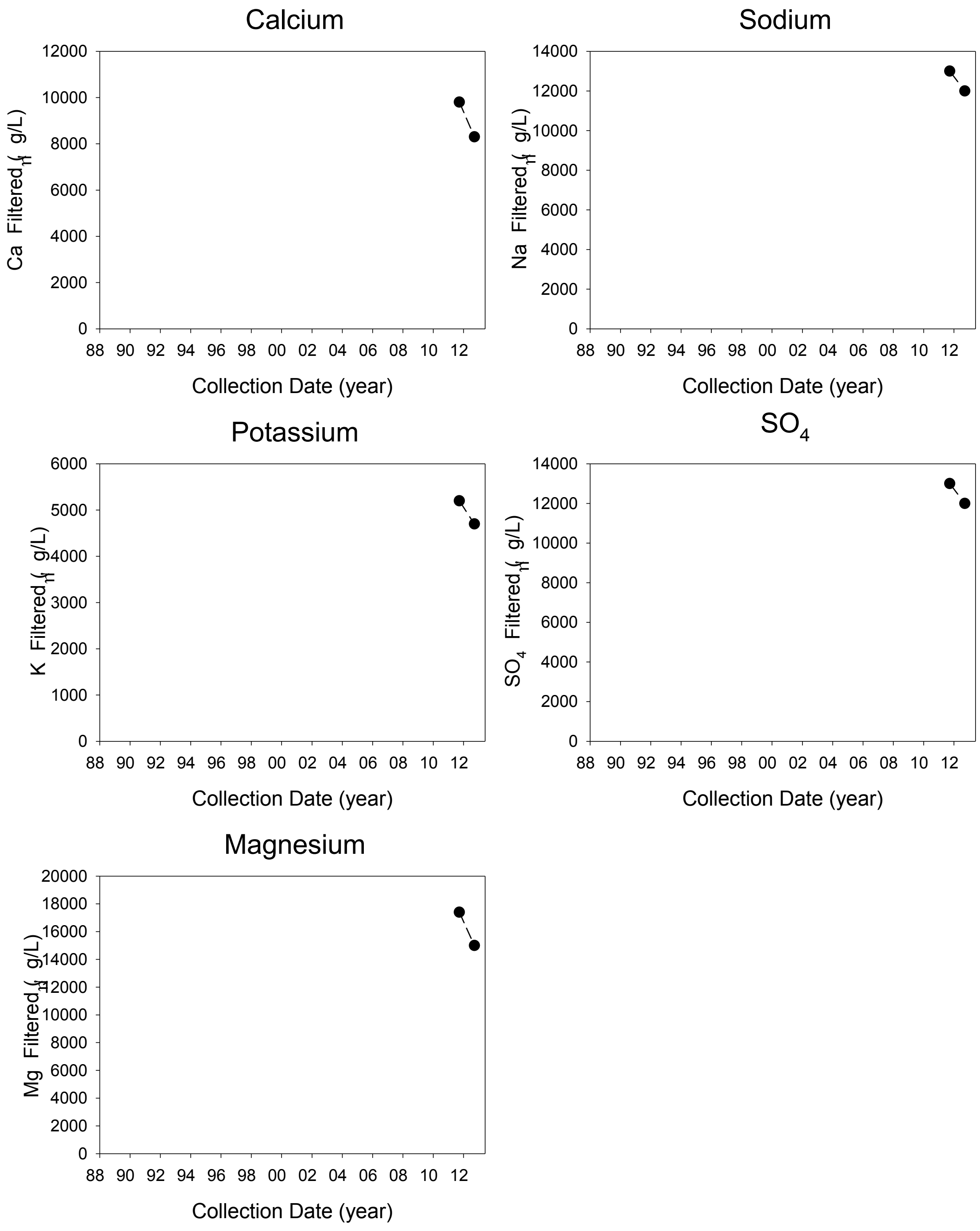

Calcium

Sodium

Potassium

SO_4

Magnesium

BORE ID - RN23931

Data - Iron, Manganese, Barium, Strontium, Uranium & Vanadium

Iron

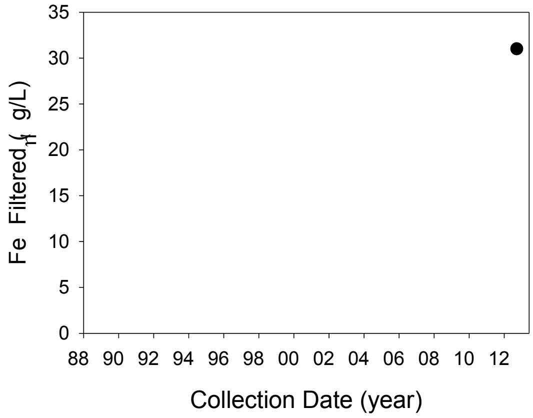

Manganese

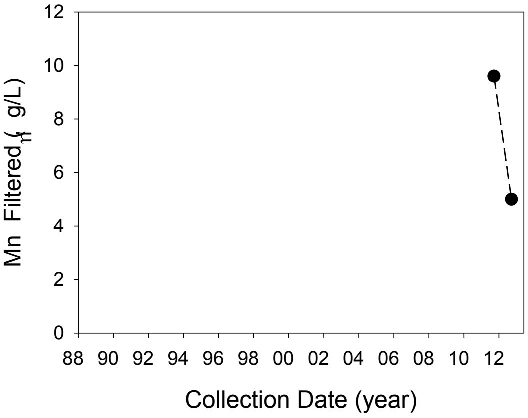

Barium

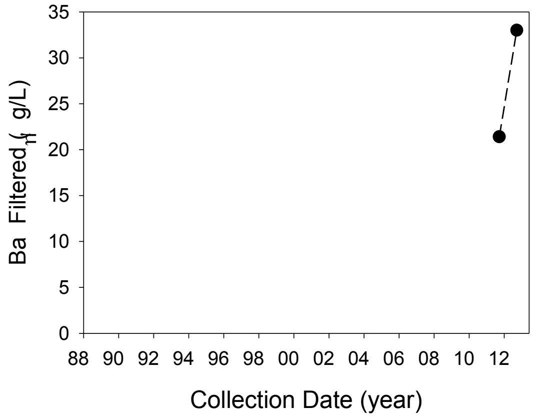

Strontium

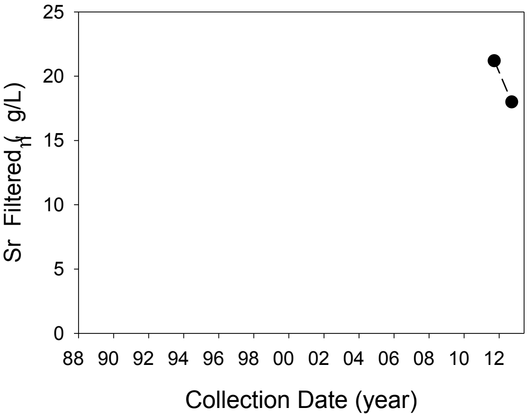

Uranium

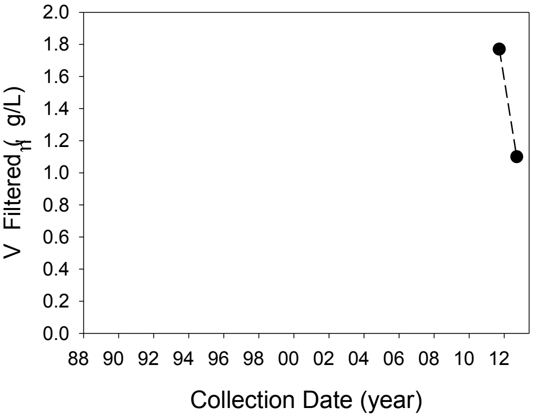

Vanadium

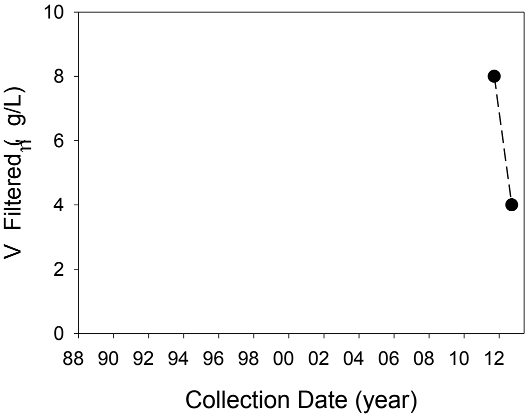

BORE ID - RN23931

Data - U-238, Ra-226, U-234:U-238 & 1/U-238
Uncertainty is 1 standard deviation based on counting statistics only

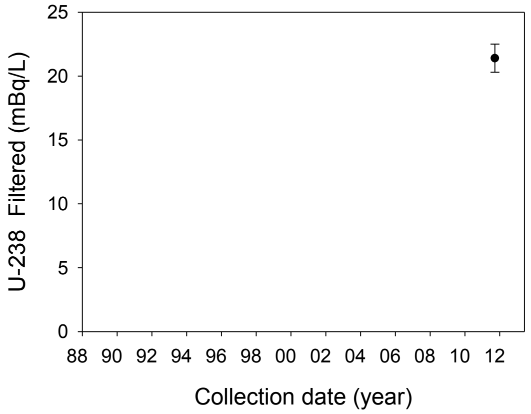
U-238 (alpha spectrometry)

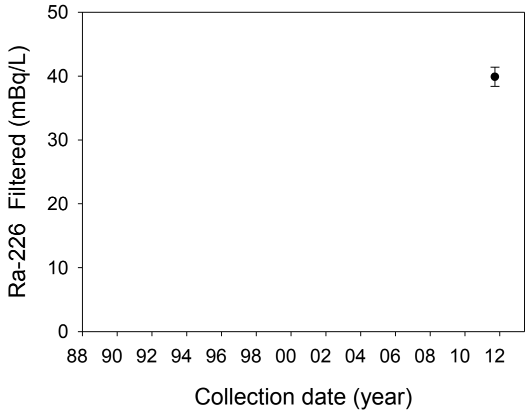
Ra-226 (alpha spectrometry)

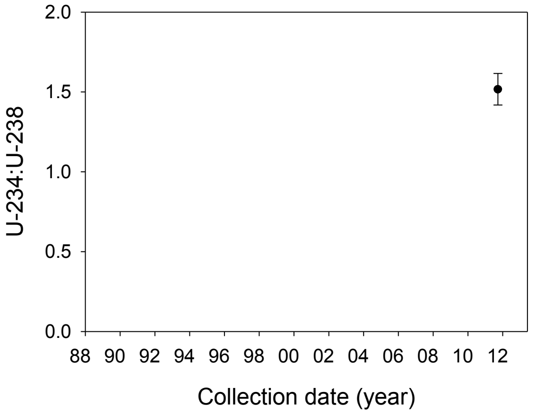
U-234:U-238 (alpha spectrometry)

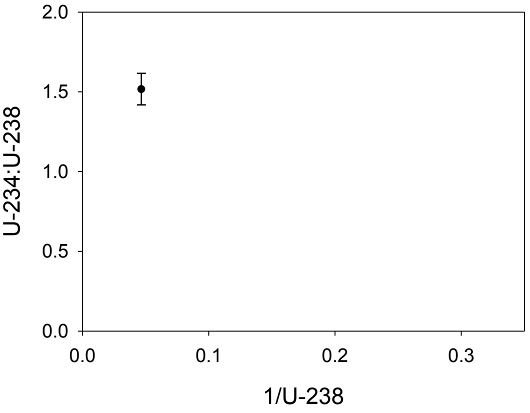
U-234:U-238 vs. 1/U-238

Bore ID – R.P. 79/ 1 Ranger

BORE ID - R.P. 79/ 1 Ranger

Data - U-238, Ra-226, U-234:U-238 & 1/U-238
Uncertainty is 1 standard deviation based on counting statistics only

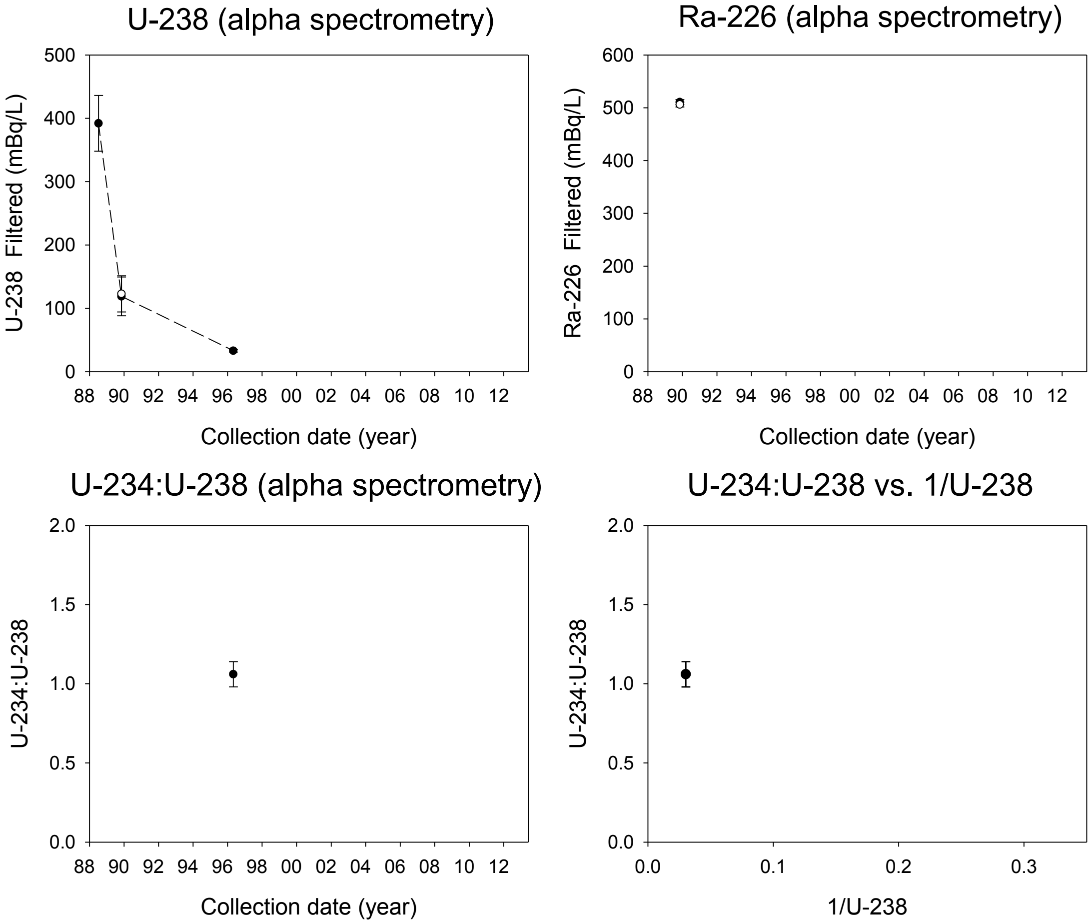

Bore ID – R.P. 79/ 2 Ranger

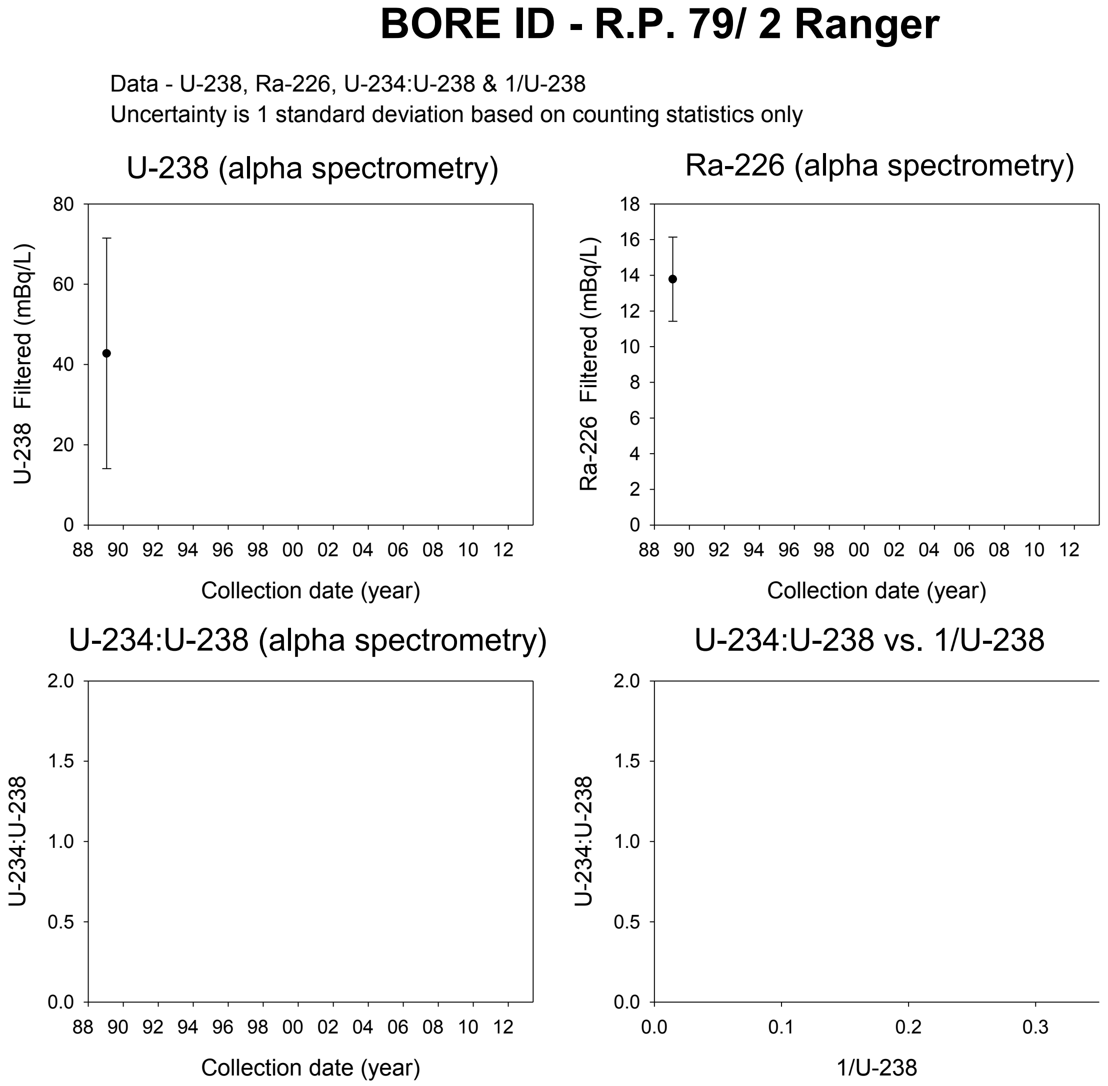

Bore ID – 79/6

BORE ID - 79/6

Data - U-238, Ra-226, U-234:U-238 & 1/U-238
Uncertainty is 1 standard deviation based on counting statistics only

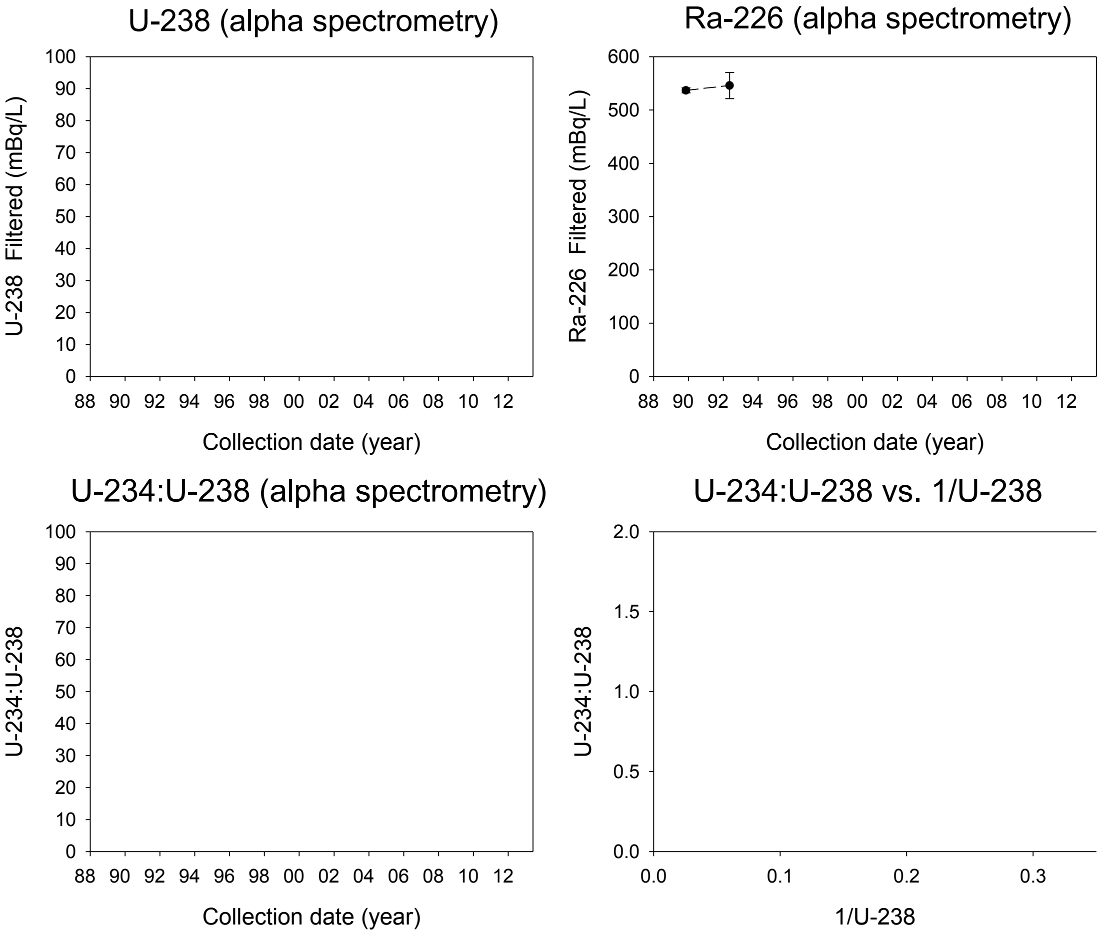

Bore ID – 79/9

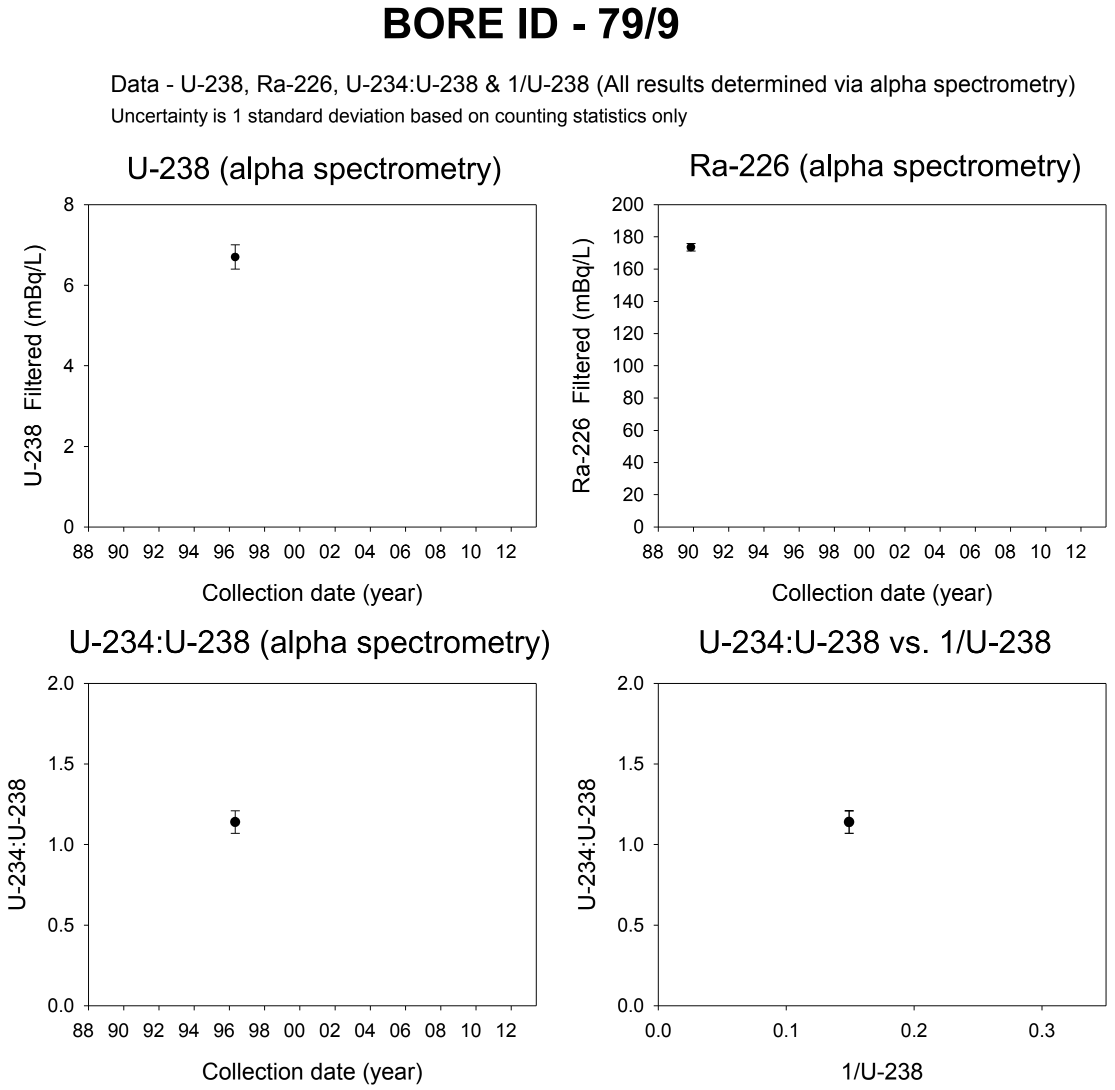
BORE ID - 79/9
Data - U-238, Ra-226, U-234:U-238 & 1/U-238 (All results determined via alpha spectrometry)
Uncertainty is 1 standard deviation based on counting statistics only
U-238 (alpha spectrometry)
U-238 Filtered (mBq/L)
0
2
4
6
8
88 90 92 94 96 98 00 02 04 06 08 10 12
Collection date (year)
Ra-226 (alpha spectrometry)
Ra-226 Filtered (mBq/L)
0
20
40
60
80
100
120
140
160
180
200
88 90 92 94 96 98 00 02 04 06 08 10 12
Collection date (year)
U-234:U-238 (alpha spectrometry)
U-234:U-238
0.0
0.5
1.0
1.5
2.0
88 90 92 94 96 98 00 02 04 06 08 10 12
Collection date (year)
U-234:U-238 vs. 1/U-238
U-234:U-238
0.0
0.5
1.0
1.5
2.0
0.0
0.1
0.2
0.3
1/U-238

Bore ID – 83_1

BORE ID - 83_1

Data - Calcium, Potassium, Magnesium,Sodium and Sulfate

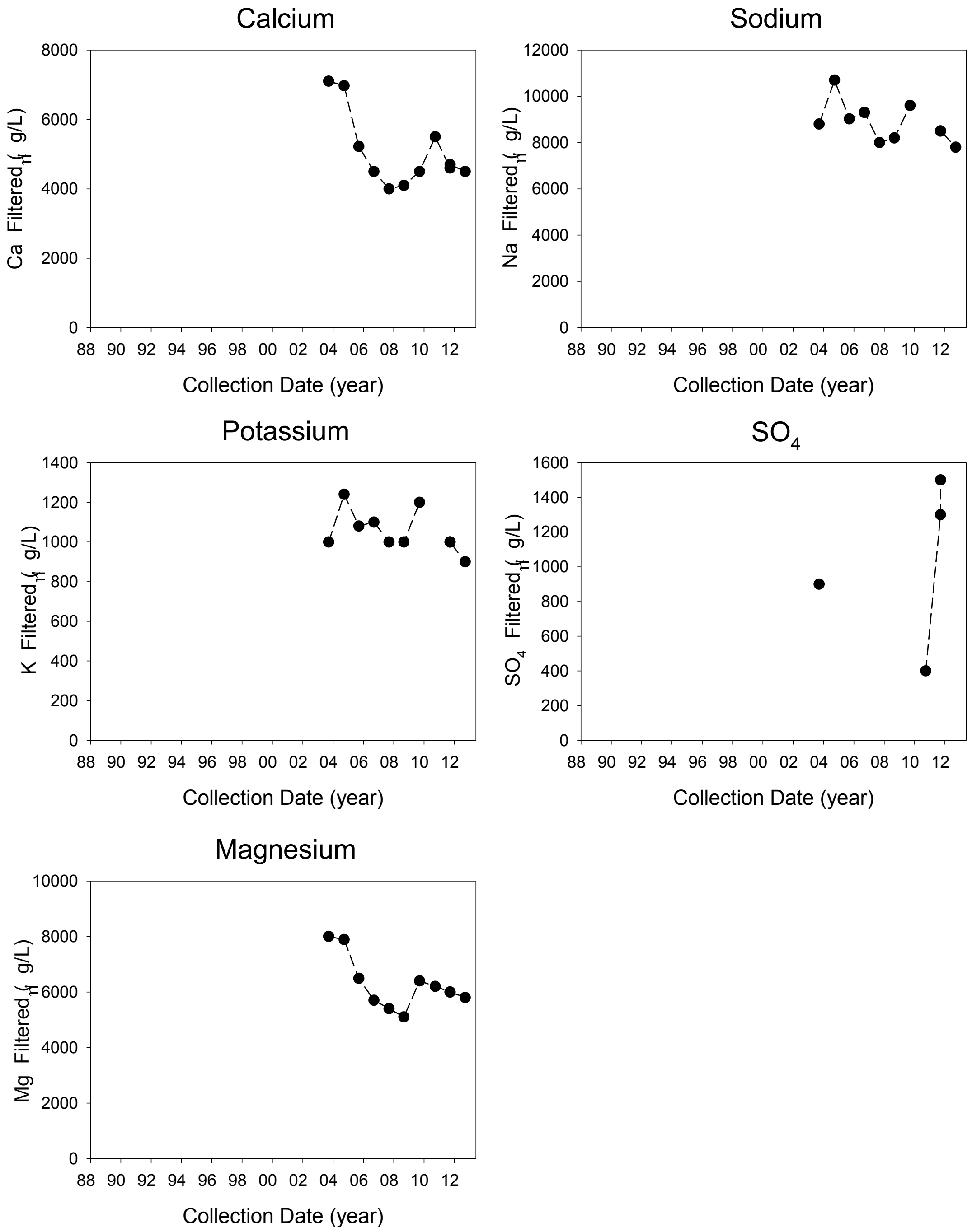

BORE ID - 83_1

Data - Iron, Manganese, Barium, Strontium, Uranium & Vanadium

Iron

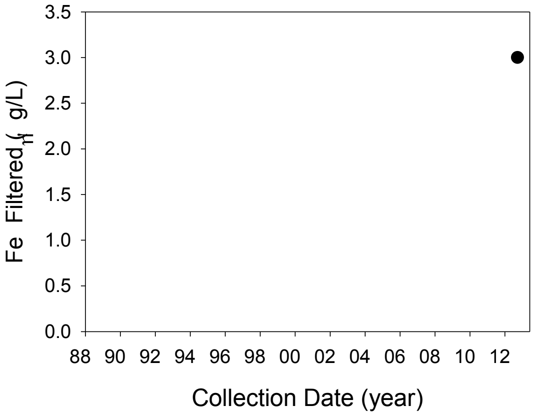

Manganese

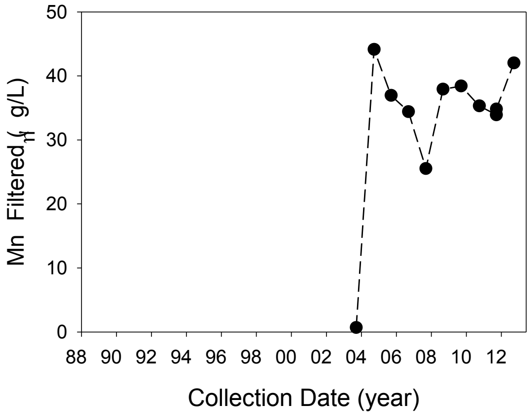

Barium

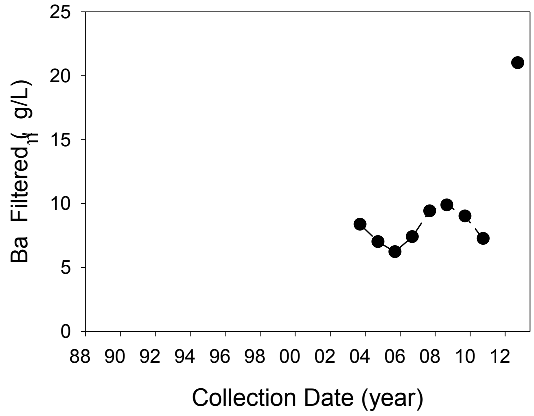

Strontium

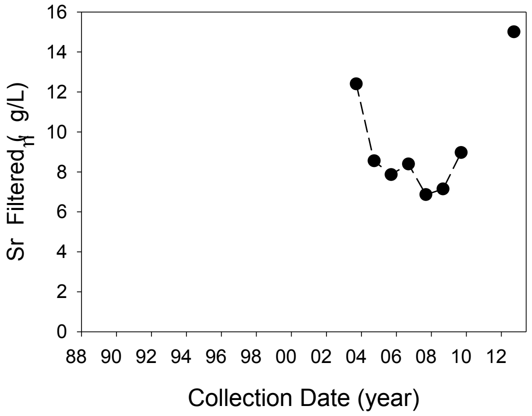

Uranium

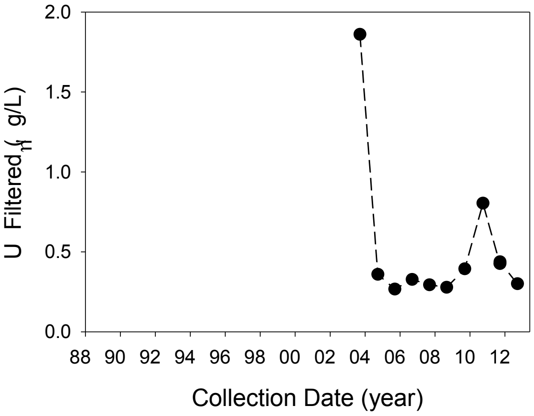

Vanadium

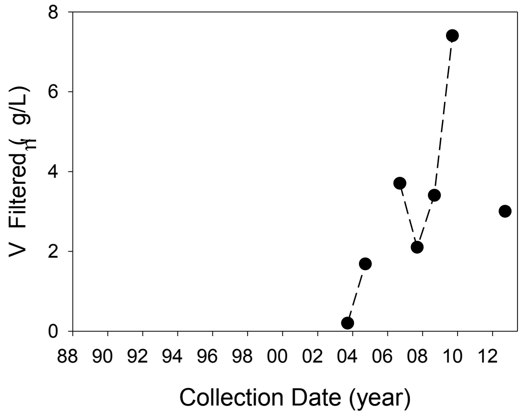

BORE ID - 83_1

Data - U-238, Ra-226, U-234:U-238 & 1/U-238
Uncertainty is 1 standard deviation based on counting statistics only

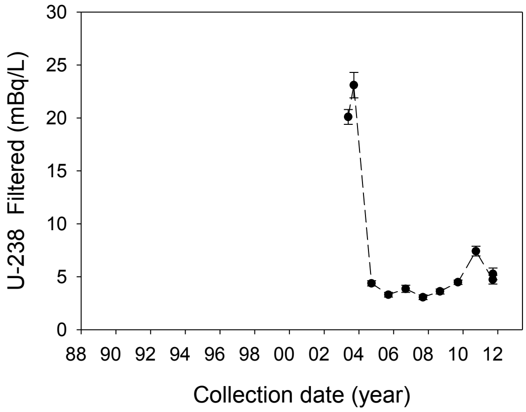
U-238 (alpha spectrometry)

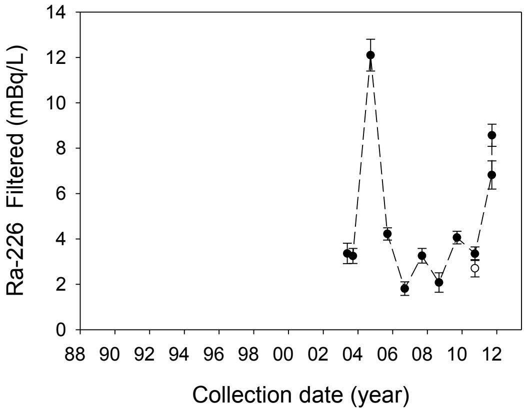
Ra-226 (alpha spectrometry)

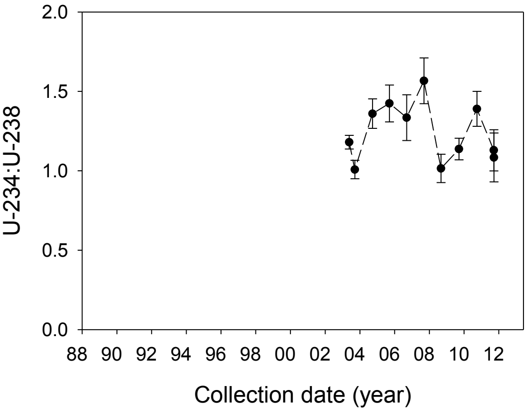
U-234:U-238 (alpha spectrometry)

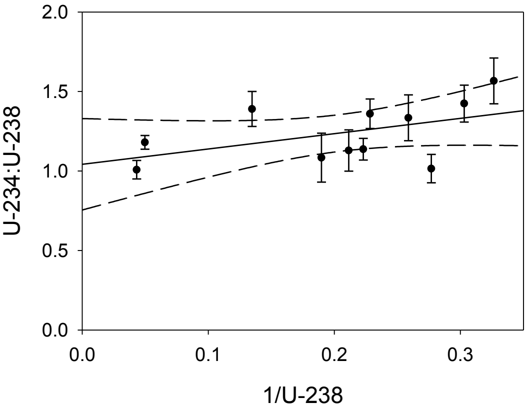
U-234:U-238 vs. 1/U-238

Bore ID – B11

BORE ID - B11

Data - Calcium, Potassium, Magnesium, Sodium and Sulfate

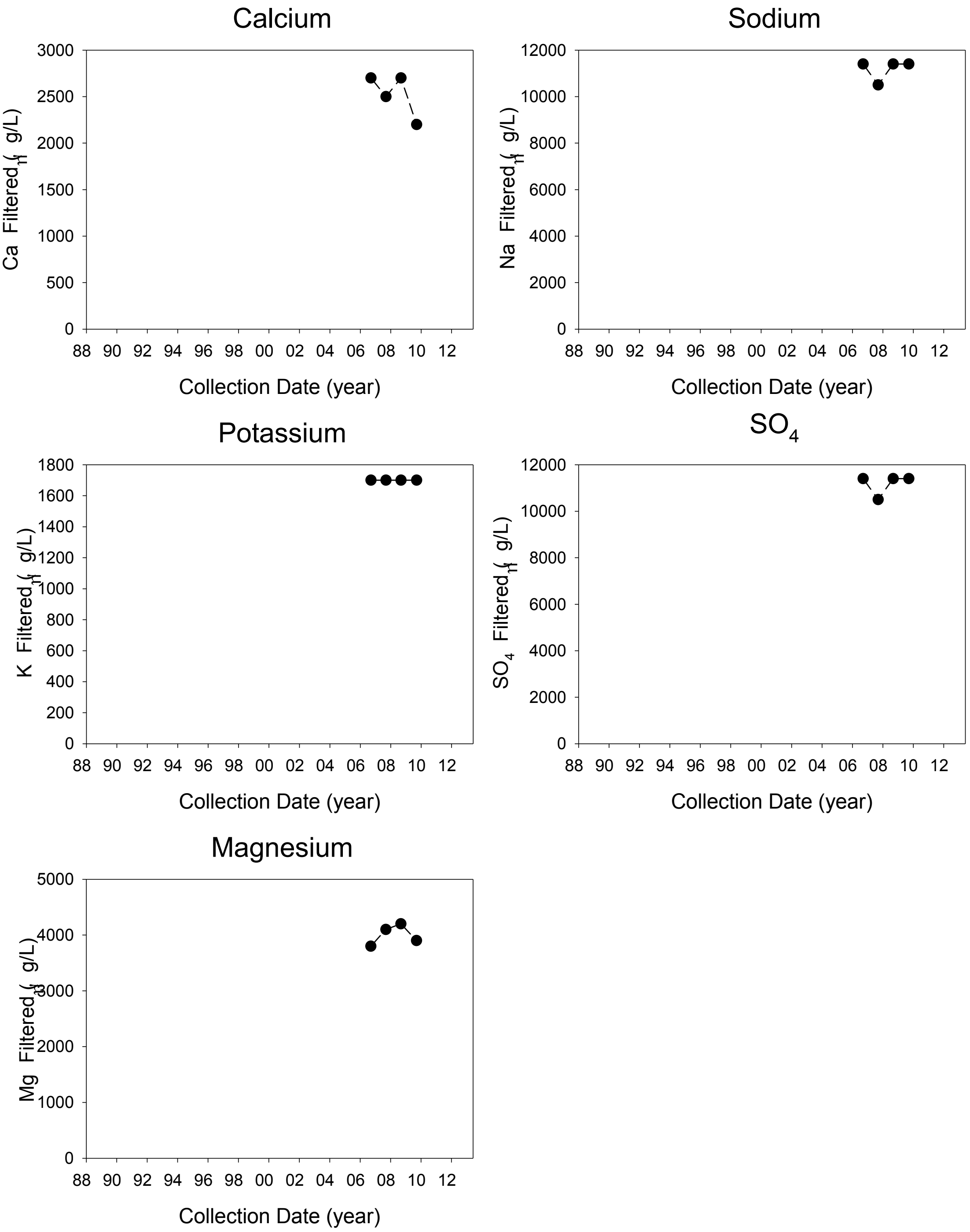

BORE ID - B11

Data - Iron, Manganese, Barium, Strontium, Uranium & Vanadium

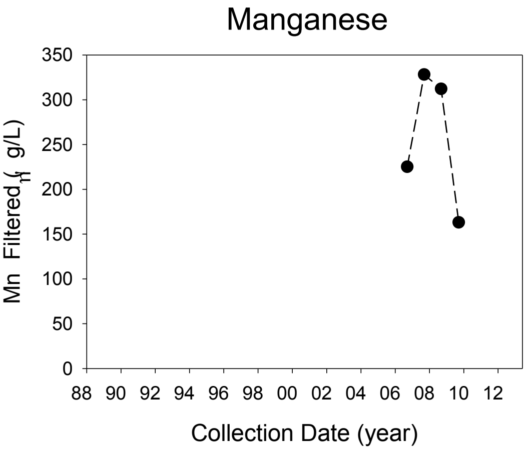

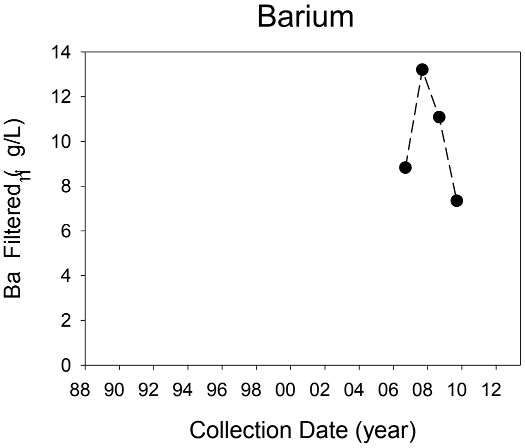

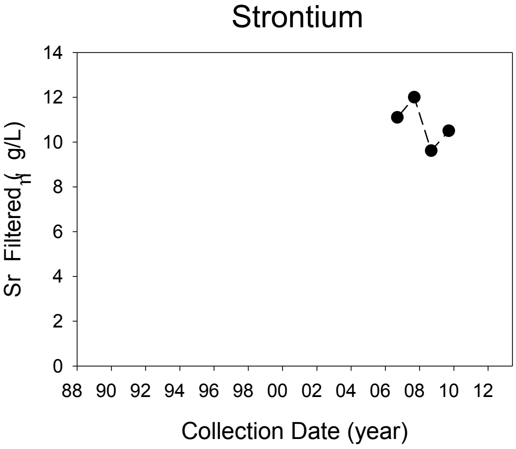

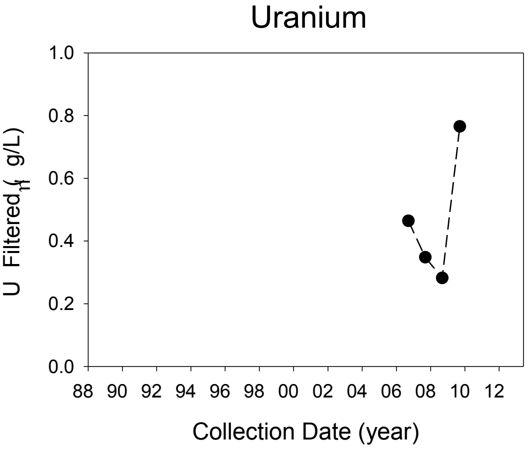

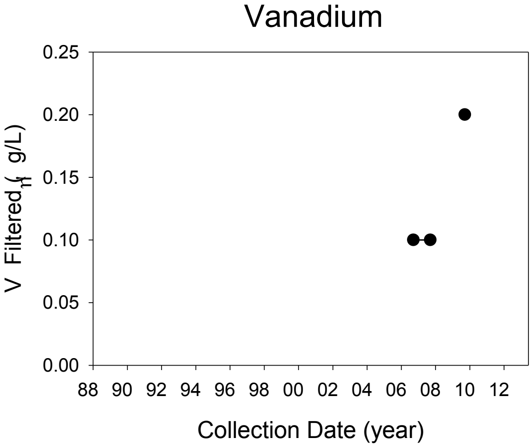

BORE ID - B11

Data - U-238, Ra-226, U-234:U-238 & 1/U-238
Uncertainty is 1 standard deviation based on counting statistics only

U-238 (alpha spectrometry)

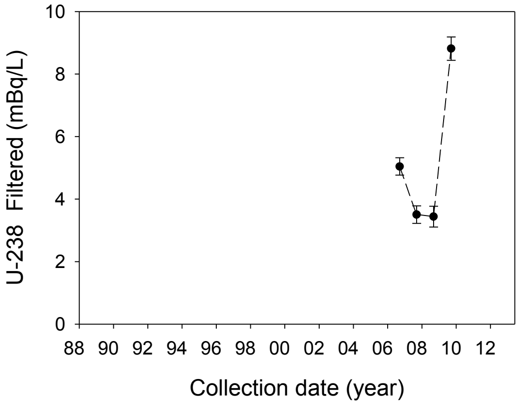

Ra-226 (alpha spectrometry)

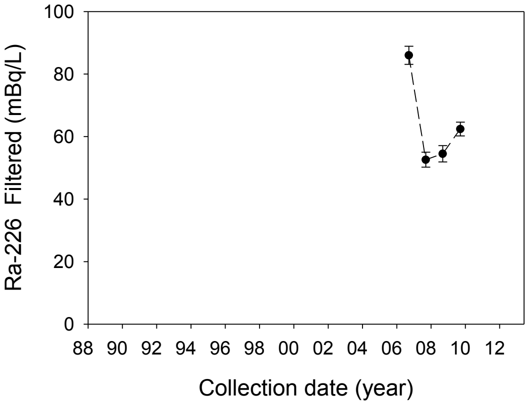

U-234:U-238 (alpha spectrometry)

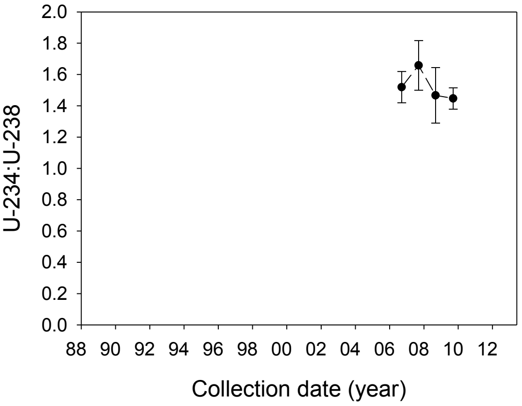

U-234:U-238 vs. 1/U-238

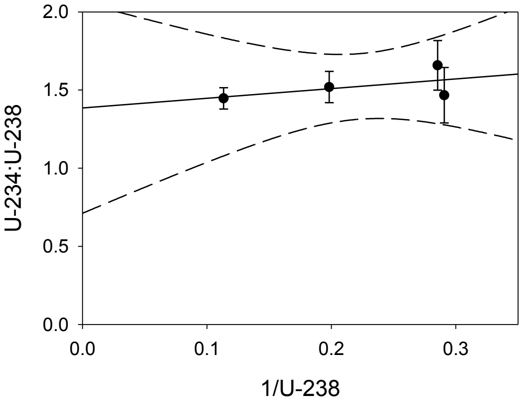

Bore ID – C12

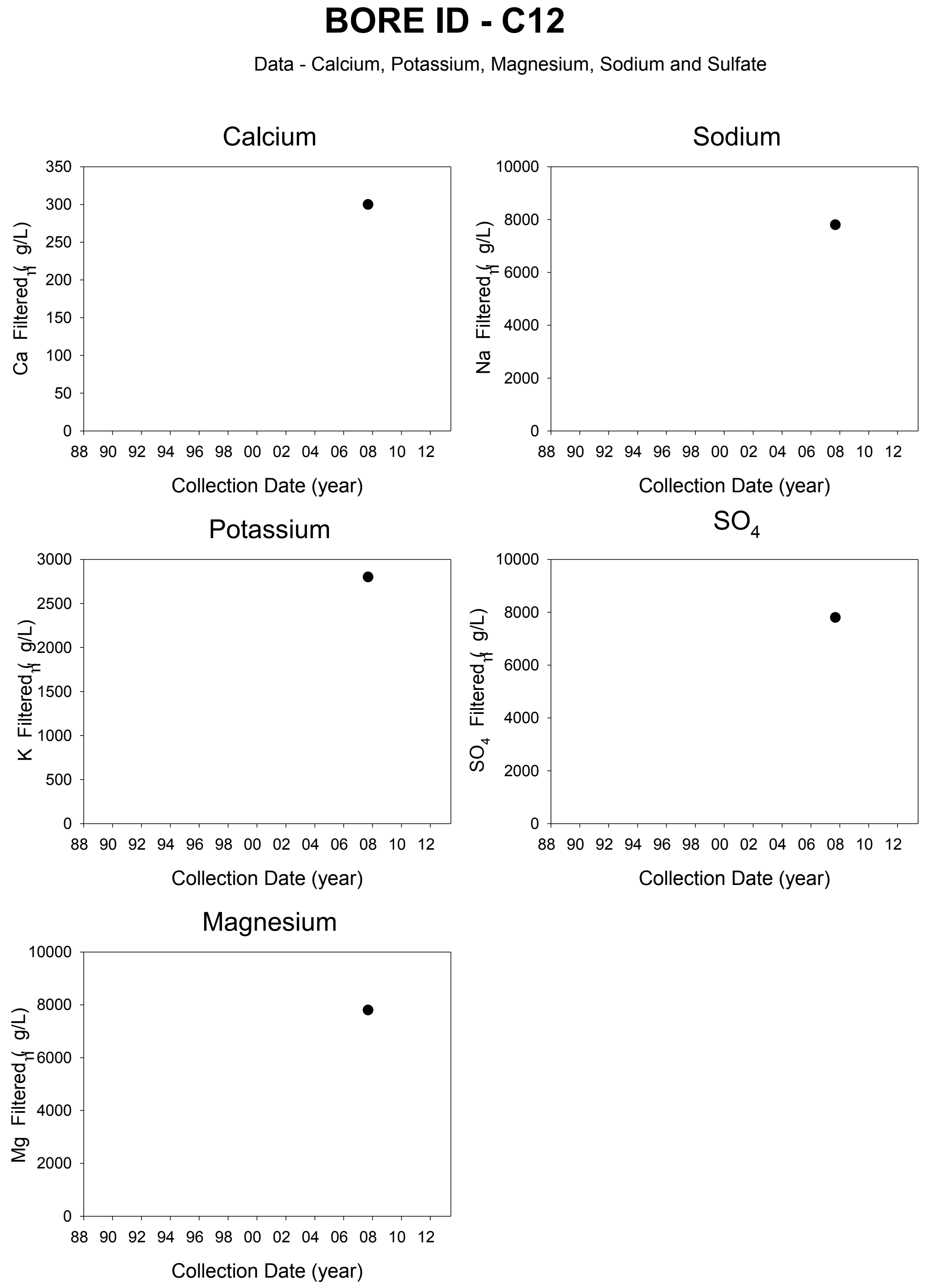

BORE ID - C12

Data - Calcium, Potassium, Magnesium, Sodium and Sulfate

BORE ID - C12

Data - Iron, Manganese, Barium, Strontium, Uranium & Vanadium

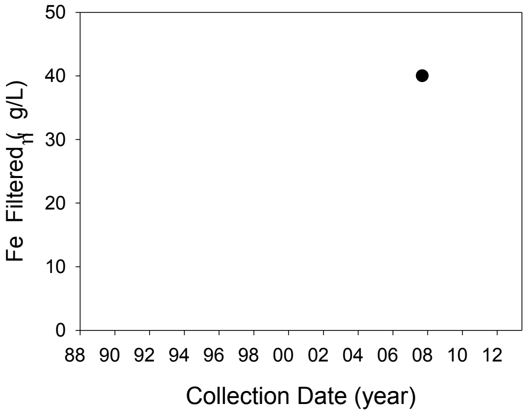
Iron

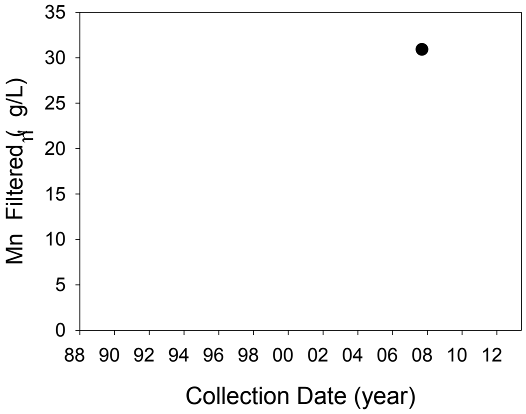
Manganese

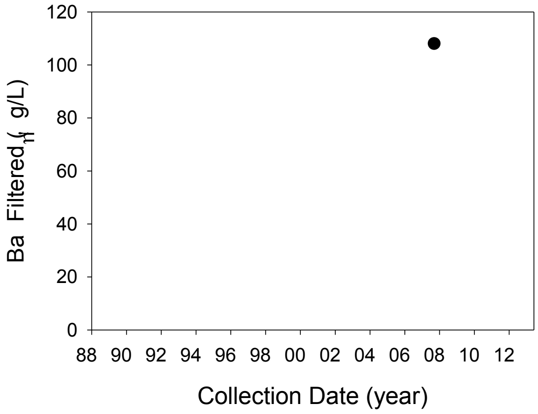
Barium

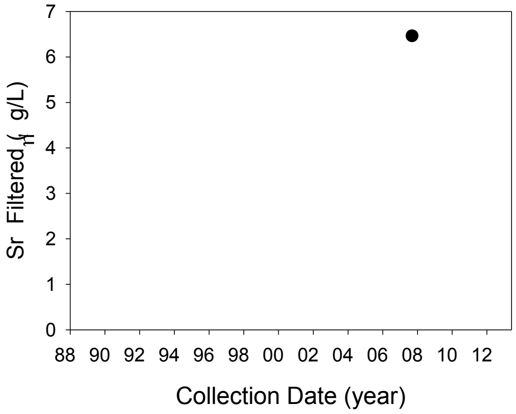
Strontium

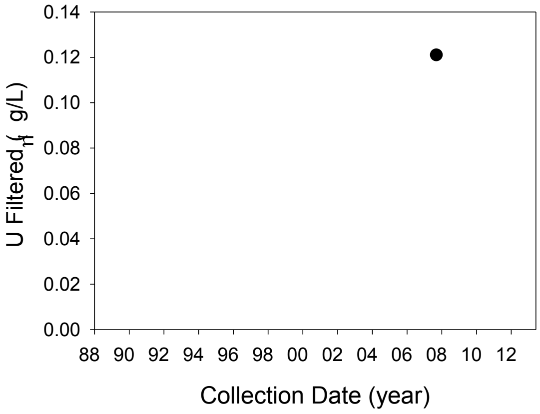
Uranium

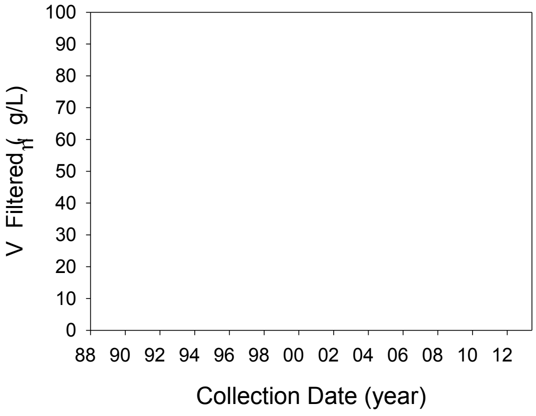
Vanadium

BORE ID - C12

Data - U-238, Ra-226, U-234:U-238 & 1/U-238
Uncertainty is 1 standard deviation based on counting statistics only

U-238 (alpha spectrometry)

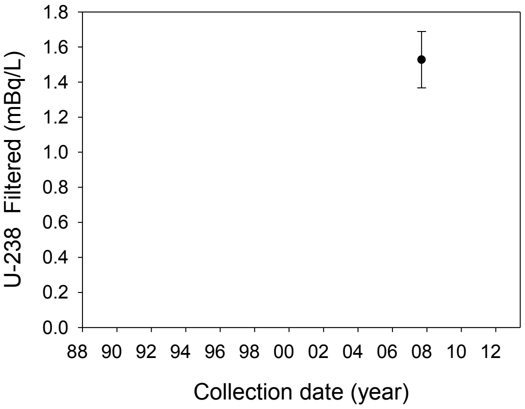

Ra-226 (alpha spectrometry)

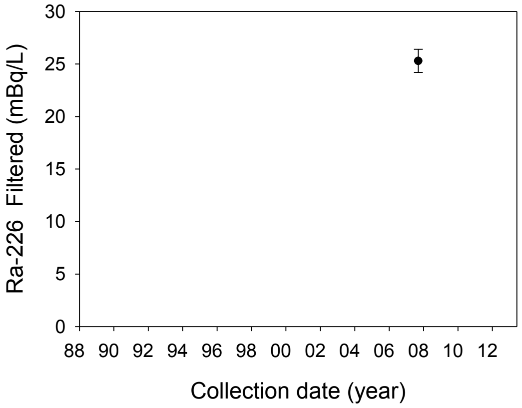

U-234:U-238 (alpha spectrometry)

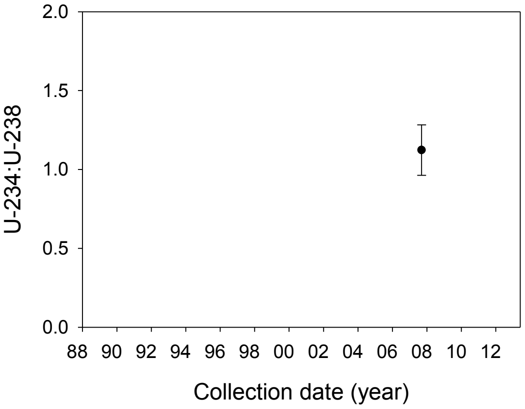

U-234:U-238 vs. 1/U-238

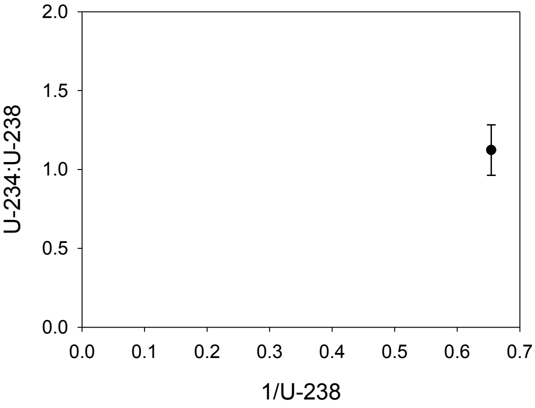

Bore ID – C1_Shallow

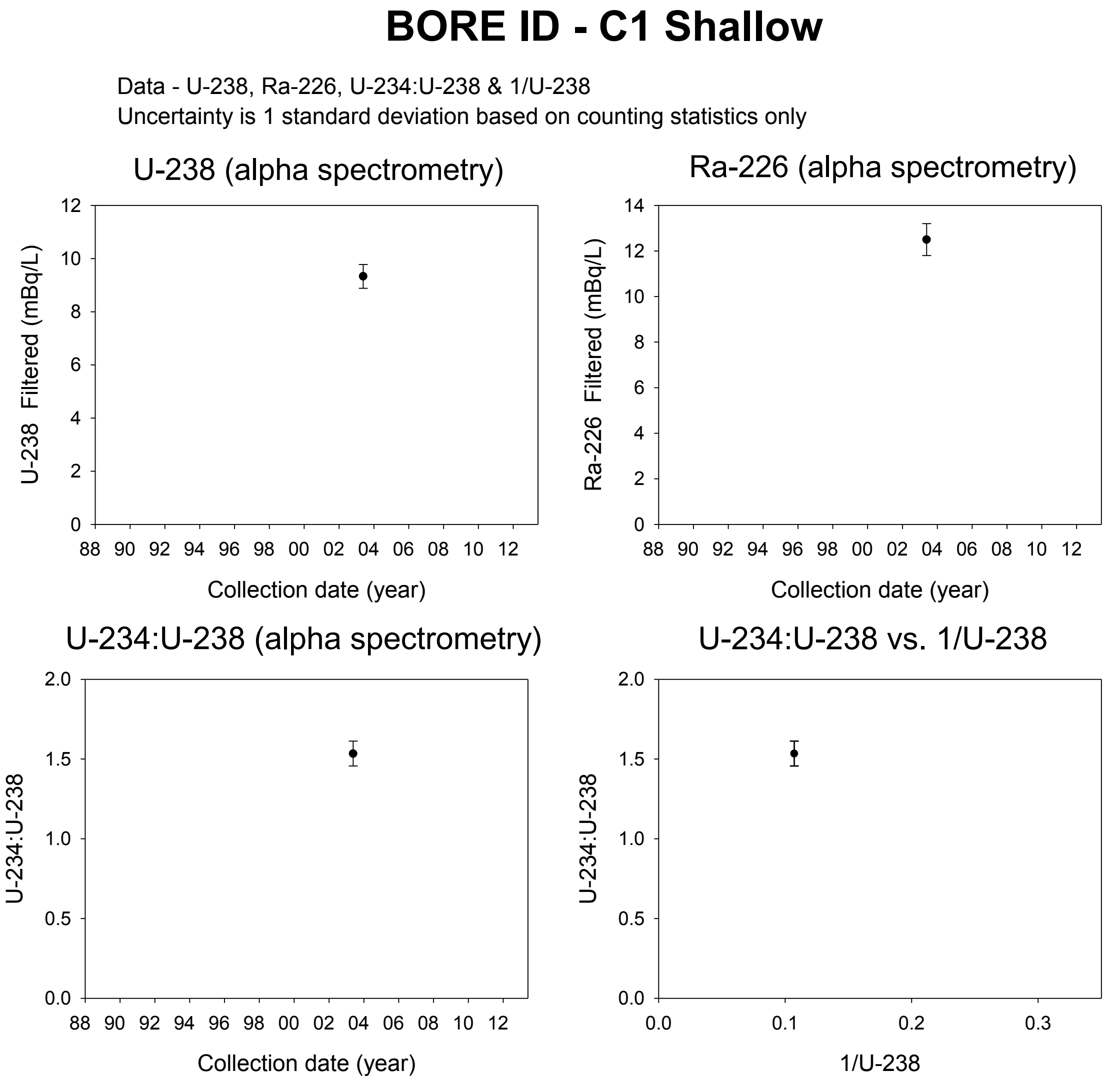

Bore ID – Magela Ck 11/80

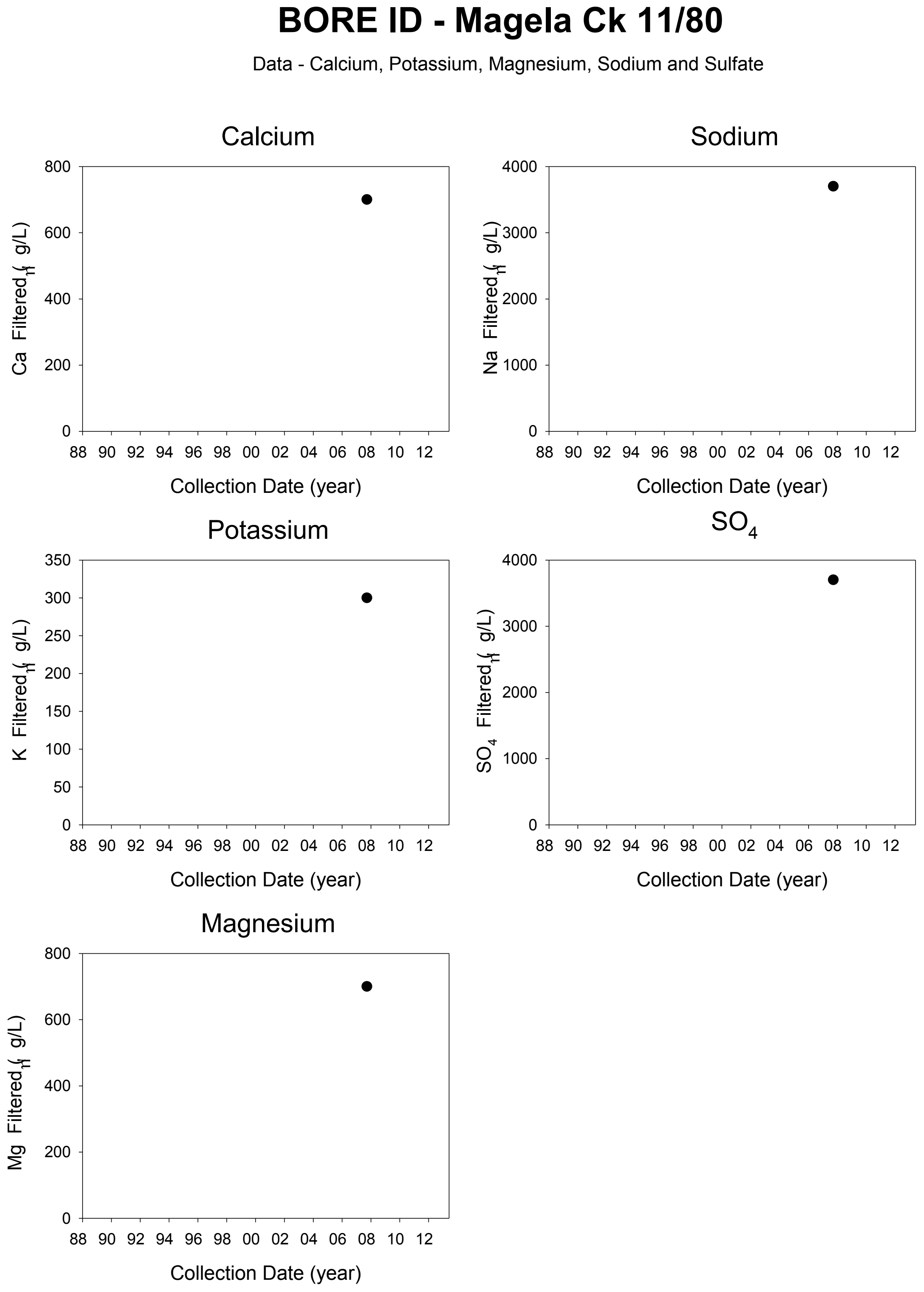

BORE ID - Magela Ck 11/80

Data - Iron, Manganese, Barium, Strontium, Uranium & Vanadium

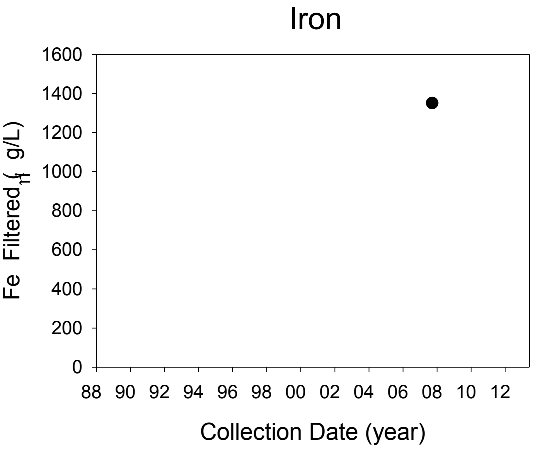
Iron

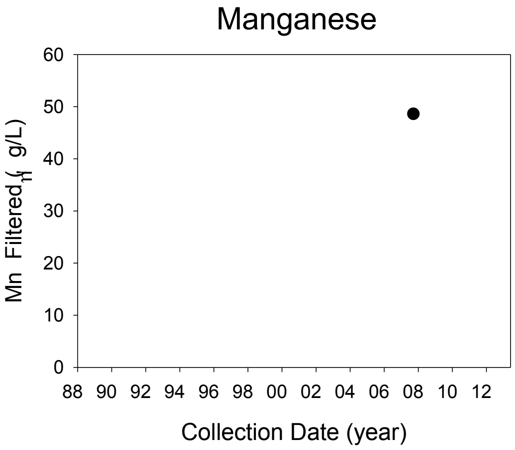
Manganese

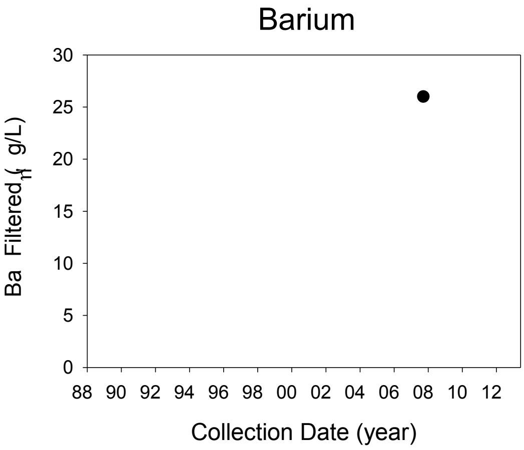
Barium

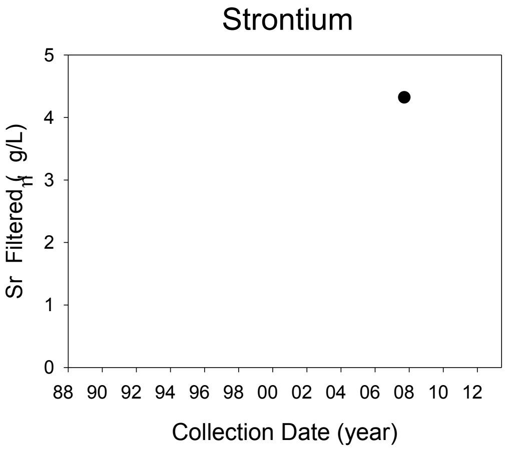
Strontium

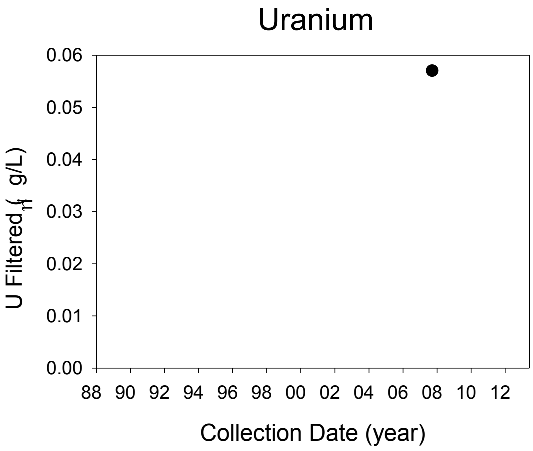
Uranium

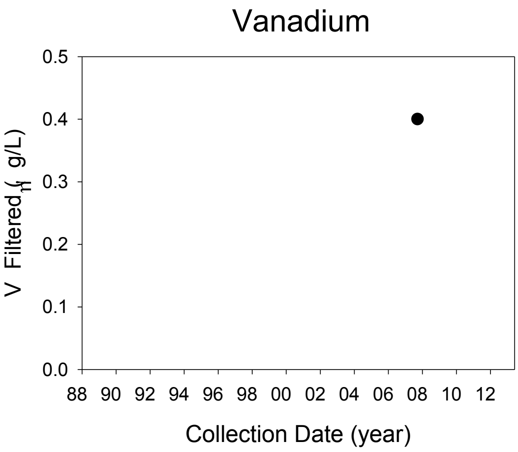
Vanadium

BORE ID - Magela Ck 11/80

Data - U-238, Ra-226, U-234:U-238 & 1/U-238
Uncertainty is 1 standard deviation based on counting statistics only

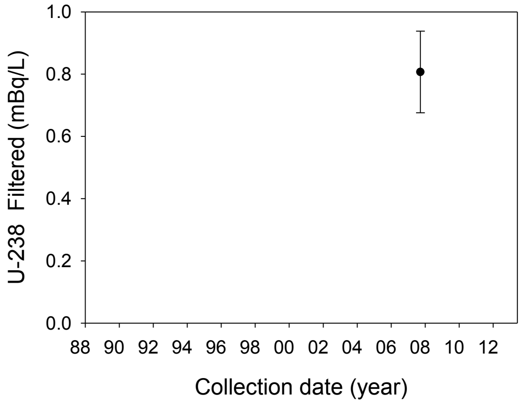
U-238 (alpha spectrometry)

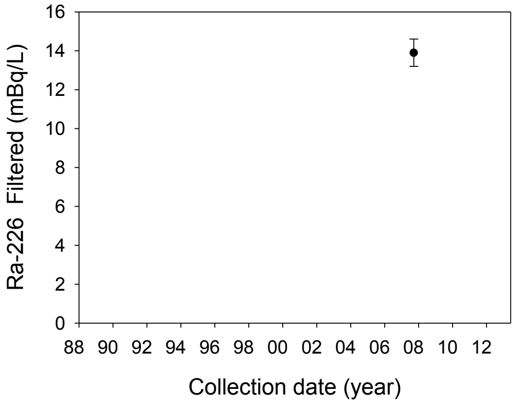
Ra-226 (alpha spectrometry)

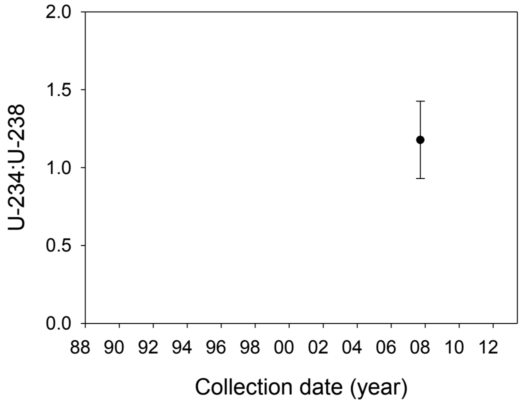
U-234:U-238 (alpha spectrometry)

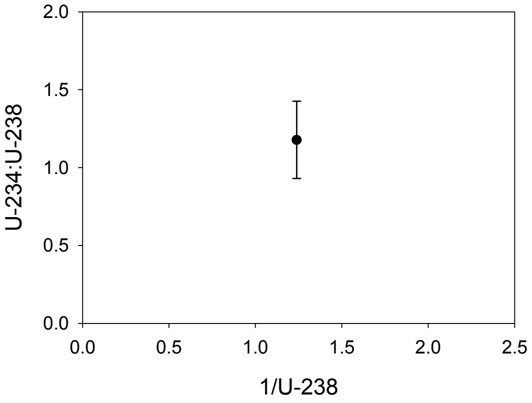
U-234:U-238 vs. 1/U-238

Bore ID – MBH

BORE ID - MBH

Data - U-238, Ra-226, U-234:U-238 & 1/U-238
Uncertainty is 1 standard deviation based on counting statistics only

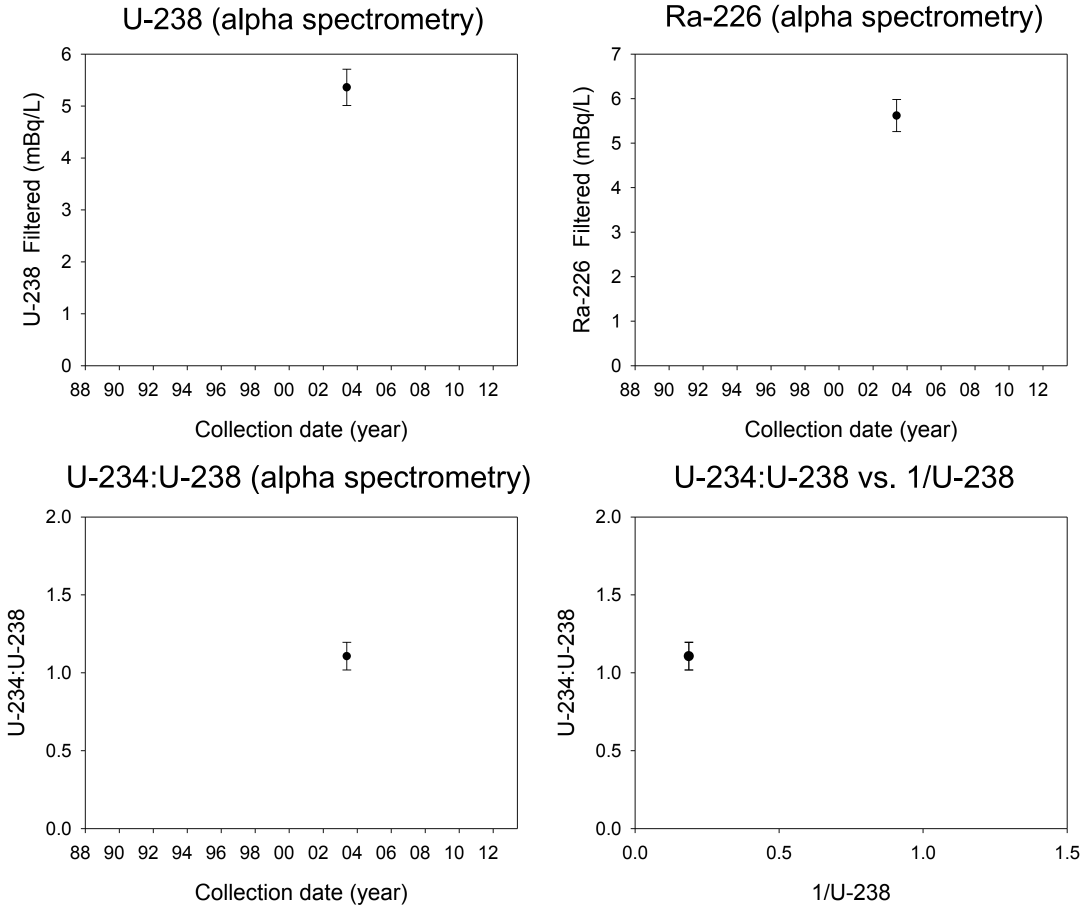

U-238 (alpha spectrometry)

Ra-226 (alpha spectrometry)

U-234:U-238 (alpha spectrometry)

U-234:U-238 vs. 1/U-238

Bore ID – MBL

BORE ID - MBL

Data - U-238, Ra-226, U-234:U-238 & 1/U-238
Uncertainty is 1 standard deviation based on counting statistics only

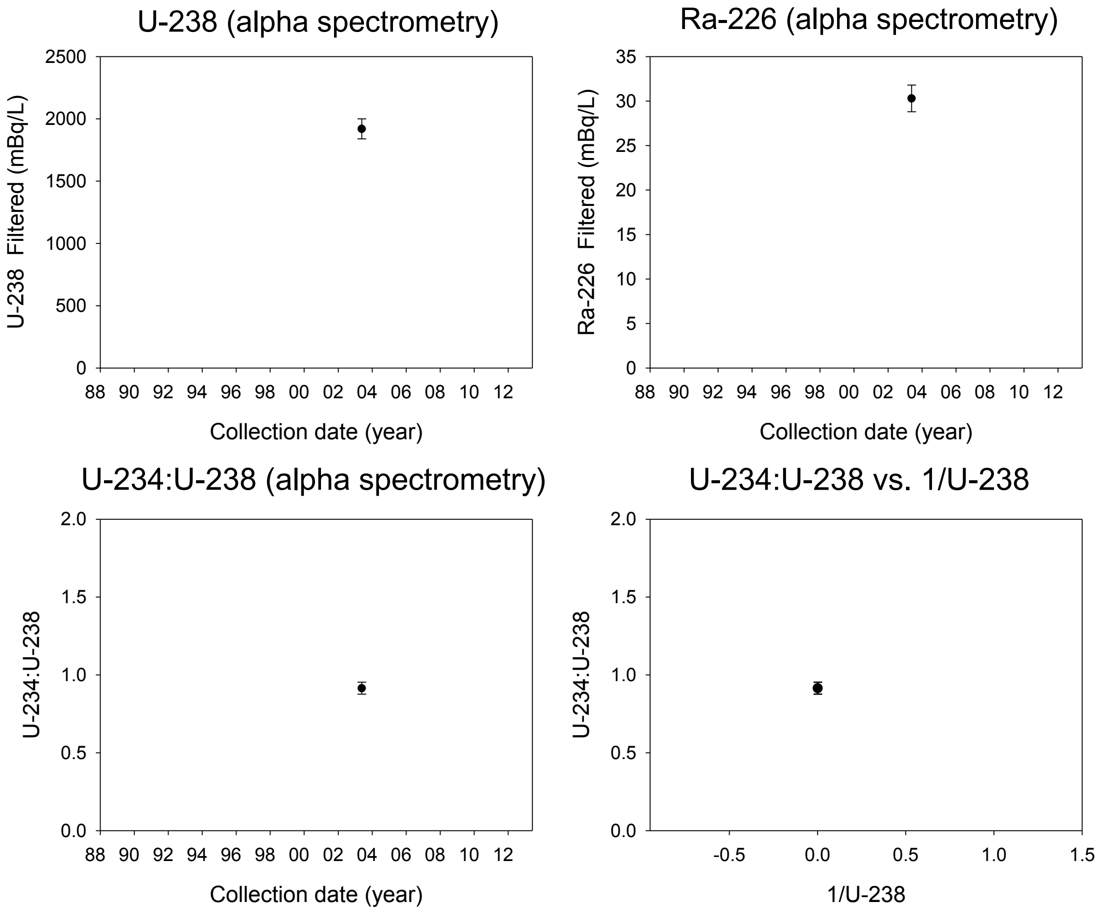

Bore ID – MC24

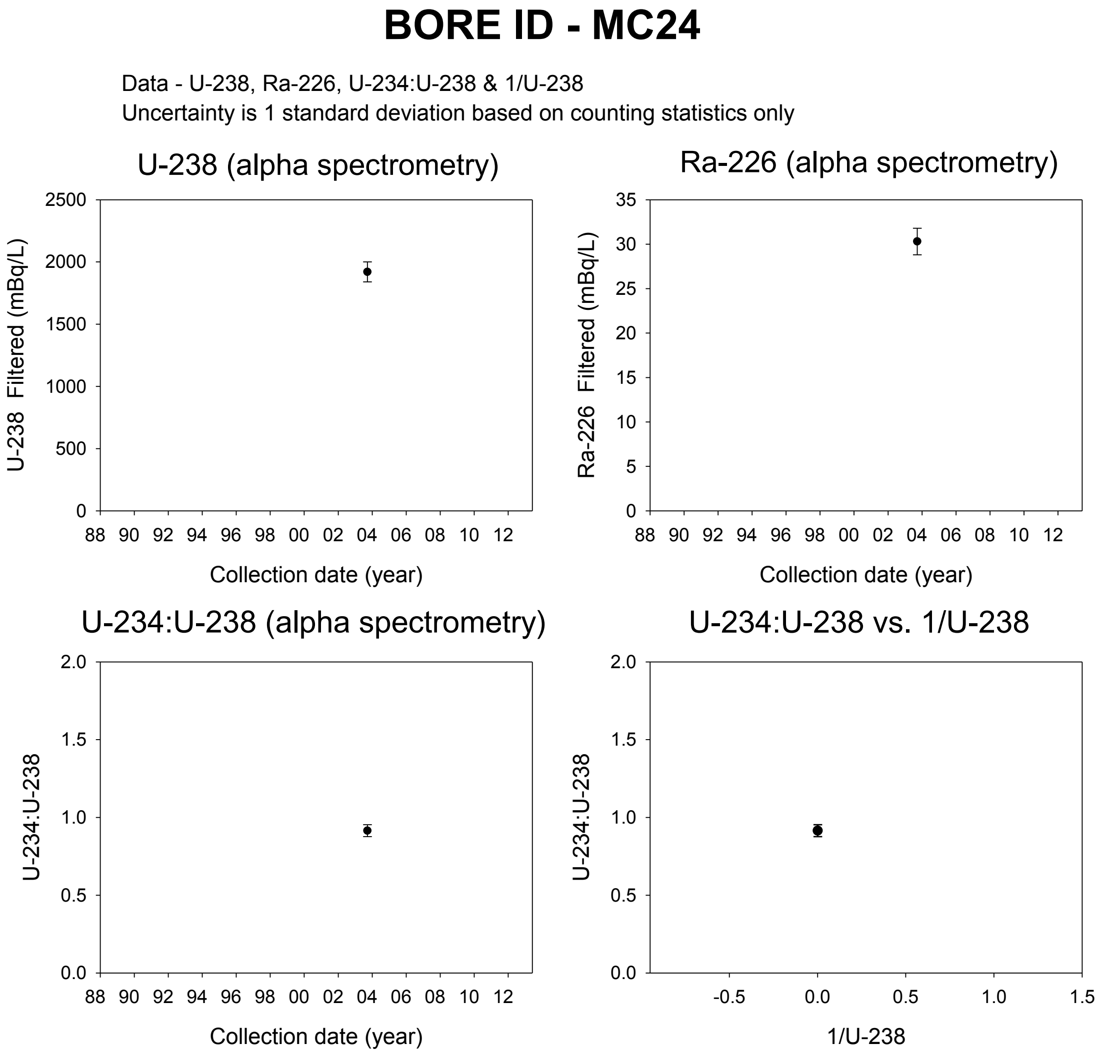
BORE ID - MC24
Data - U-238, Ra-226, U-234:U-238 & 1/U-238
Uncertainty is 1 standard deviation based on counting statistics only
U-238 (alpha spectrometry)
U-238 Filtered (mBq/L)
2500
2000
1500
1000
500
0
88 90 92 94 96 98 00 02 04 06 08 10 12
Collection date (year)
Ra-226 (alpha spectrometry)
Ra-226 Filtered (mBq/L)
35
30
25
20
15
10
5
0
88 90 92 94 96 98 00 02 04 06 08 10 12
Collection date (year)
U-234:U-238 (alpha spectrometry)
U-234:U-238
2.0
1.5
1.0
0.5
0.0
88 90 92 94 96 98 00 02 04 06 08 10 12
Collection date (year)
U-234:U-238 vs. 1/U-238
U-234:U-238
2.0
1.5
1.0
0.5
0.0
-0.5
0.0
0.5
1.0
1.5
1/U-238

Bore ID – MC27

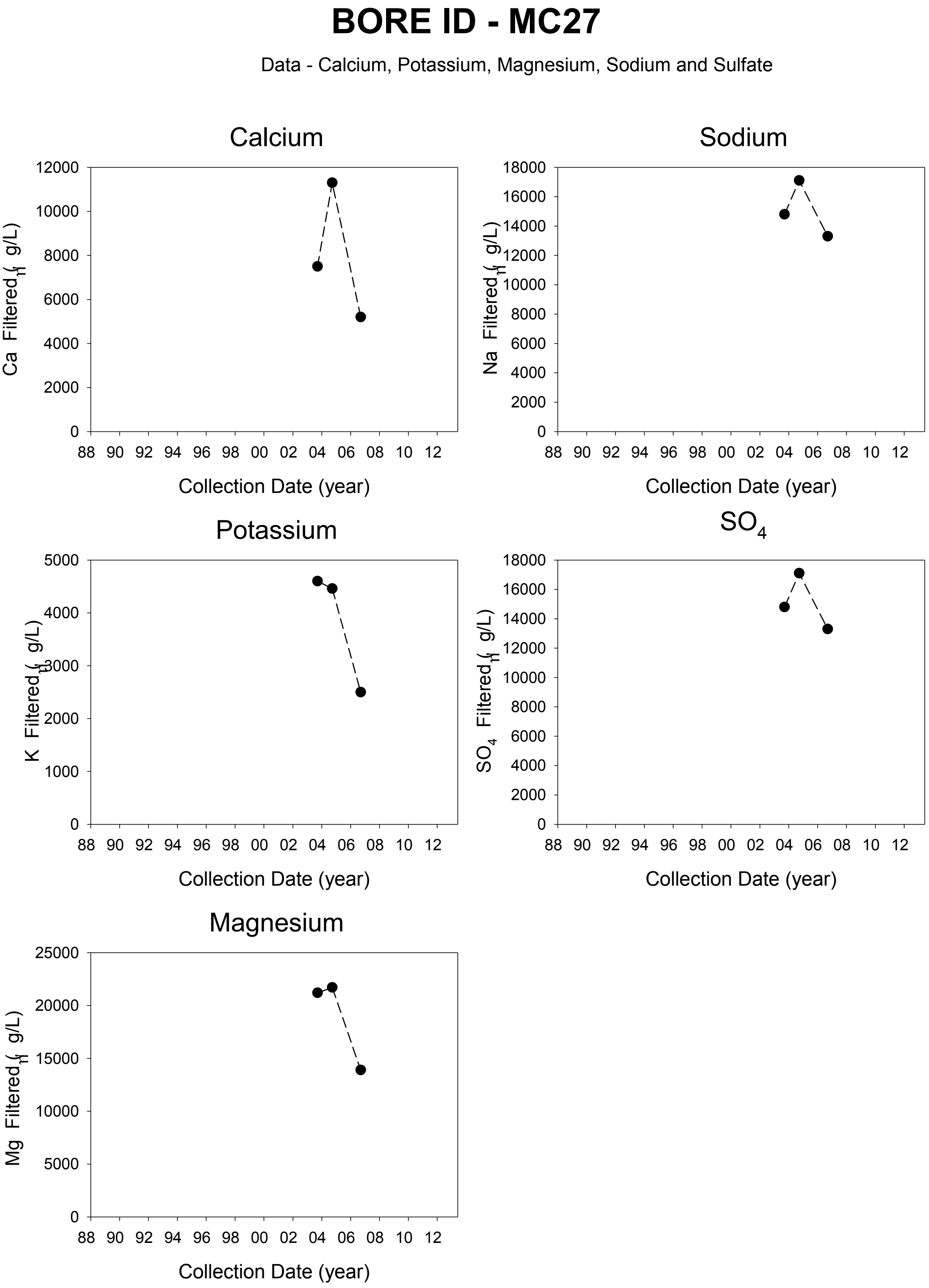
BORE ID - MC27
Data - Calcium, Potassium, Magnesium, Sodium and Sulfate
Calcium
Ca Filtered (µg/L)
0
2000
4000
6000
8000
10000
12000
Sodium
Na Filtered (µg/L)
0
2000
4000
6000
8000
10000
12000
14000
16000
18000
Potassium
K Filtered (µg/L)
0
1000
2000
3000
4000
5000
SO4
SO4 Filtered (µg/L)
0
2000
4000
6000
8000
10000
12000
14000
16000
18000
Magnesium
Mg Filtered (µg/L)
0
5000
10000
15000
20000
25000
88
90
92
94
96
98
00
02
04
06
08
10
12
Collection Date (year)

BORE ID - MC27

Data - Iron, Manganese, Barium, Strontium, Uranium & Vanadium

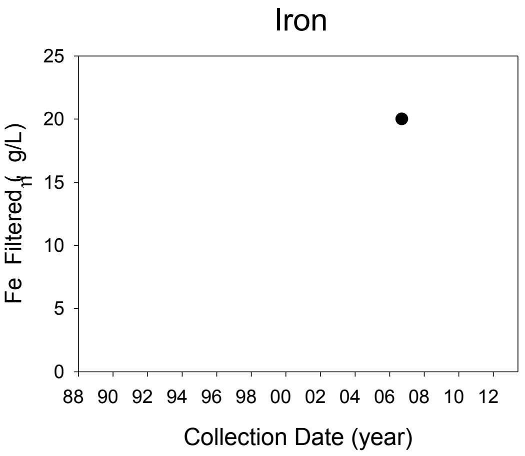

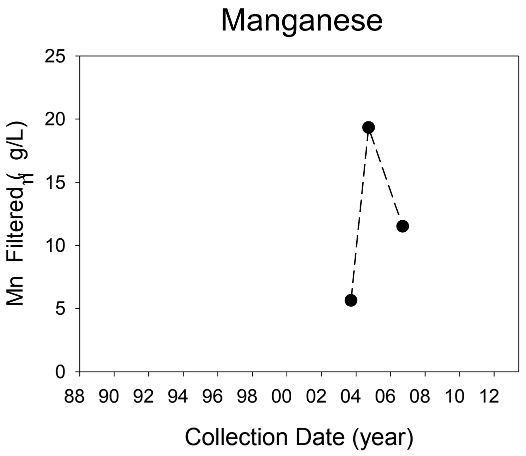

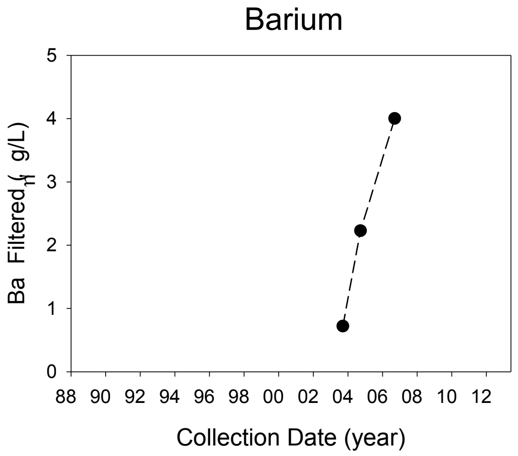

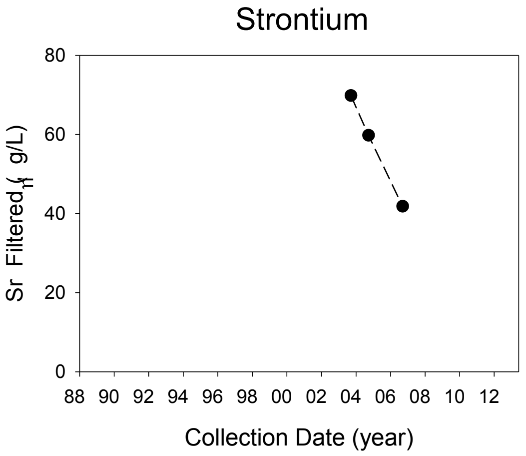

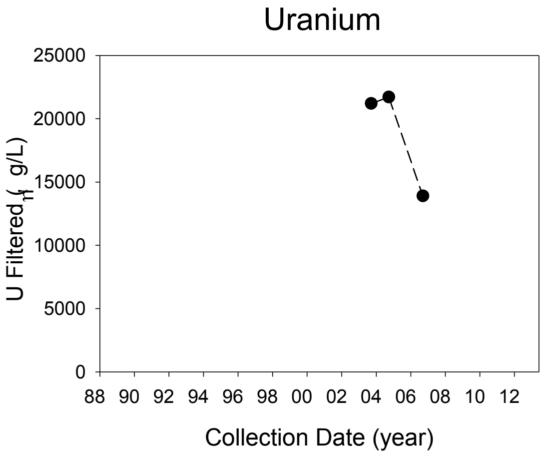

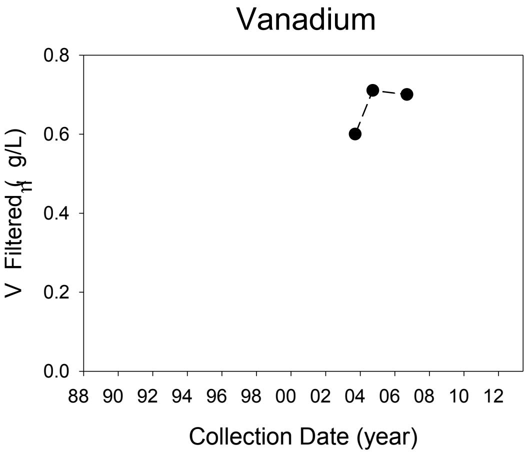

BORE ID - MC27

Data - U-238, Ra-226, U-234:U-238 & 1/U-238
Uncertainty is 1 standard deviation based on counting statistics only

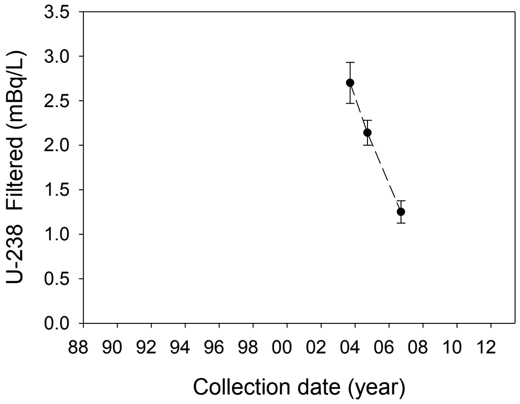
U-238 (alpha spectrometry)

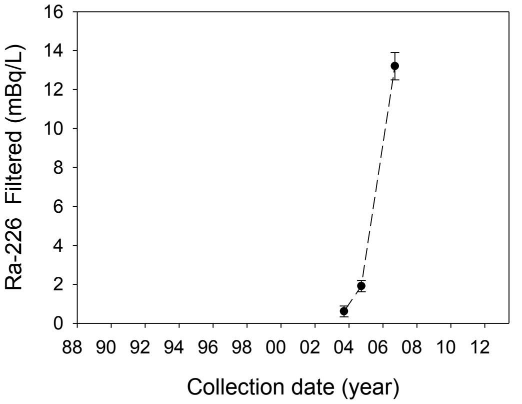
Ra-226 (alpha spectrometry)

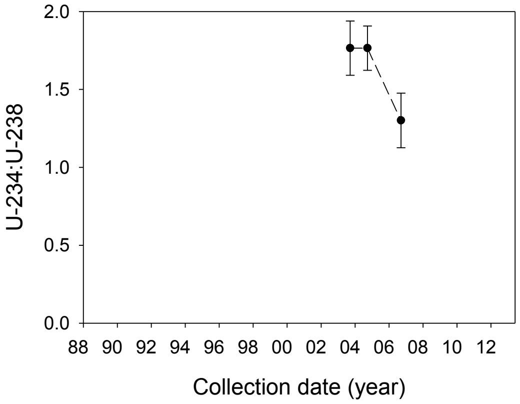
U-234:U-238 (alpha spectrometry)

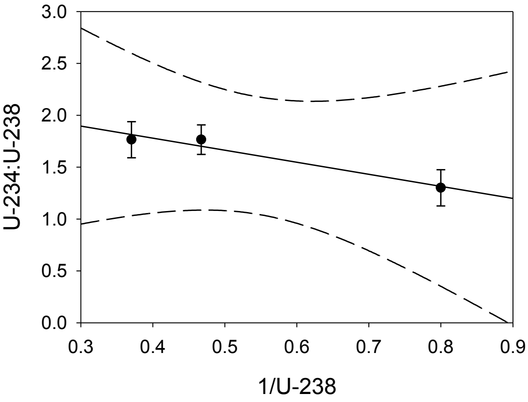
U-234:U-238 vs. 1/U-238

Bore ID – OB10A

BORE ID - OB10A

Data - Calcium, Potassium, Magnesium, Sodium and Sulfate

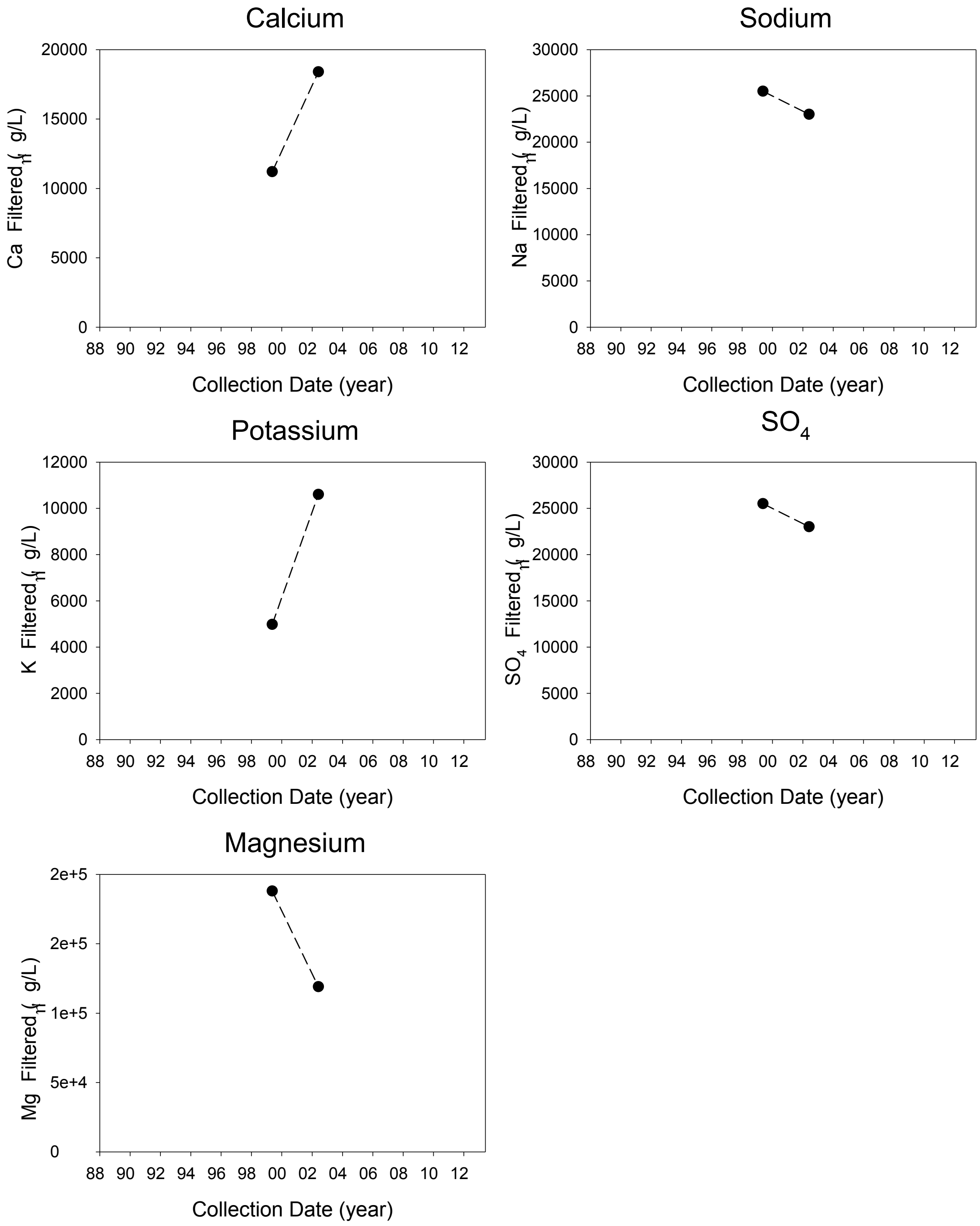

BORE ID - OB10A

Data - Iron, Manganese, Barium, Strontium, Uranium & Vanadium

Iron

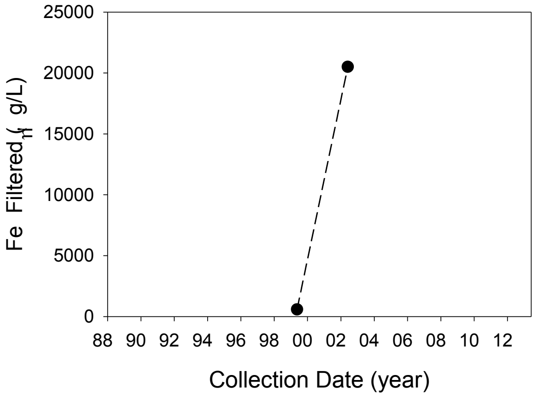

Manganese

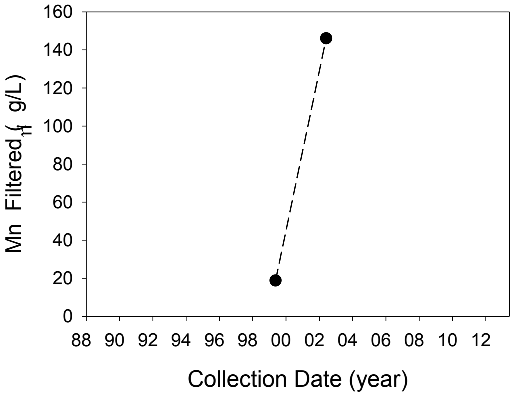

Barium

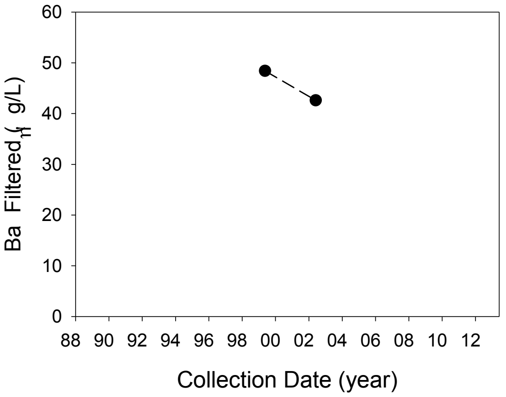

Strontium

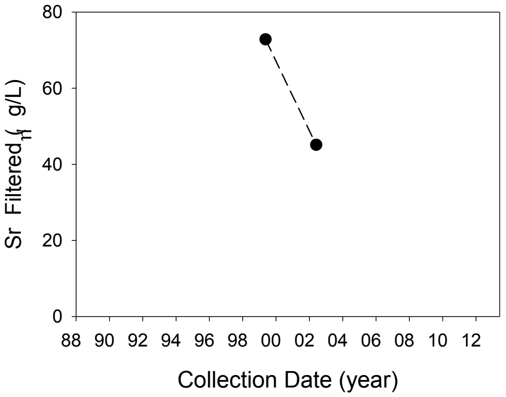

Uranium

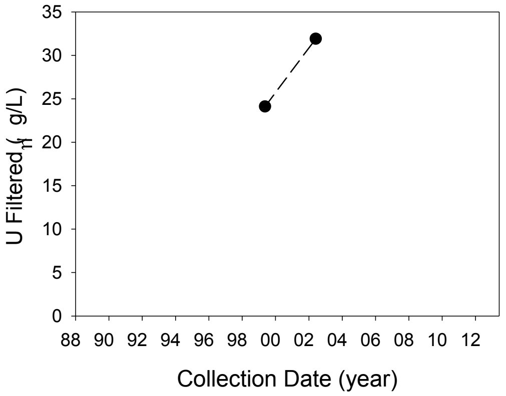

Vanadium

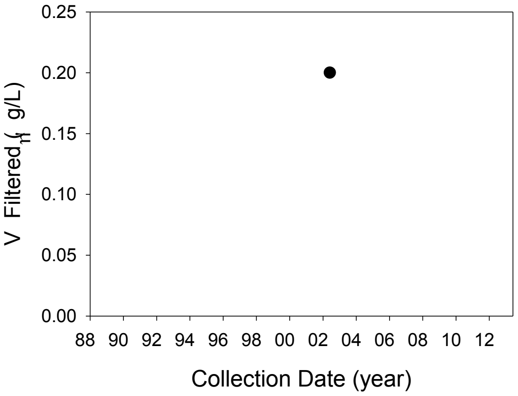

BORE ID - OB10A

Data - U-238, Ra-226, U-234:U-238 & 1/U-238
Uncertainty is 1 standard deviation based on counting statistics only

U-238 (alpha spectrometry)

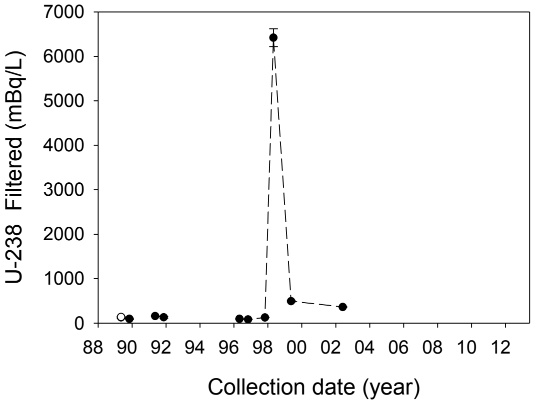

Ra-226 (alpha spectrometry)

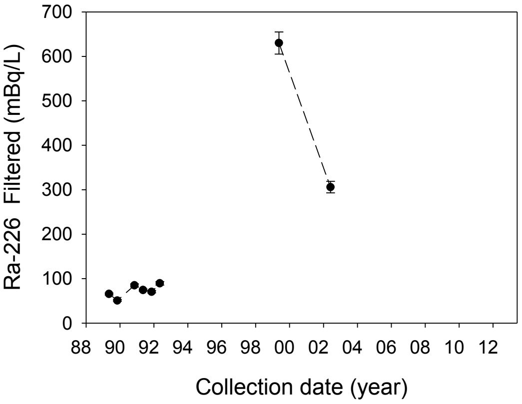

U-234:U-238 (alpha spectrometry)

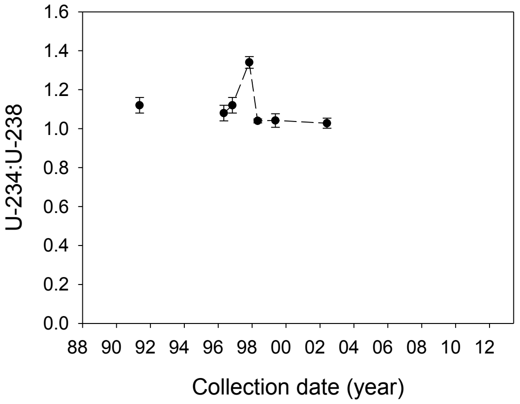

U-234:U-238 vs. 1/U-238

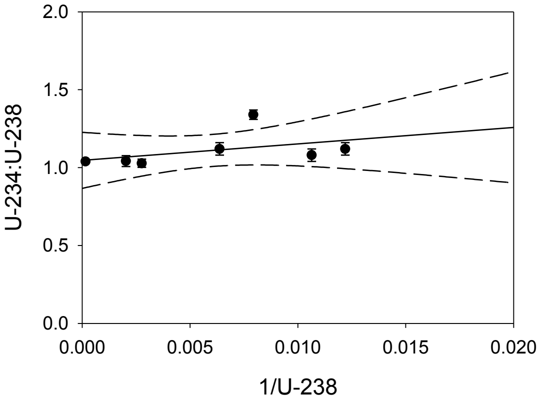

Bore ID – OB11A

BORE ID - OB11A

Data - U-238, Ra-226, U-234:U-238 & 1/U-238
Uncertainty is 1 standard deviation based on counting statistics only

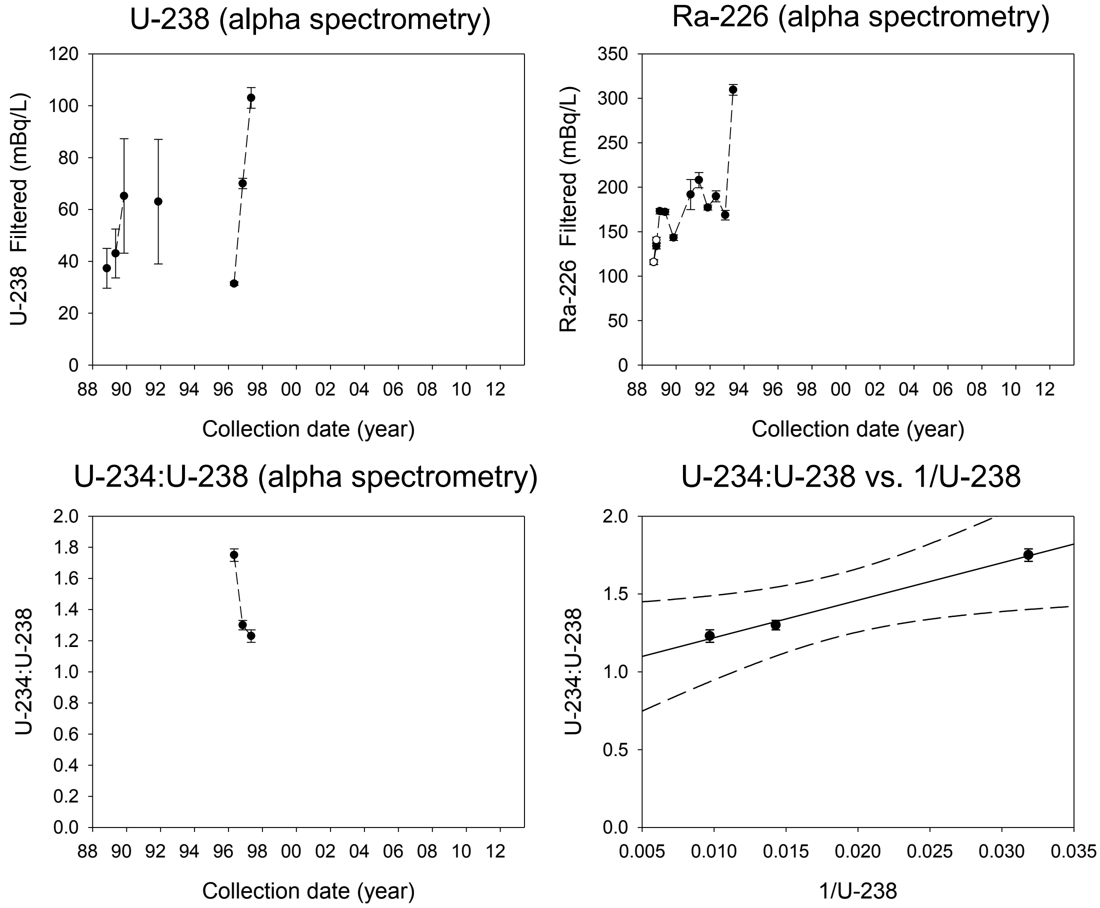

Bore ID – OB12A

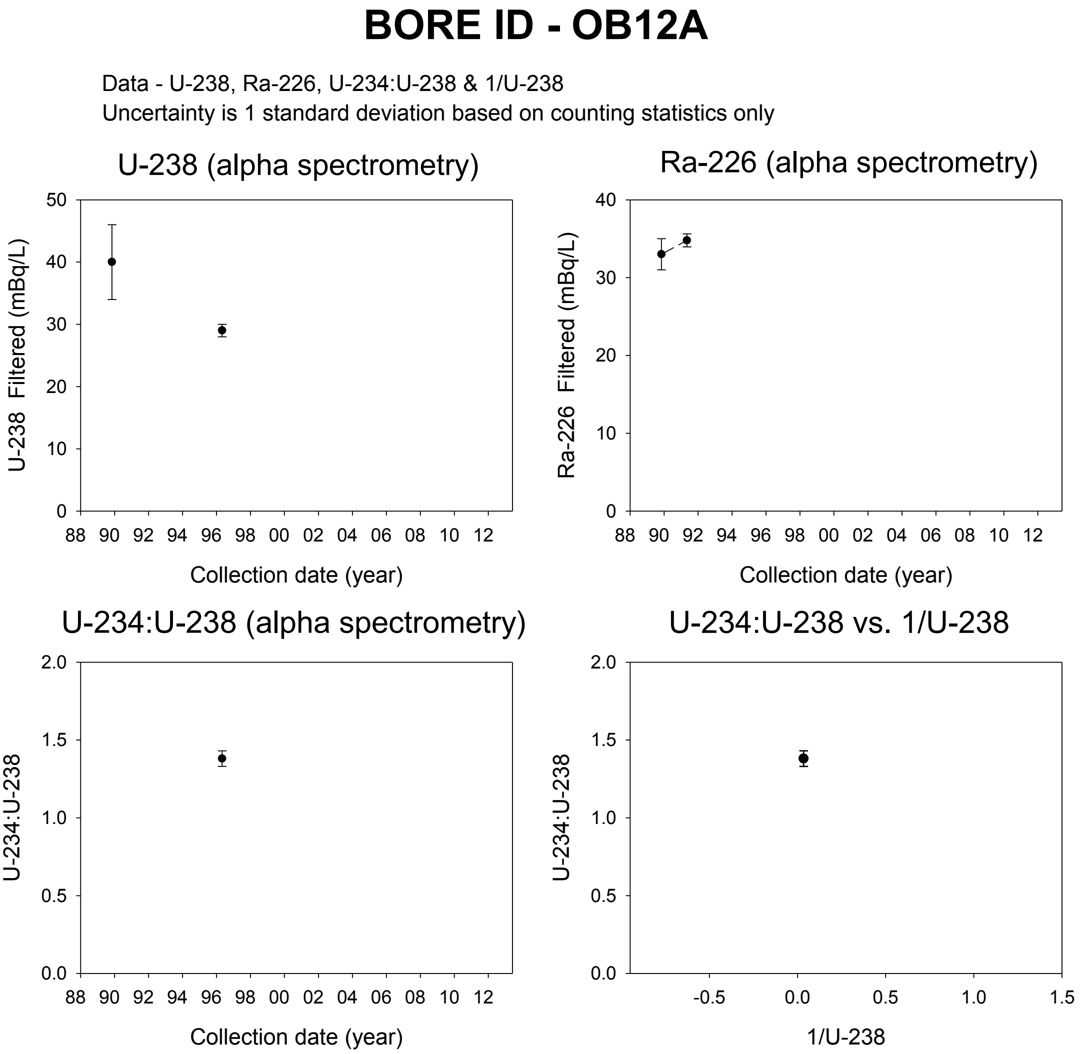

Bore ID – OB13A

BORE ID - OB13A

Data - U-238, Ra-226, U-234:U-238 & 1/U-238
Uncertainty is 1 standard deviation based on counting statistics only

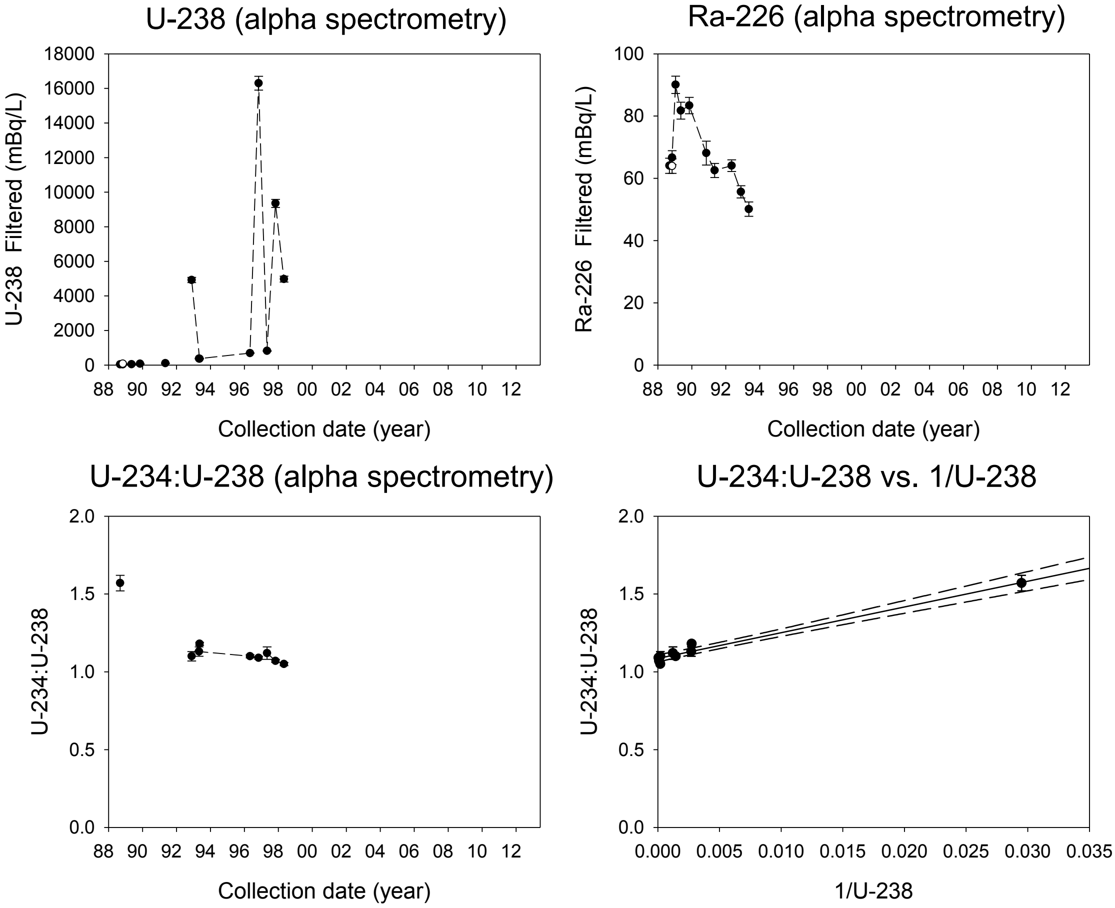

U-238 (alpha spectrometry)

Ra-226 (alpha spectrometry)

U-234:U-238 (alpha spectrometry)

U-234:U-238 vs. 1/U-238

Bore ID – OB15

BORE ID - OB15

Data - U-238, Ra-226, U-234:U-238 & 1/U-238
Uncertainty is 1 standard deviation based on counting statistics only

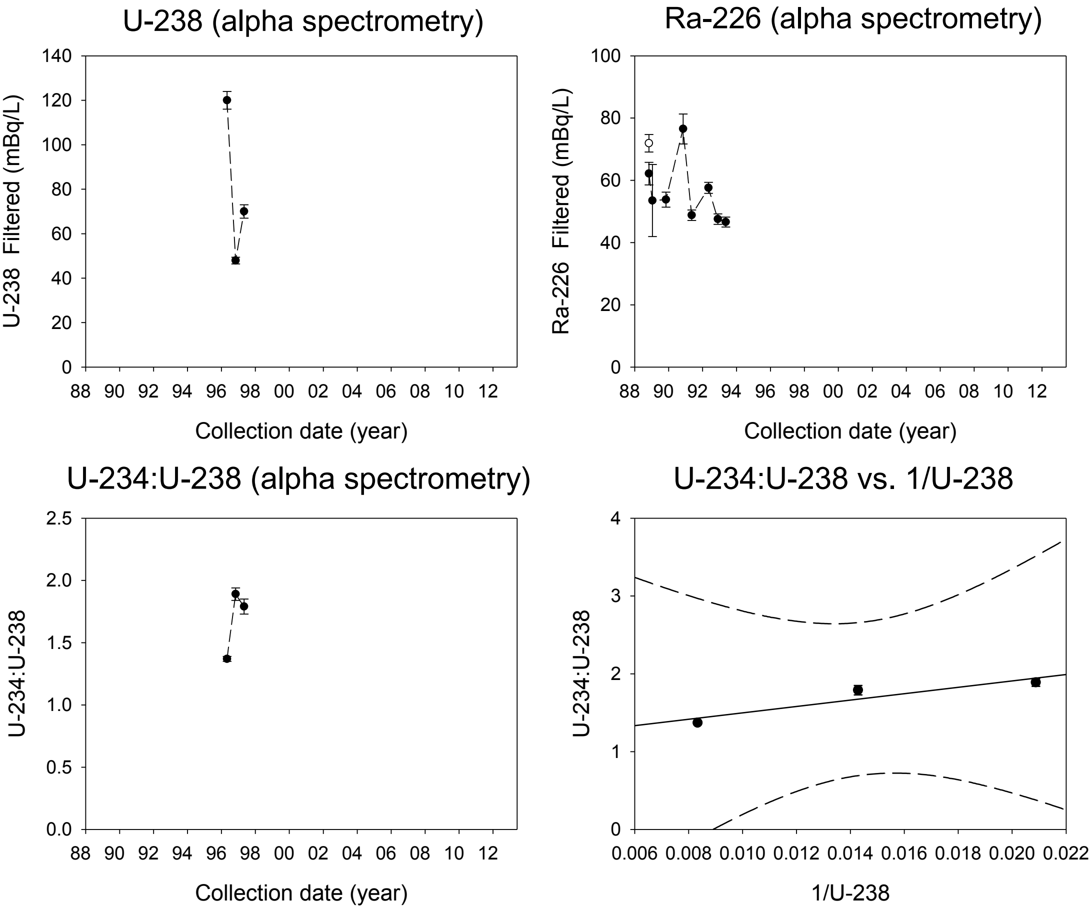

Bore ID – OB16

BORE ID - OB16

Data - U-238, Ra-226, U-234:U-238 & 1/U-238
Uncertainty is 1 standard deviation based on counting statistics only

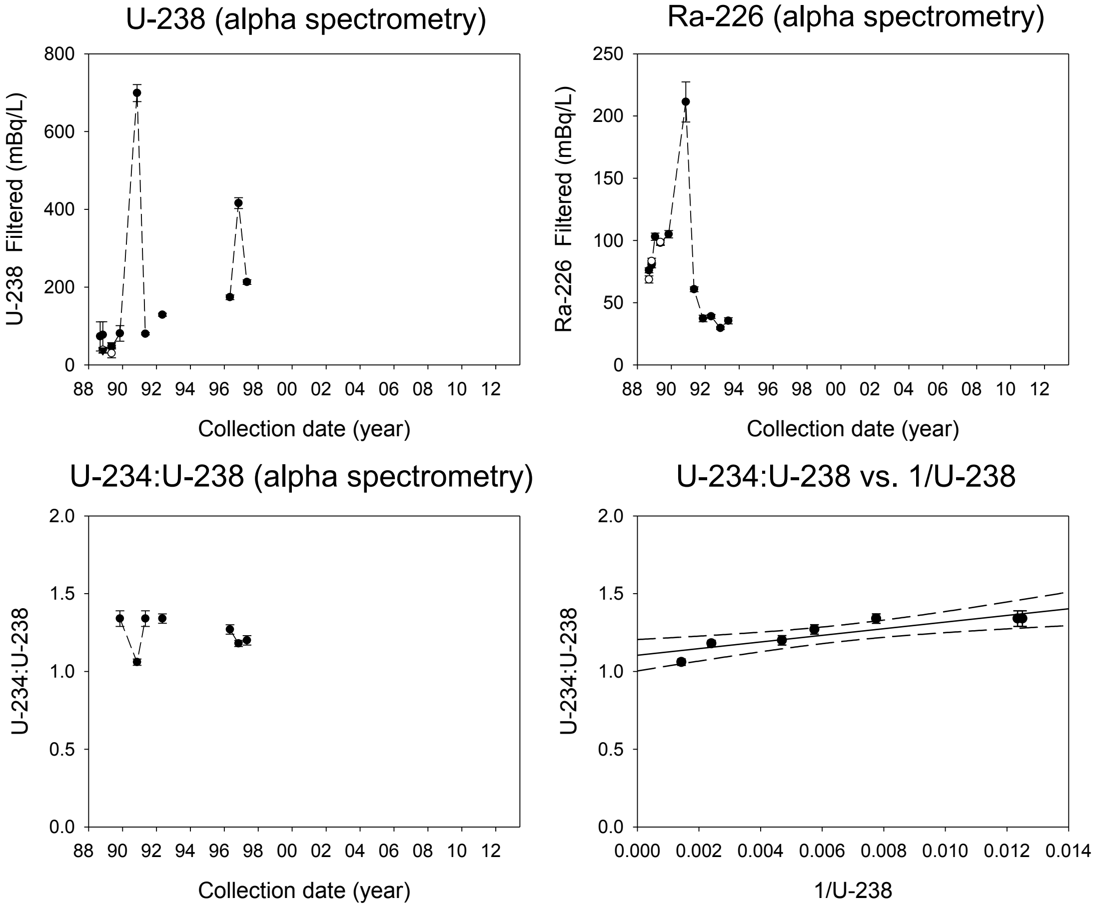

Bore ID – OB112

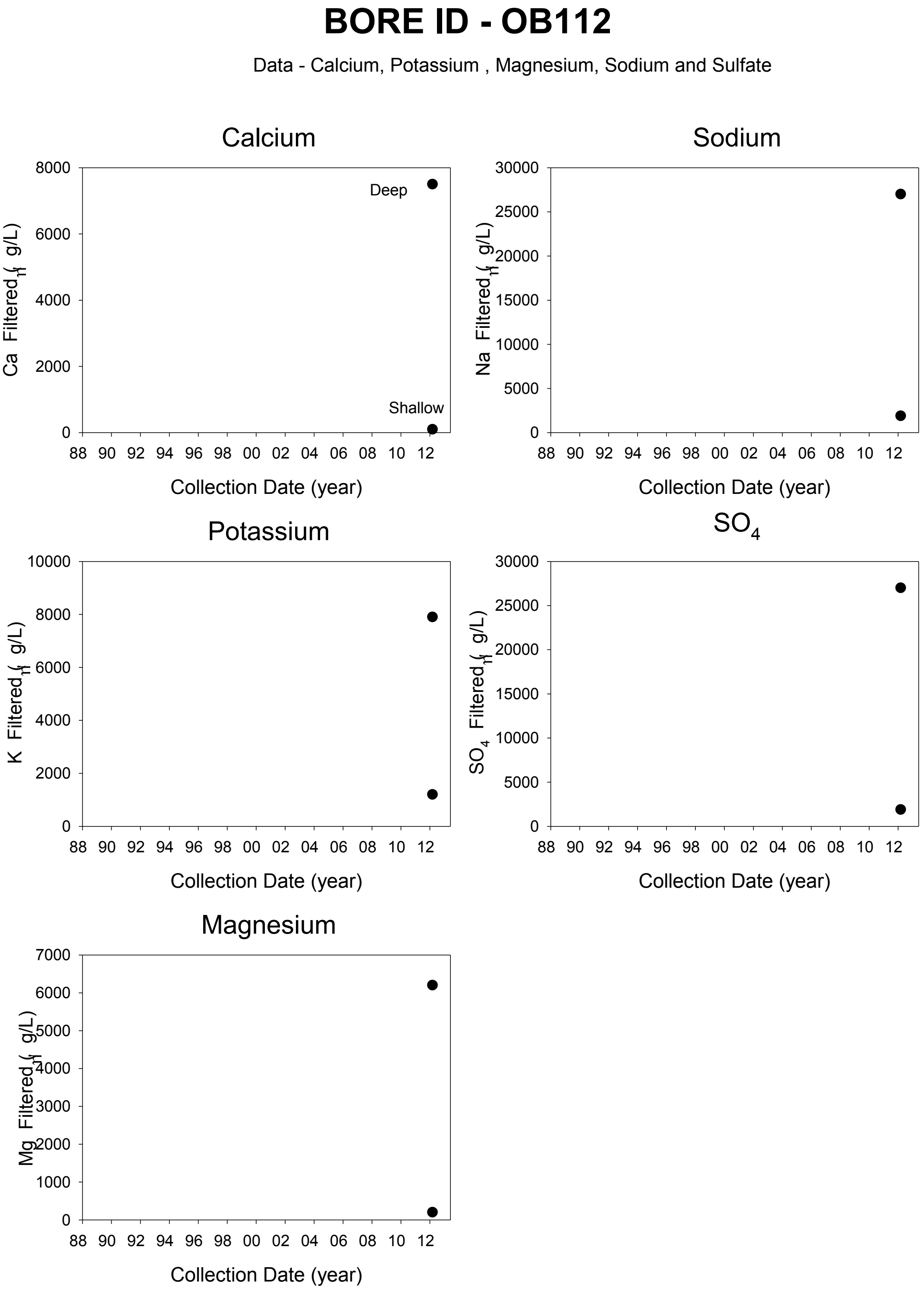

BORE ID - OB112

Data - Iron, Manganese, Barium, Strontium, Uranium& Vanadium

Iron

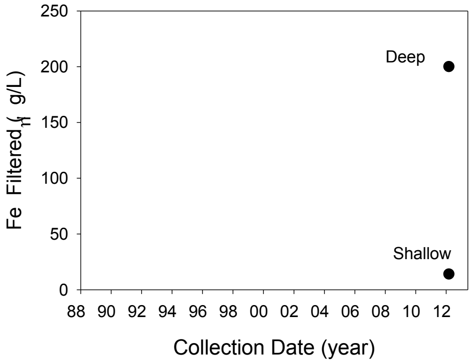

Manganese

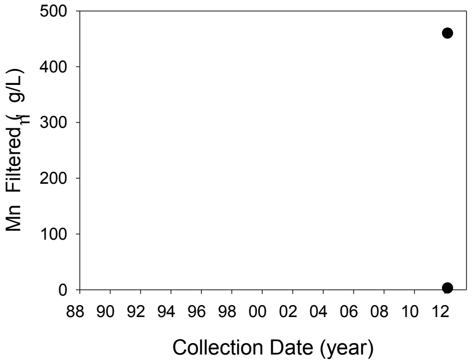

Barium

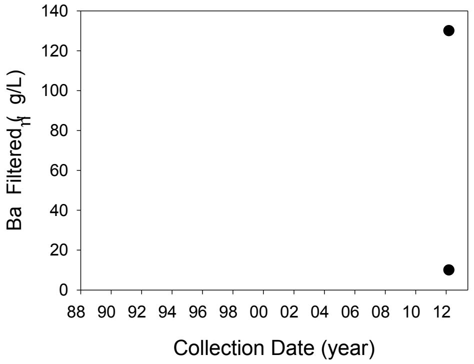

Strontium

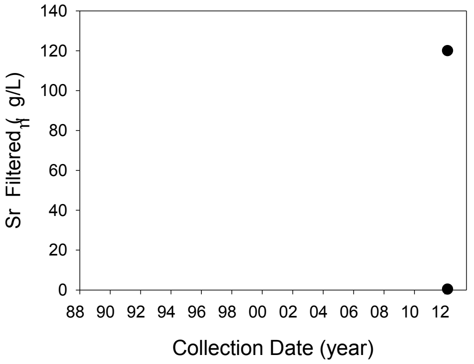

Uranium

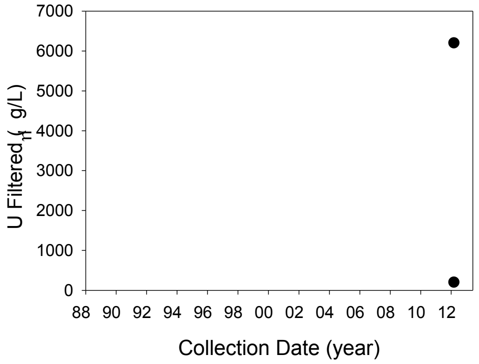

Vanadium

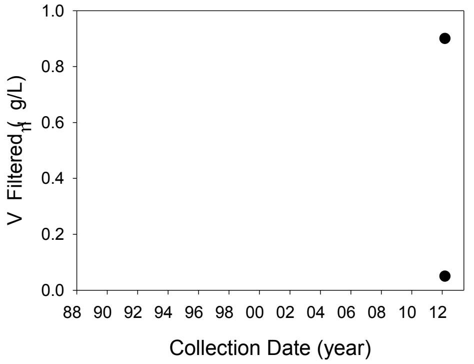

Bore ID – OB116

BORE ID - OB116

Data - Calcium, Potassium, Magnesium, Sodium and Sulfate

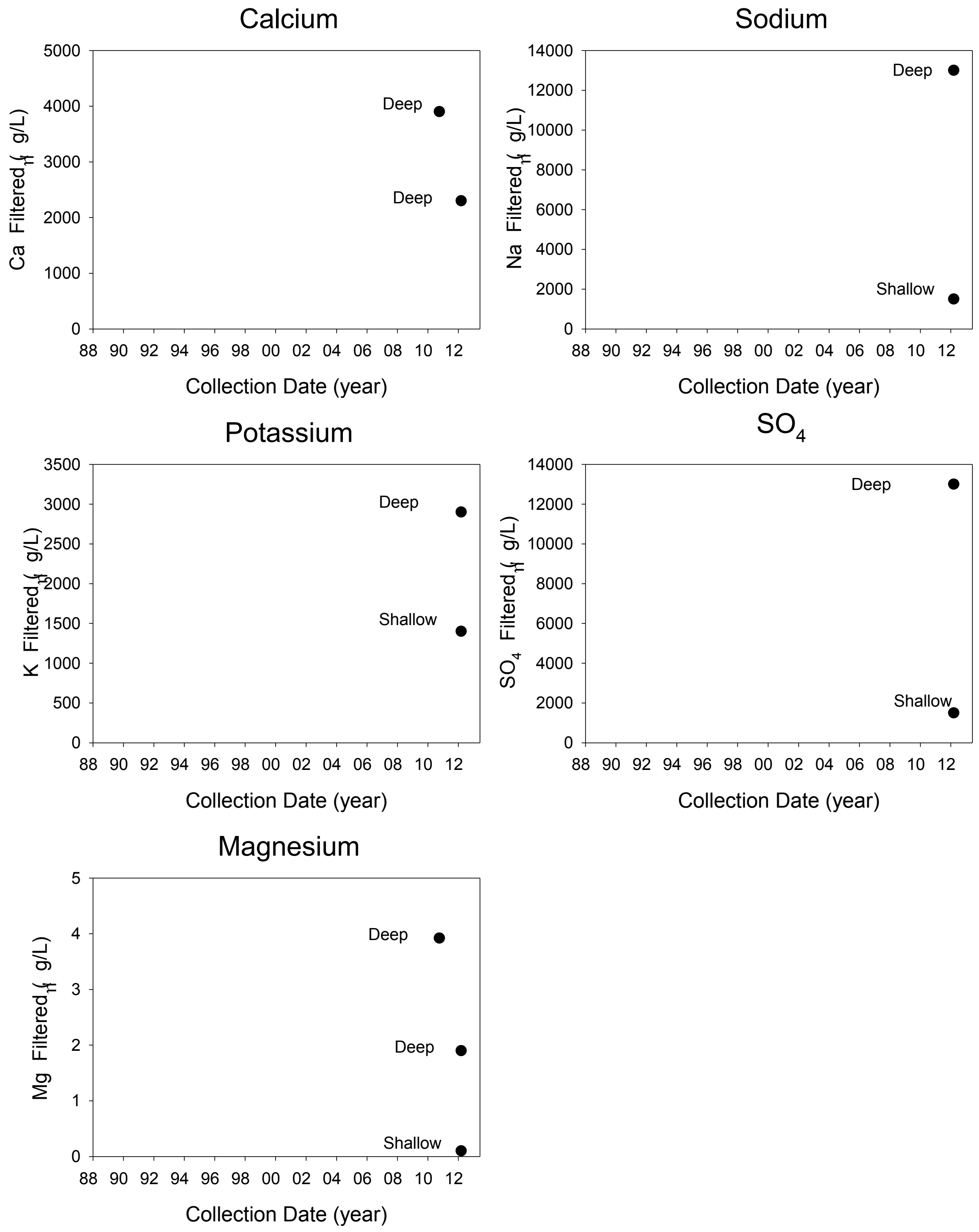

BORE ID - OB116

Data - Iron, Manganese, Barium, Strontium, Magnesium & Vanadium

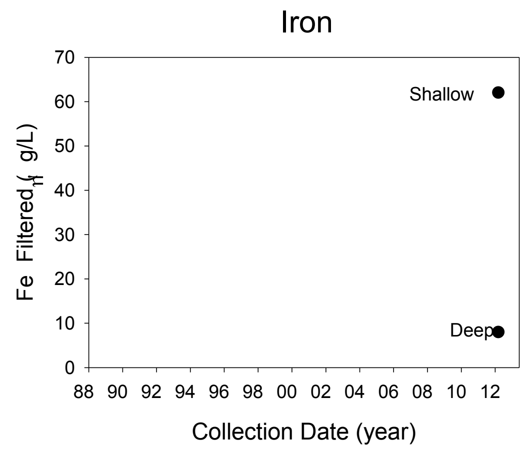

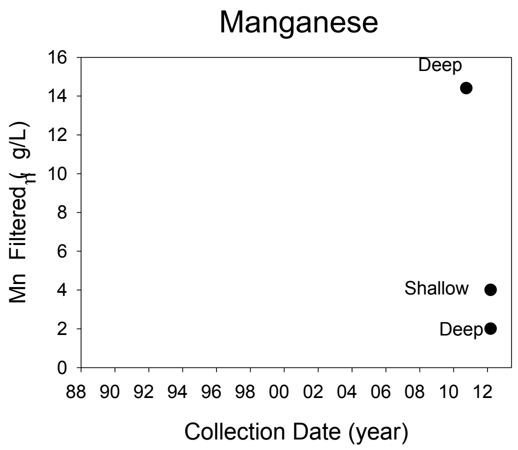

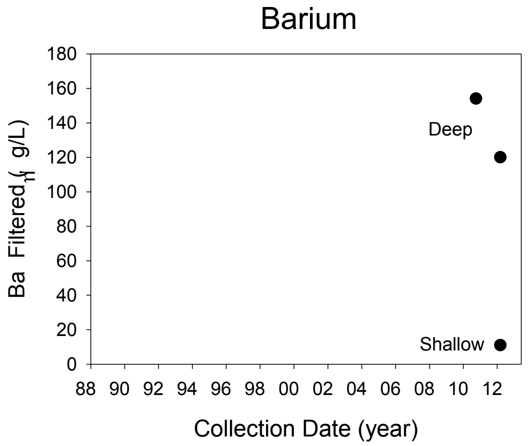

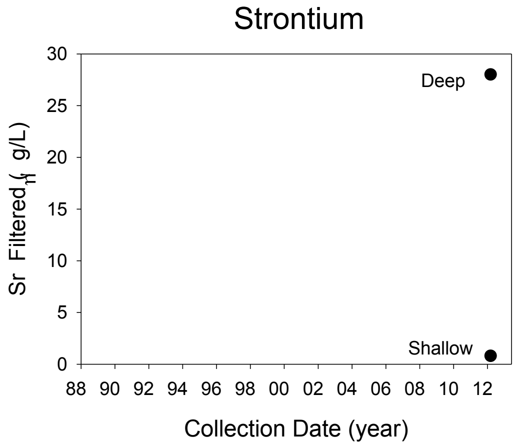

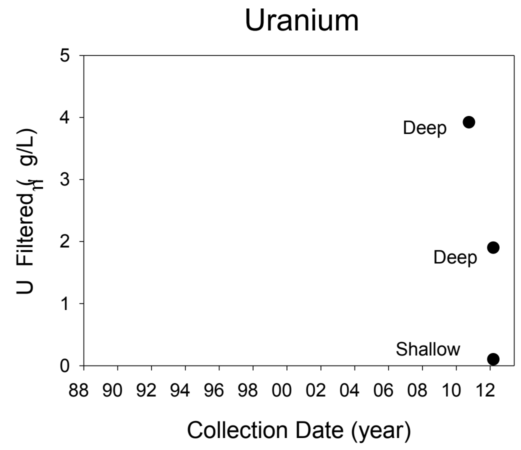

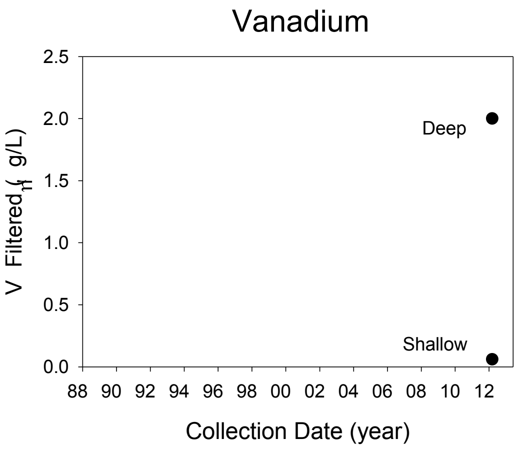

BORE ID - OB116

Data - U-238, Ra-226, U-234:U-238 & 1/U-238
Uncertainty is 1 standard deviation based on counting statistics only

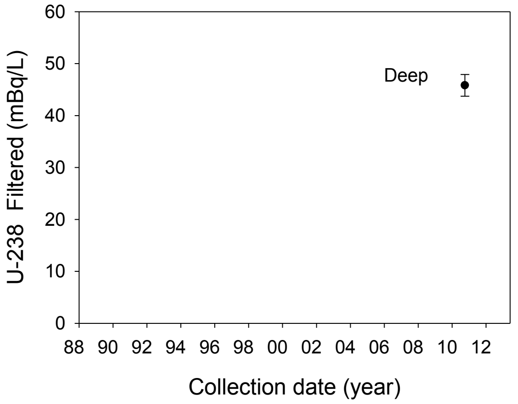
U-238 (alpha spectrometry)

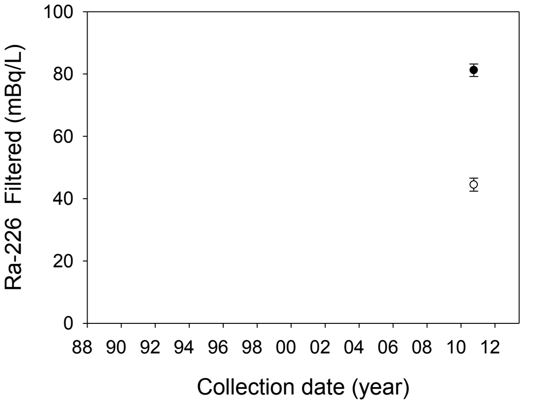
Ra-226 (alpha spectrometry)

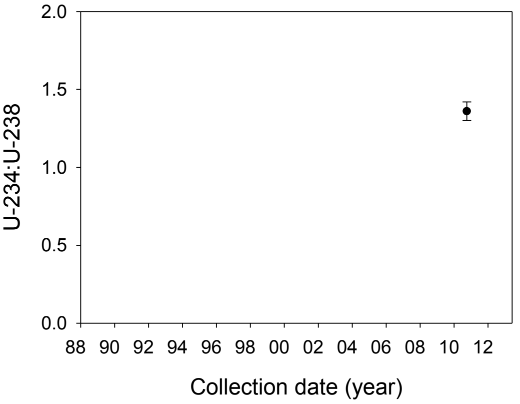
U-234:U-238 (alpha spectrometry)

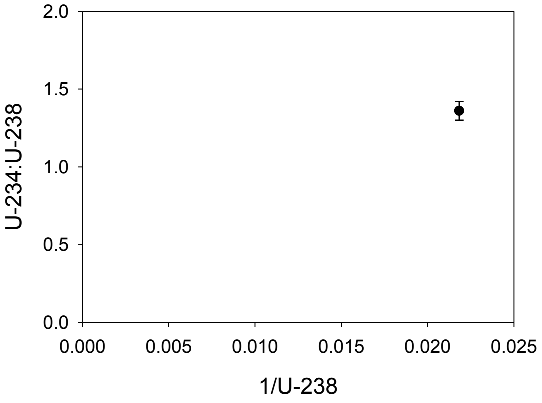
U-234:U-238 vs. 1/U-238

Bore ID – OB17A

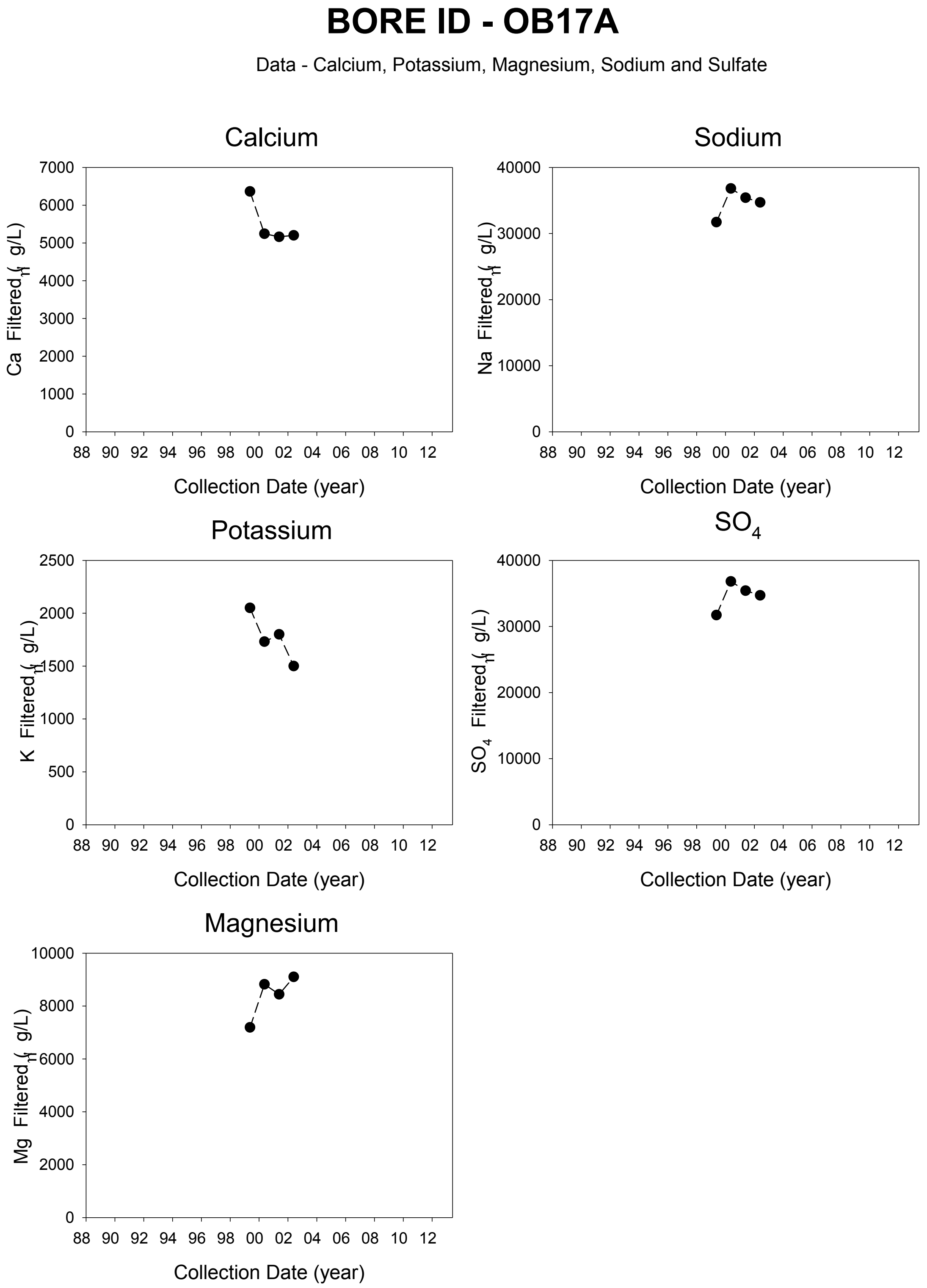

BORE ID - OB17A

Data - Iron, Manganese, Barium, Strontium, Uranium & Vanadium

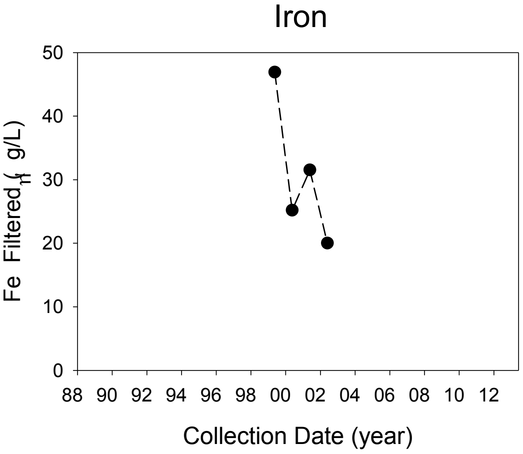
Iron

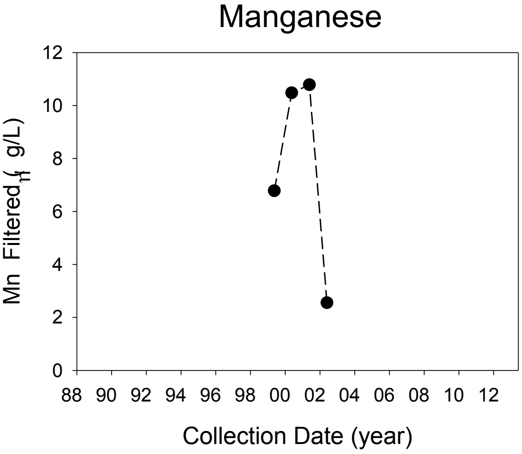
Manganese

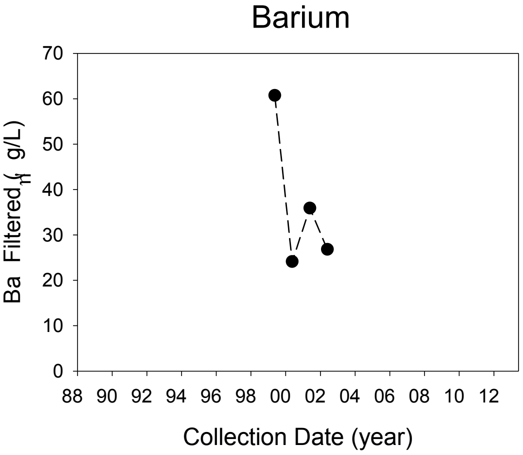
Barium

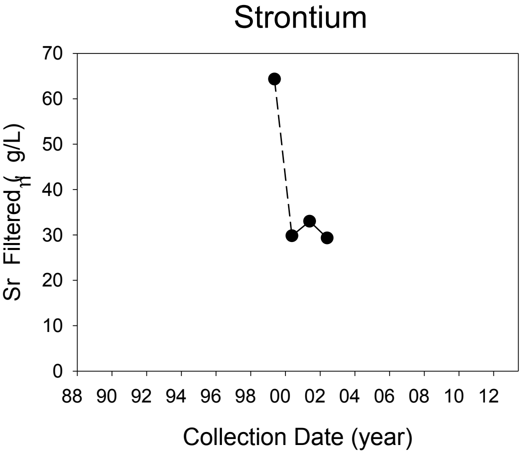
Strontium

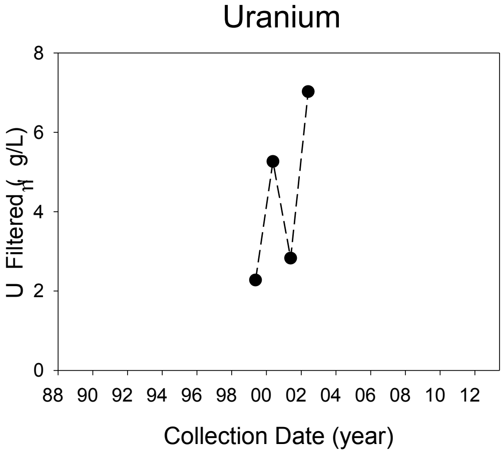
Uranium

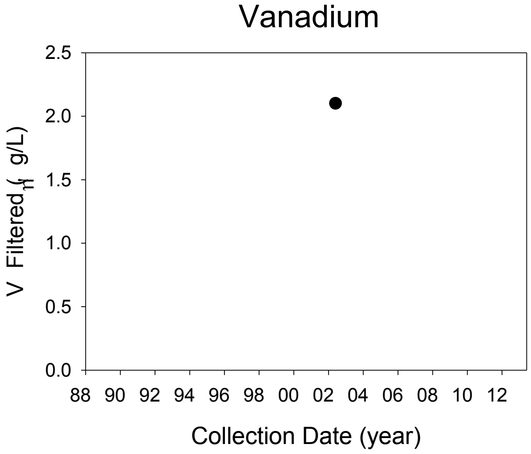
Vanadium

BORE ID - OB17A

Data - U-238, Ra-226, U-234:U-238 & 1/U-238
Uncertainty is 1 standard deviation based on counting statistics only

U-238 (alpha spectrometry)

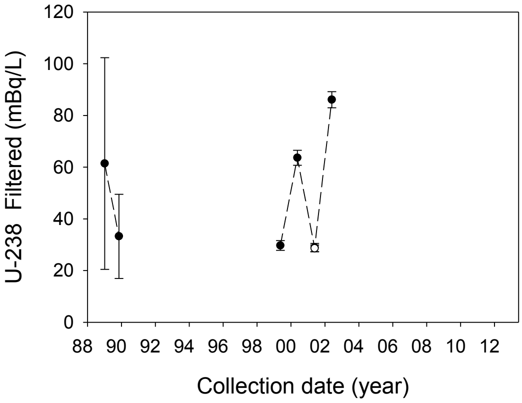

Ra-226 (alpha spectrometry)

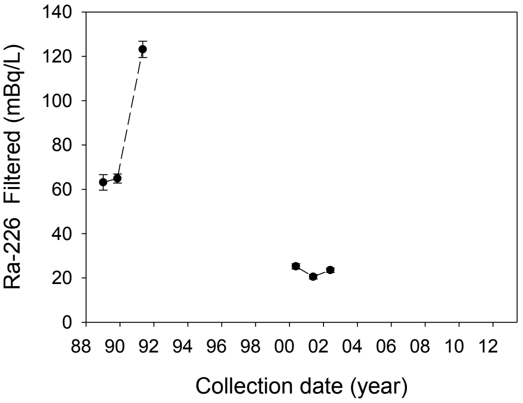

U-234:U-238 (alpha spectrometry)

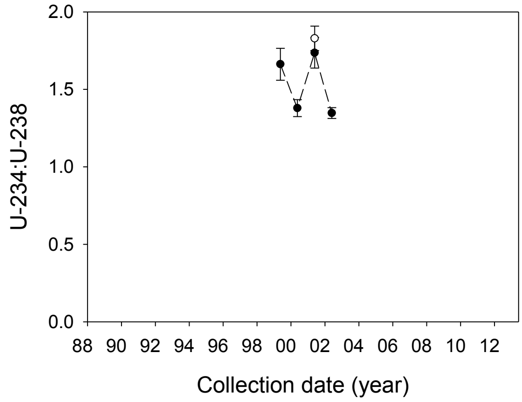

U-234:U-238 vs. 1/U-238

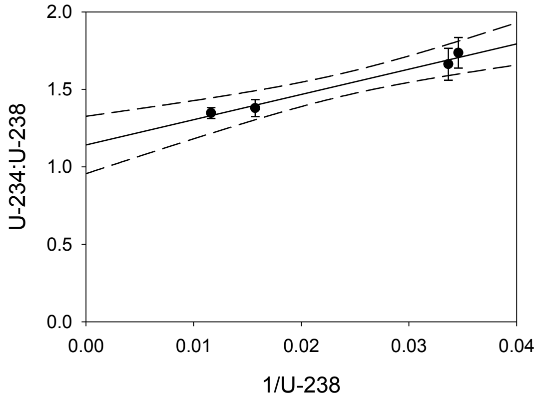

Bore ID – OB18A

BORE ID - OB18A

Data - U-238, Ra-226, U-234:U-238 & 1/U-238
Uncertainty is 1 standard deviation based on counting statistics only

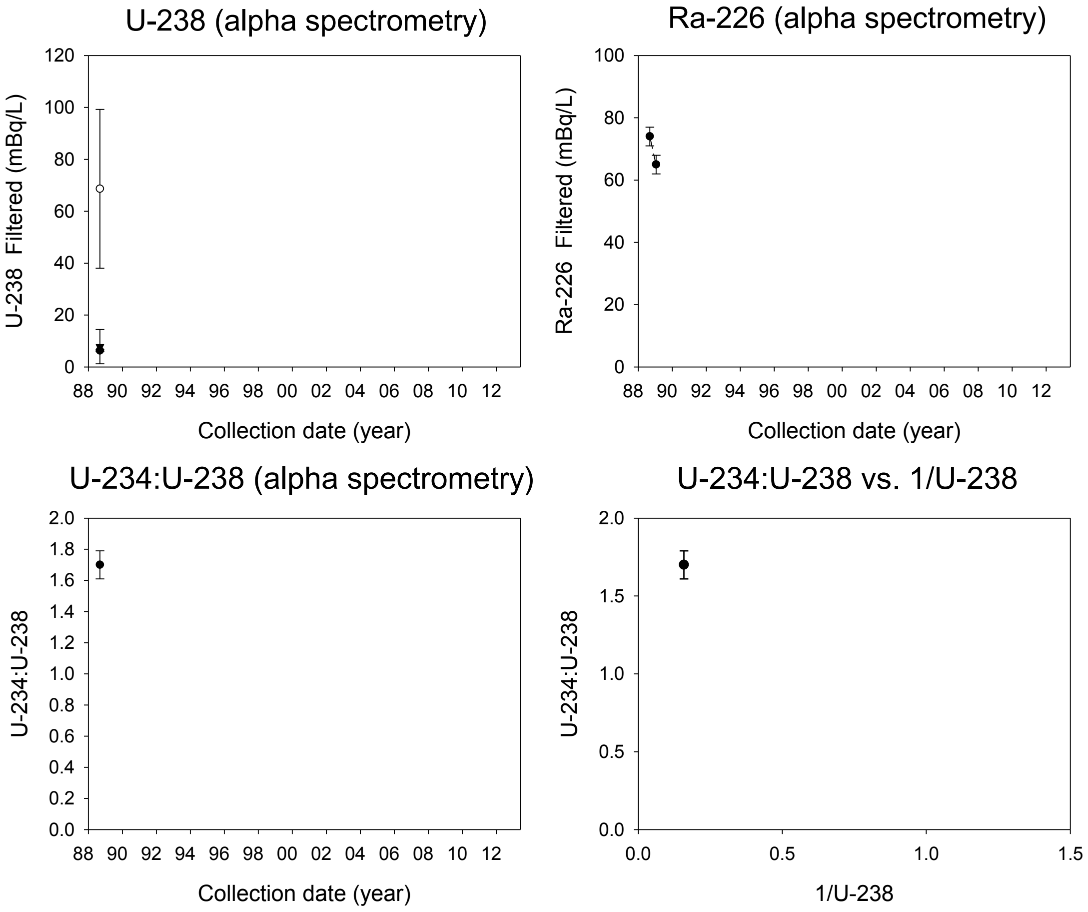

Bore ID – OB19A

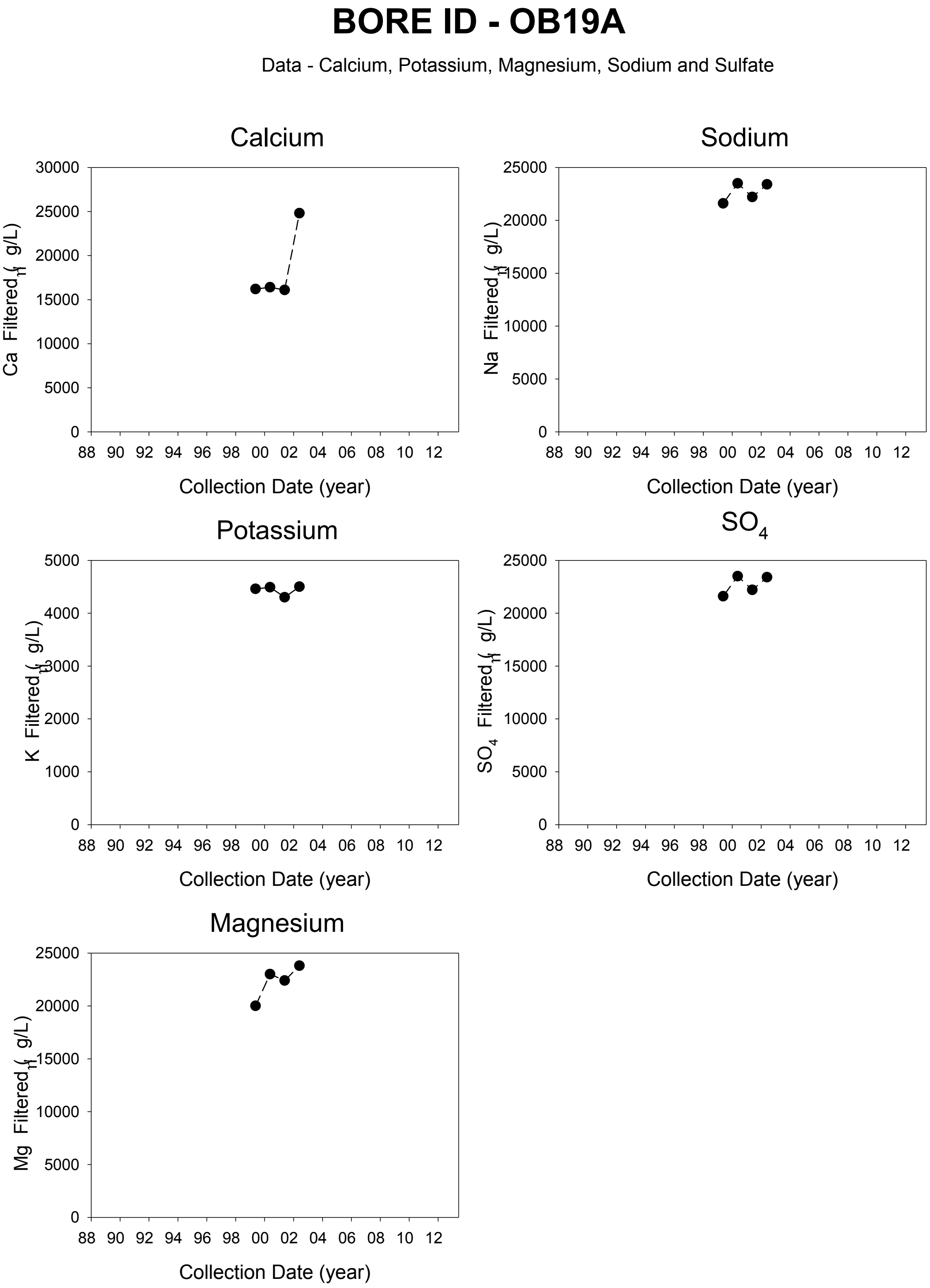

BORE ID - OB19A

Data - Iron, Manganese, Barium, Strontium, Magnesium & Vanadium

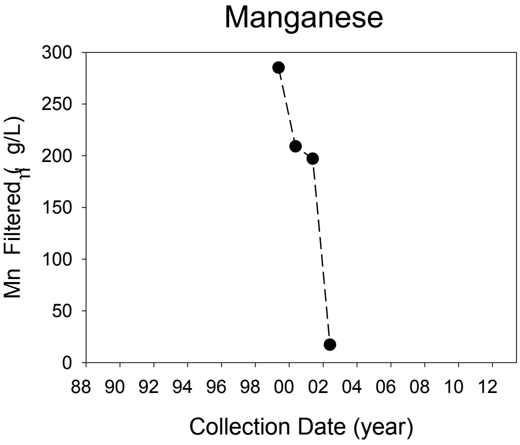

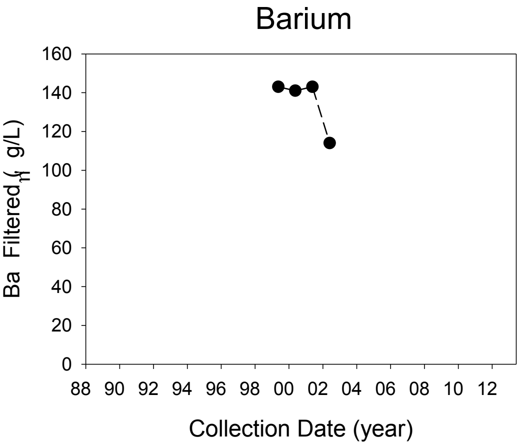

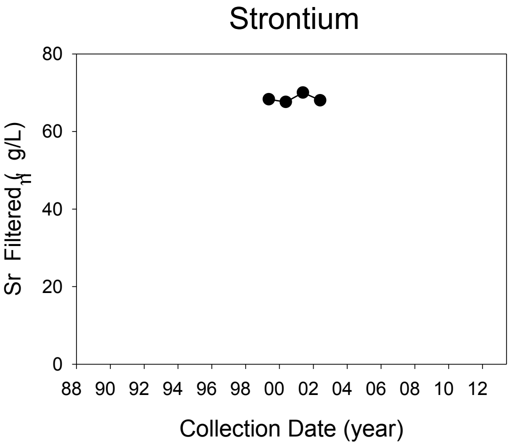

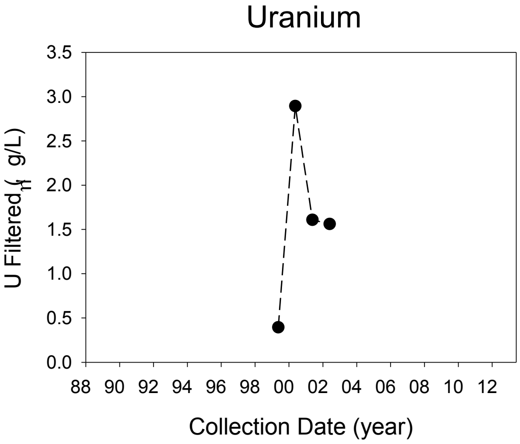

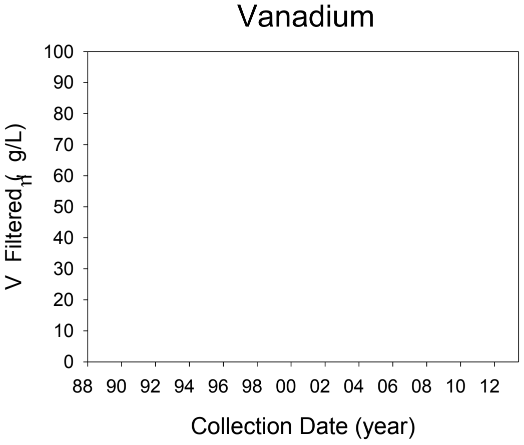

BORE ID - OB19A

Data - U-238, Ra-226, U-234:U-238 & 1/U-238
Uncertainty is 1 standard deviation based on counting statistics only

U-238 (alpha spectrometry)

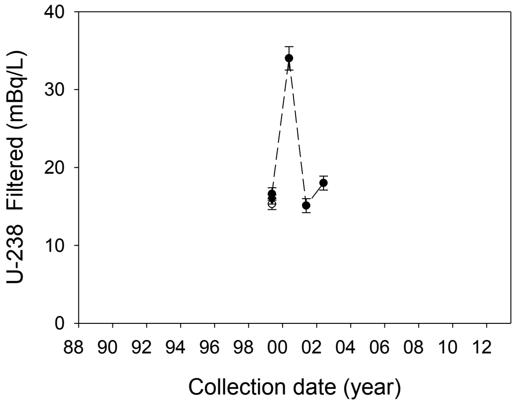

Ra-226 (alpha spectrometry)

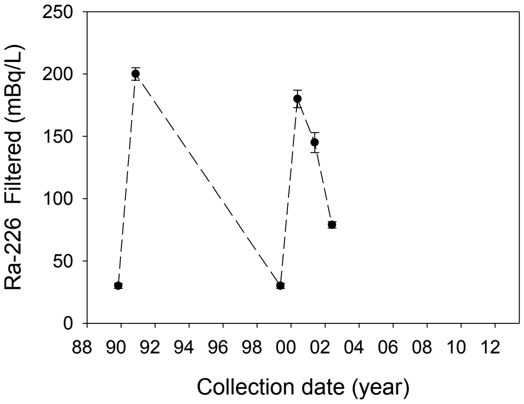

U-234:U-238 (alpha spectrometry)

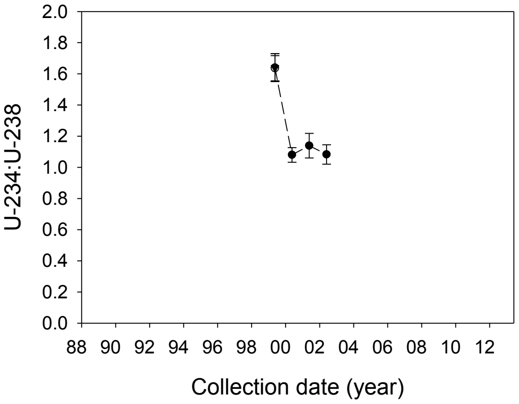

U-234:U-238 vs. 1/U-238

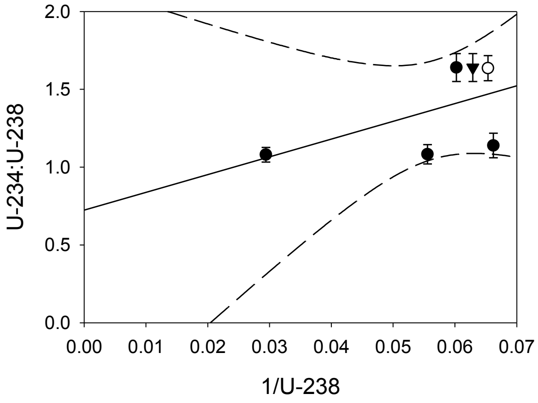

Bore ID – OB1A

BORE ID - OB1A

Data - Calcium, Potassium, Magnesium, Sodium and Sulfate

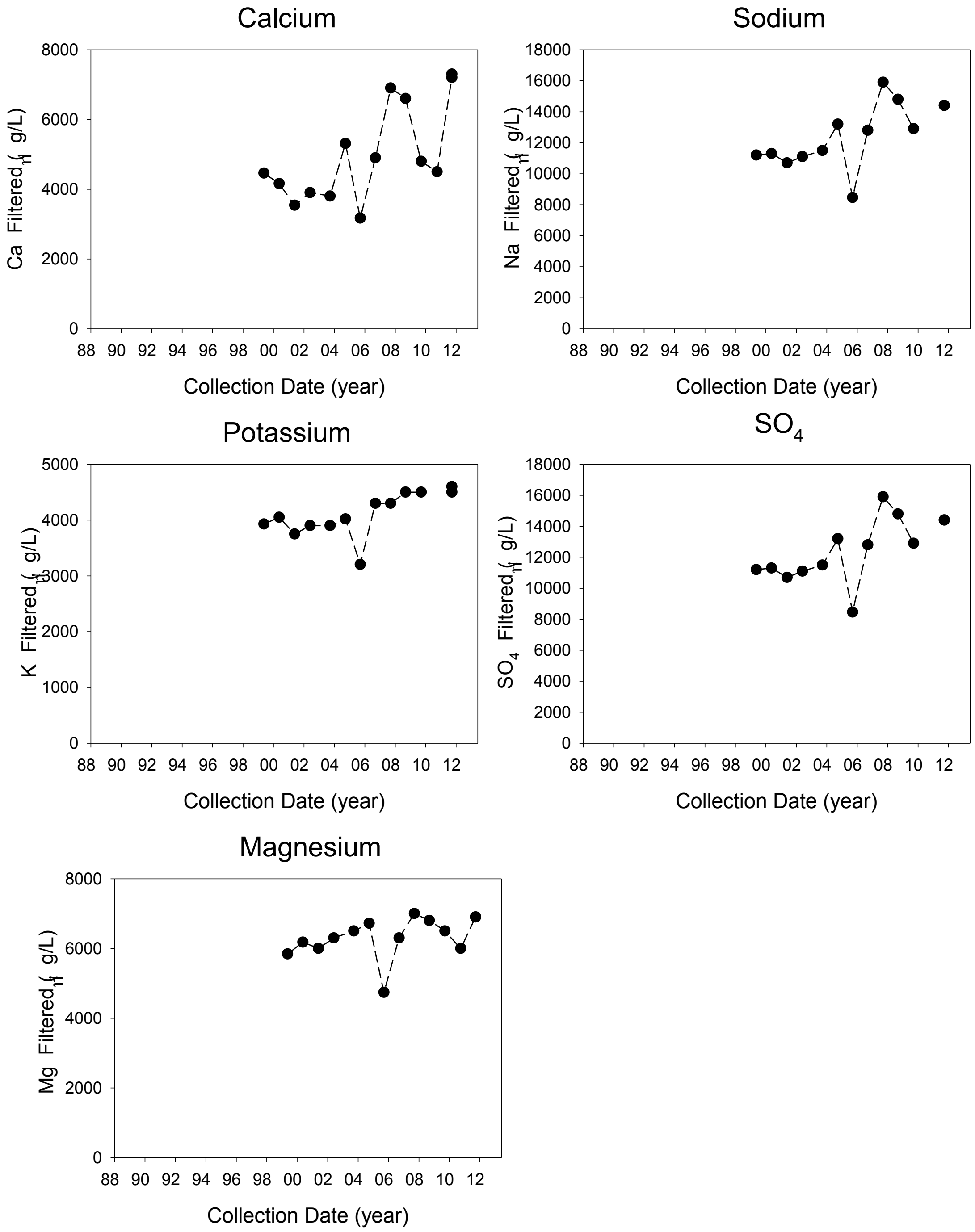

BORE ID - OB1A

Data - Iron, Manganese, Barium, Strontium, Uranium & Vanadium

Iron

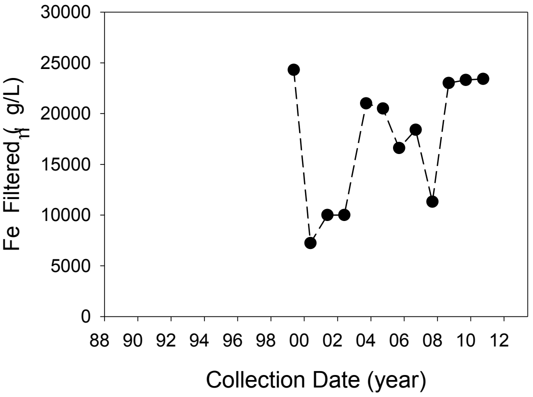

Manganese

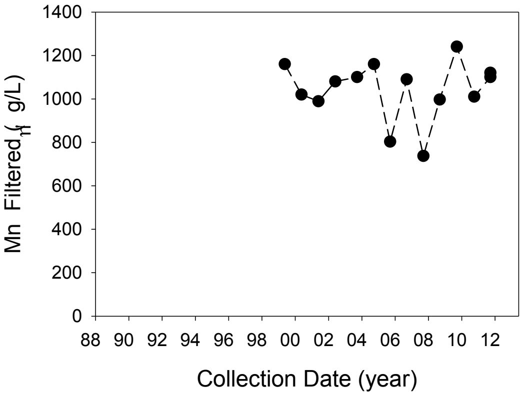

Barium

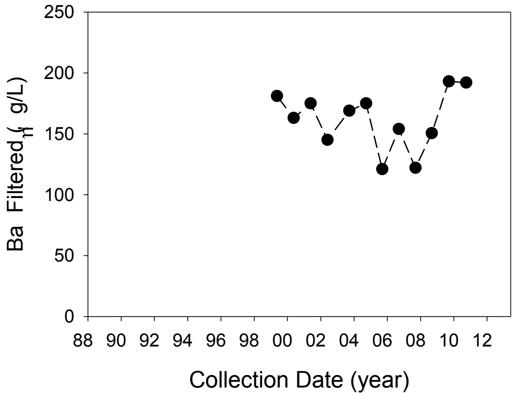

Strontium

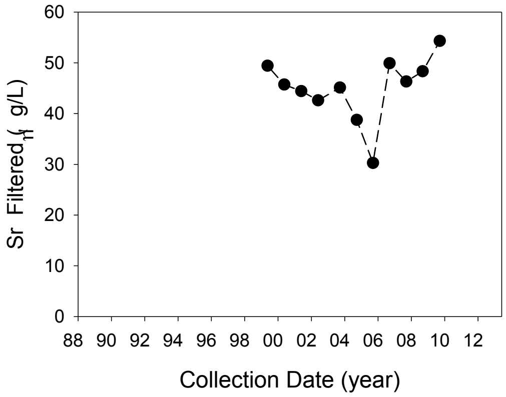

Uranium

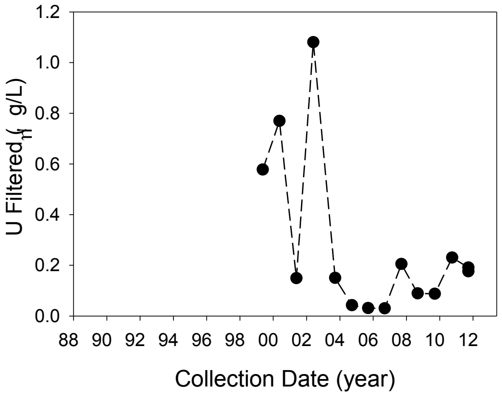

Vanadium

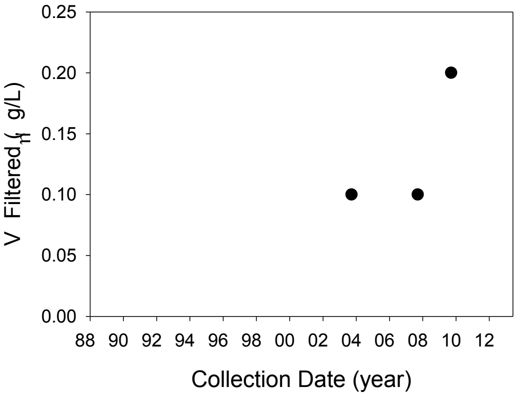

BORE ID - OB1A

Data - U-238, Ra-226, U-234:U-238 & 1/U-238
Uncertainty is 1 standard deviation based on counting statistics only

U-238 (alpha spectrometry)

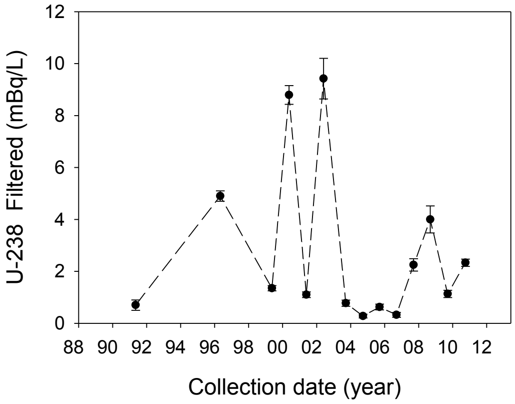

Ra-226 (alpha spectrometry)

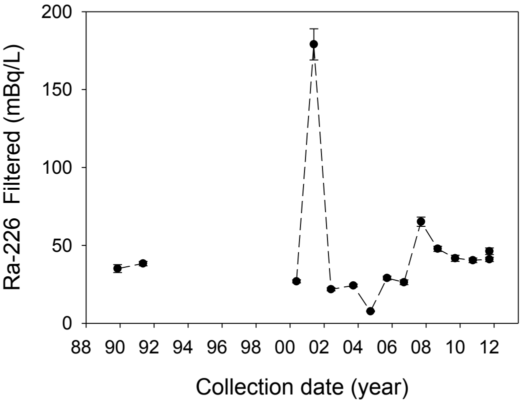

U-234:U-238 (alpha spectrometry)

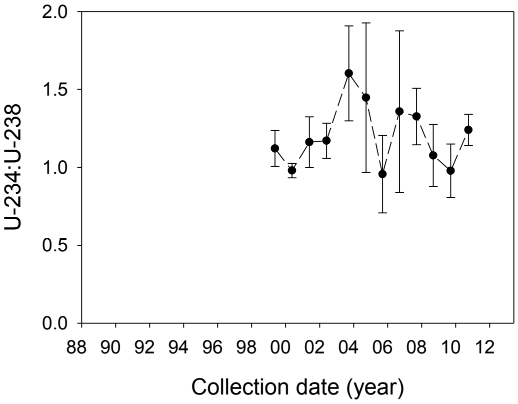

U-234:U-238 vs. 1/U-238

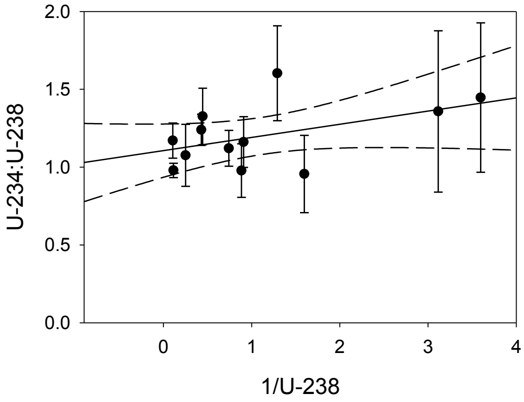

Bore ID – OB20

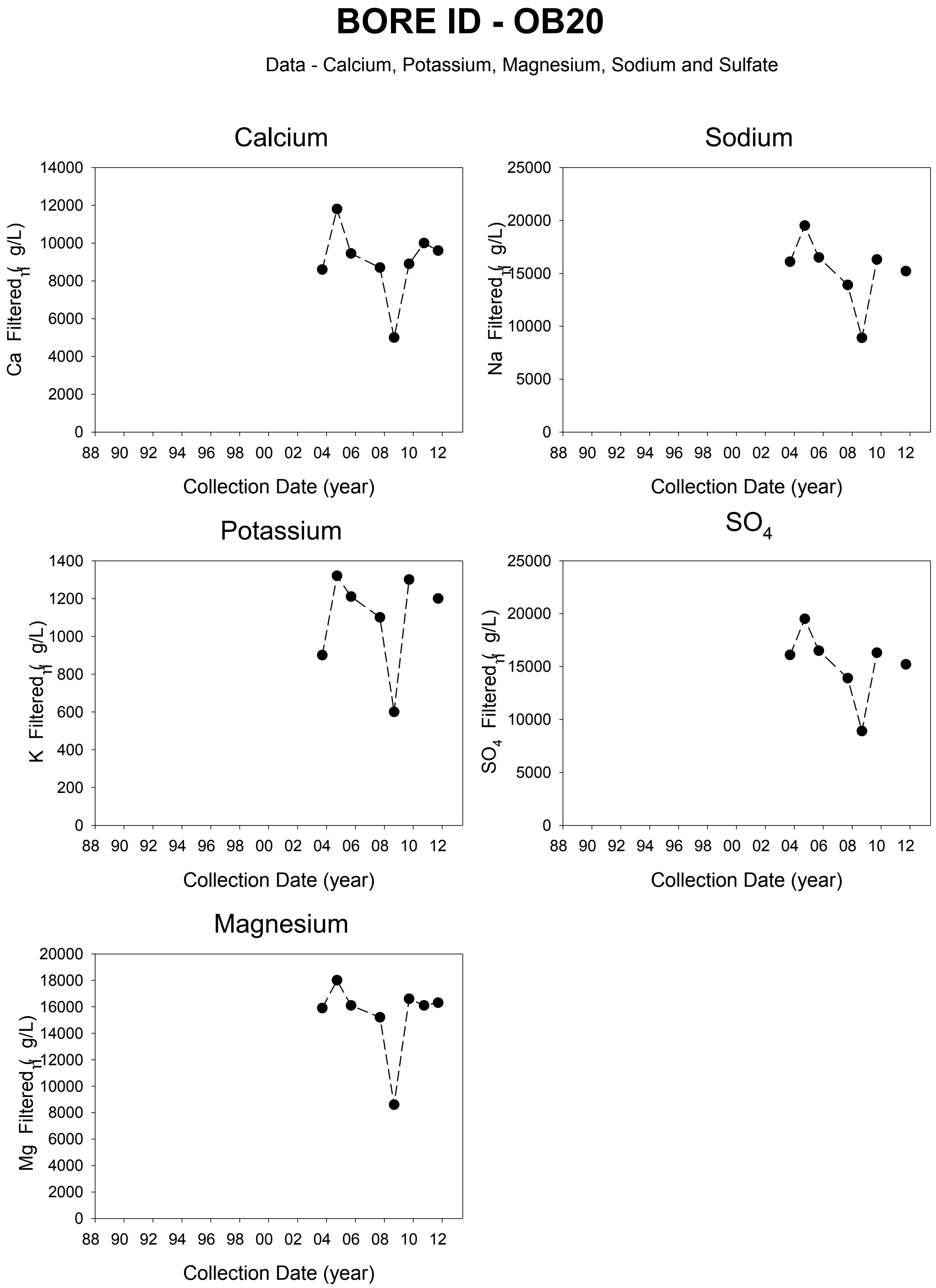
BORE ID - OB20
Data - Calcium, Potassium, Magnesium, Sodium and Sulfate
Calcium
Ca Filtered (µg/L)
0
2000
4000
6000
8000
10000
12000
14000
Sodium
Na Filtered (µg/L)
0
5000
10000
15000
20000
25000
Potassium
K Filtered (µg/L)
0
200
400
600
800
1000
1200
1400
SO4
SO4 Filtered (µg/L)
0
5000
10000
15000
20000
25000
Magnesium
Mg Filtered (µg/L)
0
2000
4000
6000
8000
10000
12000
14000
16000
18000
20000
88
90
92
94
96
98
00
02
04
06
08
10
12
Collection Date (year)

BORE ID - OB20

Data - Iron, Manganese, Barium, Strontium, Uranium & Vanadium

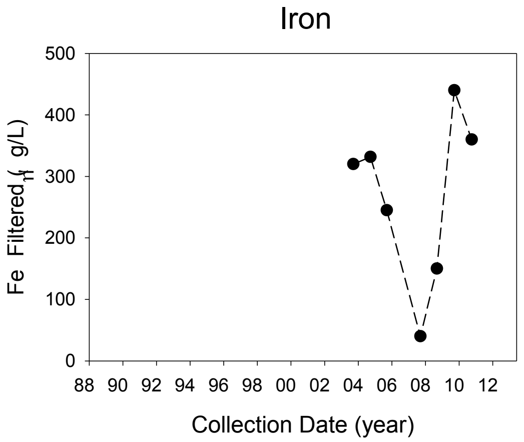
Iron

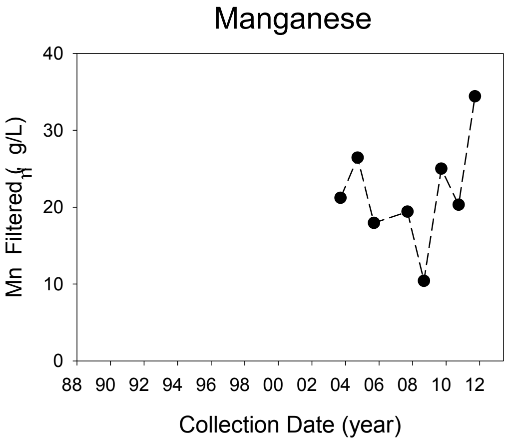
Manganese

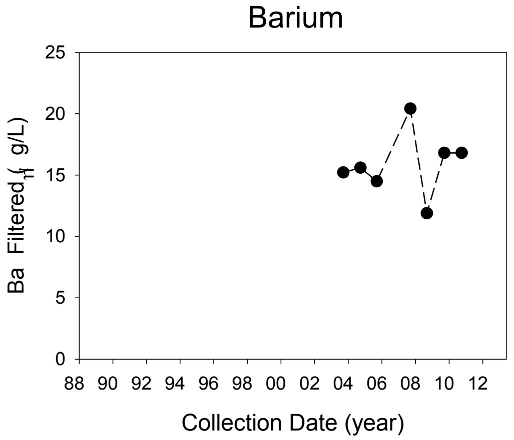
Barium

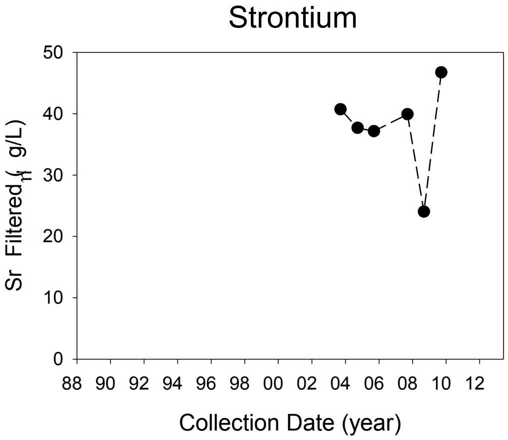
Strontium

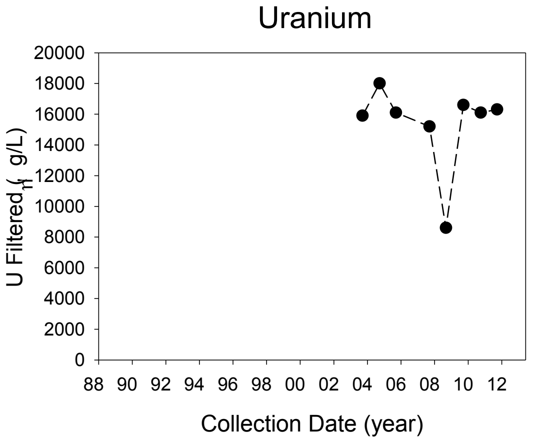
Uranium

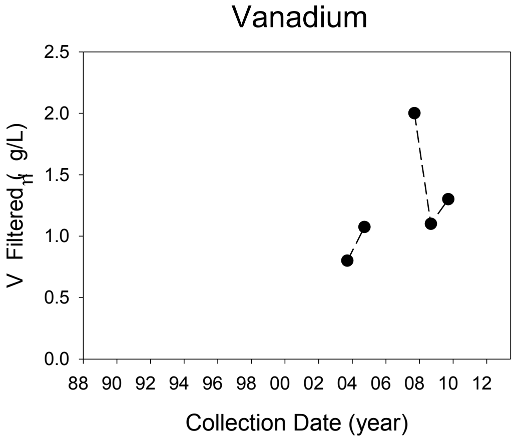
Vanadium

BORE ID - OB20

Data - U-238, Ra-226, U-234:U-238 & 1/U-238
Uncertainty is 1 standard deviation based on counting statistics only

U-238 (alpha spectrometry)

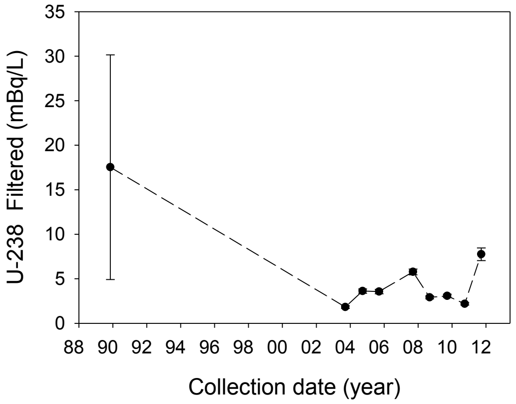

Ra-226 (alpha spectrometry)

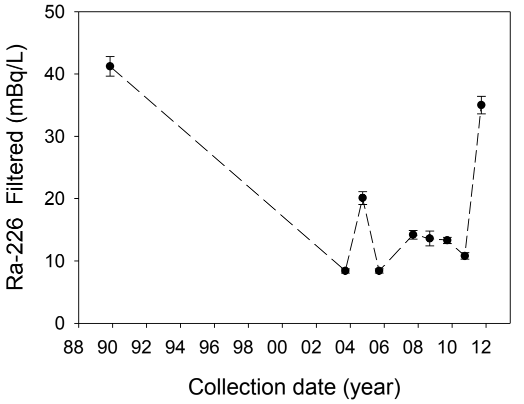

U-234:U-238 (alpha spectrometry)

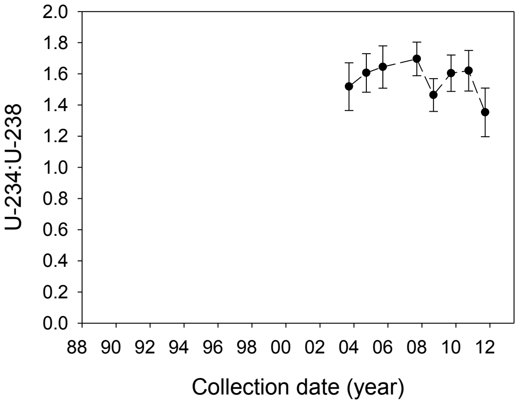

U-234:U-238 vs. 1/U-238

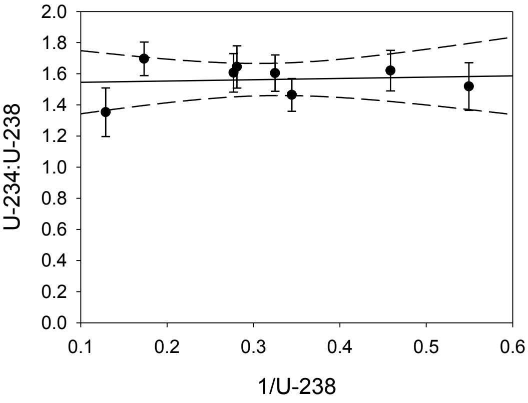

Bore ID – OB21A

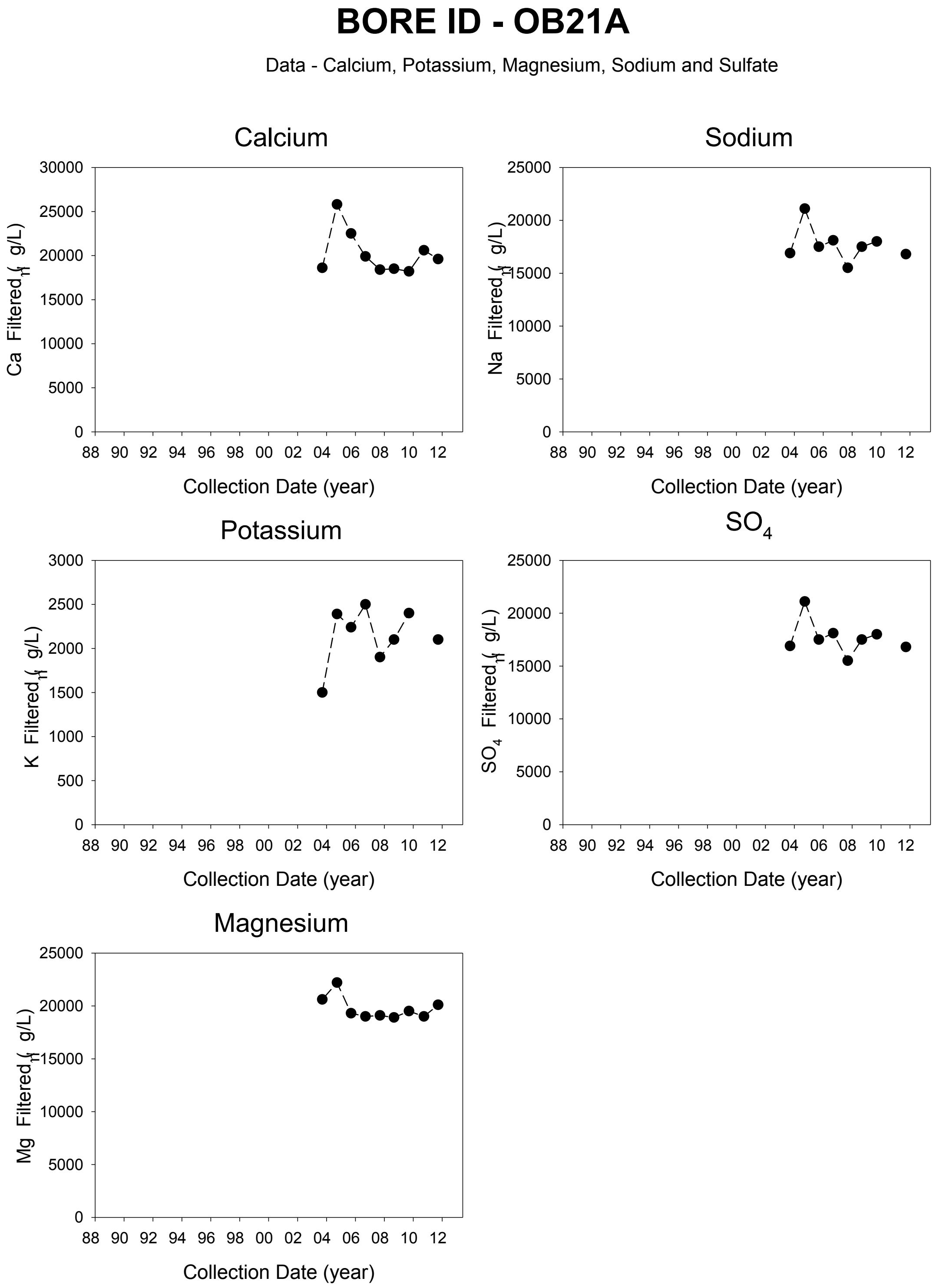

BORE ID - OB21A

Data - Iron, Manganese, Barium, Strontium, Uranium & Vanadium

Iron

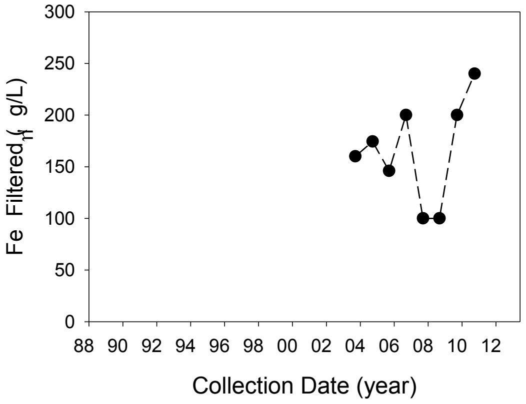

Manganese

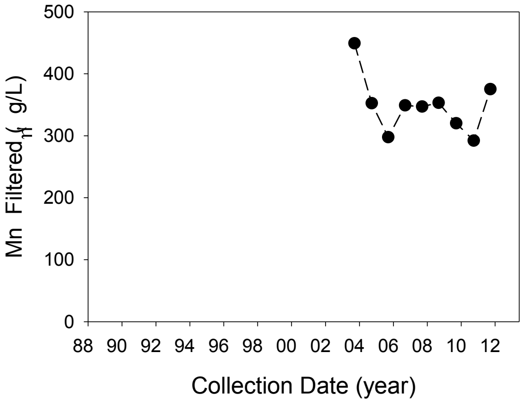

Barium

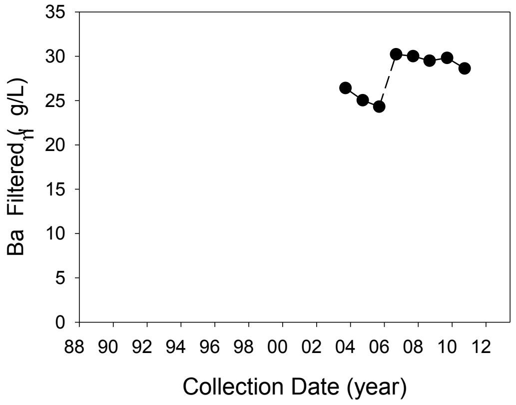

Strontium

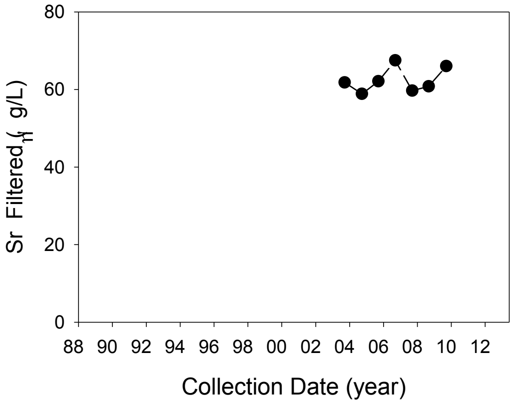

Uranium

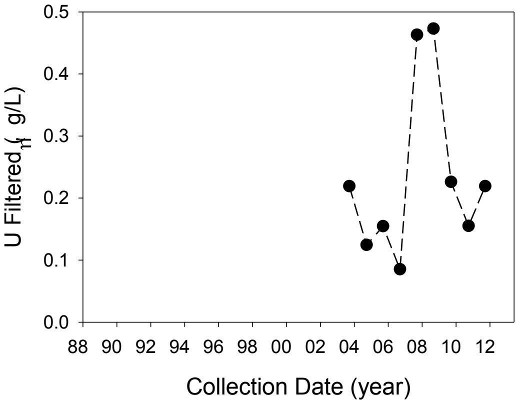

Vanadium

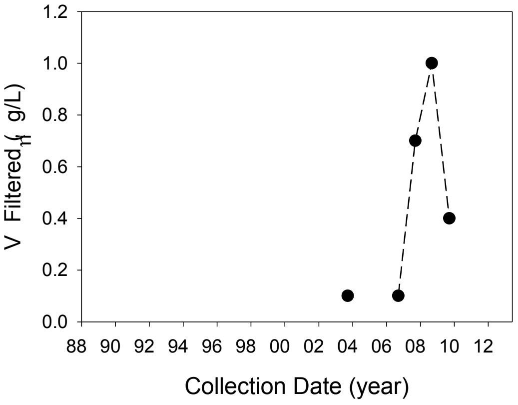

BORE ID - OB21A

Data - U-238, Ra-226, U-234:U-238 & 1/U-238
Uncertainty is 1 standard deviation based on counting statistics only

U-238 (alpha spectrometry)

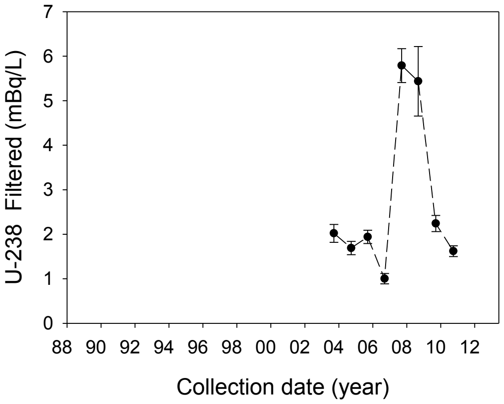

Ra-226 (alpha spectrometry)

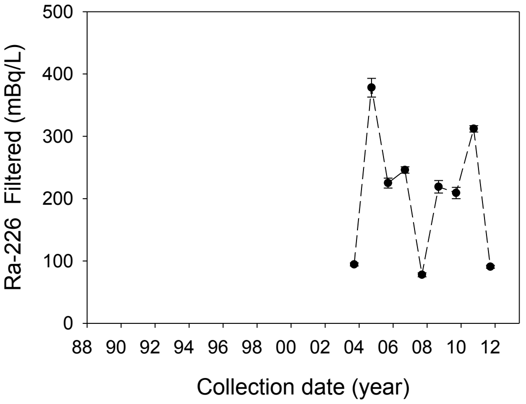

U-234:U-238 (alpha spectrometry)

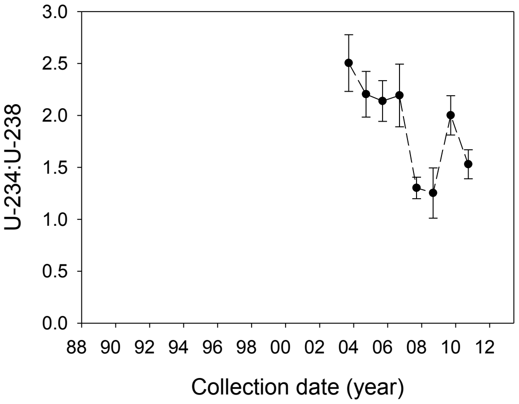

U-234:U-238 vs. 1/U-238

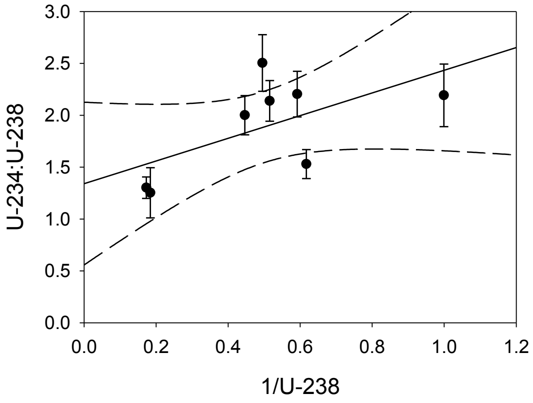

Bore ID – OB22

BORE ID - OB22

Data - U-238, Ra-226, U-234:U-238 & 1/U-238
Uncertainty is 1 standard deviation based on counting statistics only

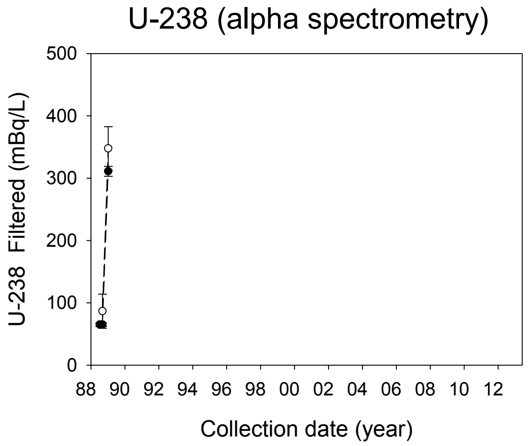

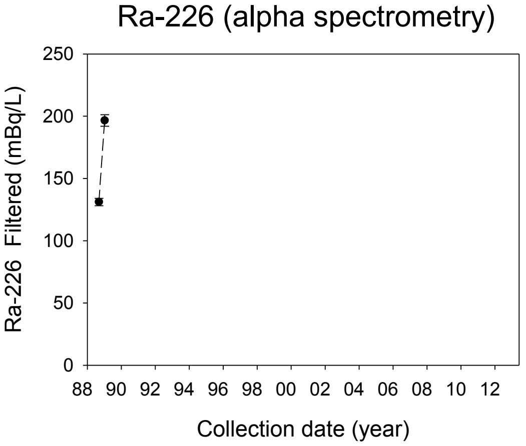

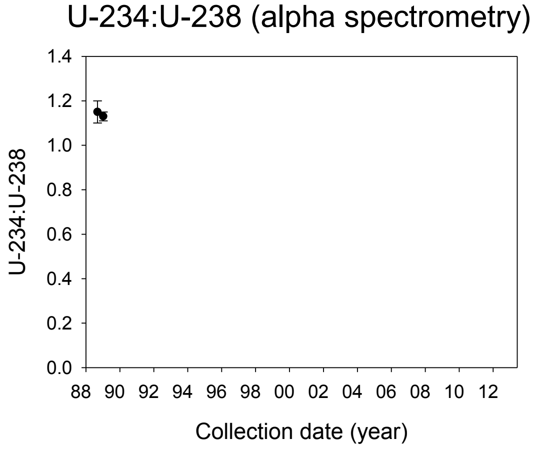

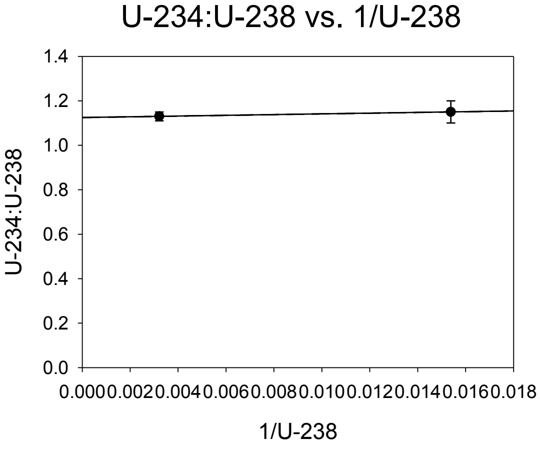

Bore ID – OB23

BORE ID - OB23

Data - Calcium, Potassium, Magnesium, Sodium and Sulfate

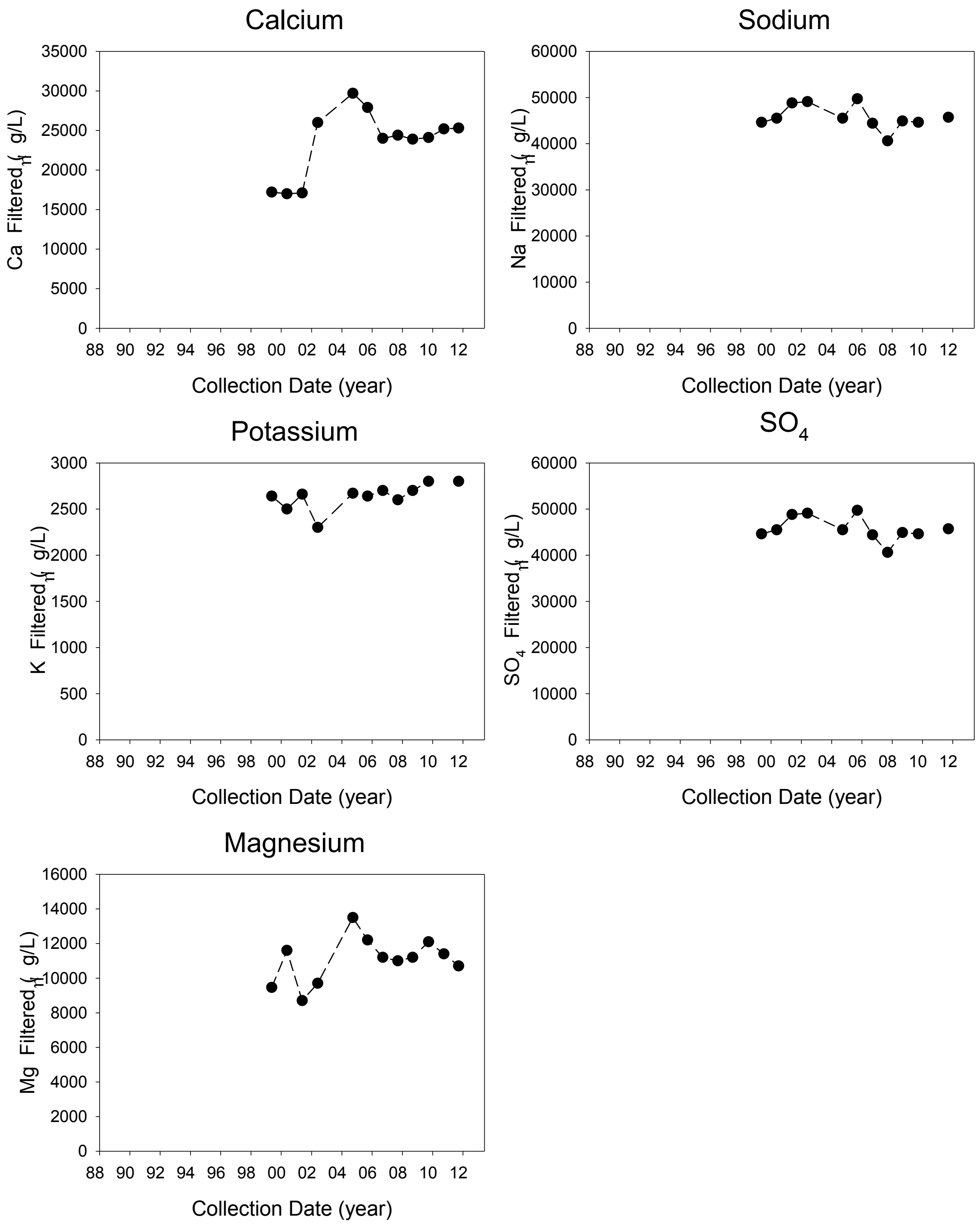

BORE ID - OB23

Data - Iron, Manganese, Barium, Strontium, Uranium & Vanadium

Iron

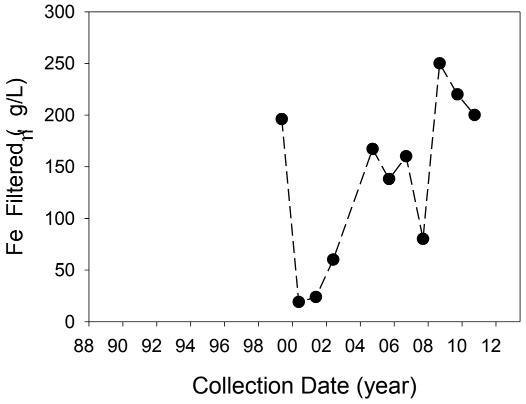

Manganese

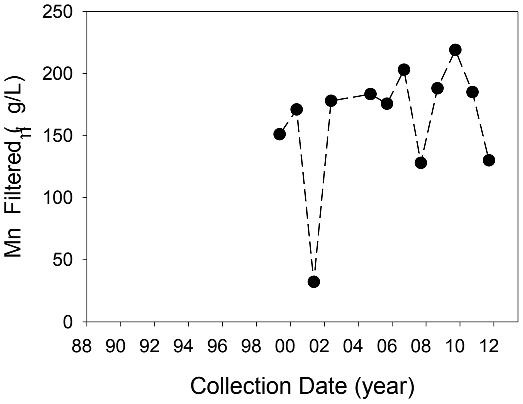

Barium

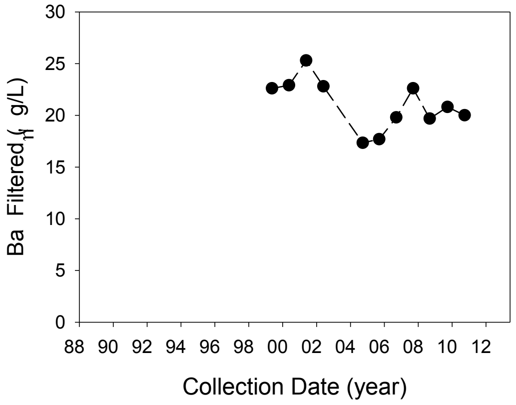

Strontium

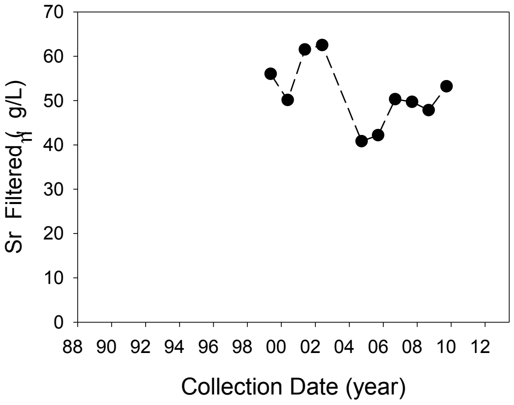

Uranium

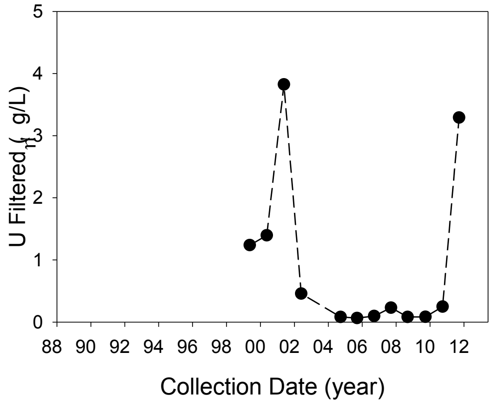

Vanadium

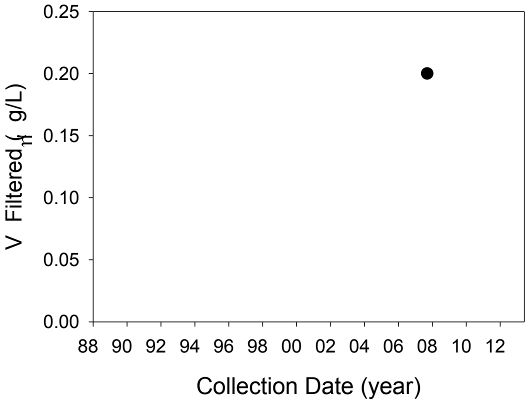

BORE ID - OB23

Data - U-238, Ra-226, U-234:U-238 & 1/U-238
Uncertainty is 1 standard deviation based on counting statistics only

U-238 (alpha spectrometry)

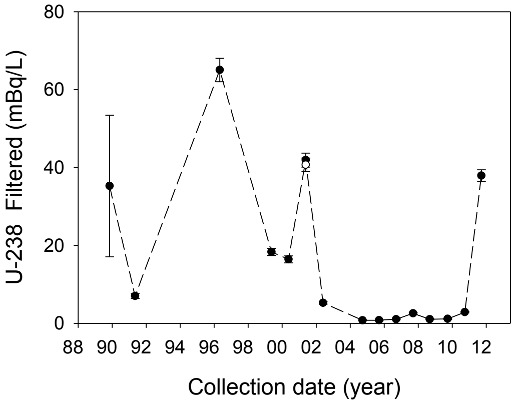

Ra-226 (alpha spectrometry)

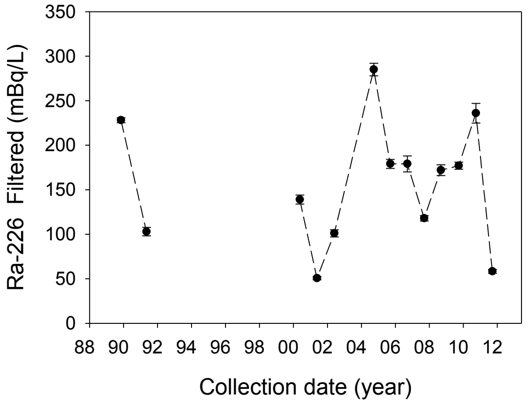

U-234:U-238 (alpha spectrometry)

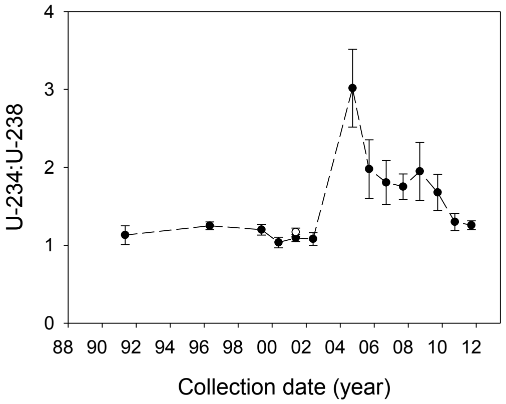

U-234:U-238 vs. 1/U-238

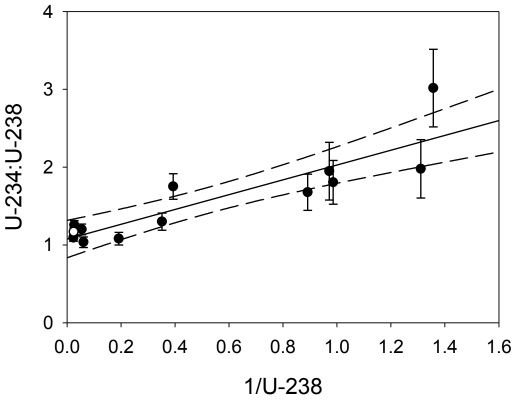

Bore ID – OB24

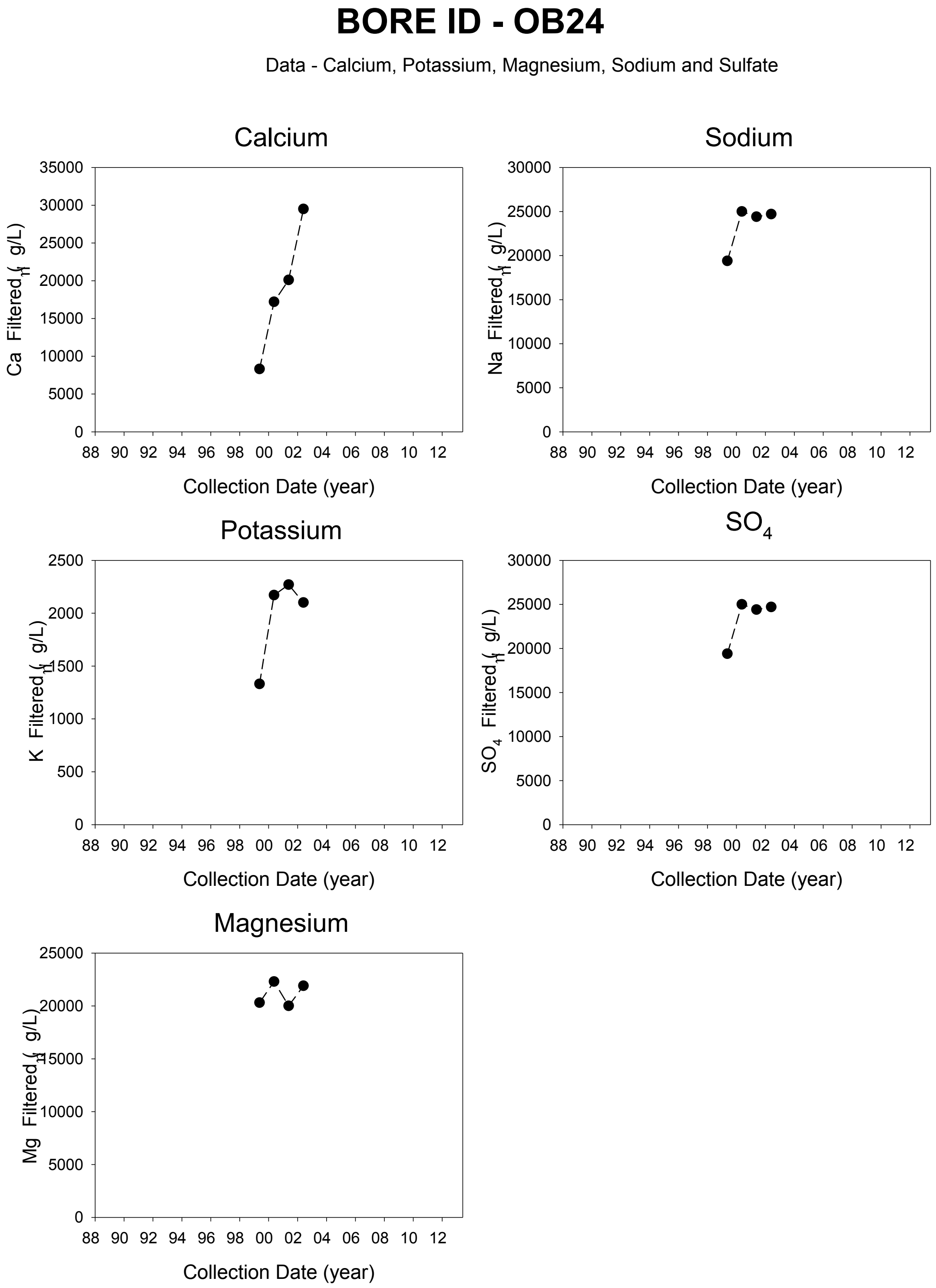
BORE ID - OB24
Data - Calcium, Potassium, Magnesium, Sodium and Sulfate
Calcium
Ca Filtered (µg/L)
0
5000
10000
15000
20000
25000
30000
35000
Collection Date (year)
88
90
92
94
96
98
00
02
04
06
08
10
12
Sodium
Na Filtered (µg/L)
0
5000
10000
15000
20000
25000
30000
Collection Date (year)
Potassium
K Filtered (µg/L)
0
500
1000
1500
2000
2500
Collection Date (year)
SO4
SO4 Filtered (µg/L)
0
5000
10000
15000
20000
25000
30000
Collection Date (year)
Magnesium
Mg Filtered (µg/L)
0
5000
10000
15000
20000
25000
Collection Date (year)

BORE ID - OB24

Data - Iron, Manganese, Barium, Strontium, Uranium & Vanadium

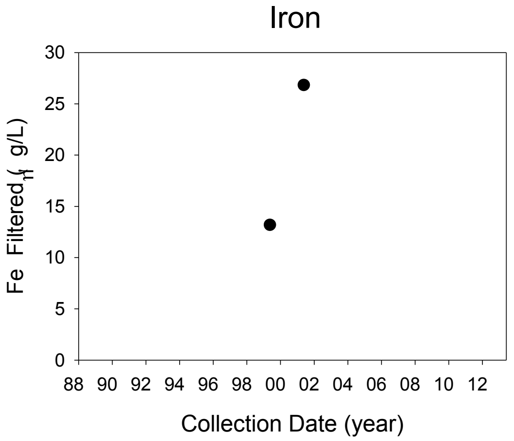

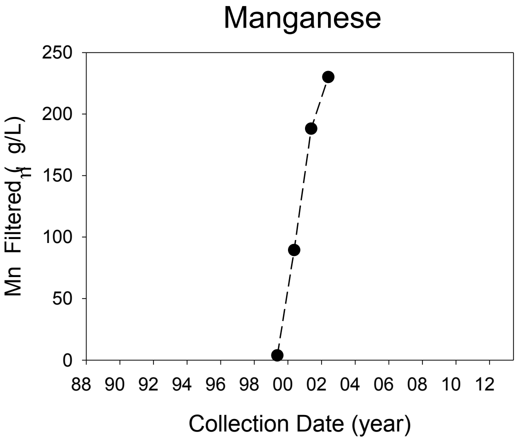

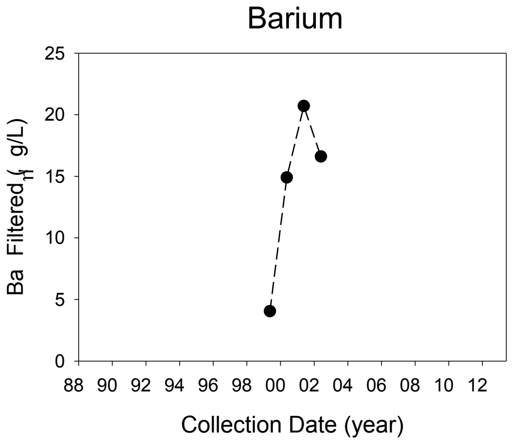

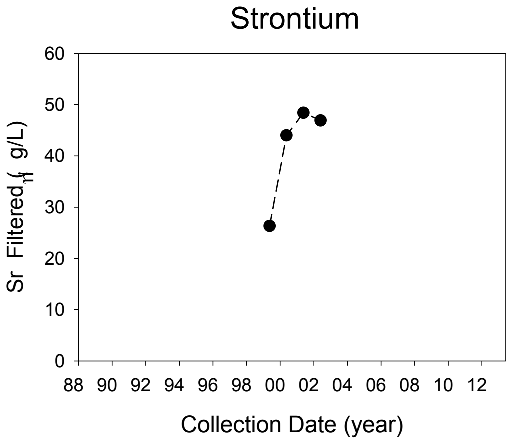

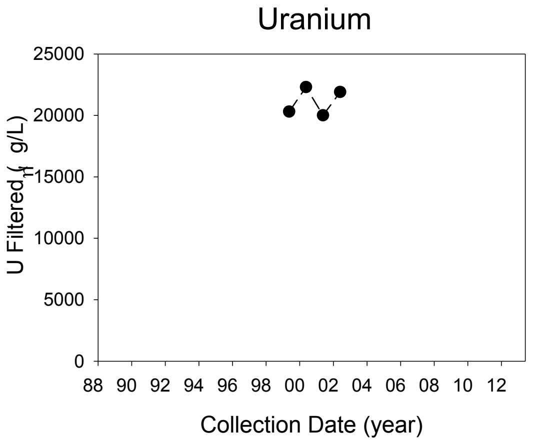

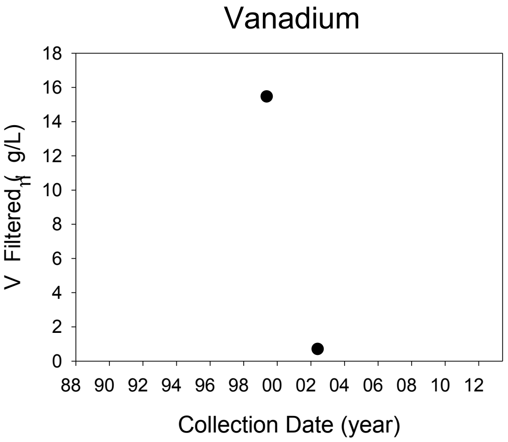

BORE ID - OB24

Data - U-238, Ra-226, U-234:U-238 & 1/U-238
Uncertainty is 1 standard deviation based on counting statistics only

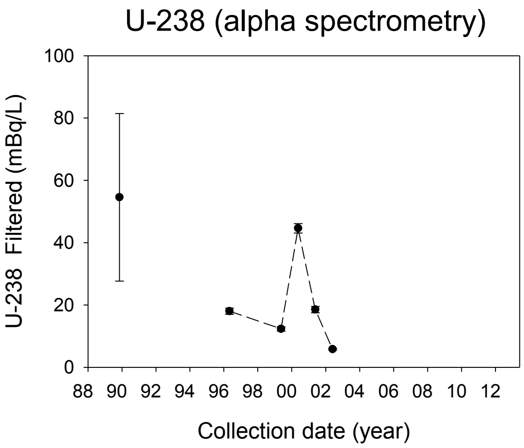

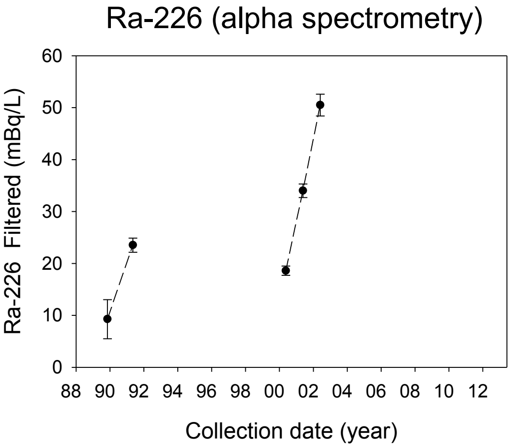

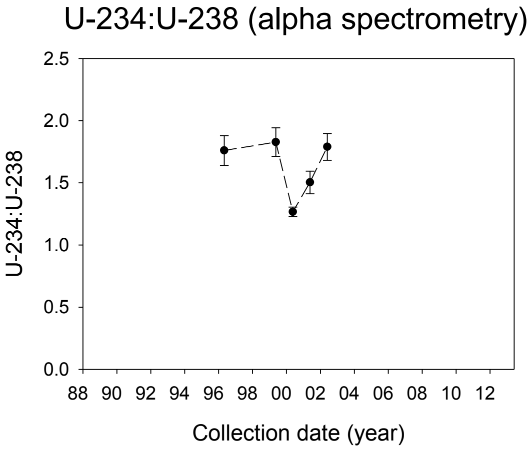

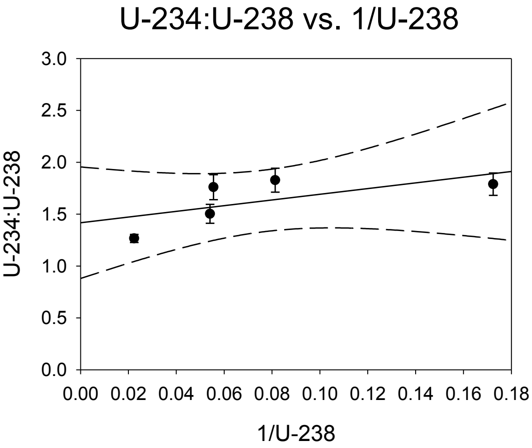

Bore ID – OB26

BORE ID - OB26

Data - U-238, Ra-226, U-234:U-238 & 1/U-238
Uncertainty is 1 standard deviation based on counting statistics only

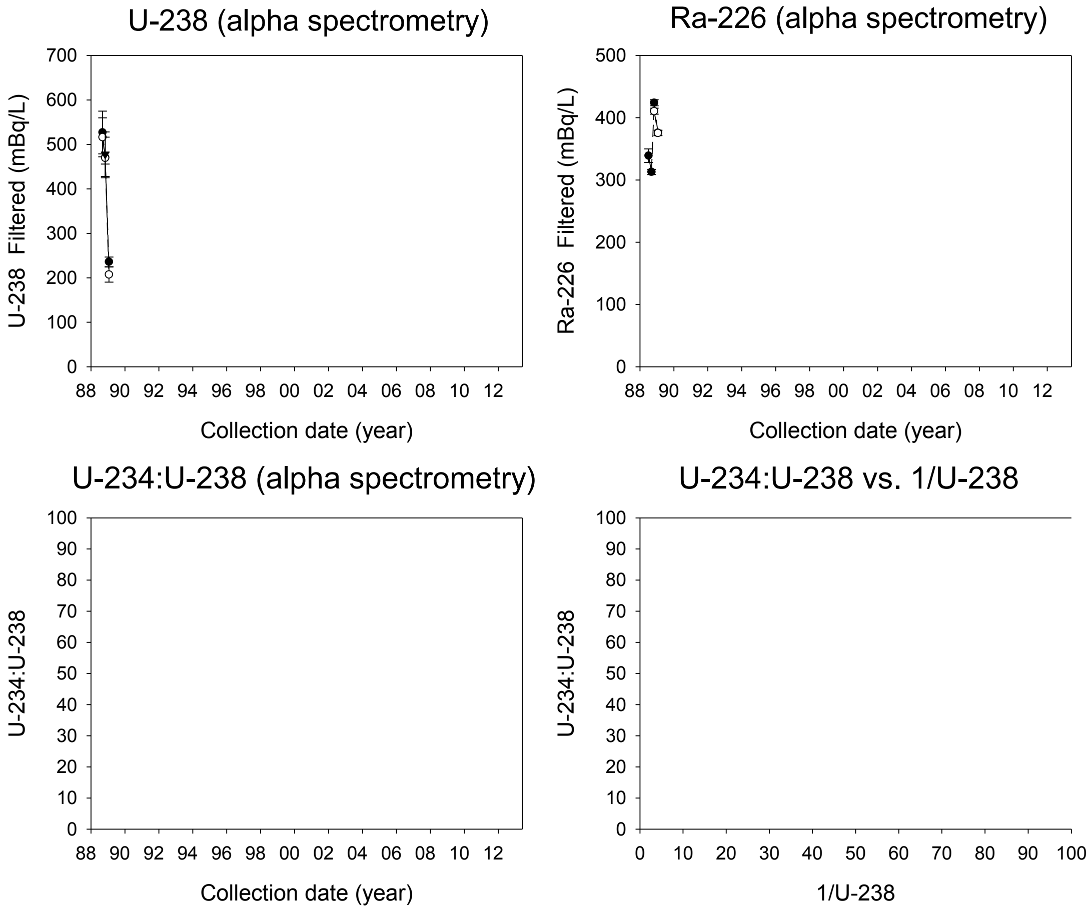

Bore ID – OB27

BORE ID - OB27

Data - Calcium, Potassium, Magnesium, Sodium and Sulfate

Calcium

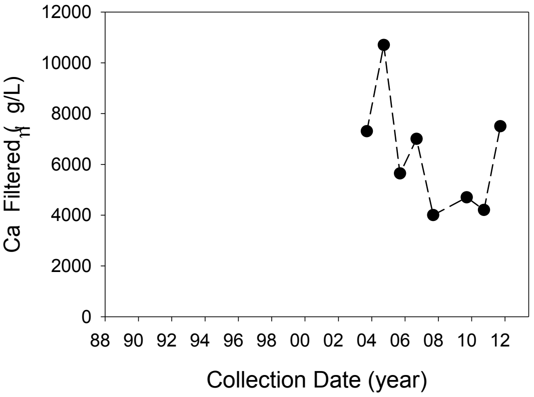

Sodium

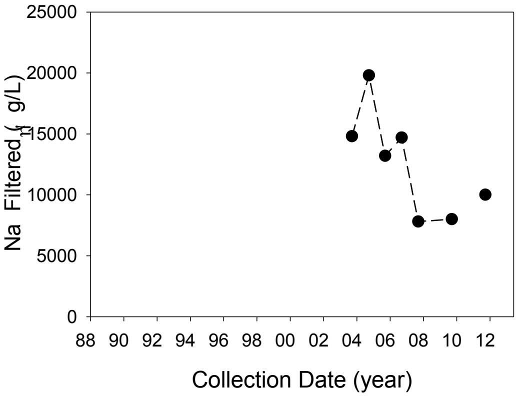

Potassium

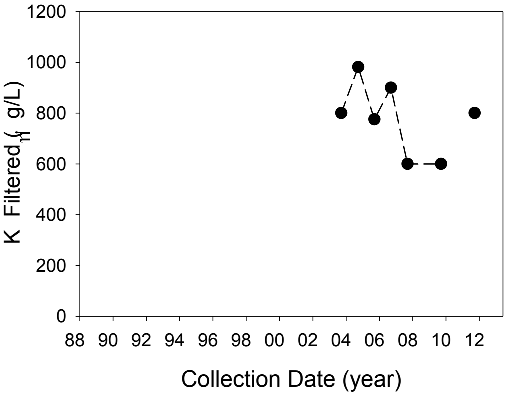

SO_4

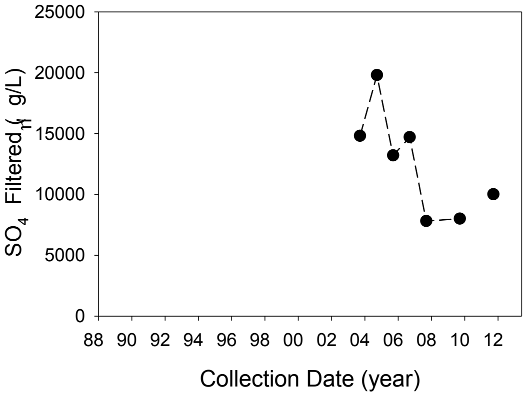

Magnesium

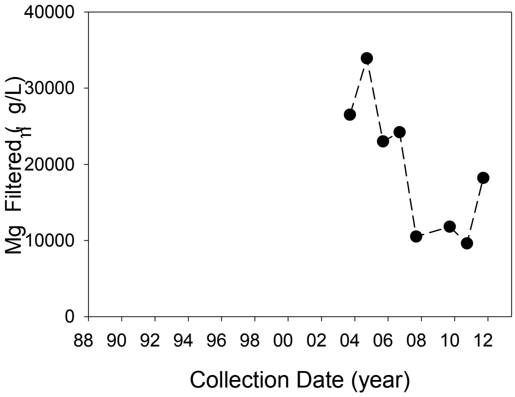

BORE ID - OB27

Data - Iron, Manganese, Barium, Strontium, Uranium & Vanadium

Iron

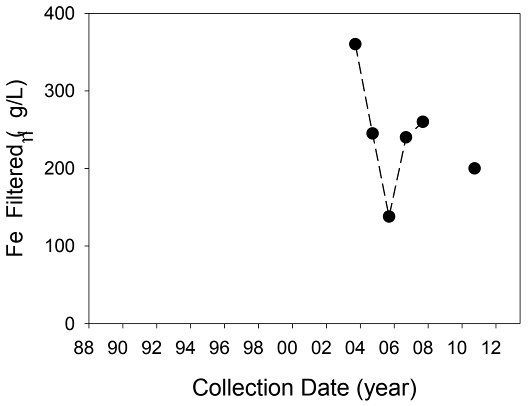

Manganese

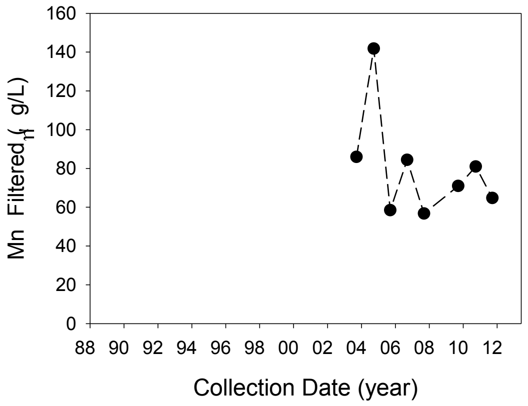

Barium

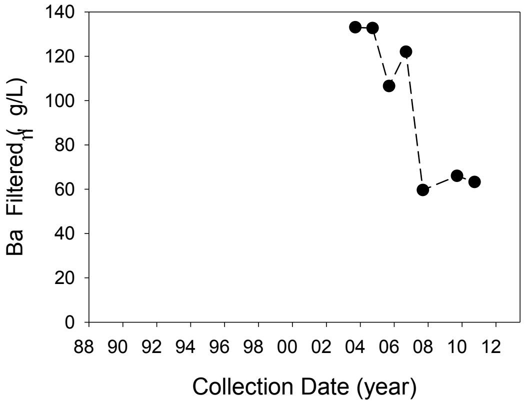

Strontium

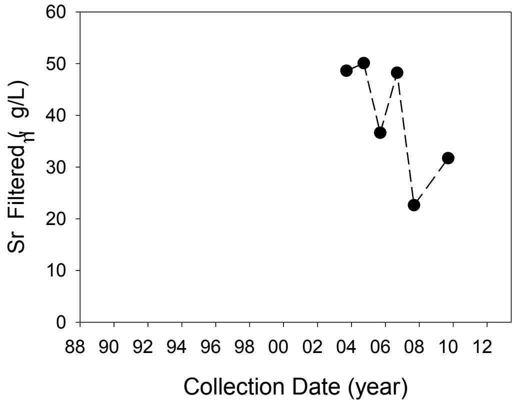

Uranium

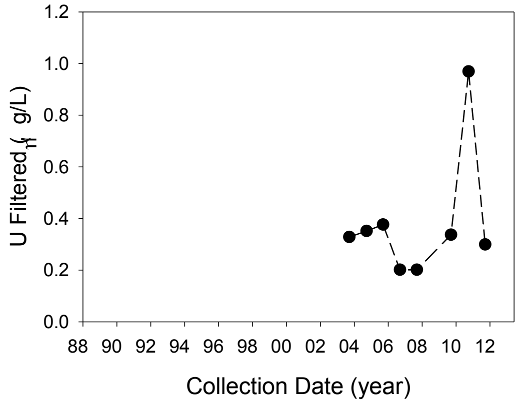

Vanadium

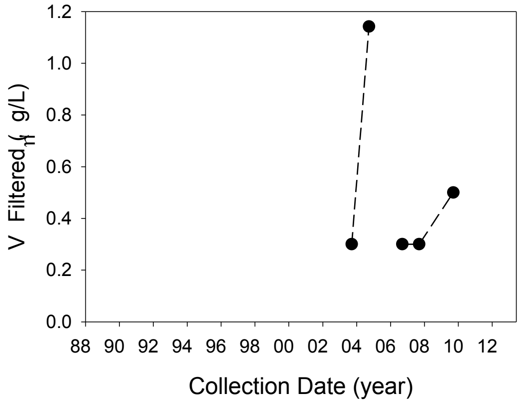

BORE ID - OB27

Data - U-238, Ra-226, U-234:U-238 & 1/U-238
Uncertainty is 1 standard deviation based on counting statistics only

U-238 (alpha spectrometry)

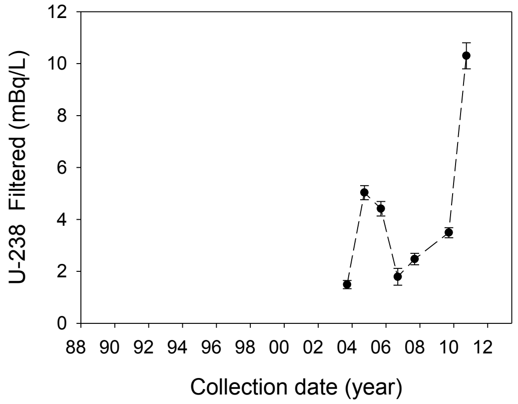

Ra-226 (alpha spectrometry)

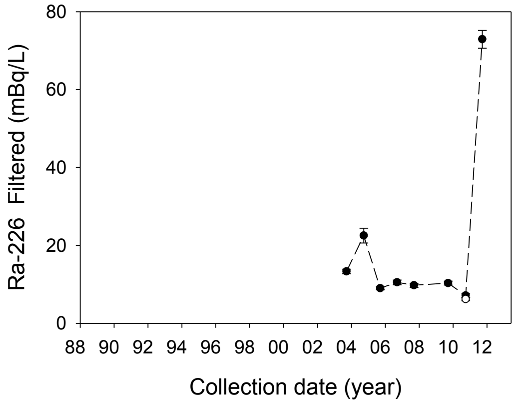

U-234:U-238 (alpha spectrometry)

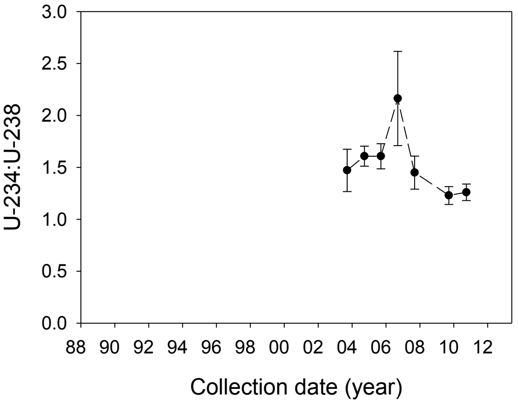

U-234:U-238 vs. 1/U-238

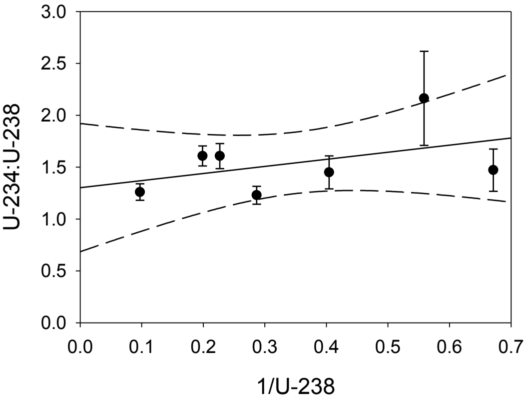

Bore ID – OB28

BORE ID - OB28

Data - Calcium, Potassium, Magnesium, Sodium and Sulfate

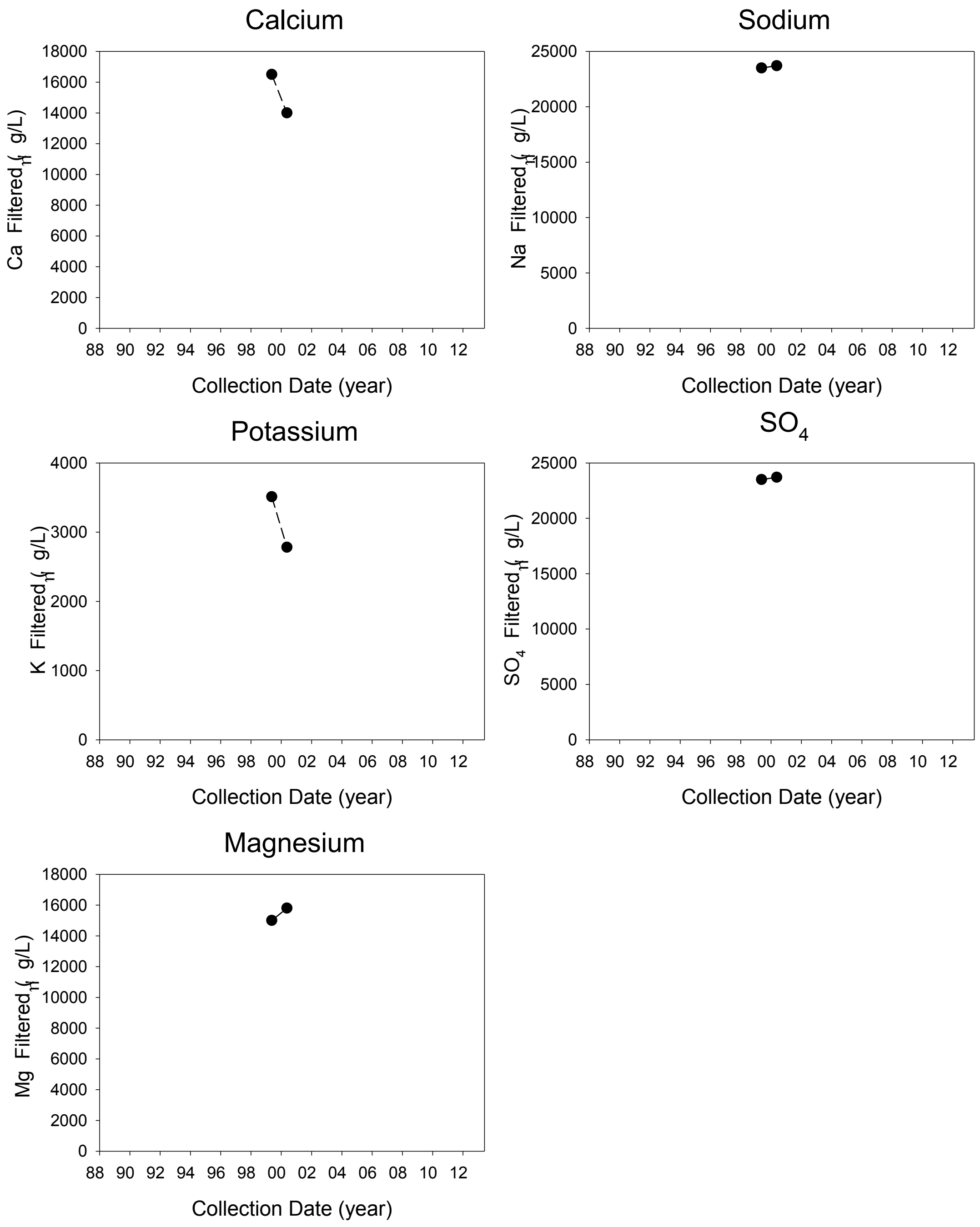

BORE ID - OB28

Data - Iron, Manganese, Barium, Strontium, Uranium & Vanadium

Iron

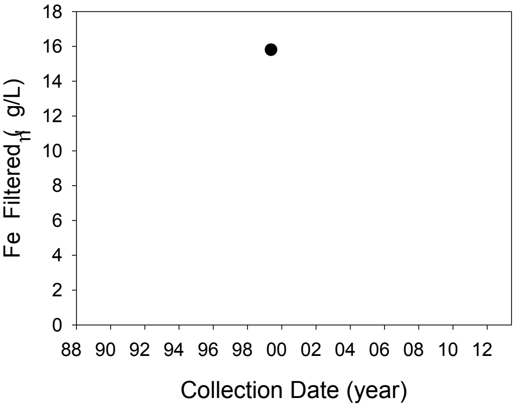

Manganese

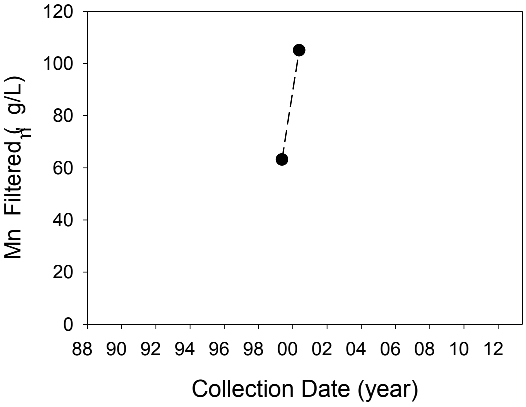

Barium

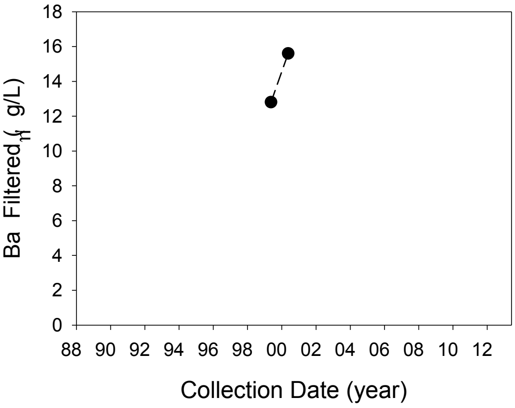

Strontium

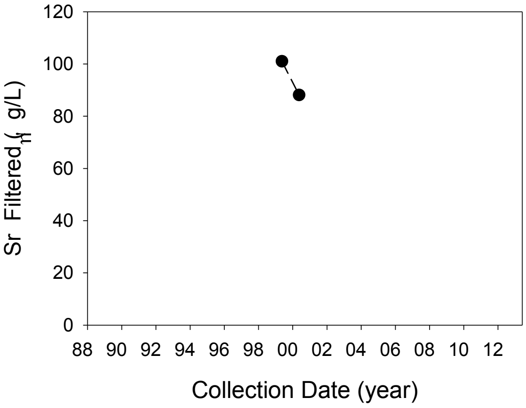

Uranium

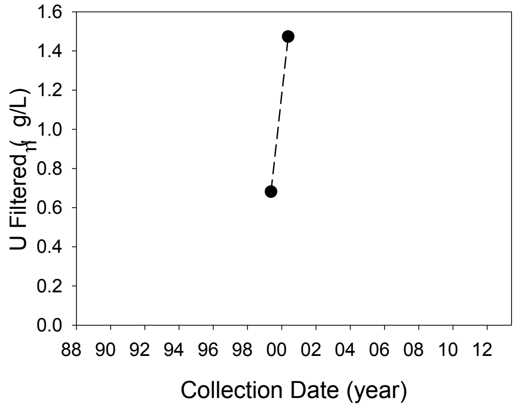

Vanadium

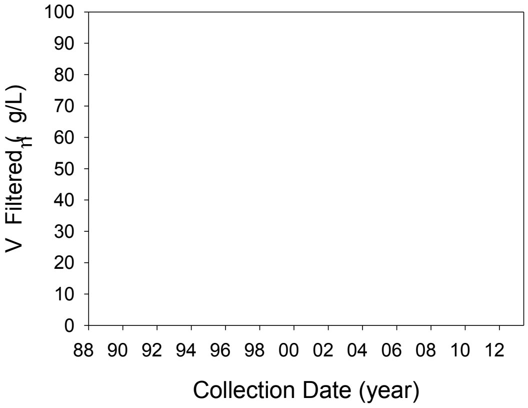

BORE ID - OB28

Data - U-238, Ra-226, U-234:U-238 & 1/U-238
Uncertainty is 1 standard deviation based on counting statistics only

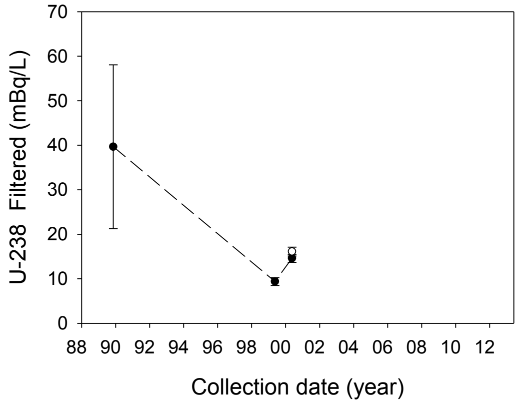
U-238 (alpha spectrometry)

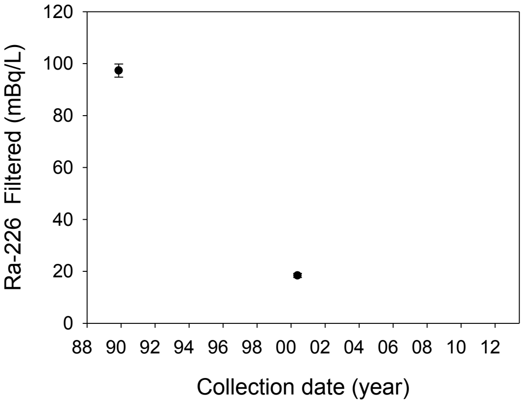
Ra-226 (alpha spectrometry)

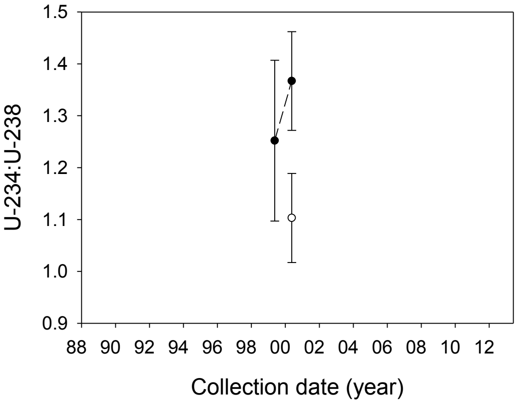
U-234:U-238 (alpha spectrometry)

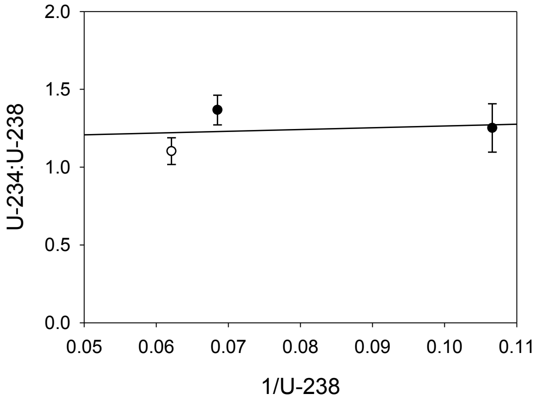
U-234:U-238 vs. 1/U-238

Bore ID – OB29

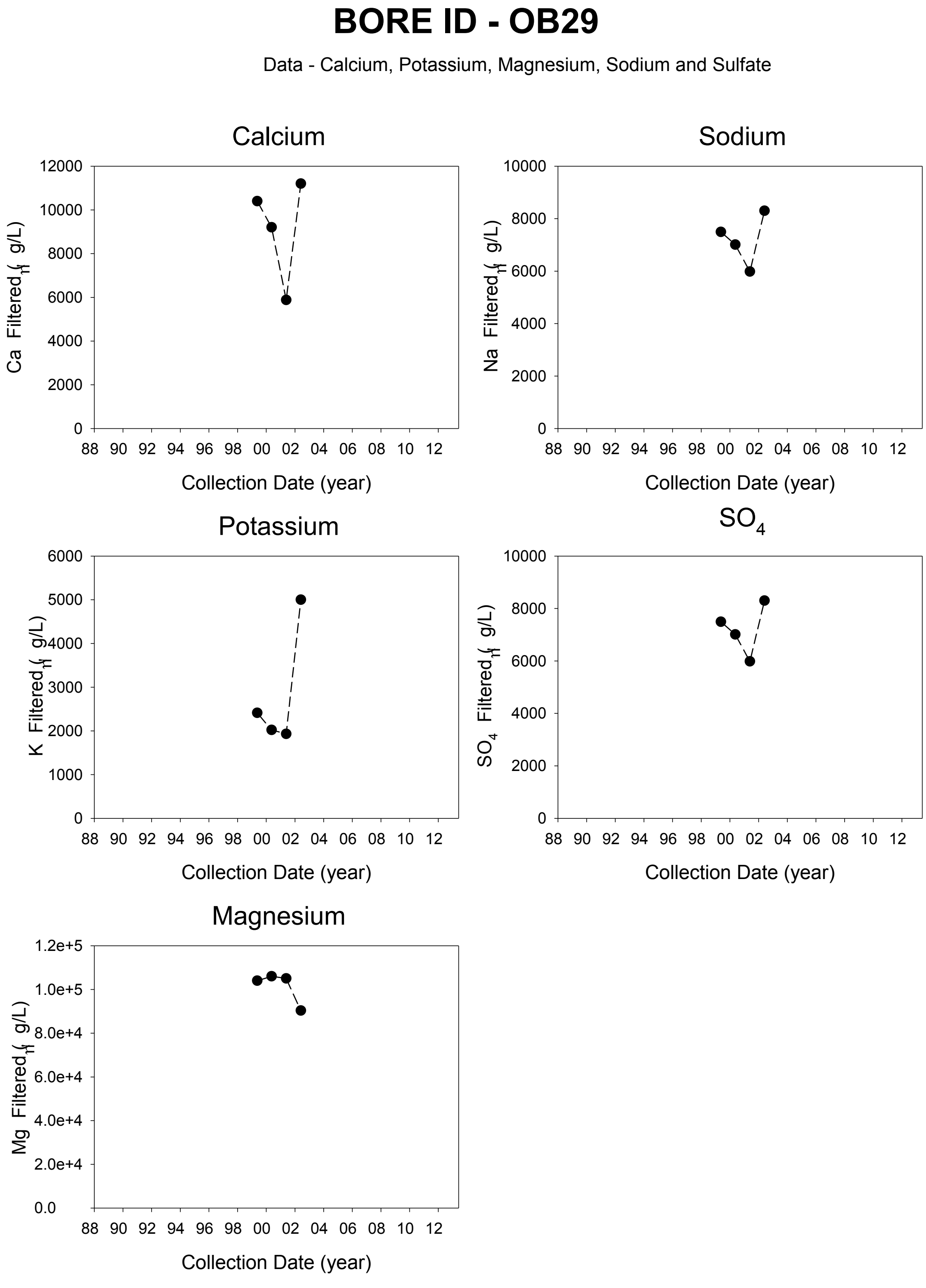
BORE ID - OB29
Data - Calcium, Potassium, Magnesium, Sodium and Sulfate
Calcium
Ca Filtered (µg/L)
0
2000
4000
6000
8000
10000
12000
88 90 92 94 96 98 00 02 04 06 08 10 12
Collection Date (year)
Sodium
Na Filtered (µg/L)
0
2000
4000
6000
8000
10000
88 90 92 94 96 98 00 02 04 06 08 10 12
Collection Date (year)
Potassium
K Filtered (µg/L)
0
1000
2000
3000
4000
5000
6000
88 90 92 94 96 98 00 02 04 06 08 10 12
Collection Date (year)
SO_4
SO_4 Filtered (µg/L)
0
2000
4000
6000
8000
10000
88 90 92 94 96 98 00 02 04 06 08 10 12
Collection Date (year)
Magnesium
Mg Filtered (µg/L)
0.0
2.0e+4
4.0e+4
6.0e+4
8.0e+4
1.0e+5
1.2e+5
88 90 92 94 96 98 00 02 04 06 08 10 12
Collection Date (year)

BORE ID - OB29

Data - Iron, Manganese, Barium, Strontium, Uranium & Vanadium

Iron

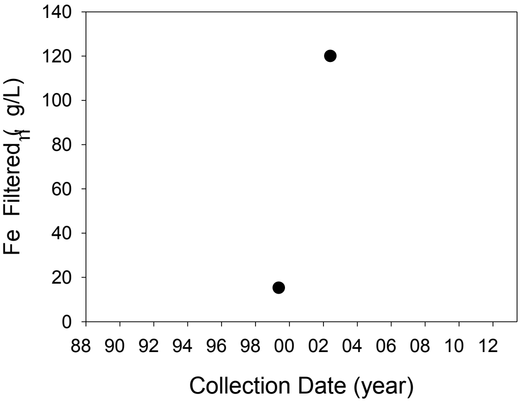

Manganese

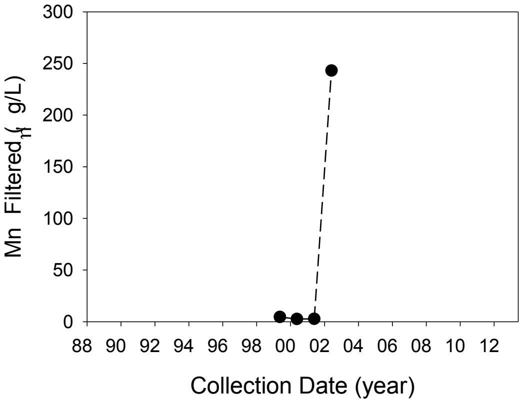

Barium

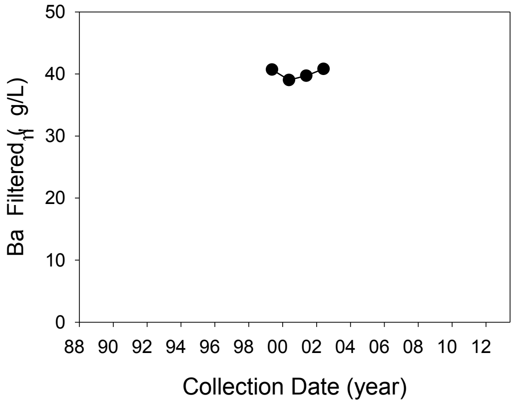

Strontium

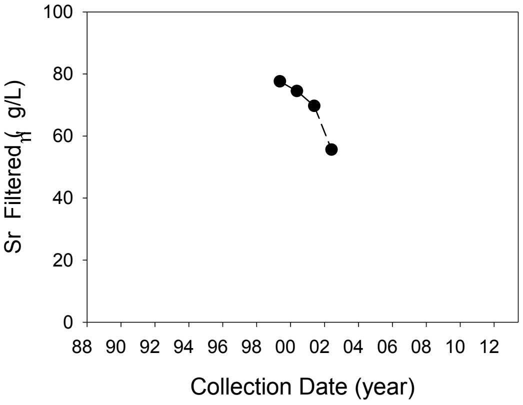

Uranium

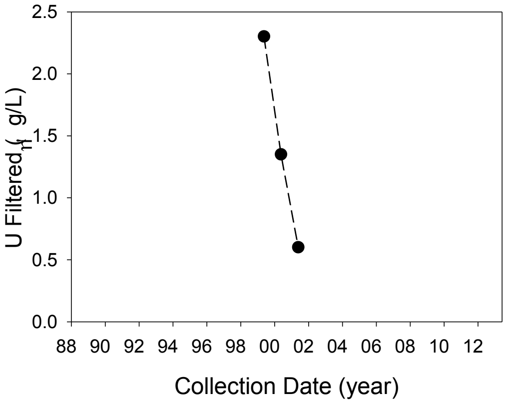

Vanadium

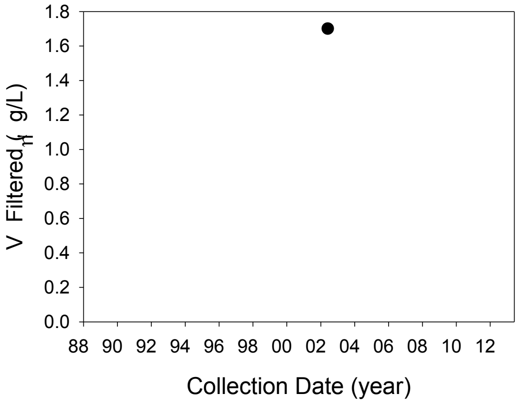

BORE ID - OB29

Data - U-238, Ra-226, U-234:U-238 & 1/U-238
Uncertainty is 1 standard deviation based on counting statistics only

U-238 (alpha spectrometry)

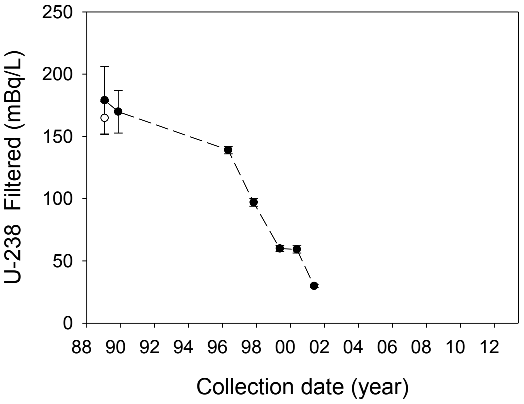

Ra-226 (alpha spectrometry)

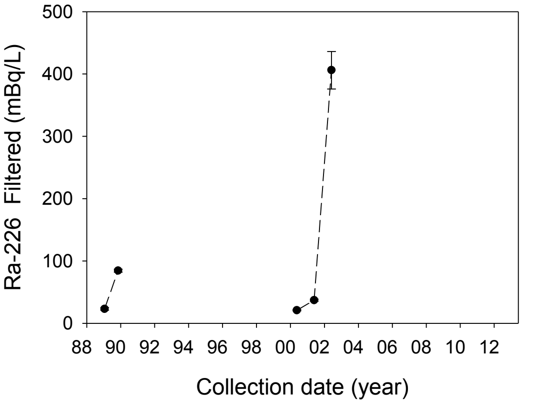

U-234:U-238 (alpha spectrometry)

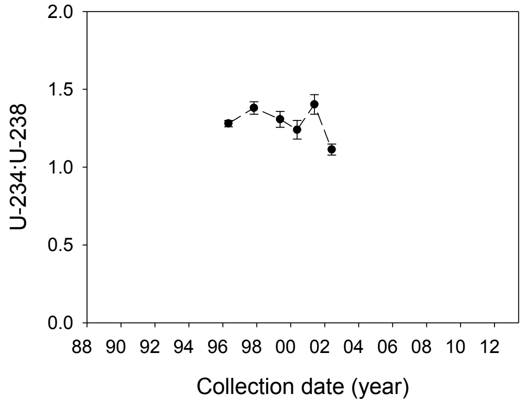

U-234:U-238 vs. 1/U-238

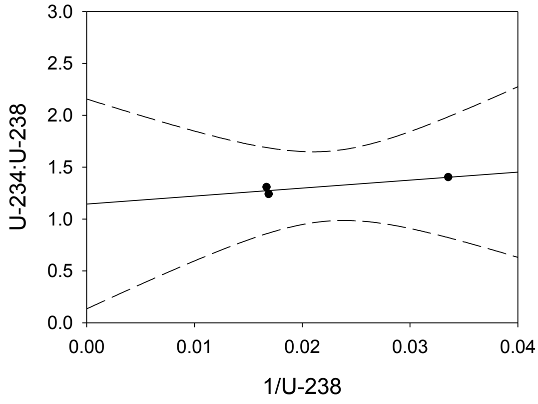

Bore ID – OB30

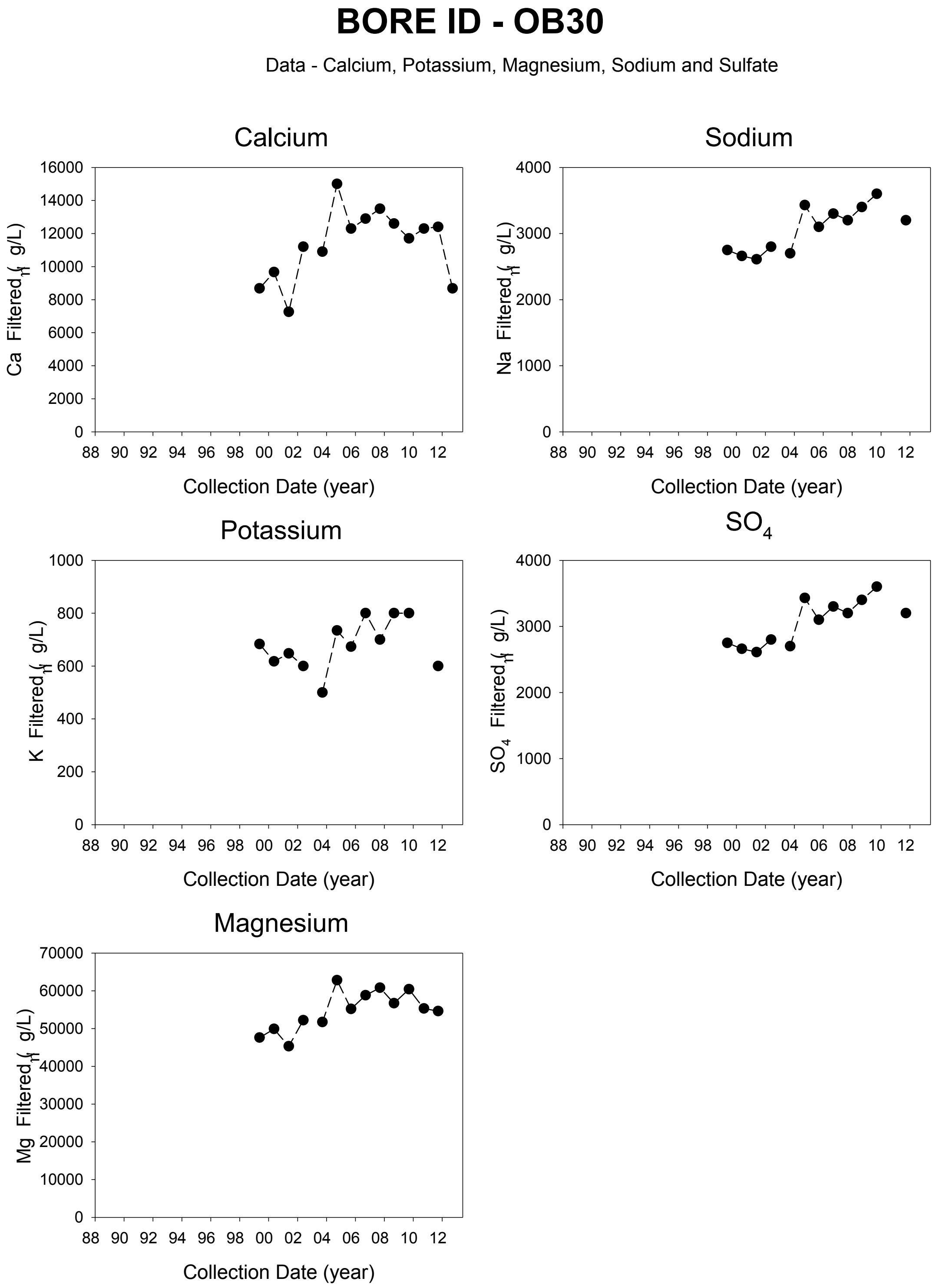

BORE ID - OB30

Data - Calcium, Potassium, Magnesium, Sodium and Sulfate

BORE ID - OB30

Data - Iron, Manganese, Barium, Strontium, Uranium & Vanadium

Iron

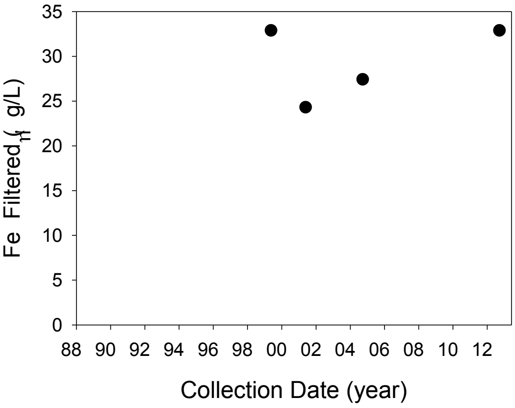

Manganese

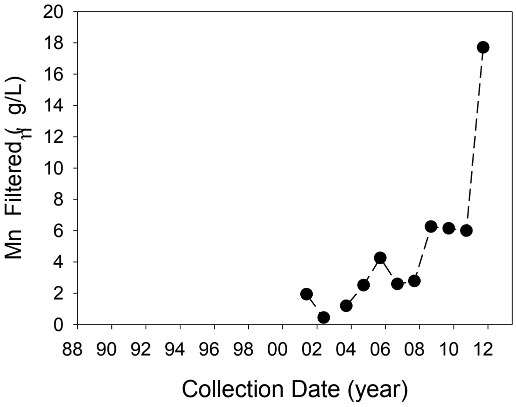

Barium

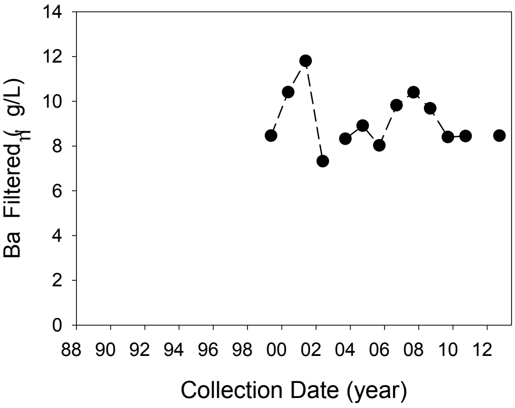

Strontium

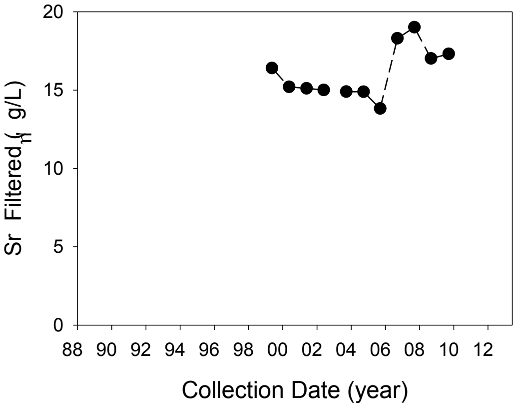

Uranium

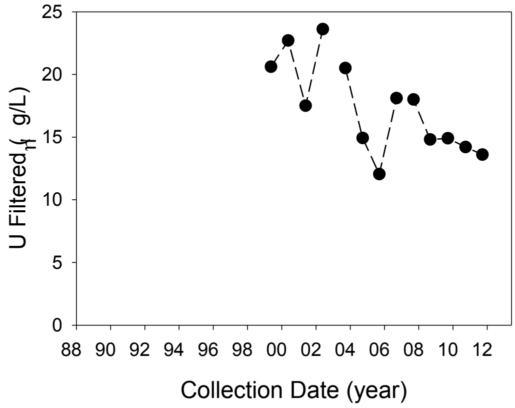

Vanadium

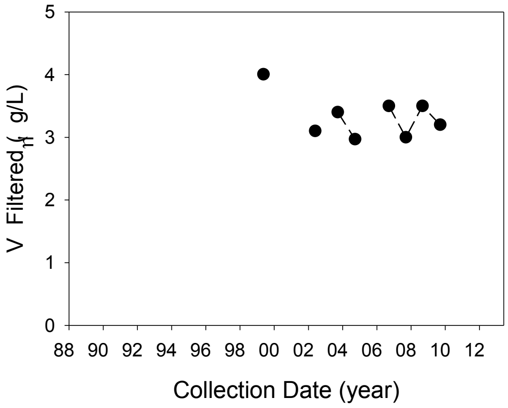

BORE ID - OB30

Data - U-238, Ra-226, U-234:U-238 & 1/U-238
Uncertainty is 1 standard deviation based on counting statistics only

U-238 (alpha spectrometry)

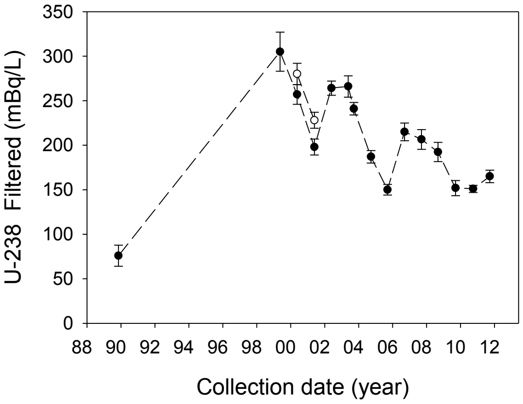

Ra-226 (alpha spectrometry)

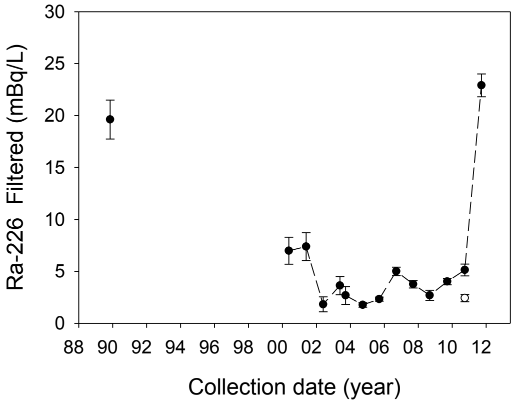

U-234:U-238 (alpha spectrometry)

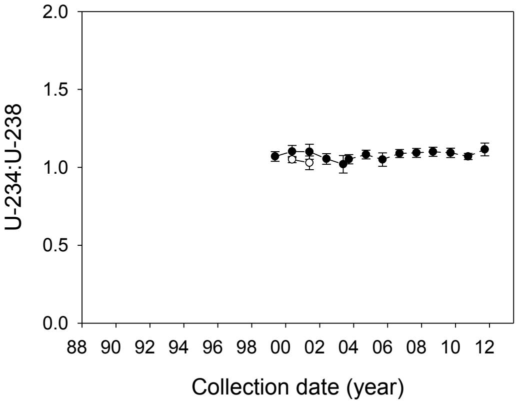

U-234:U-238 vs. 1/U-238

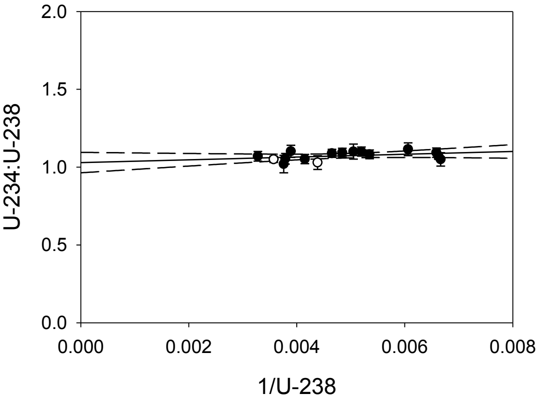

Bore ID – OB2A

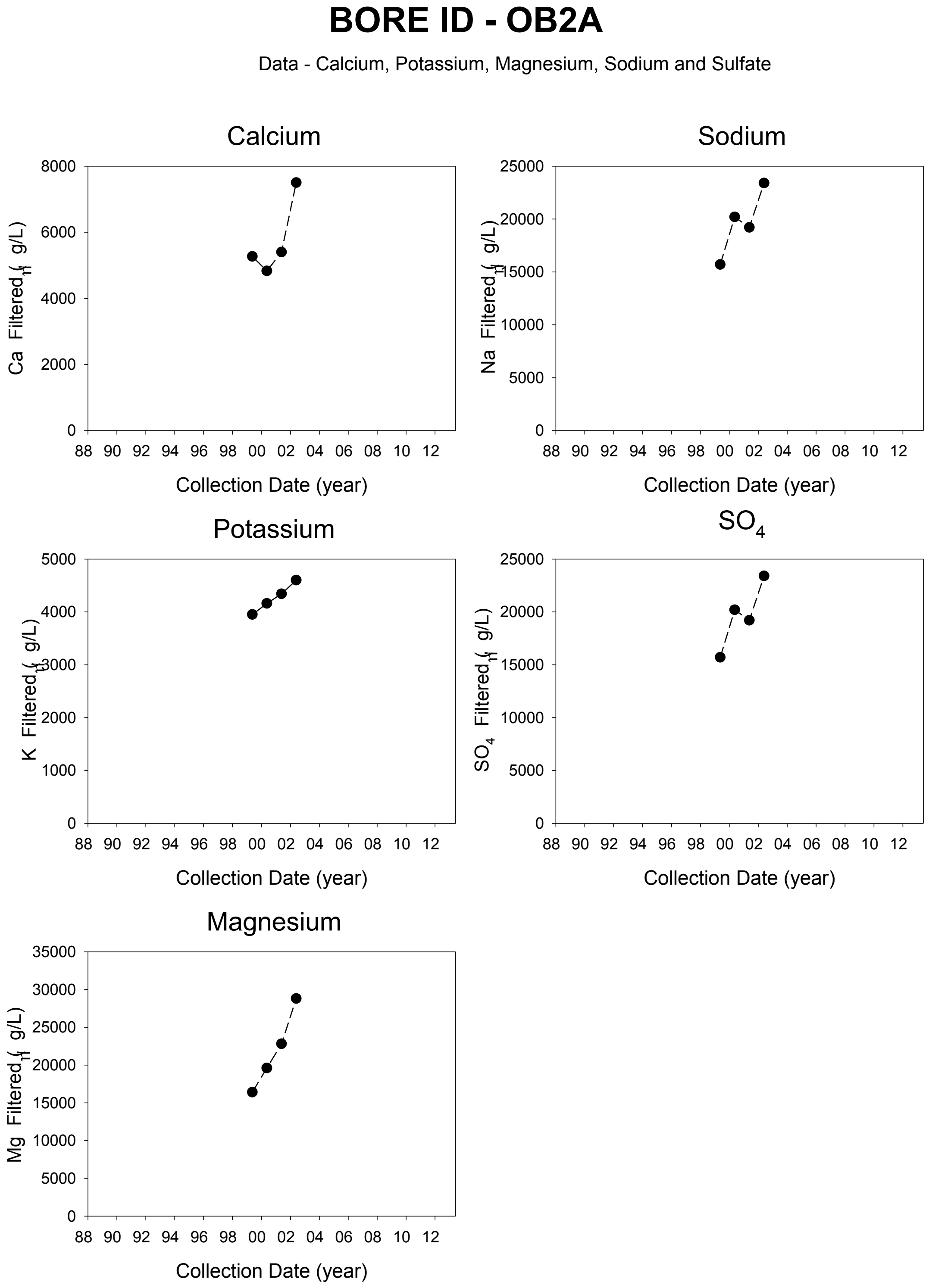
BORE ID - OB2A
Data - Calcium, Potassium, Magnesium, Sodium and Sulfate
Calcium
Ca Filtered (μg/L)
0
2000
4000
6000
8000
Sodium
Na Filtered (μg/L)
0
5000
10000
15000
20000
25000
Potassium
K Filtered (μg/L)
0
1000
2000
3000
4000
5000
SO_4
SO_4 Filtered (μg/L)
0
5000
10000
15000
20000
25000
Magnesium
Mg Filtered (μg/L)
0
5000
10000
15000
20000
25000
30000
35000
88 90 92 94 96 98 00 02 04 06 08 10 12
Collection Date (year)

BORE ID - OB2A

Data - Iron, Manganese, Barium, Strontium, Uranium & Vanadium

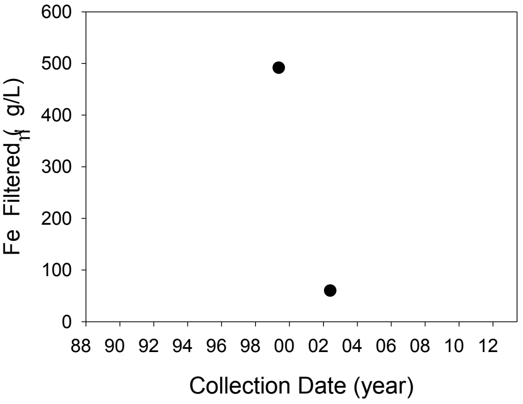
Iron

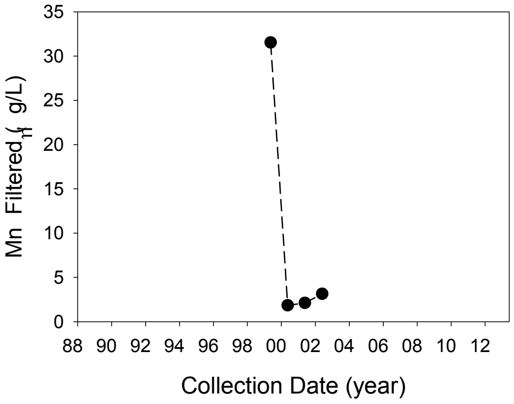
Manganese

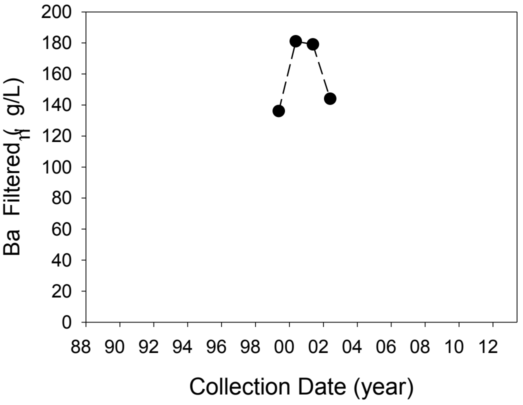
Barium

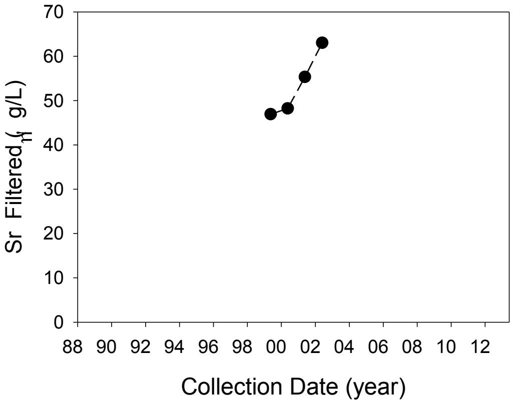
Strontium

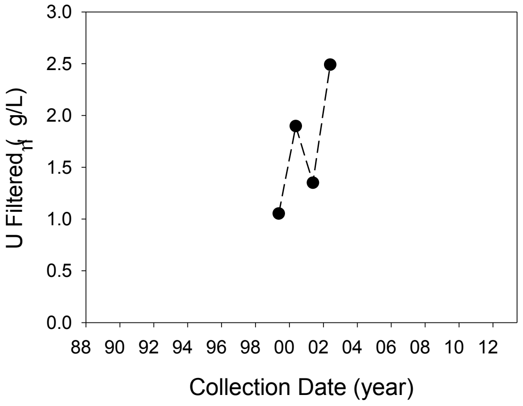
Uranium

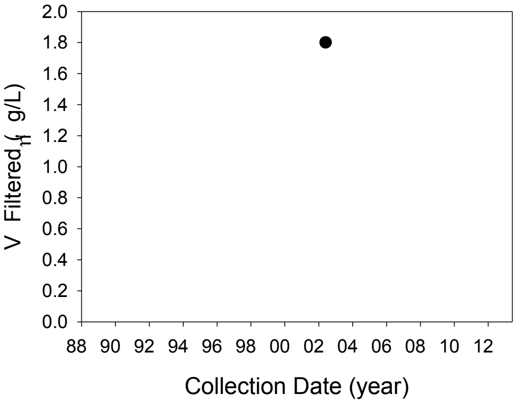
Vanadium

BORE ID - OB2A

Data - U-238, Ra-226, U-234:U-238 & 1/U-238
Uncertainty is 1 standard deviation based on counting statistics only

U-238 (alpha spectrometry)

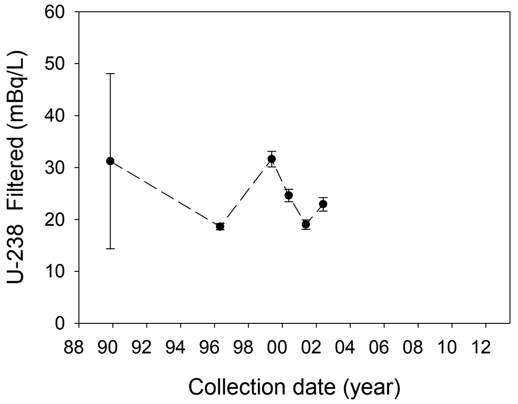

Ra-226 (alpha spectrometry)

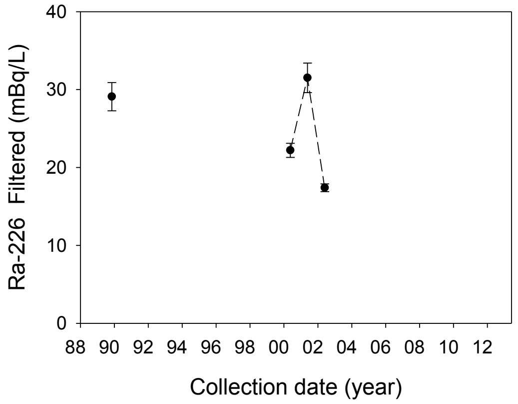

U-234:U-238 (alpha spectrometry)

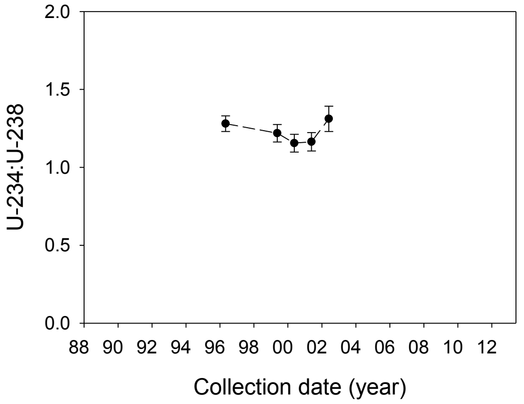

U-234:U-238 vs. 1/U-238

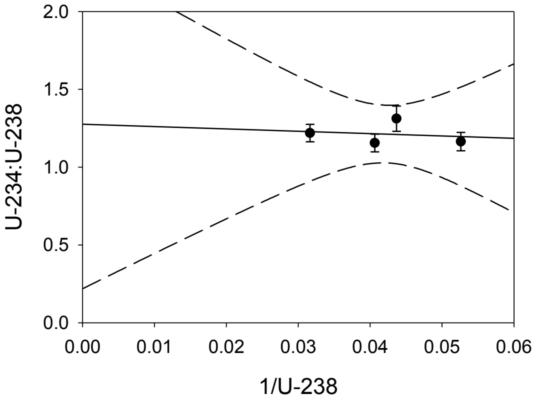

Bore ID – OB44

BORE ID - OB44

Data - Calcium, Potassium, Magnesium, Sodium and Sulfate

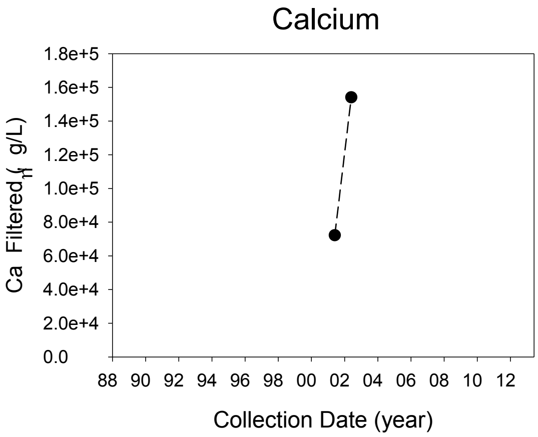

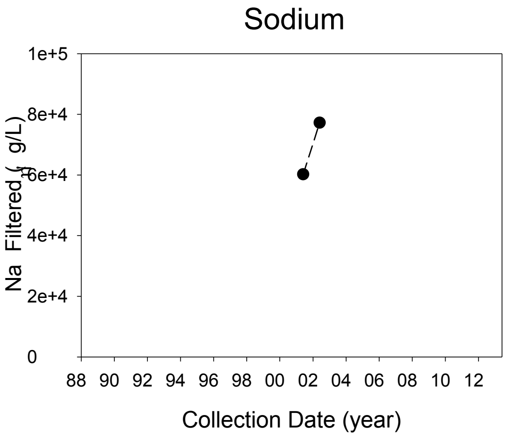

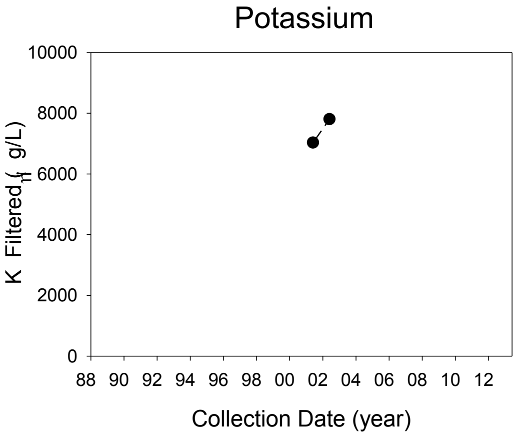

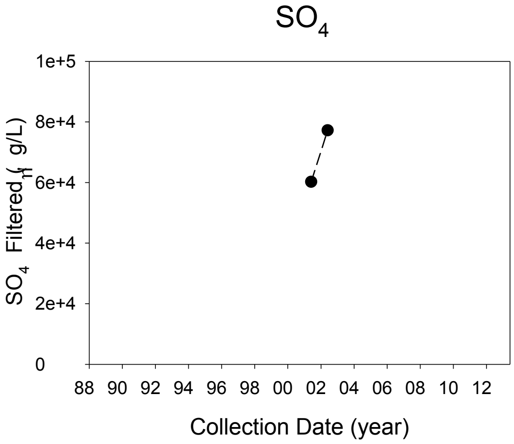

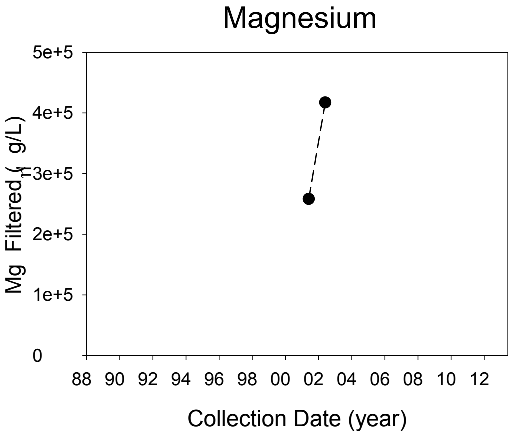

BORE ID - OB44

Data - Iron, Manganese, Barium, Strontium, Uranium & Vanadium

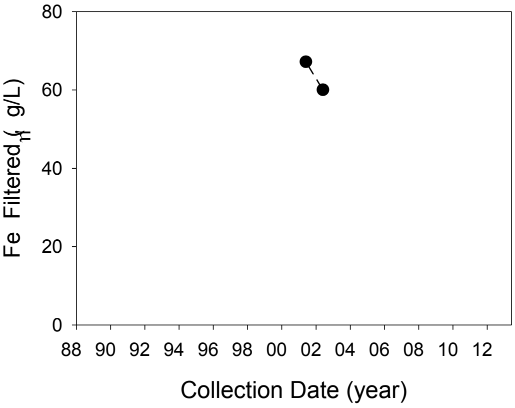
Iron

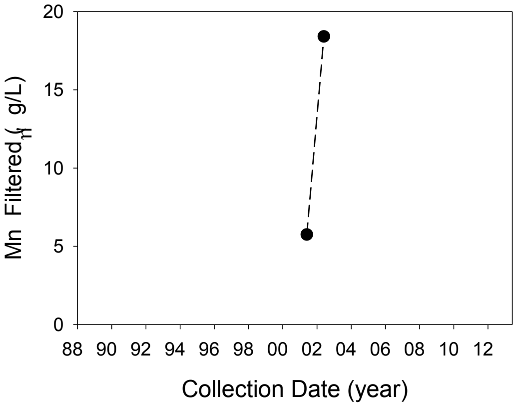
Manganese

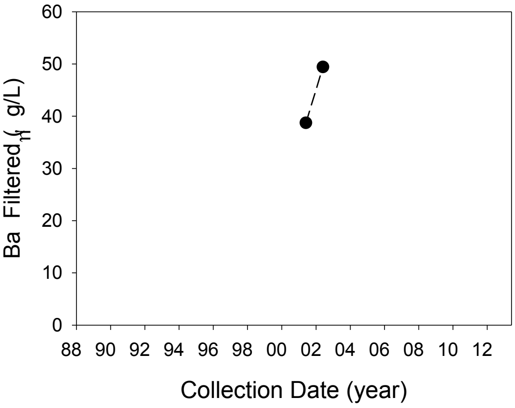
Barium

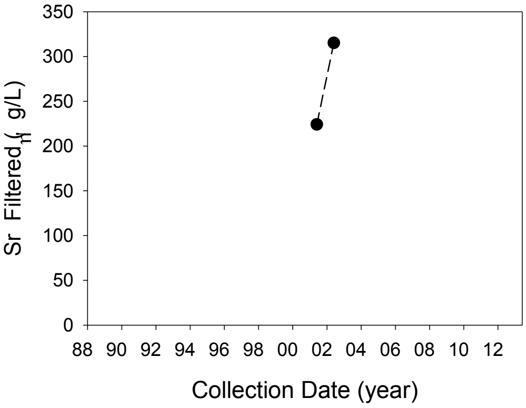
Strontium

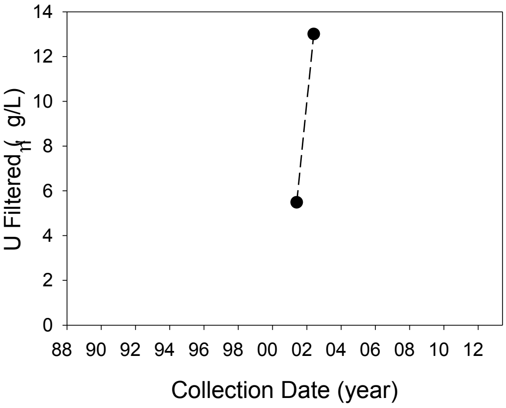
Uranium

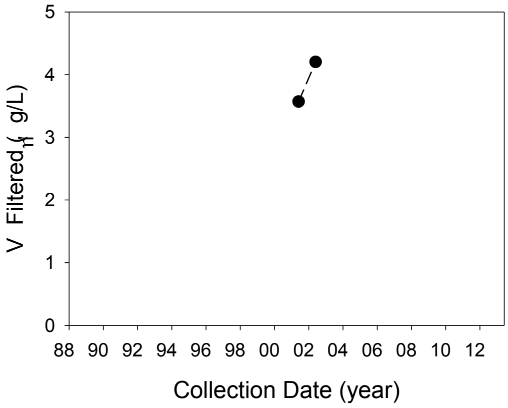
Vanadium

BORE ID - OB44

Data - U-238, Ra-226, U-234:U-238 & 1/U-238
Uncertainty is 1 standard deviation based on counting statistics only

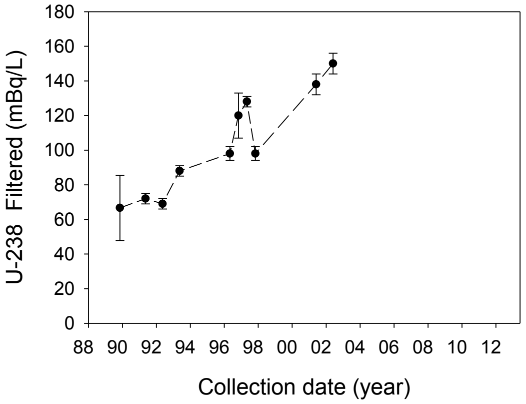
U-238 (alpha spectrometry)

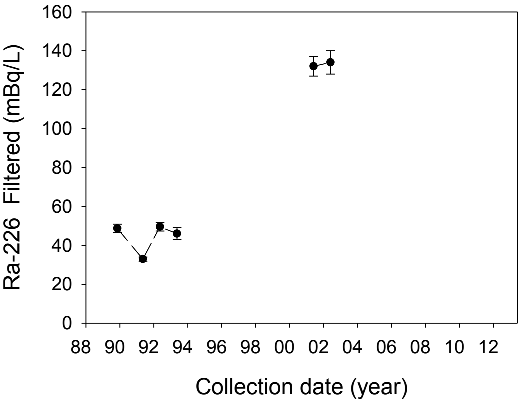
Ra-226 (alpha spectrometry)

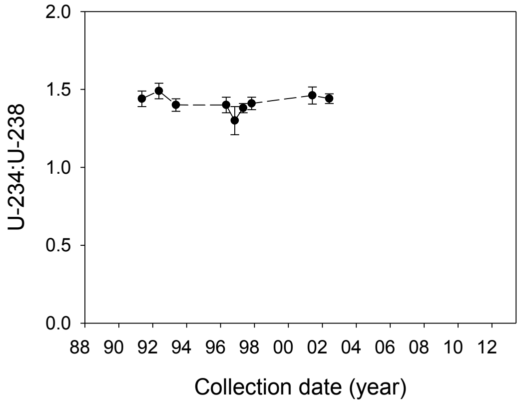
U-234:U-238 (alpha spectrometry)

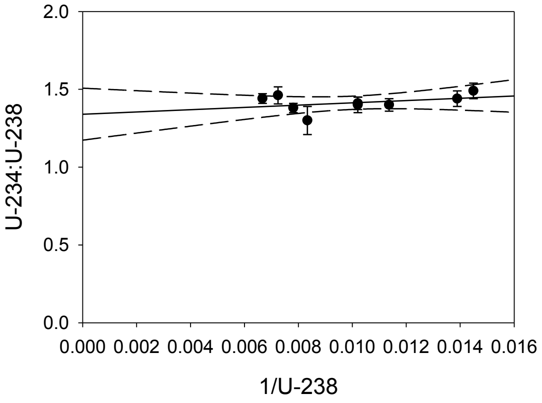
U-234:U-238 vs. 1/U-238

Bore ID –OB46

BORE ID - OB46

Data - U-238, Ra-226, U-234:U-238 & 1/U-238
Uncertainty is 1 standard deviation based on counting statistics only

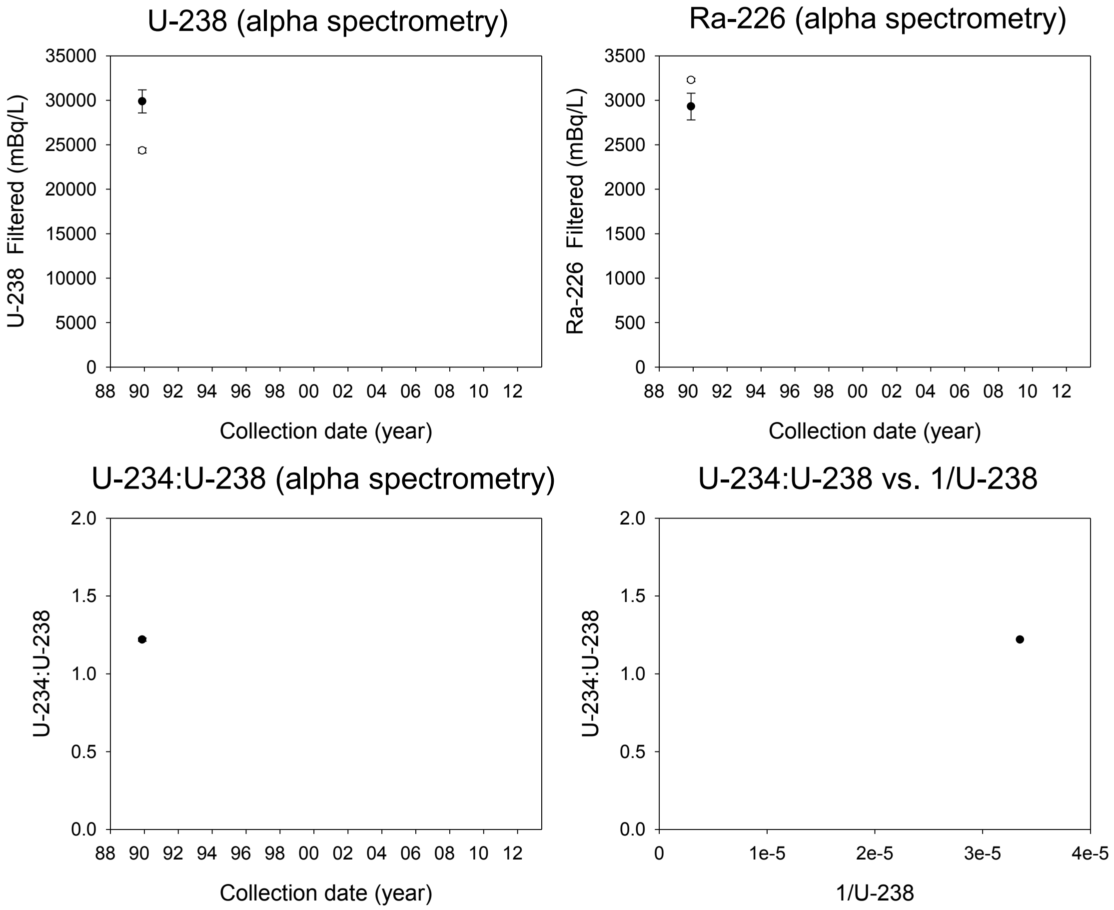

Bore ID –OB47

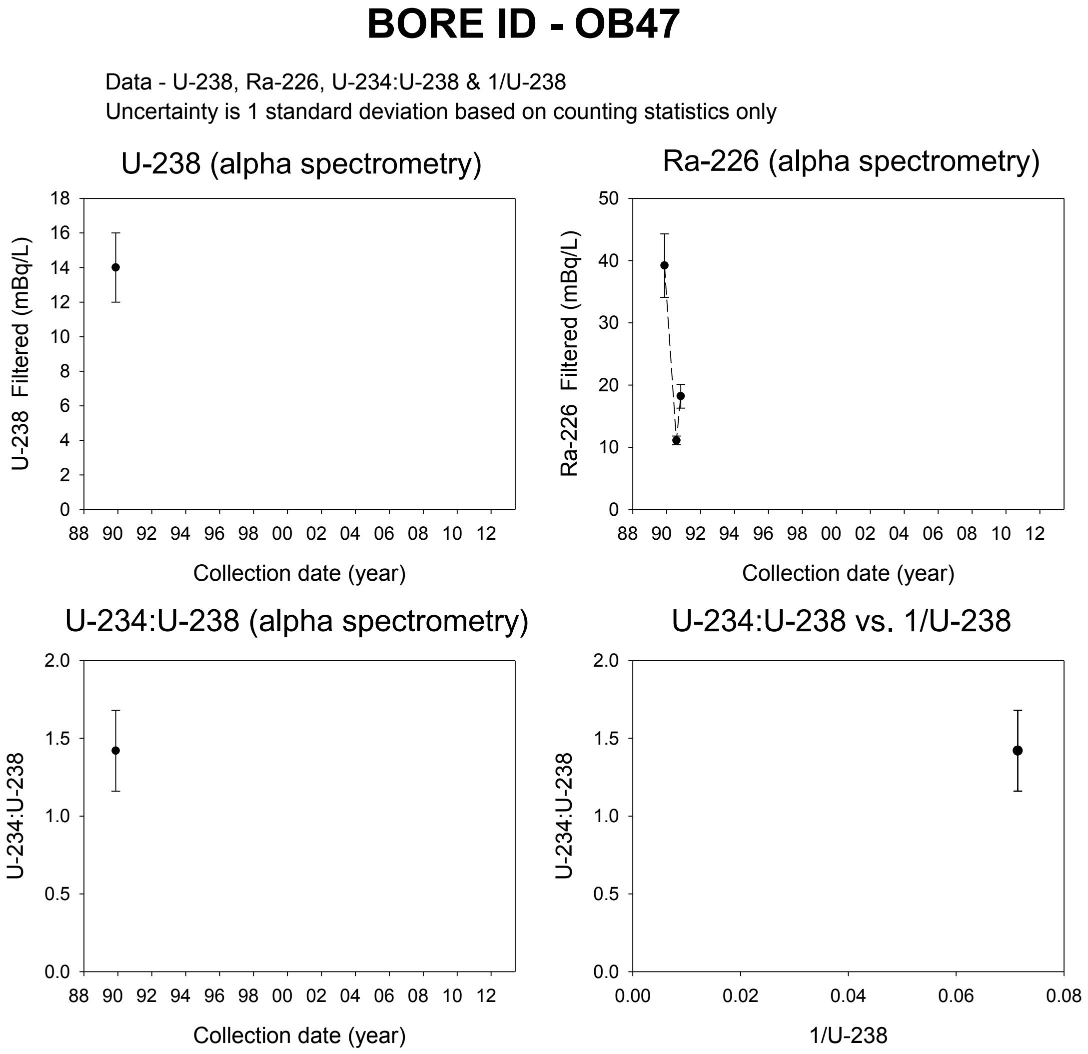

BORE ID - OB47

Data - U-238, Ra-226, U-234:U-238 & 1/U-238
Uncertainty is 1 standard deviation based on counting statistics only

U-238 (alpha spectrometry)

Ra-226 (alpha spectrometry)

U-234:U-238 (alpha spectrometry)

U-234:U-238 vs. 1/U-238

Bore ID –OB48

BORE ID - OB48

Data - U-238, Ra-226, U-234:U-238 & 1/U-238
Uncertainty is 1 standard deviation based on counting statistics only

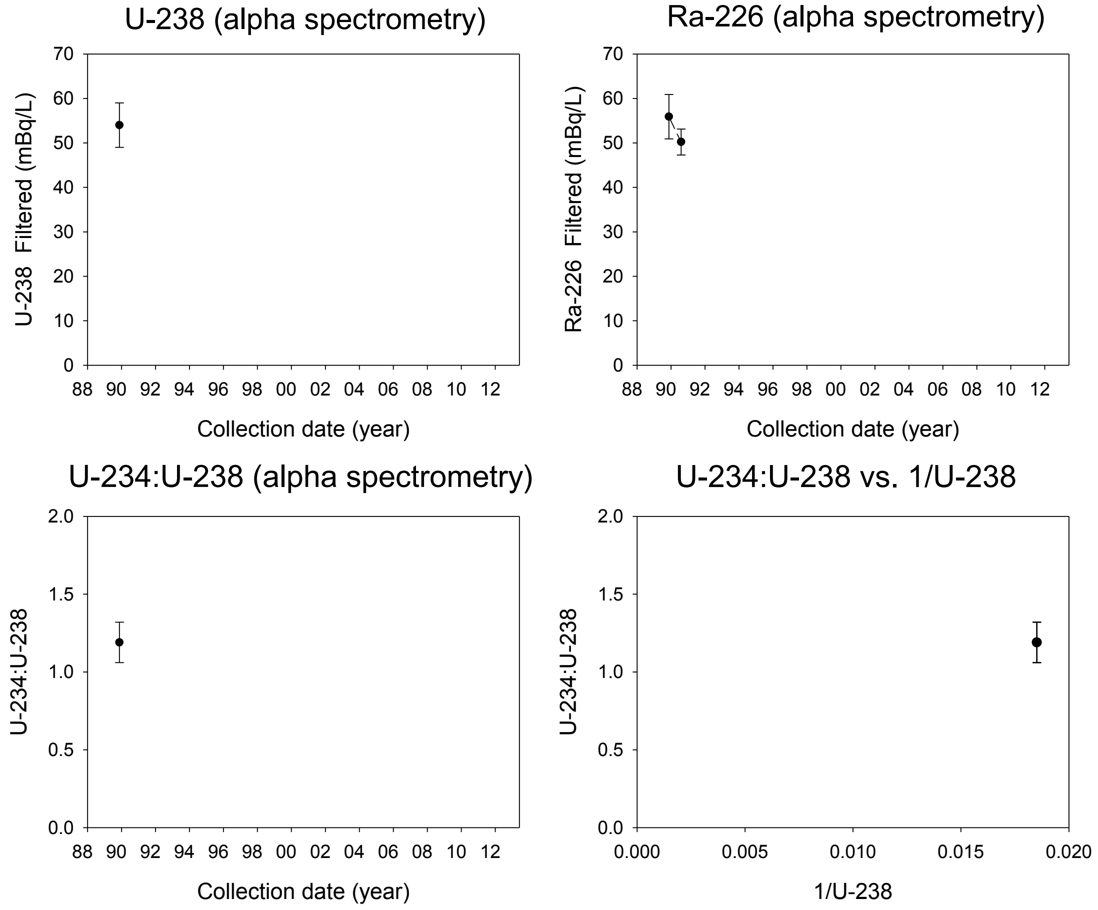

Bore ID –OB49

BORE ID - OB49

Data - U-238, Ra-226, U-234:U-238 & 1/U-238
Uncertainty is 1 standard deviation based on counting statistics only

U-238 (alpha spectrometry)

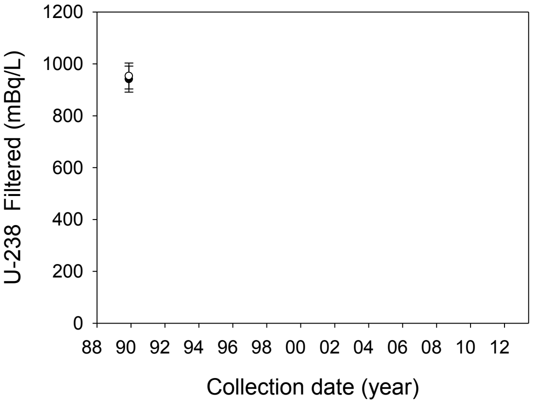

Ra-226 (alpha spectrometry)

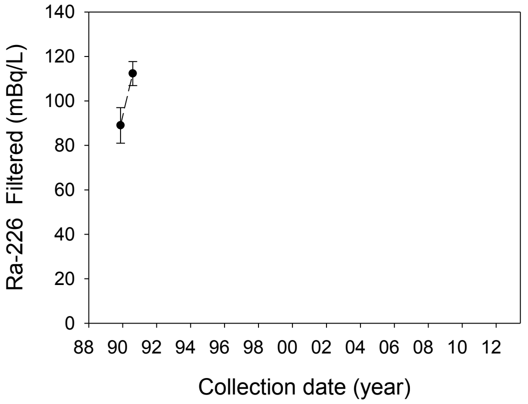

U-234:U-238 (alpha spectrometry)

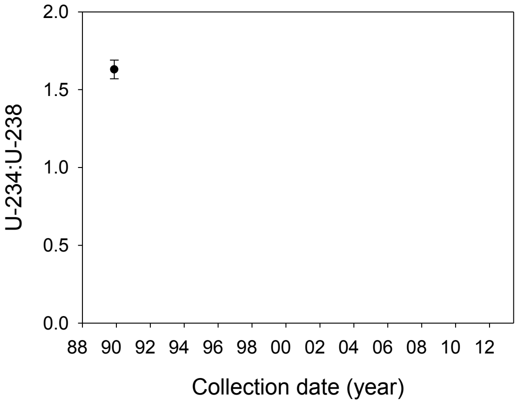

U-234:U-238 vs. 1/U-238

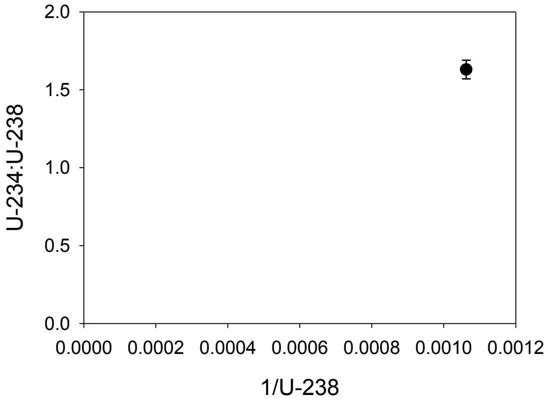

Bore ID –OB50

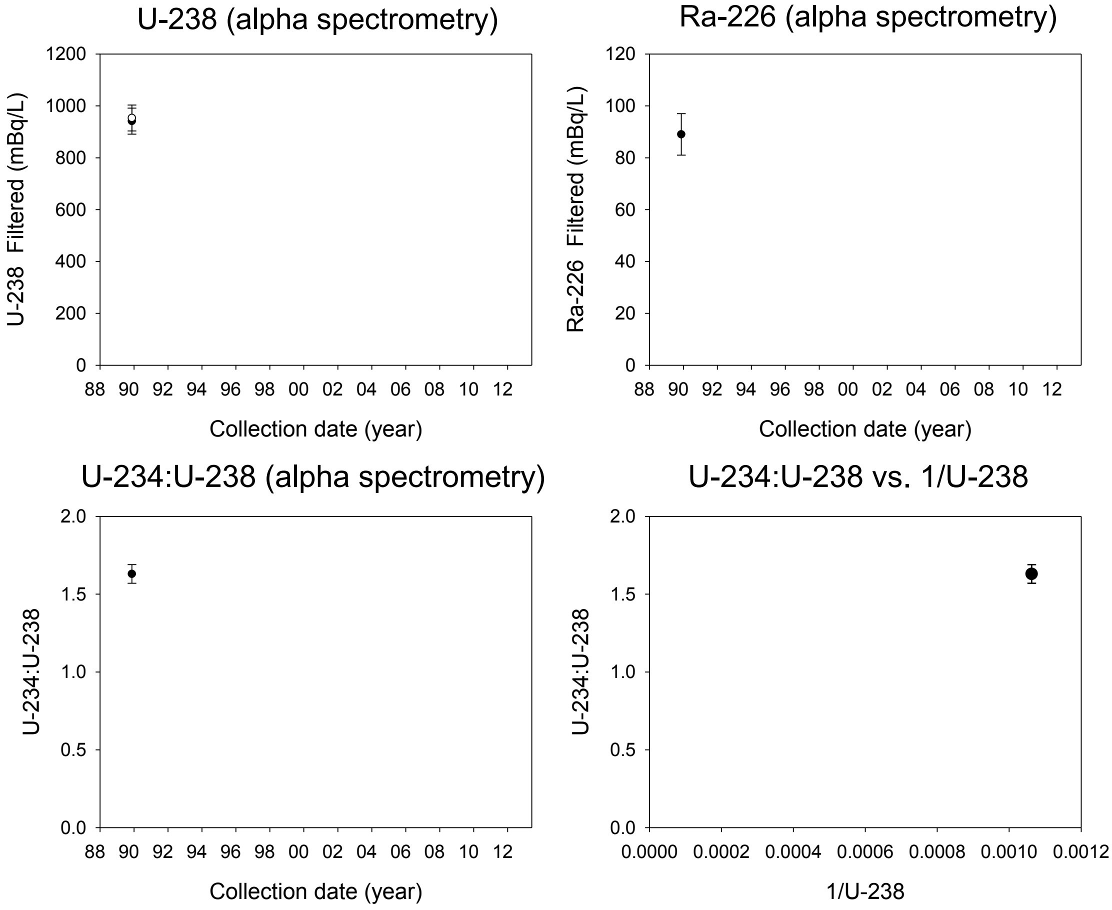

BORE ID - OB50

Data - U-238, Ra-226, U-234:U-238 & 1/U-238
Uncertainty is 1 standard deviation based on counting statistics only

Bore ID –OB51

BORE ID - OB51

Data - U-238, Ra-226, U-234:U-238 & 1/U-238
Uncertainty is 1 standard deviation based on counting statistics only

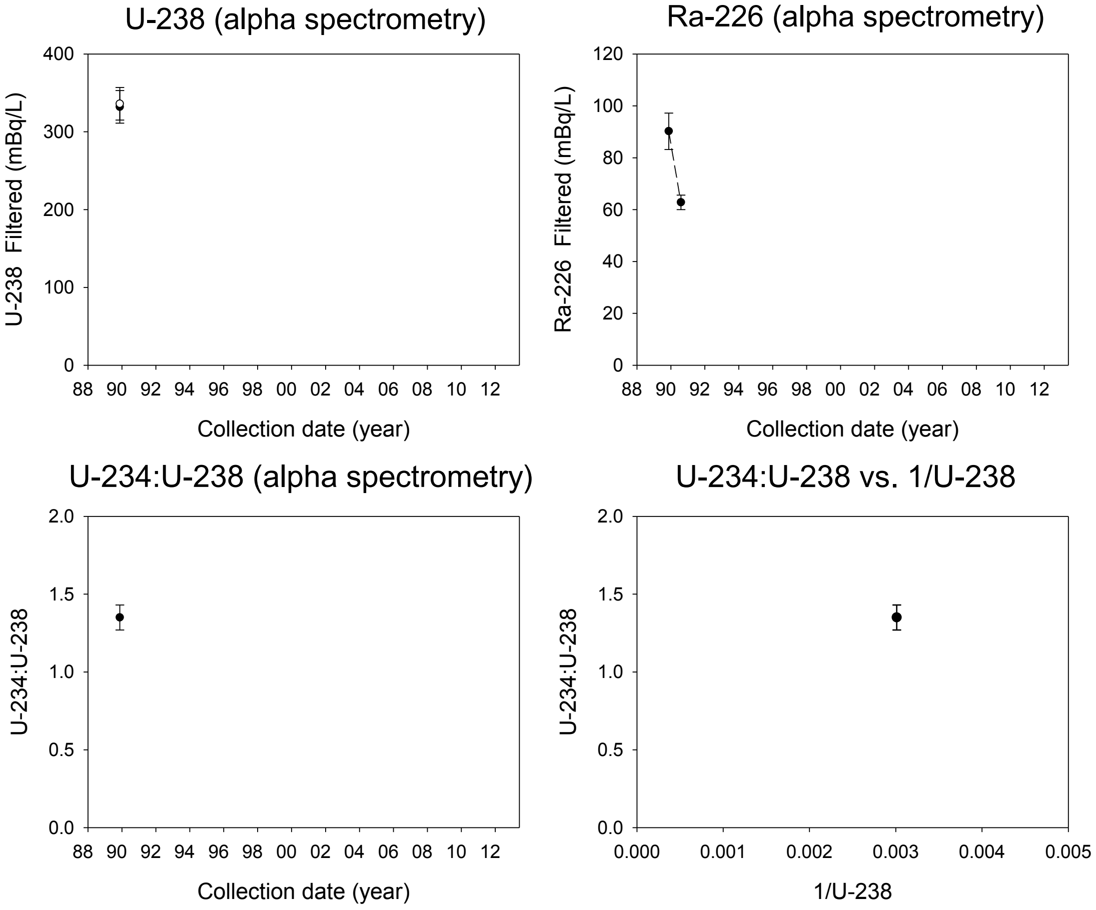

Bore ID –OB4A

BORE ID - OB4A

Data - Calcium, Potassium, Magnesium, Sodium and Sulfate

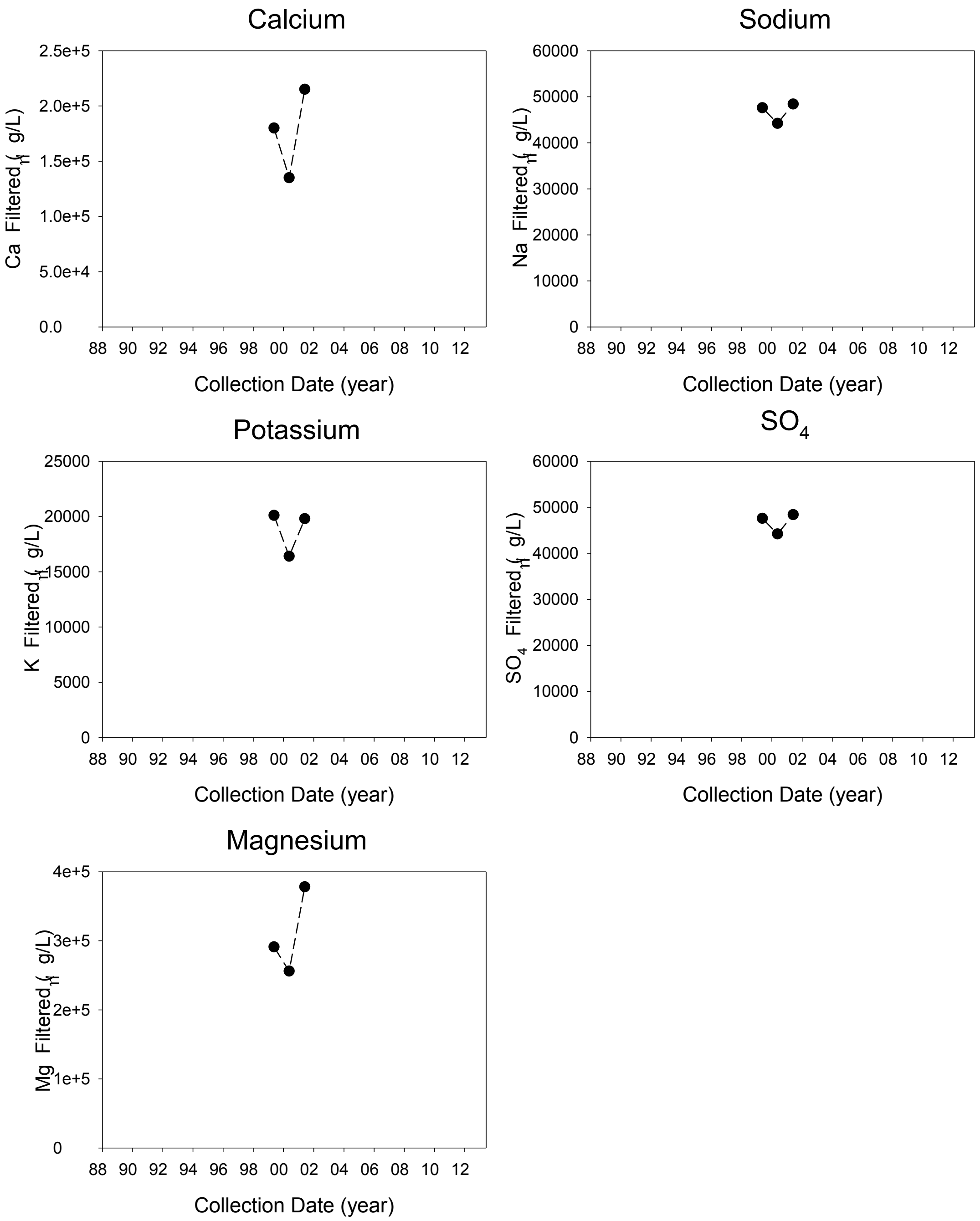

BORE ID - OB4A

Data - Iron, Manganese, Barium, Strontium, Uranium & Vanadium

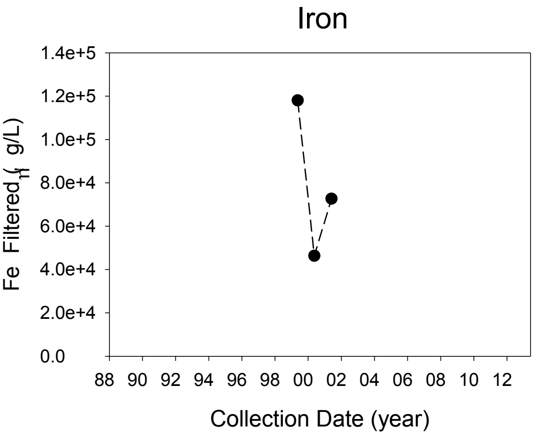

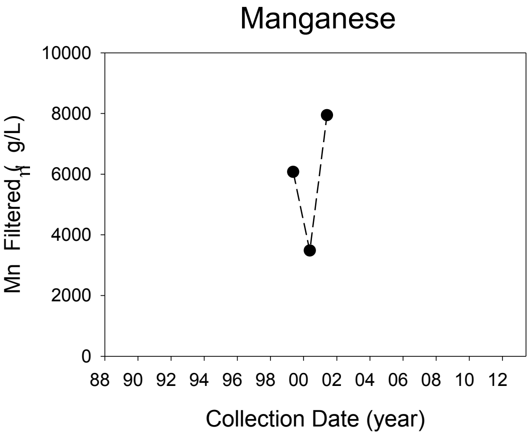

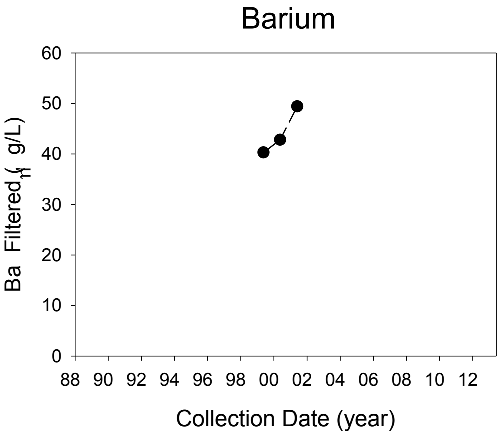

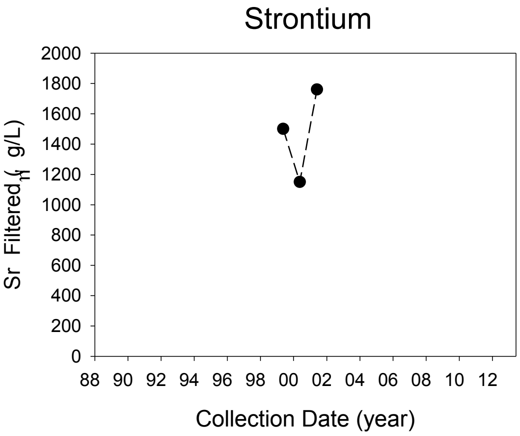

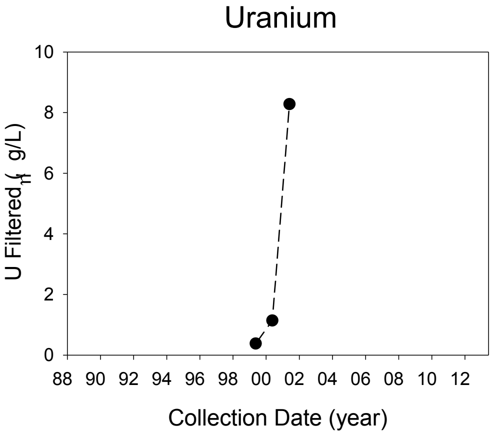

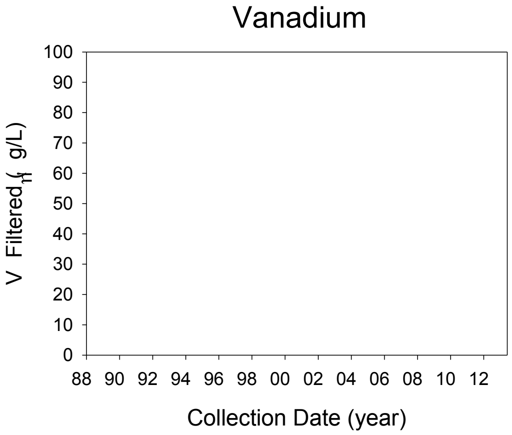

BORE ID - OB4A

Data - U-238, Ra-226, U-234:U-238 & 1/U-238
Uncertainty is 1 standard deviation based on counting statistics only

U-238 (alpha spectrometry)

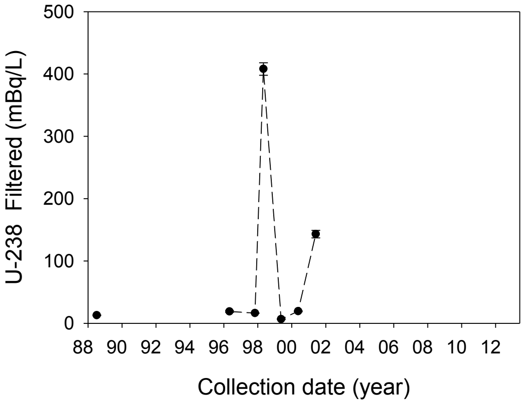

Ra-226 (alpha spectrometry)

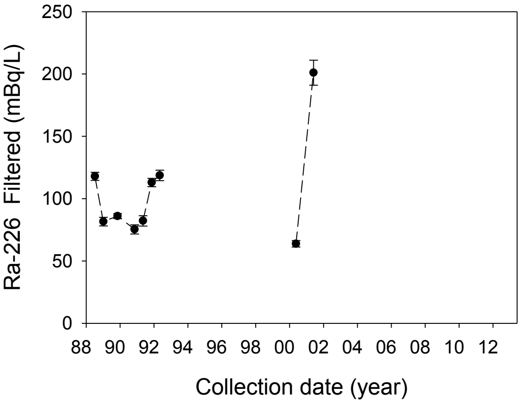

U-234:U-238 (alpha spectrometry)

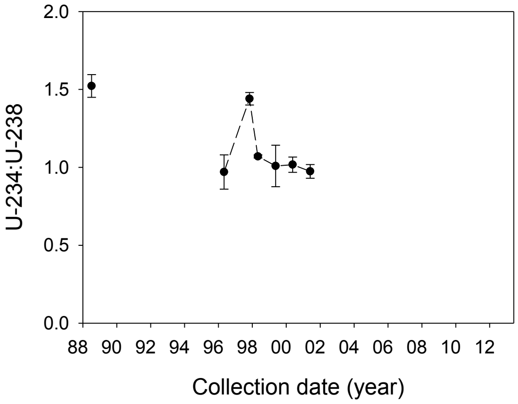

U-234:U-238 vs. 1/U-238

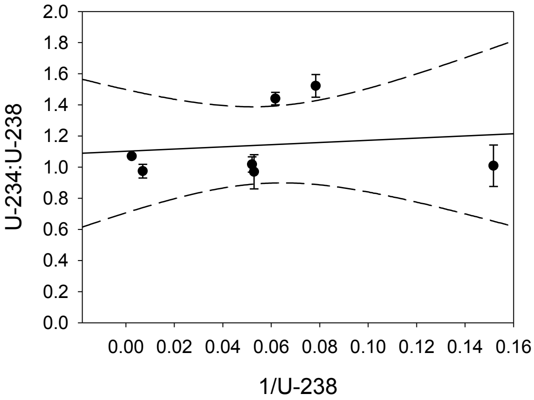

Bore ID –OB6

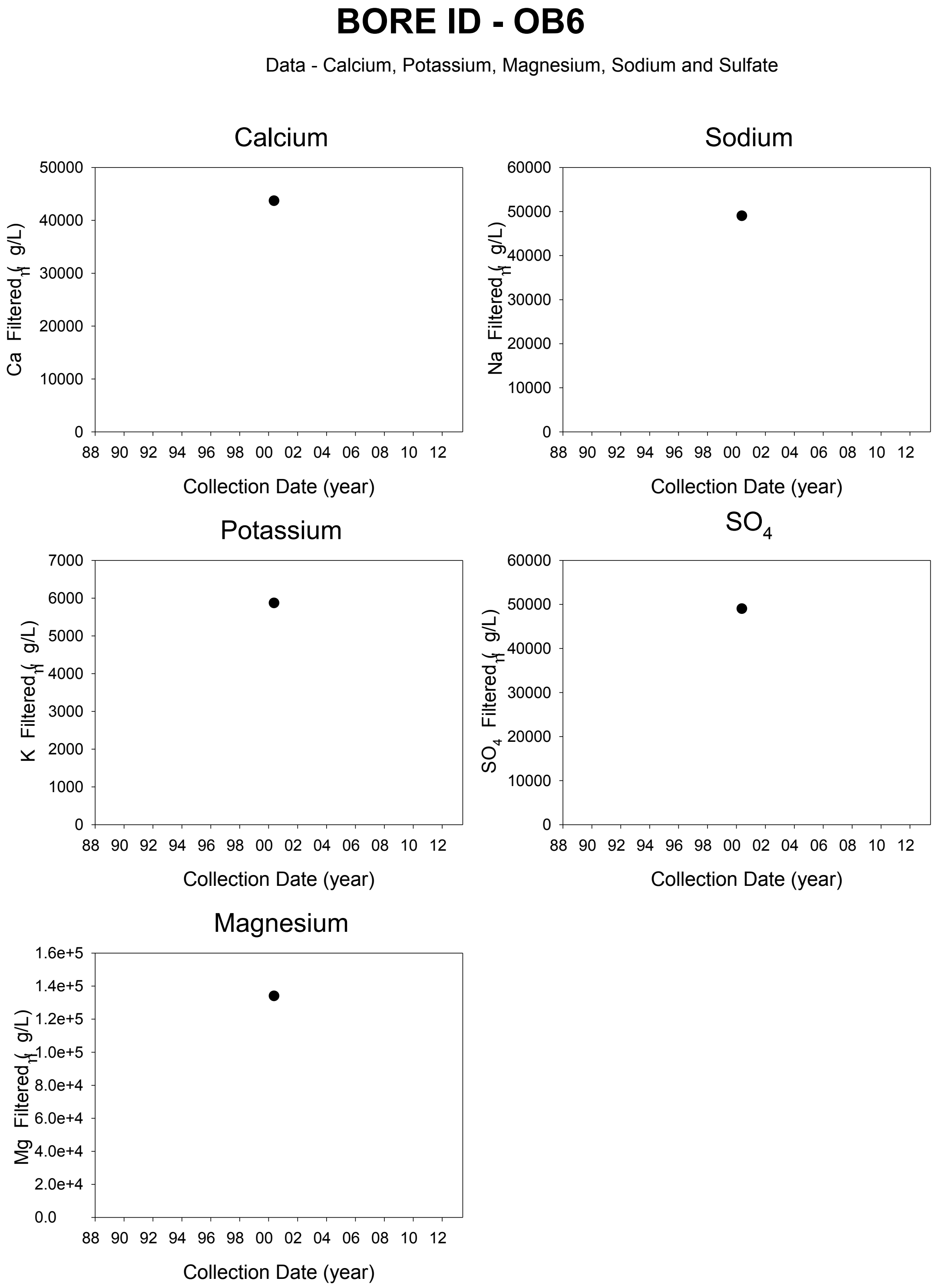
BORE ID - OB6
Data - Calcium, Potassium, Magnesium, Sodium and Sulfate
Calcium
Ca Filtered (µg/L)
0
10000
20000
30000
40000
50000
88 90 92 94 96 98 00 02 04 06 08 10 12
Collection Date (year)
Sodium
Na Filtered (µg/L)
0
10000
20000
30000
40000
50000
60000
88 90 92 94 96 98 00 02 04 06 08 10 12
Collection Date (year)
Potassium
K Filtered (µg/L)
0
1000
2000
3000
4000
5000
6000
7000
88 90 92 94 96 98 00 02 04 06 08 10 12
Collection Date (year)
SO4
SO4 Filtered (µg/L)
0
10000
20000
30000
40000
50000
60000
88 90 92 94 96 98 00 02 04 06 08 10 12
Collection Date (year)
Magnesium
Mg Filtered (µg/L)
0.0
2.0e+4
4.0e+4
6.0e+4
8.0e+4
1.0e+5
1.2e+5
1.4e+5
1.6e+5
88 90 92 94 96 98 00 02 04 06 08 10 12
Collection Date (year)

BORE ID - OB6

Data - Iron, Manganese, Barium, Strontium, Uranium & Vanadium

Iron

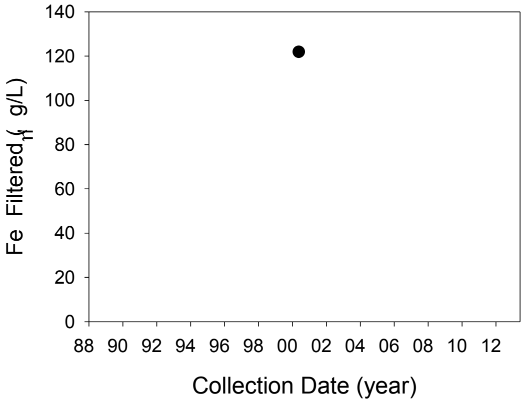

Manganese

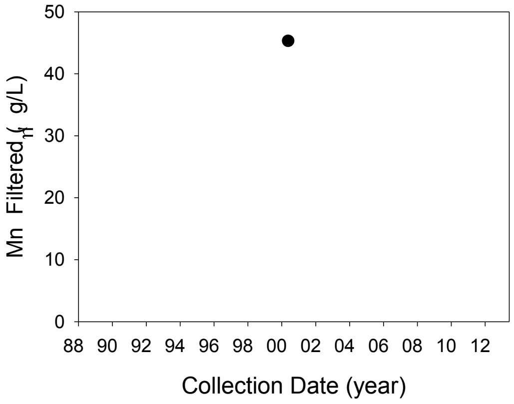

Barium

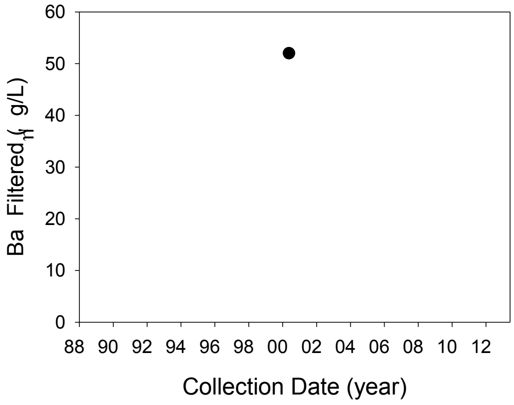

Strontium

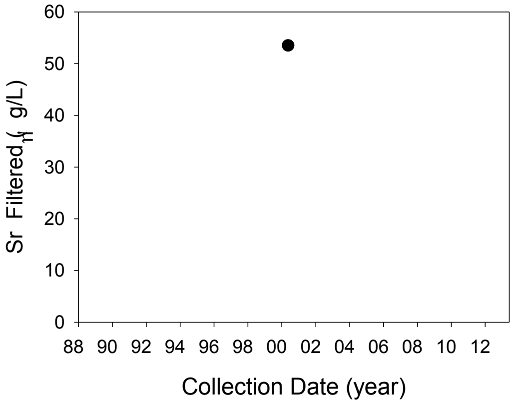

Uranium

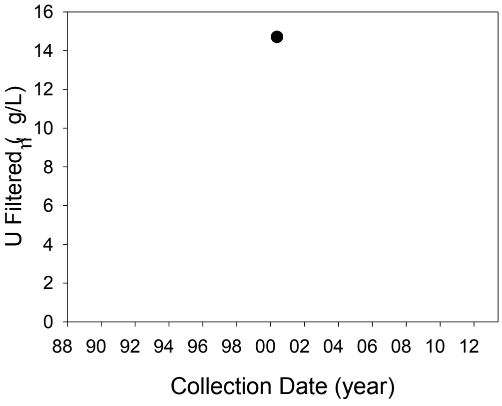

Vanadium

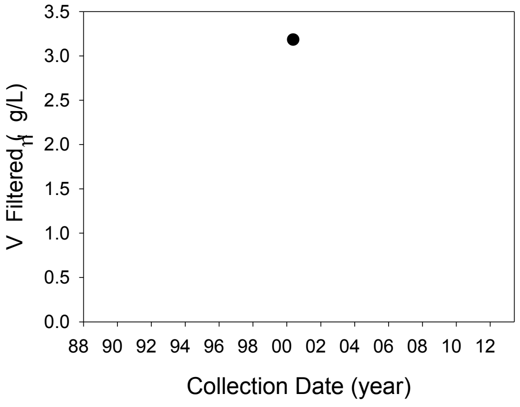

BORE ID - OB6

Data - U-238, Ra-226, U-234:U-238 & 1/U-238
Uncertainty is 1 standard deviation based on counting statistics only

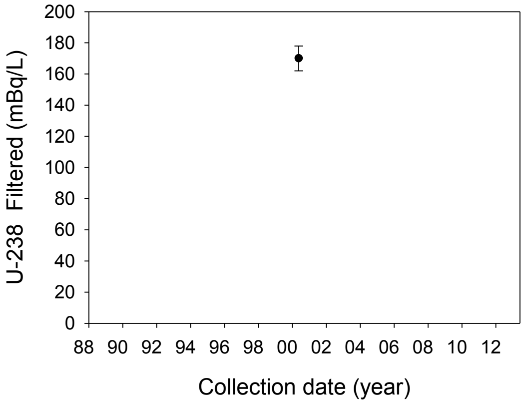
U-238 (alpha spectrometry)

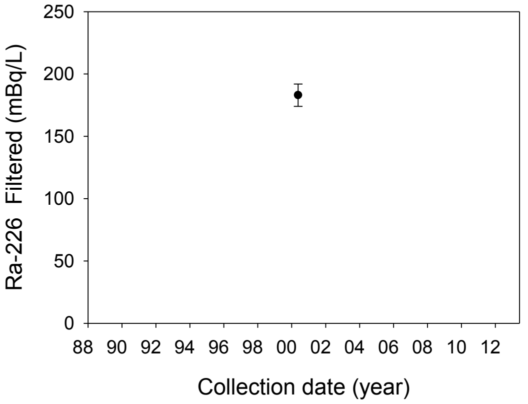
Ra-226 (alpha spectrometry)

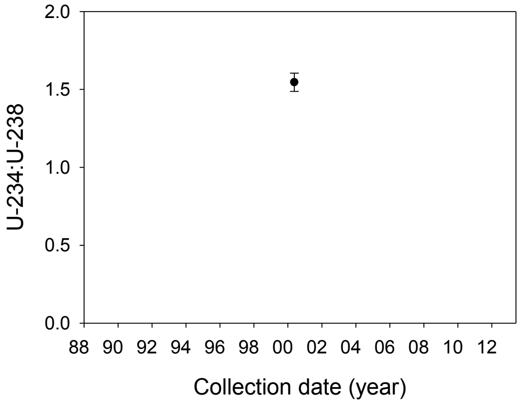
U-234:U-238 (alpha spectrometry)

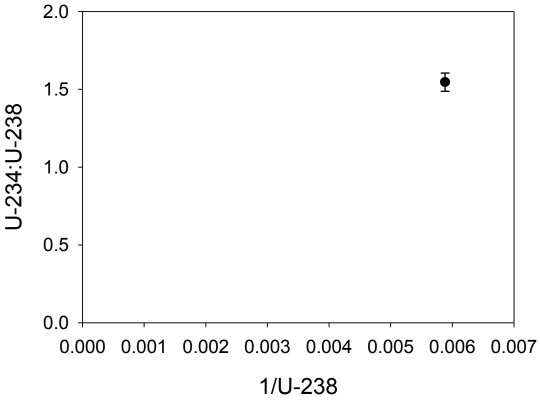
U-234:U-238 vs. 1/U-238

Bore ID –OB6A

BORE ID - OB6A

Data - Calcium, Potassium, Magnesium, Sodium and Sulfate

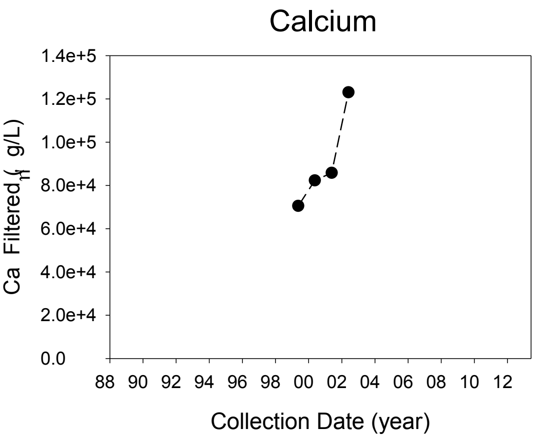

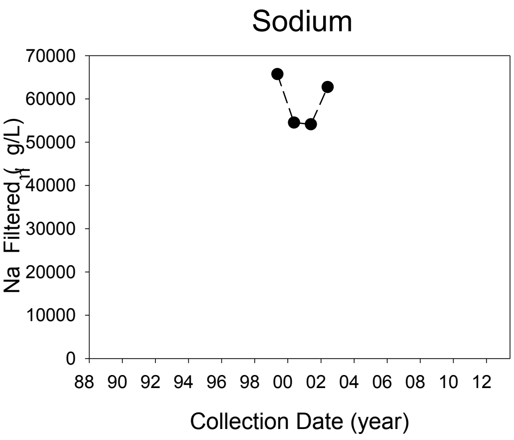

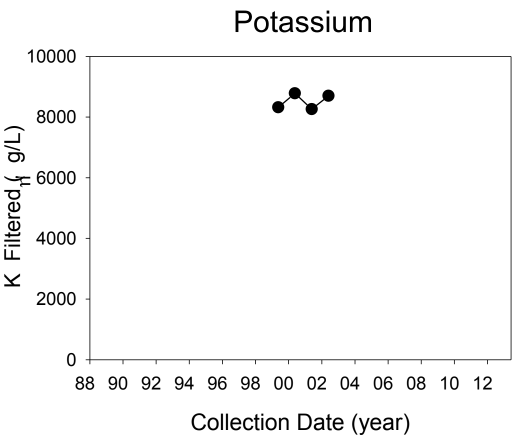

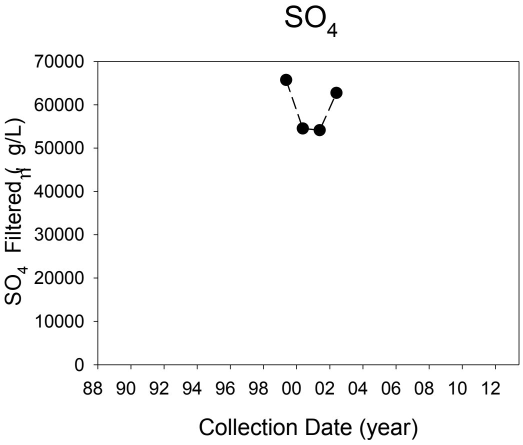

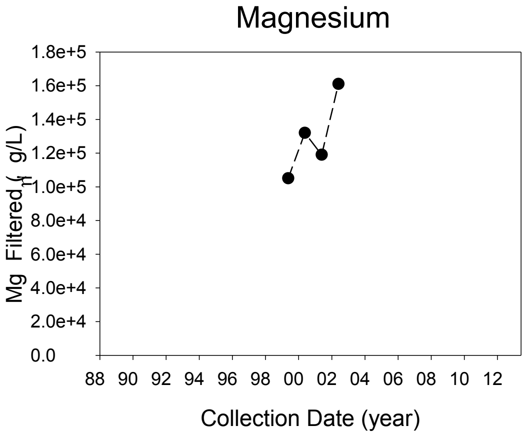

BORE ID - OB6A

Data - Iron, Manganese, Barium, Strontium, Uranium & Vanadium

Iron

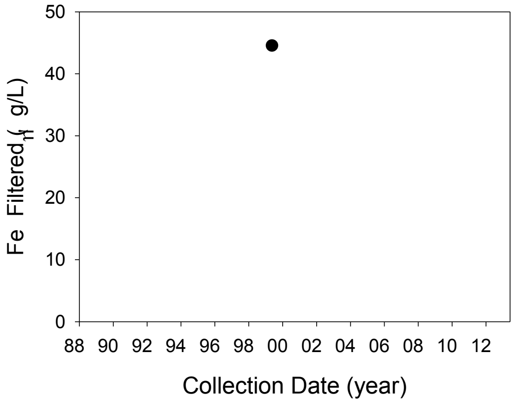

Manganese

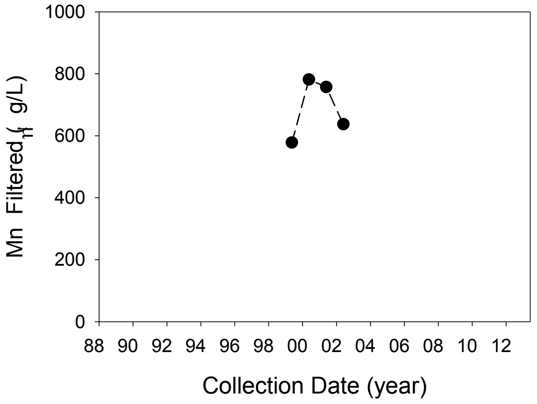

Barium

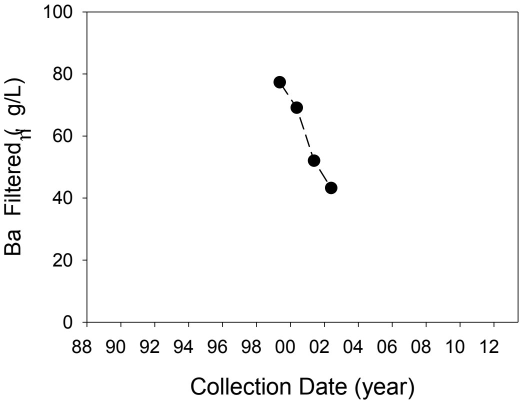

Strontium

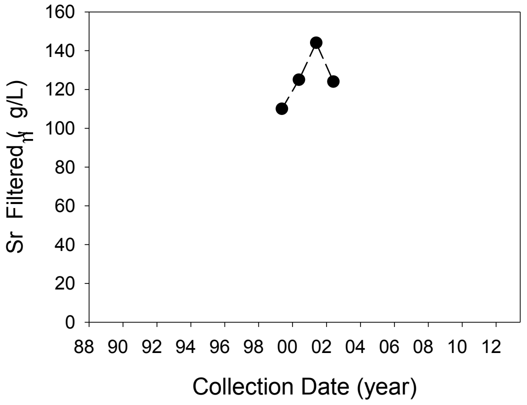

Uranium

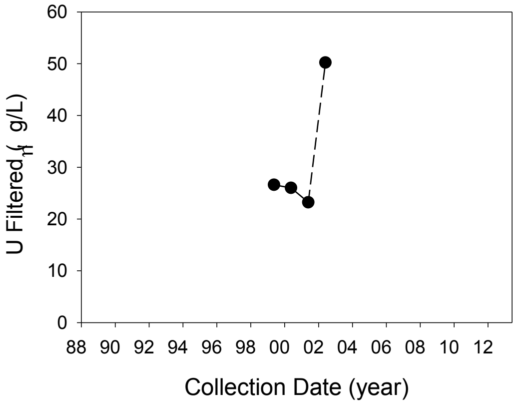

Vanadium

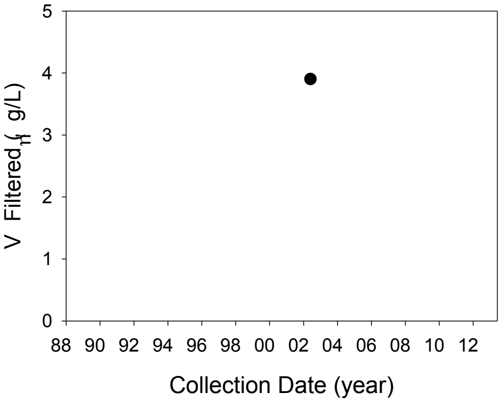

BORE ID - OB6A

Data - U-238, Ra-226, U-234:U-238 & 1/U-238
Uncertainty is 1 standard deviation based on counting statistics only

U-238 (alpha spectrometry)

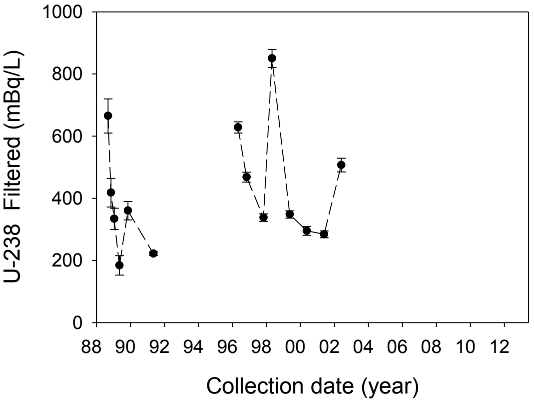

Ra-226 (alpha spectrometry)

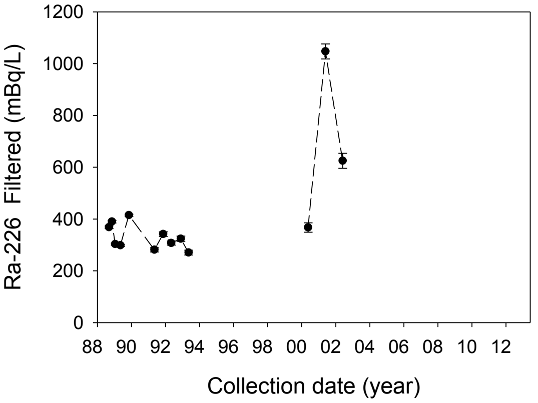

U-234:U-238 (alpha spectrometry)

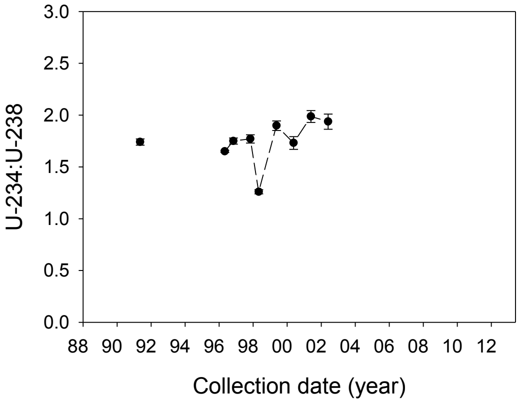

U-234:U-238 vs. 1/U-238

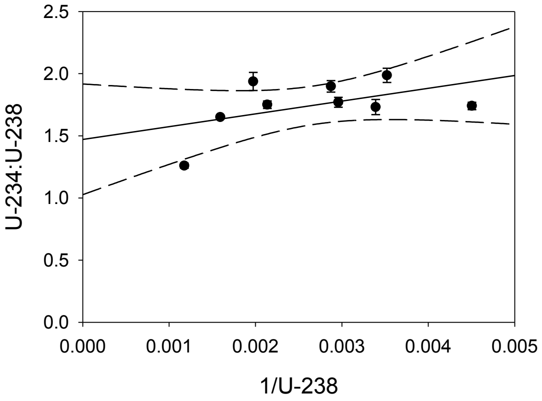

Bore ID –OB7A

BORE ID - OB7A

Data - Calcium, Potassium, Magnesium, Sodium and Sulfate

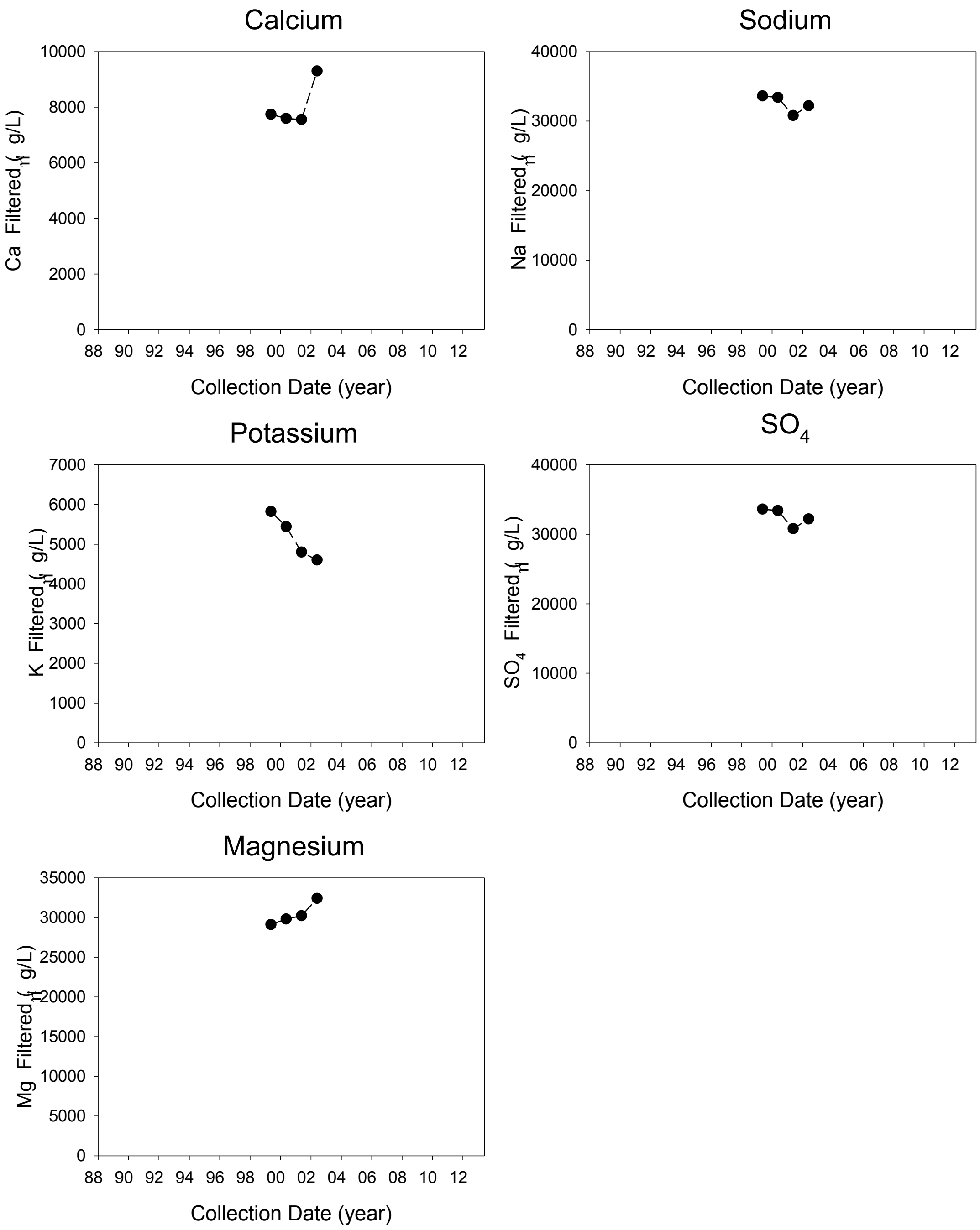

BORE ID - OB7A

Data - Iron, Manganese, Barium, Strontium, Uranium & Vanadium

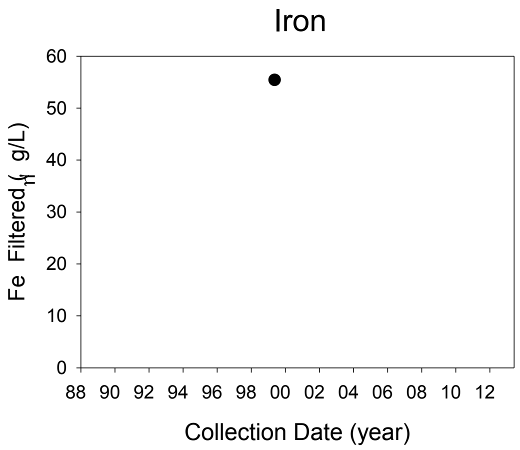
Iron

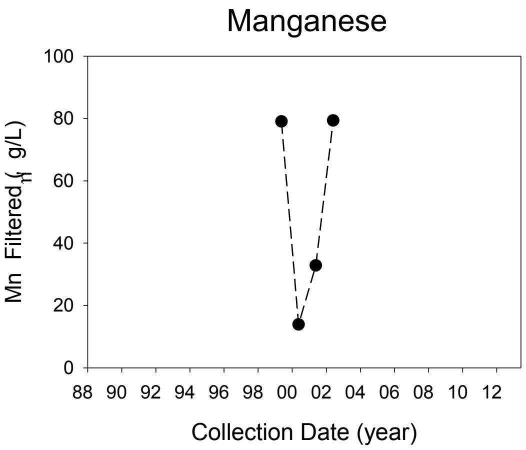
Manganese

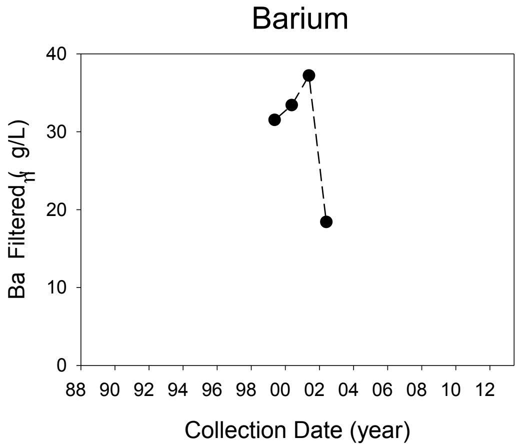
Barium

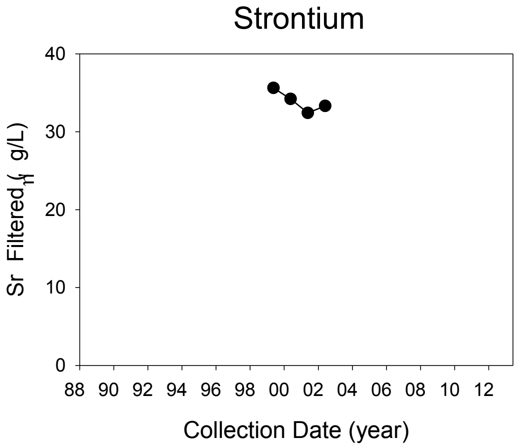
Strontium

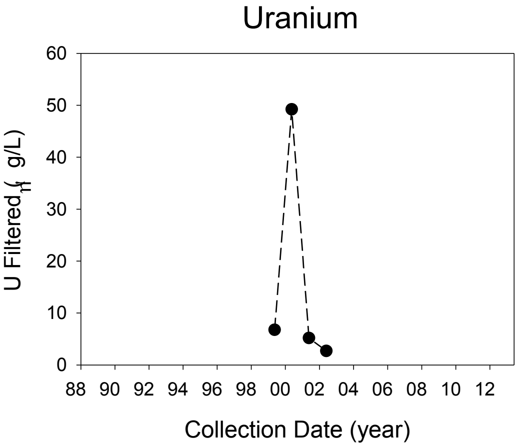
Uranium

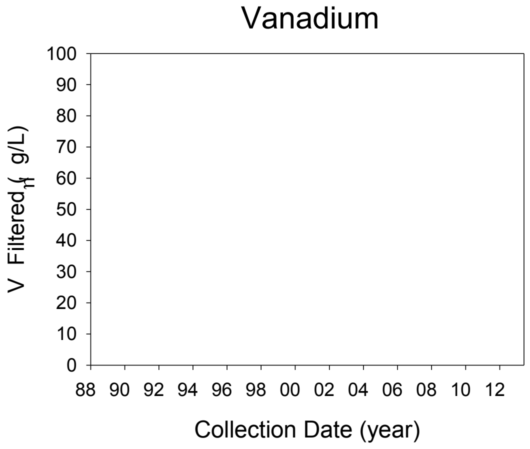
Vanadium

BORE ID - OB7A

Data - U-238, Ra-226, U-234:U-238 & 1/U-238
Uncertainty is 1 standard deviation based on counting statistics only

U-238 (alpha spectrometry)

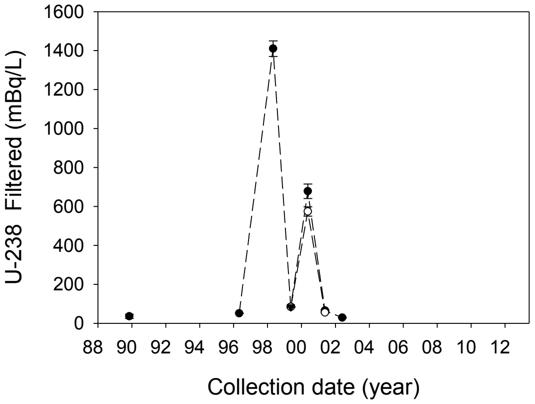

Ra-226 (alpha spectrometry)

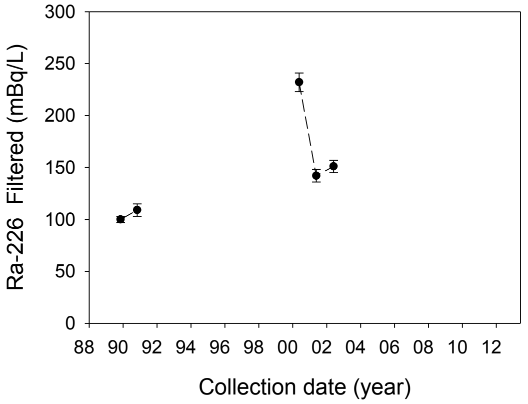

U-234:U-238 (alpha spectrometry)

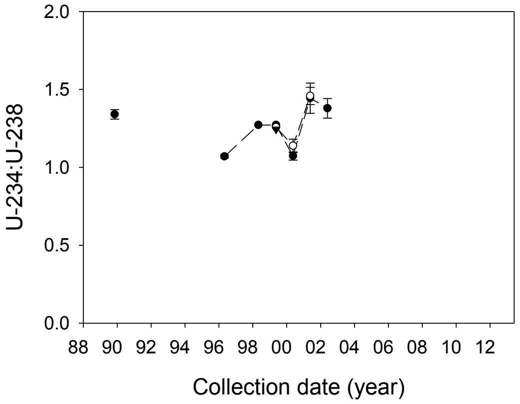

U-234:U-238 vs. 1/U-238

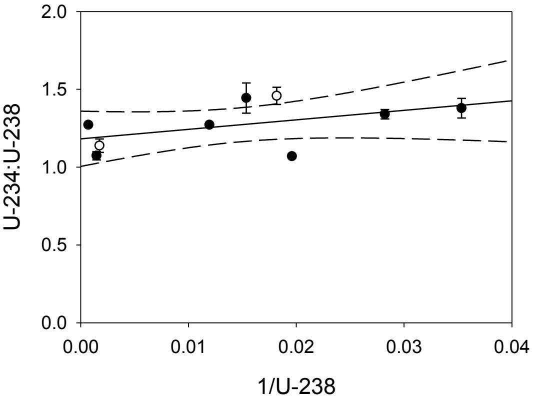

Bore ID –OB9A

BORE ID - OB9A

Data - U-238, Ra-226, U-234:U-238 & 1/U-238
Uncertainty is 1 standard deviation based on counting statistics only

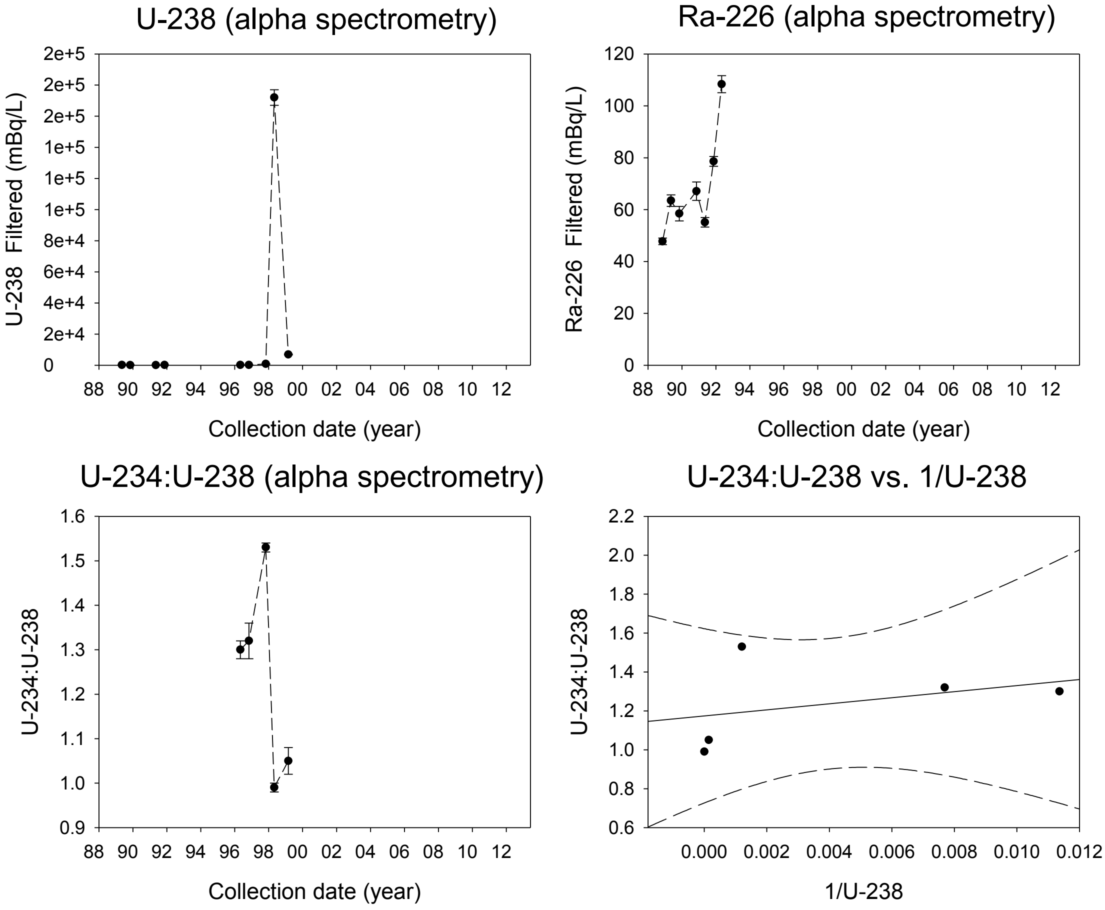

Bore ID – RN22211

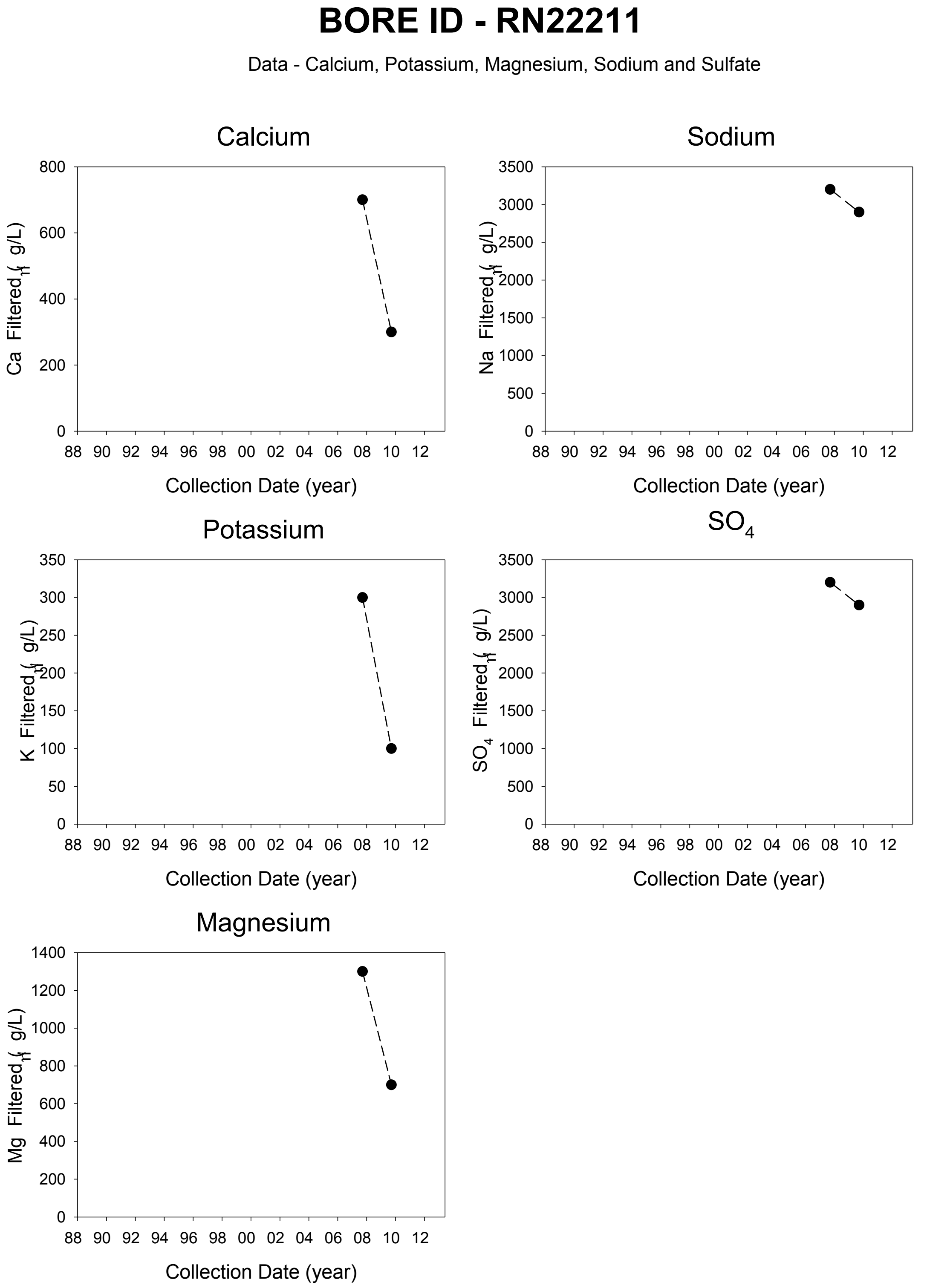

BORE ID - RN22211

Data - Iron, Manganese, Barium, Strontium, Uranium & Vanadium

Iron

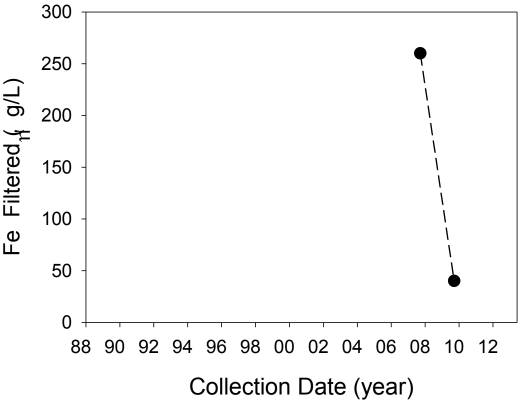

Manganese

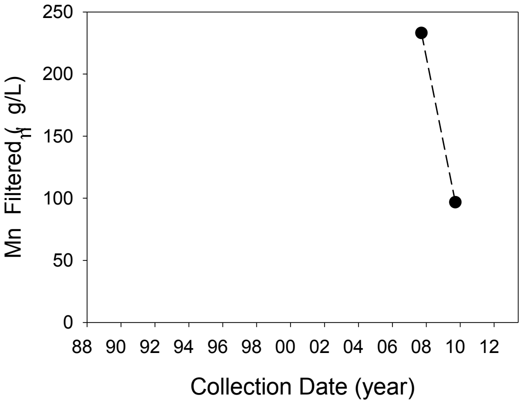

Barium

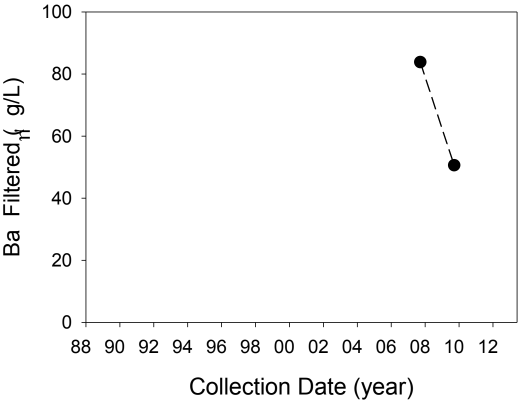

Strontium

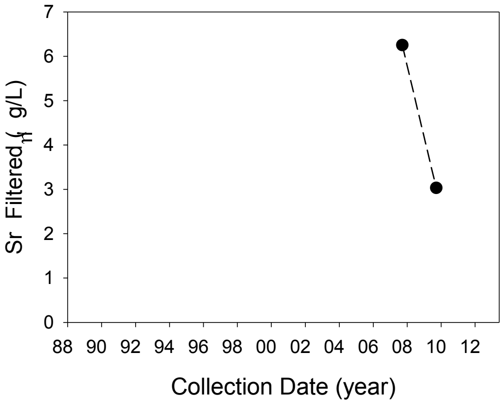

Uranium

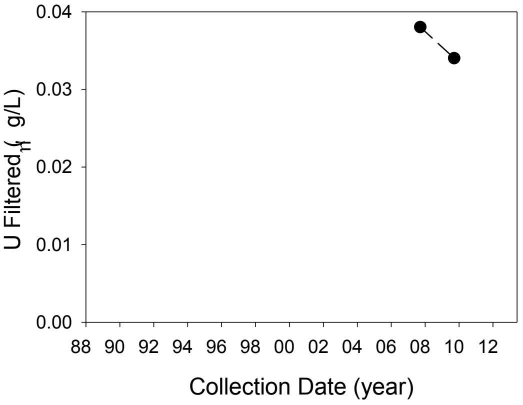

Vanadium

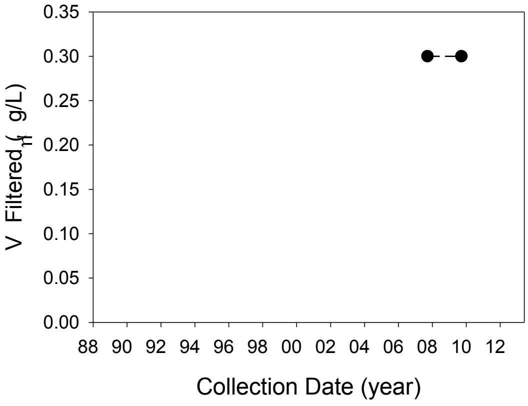

BORE ID - RN22211

Data - U-238, Ra-226, U-234:U-238 & 1/U-238
Uncertainty is 1 standard deviation based on counting statistics only

U-238 (alpha spectrometry)

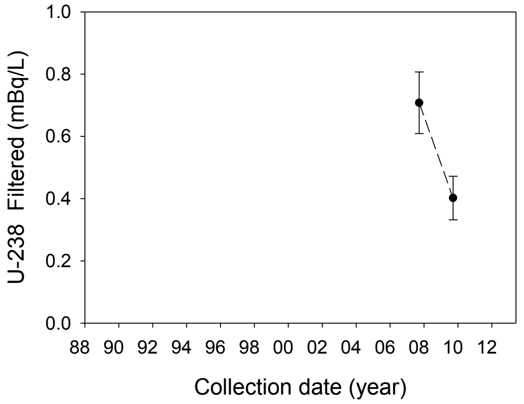

Ra-226 (alpha spectrometry)

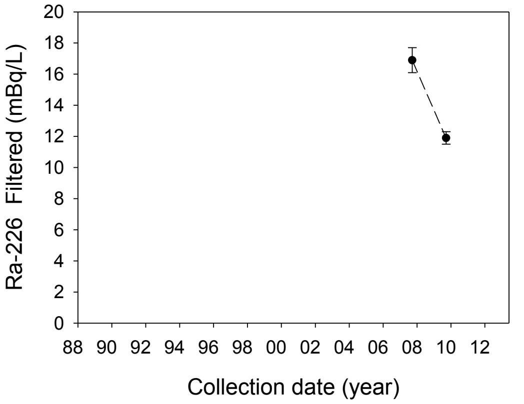

U-234:U-238 (alpha spectrometry)

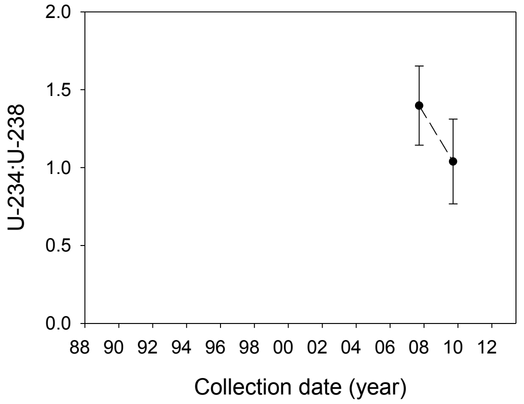

U-234:U-238 vs. 1/U-238

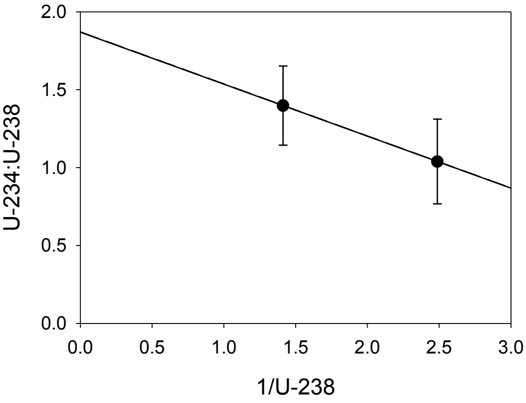

Bore ID – RN23551

BORE ID - RN23551

Data - Calcium, Potassium, Magnesium, Sodium and Sulfate

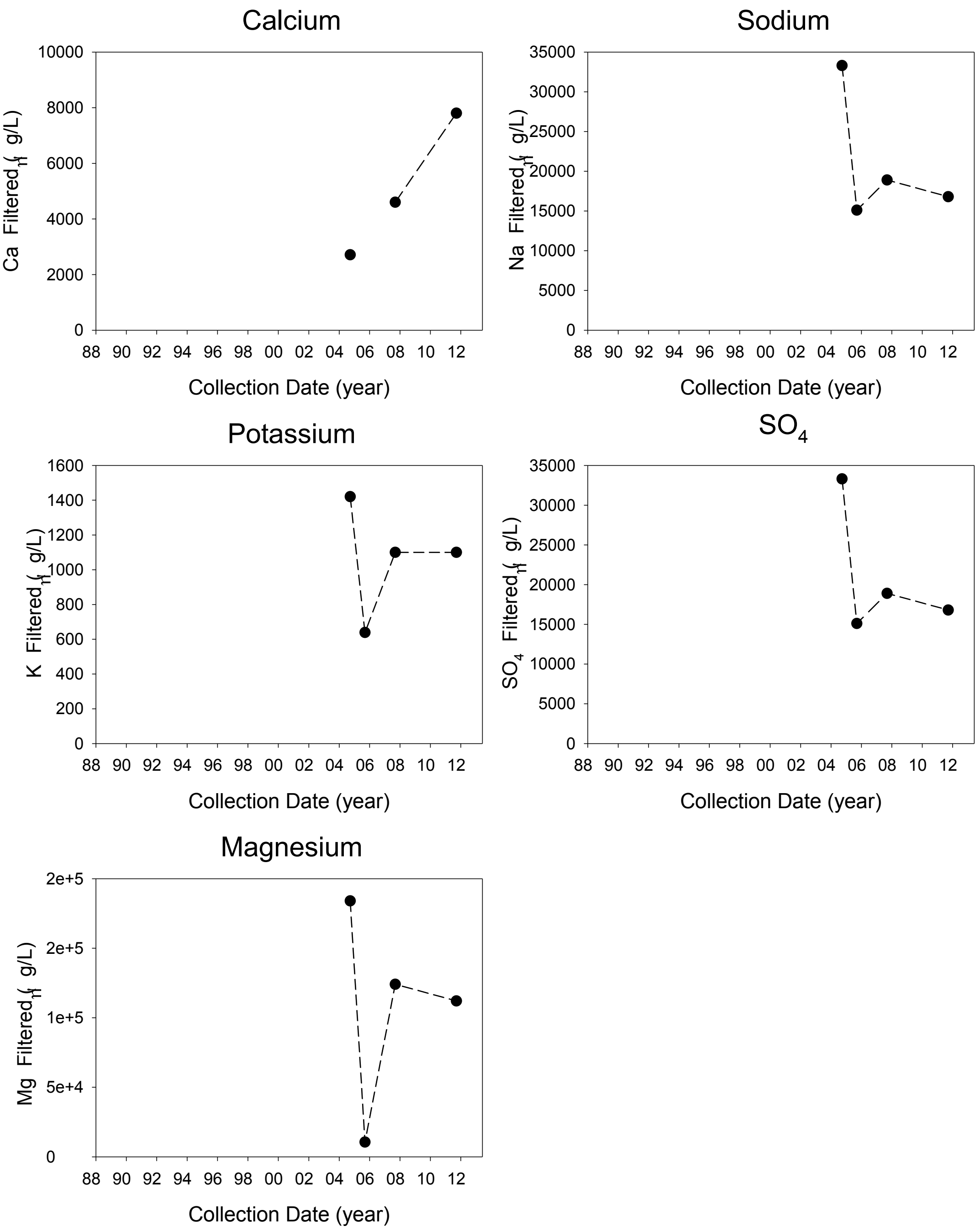

BORE ID - RN23551

Data - Iron, Manganese, Barium, Strontium, Uranium & Vanadium

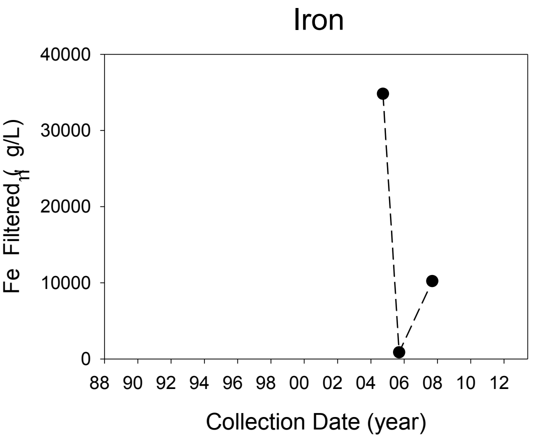

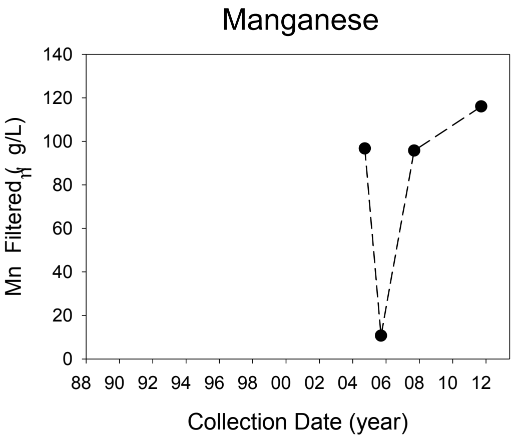

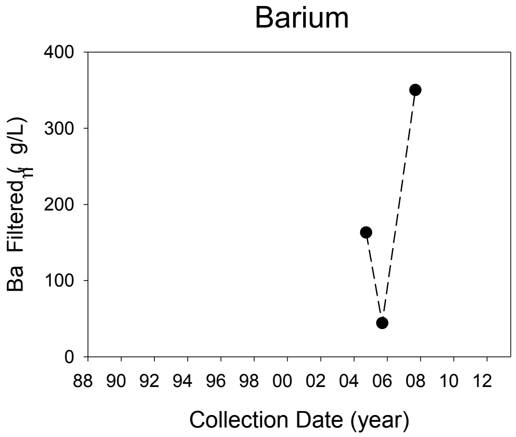

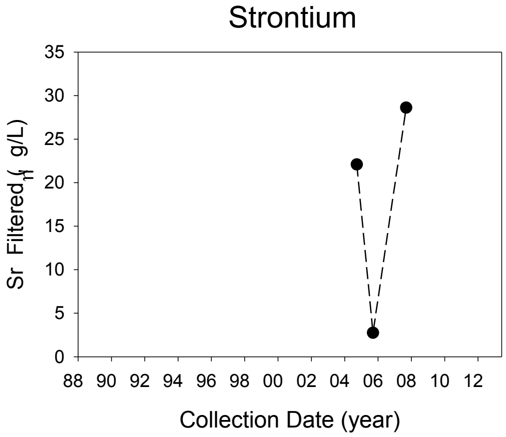

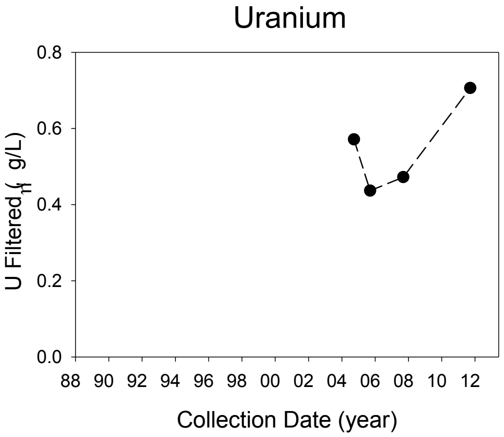

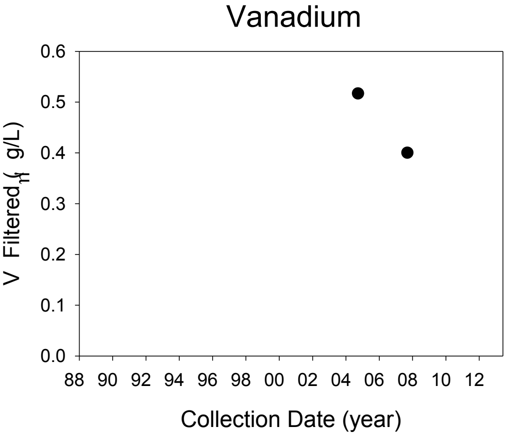

BORE ID - RN23551

Data - U-238, Ra-226, U-234:U-238 & 1/U-238
Uncertainty is 1 standard deviation based on counting statistics only

U-238 (alpha spectrometry)

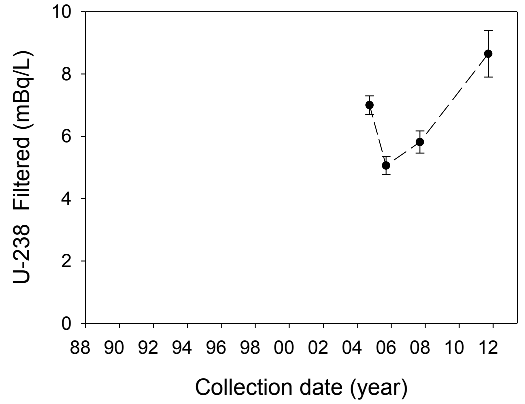

Ra-226 (alpha spectrometry)

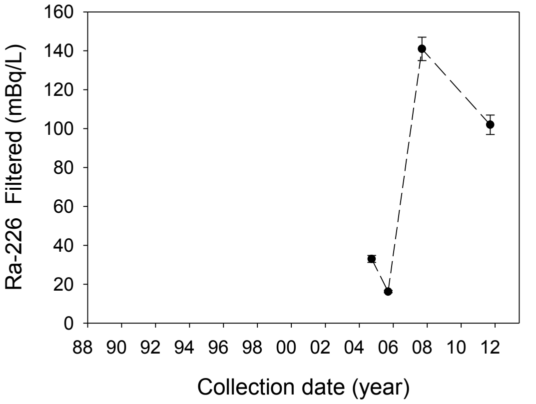

U-234:U-238 (alpha spectrometry)

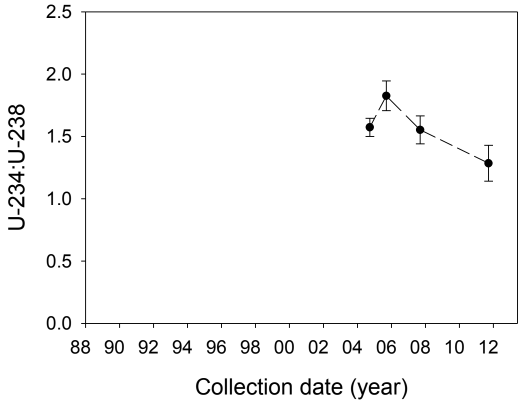

U-234:U-238 vs. 1/U-238

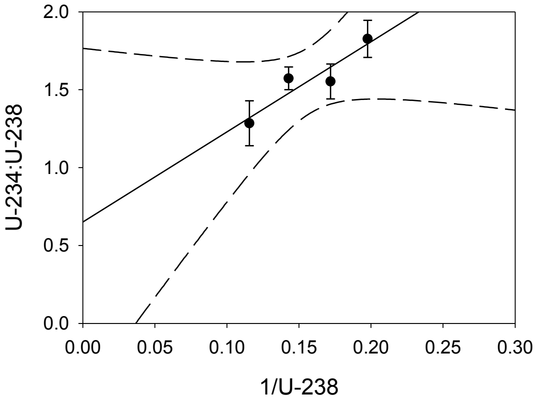

Bore ID – RN23556

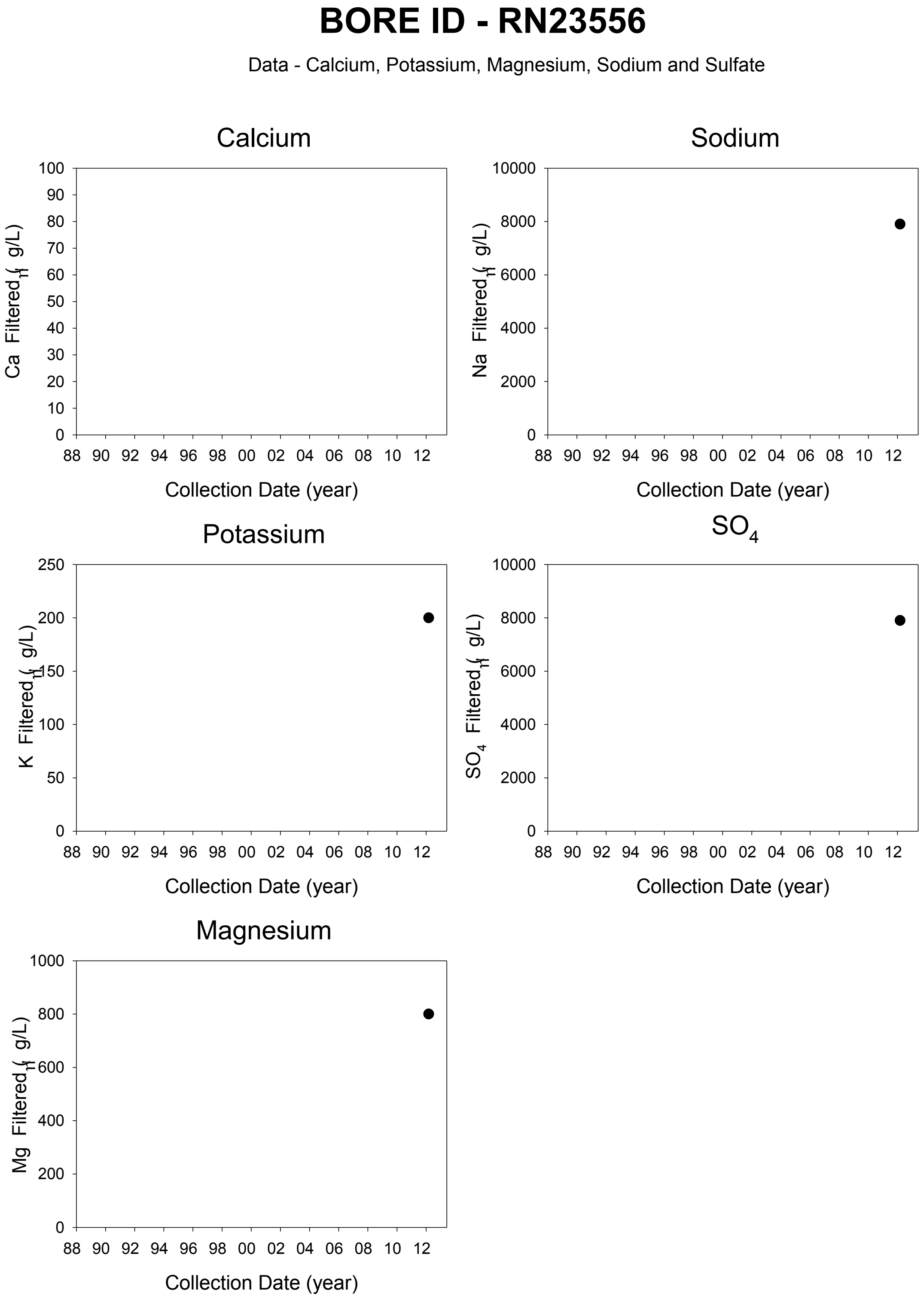

BORE ID - RN23556

Data - Iron, Manganese, Barium, Strontium, Uranium & Vanadium

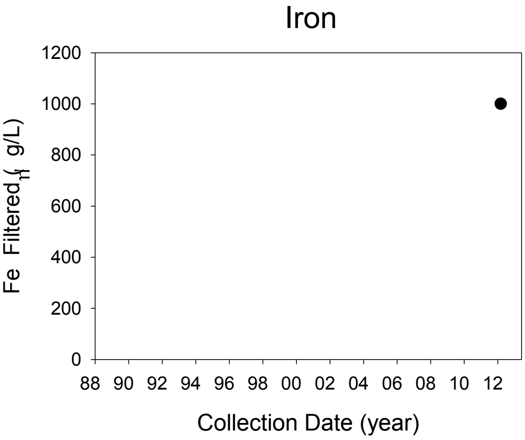
Iron

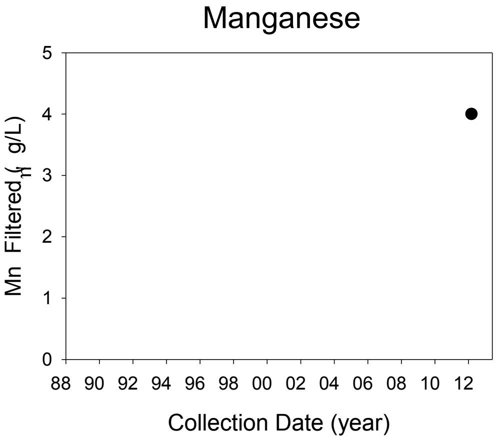
Manganese

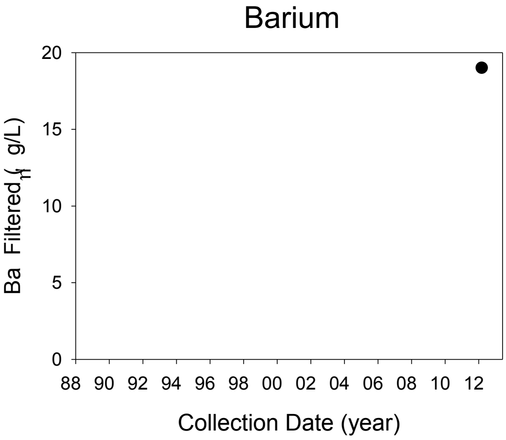
Barium

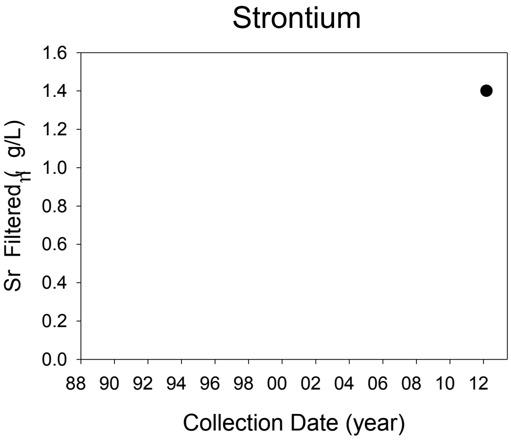
Strontium

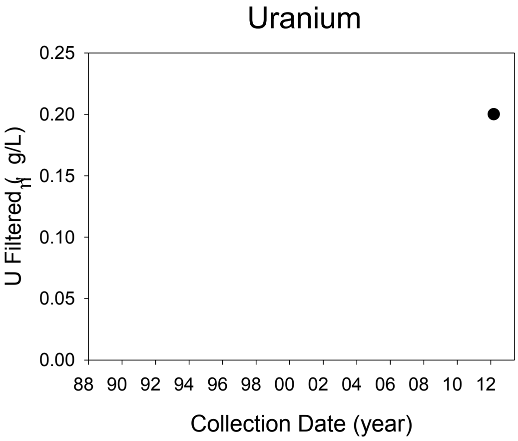
Uranium

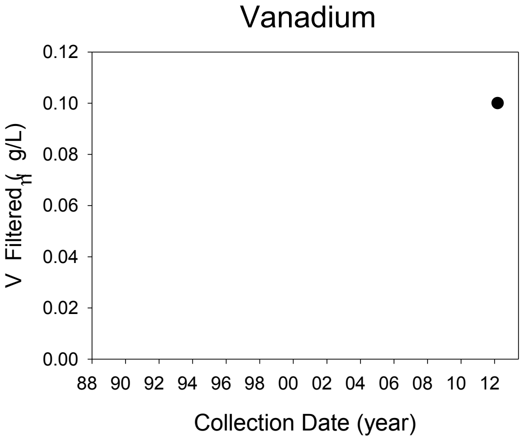
Vanadium

BORE ID - RN23556

Data - U-238, Ra-226, U-234:U-238 & 1/U-238
Uncertainty is 1 standard deviation based on counting statistics only

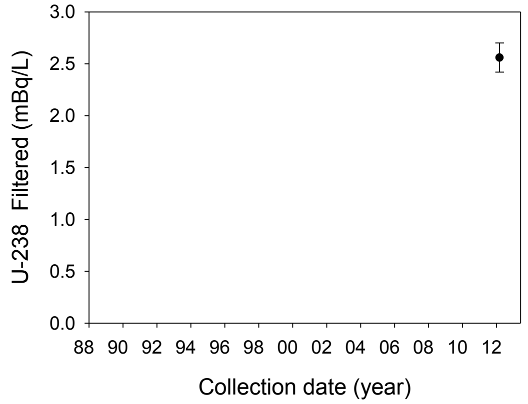
U-238 (alpha spectrometry)

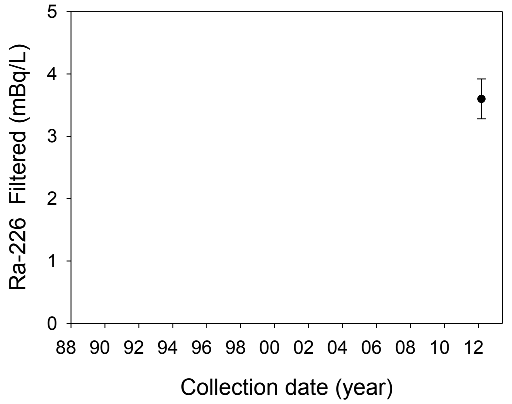
Ra-226 (alpha spectrometry)

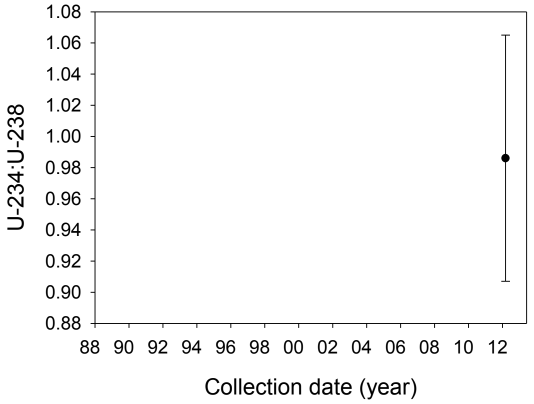
U-234:U-238 (alpha spectrometry)

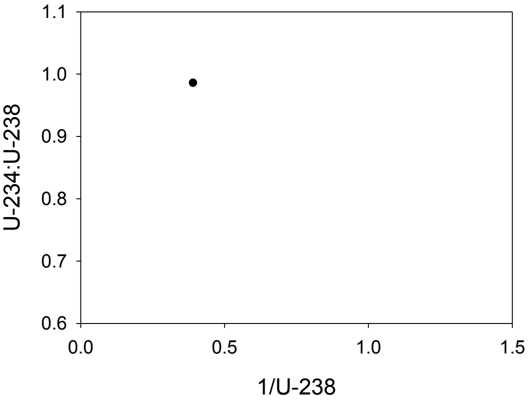
U-234:U-238 vs. 1/U-238

Bore ID – RN23562

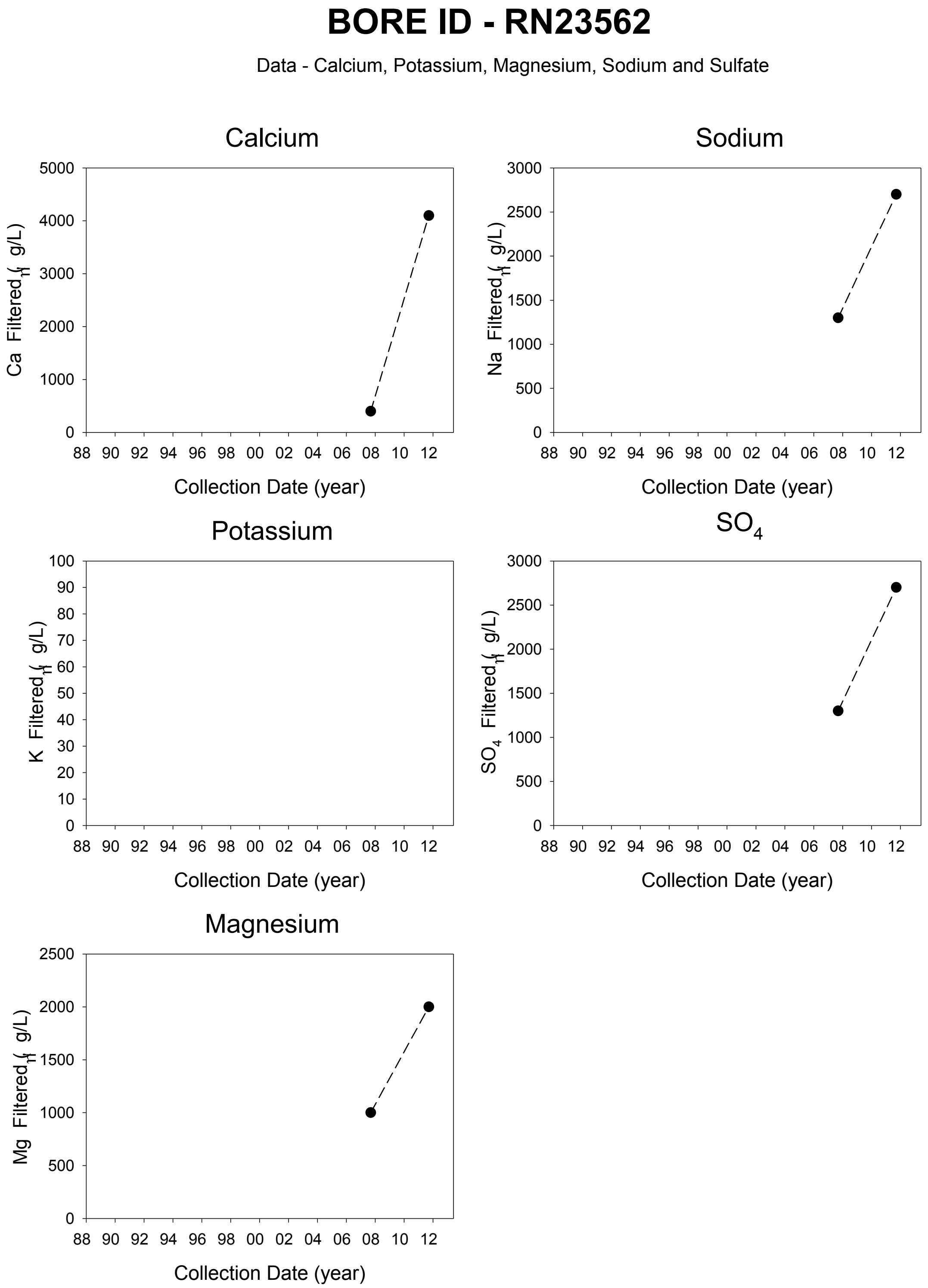

BORE ID - RN23562

Data - Calcium, Potassium, Magnesium, Sodium and Sulfate

BORE ID - RN23562

Data - Iron, Manganese, Barium, Strontium, Uranium & Vanadium

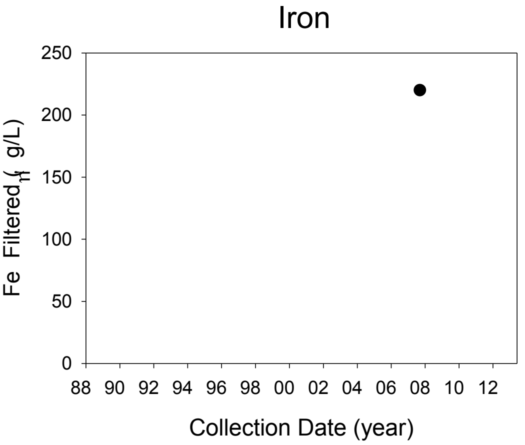

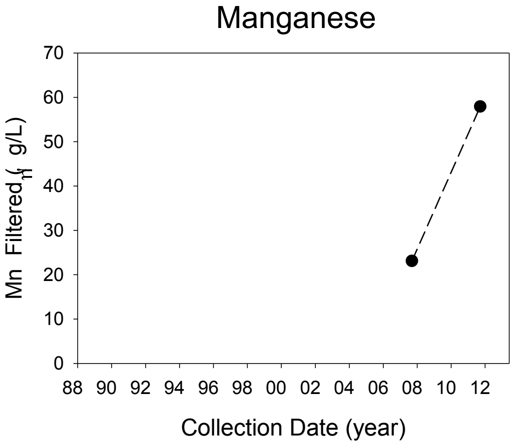

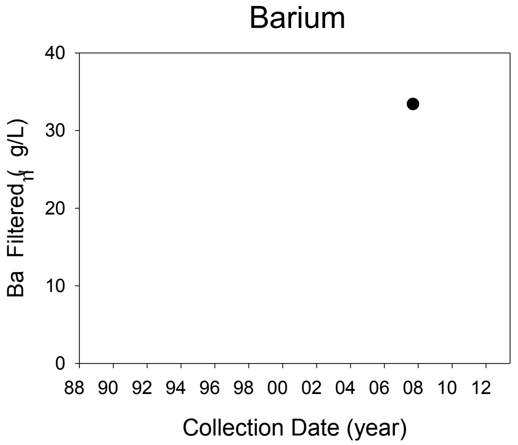

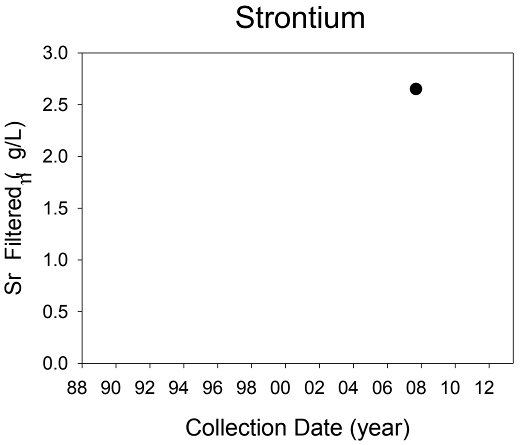

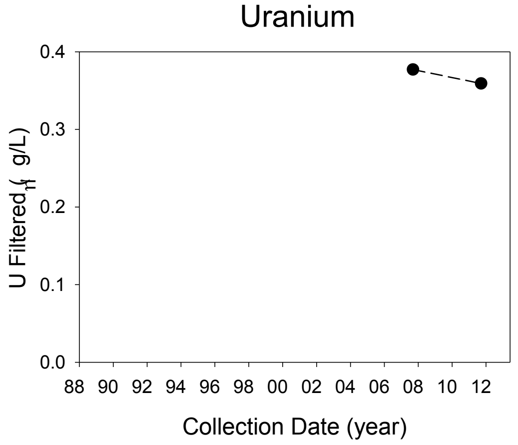

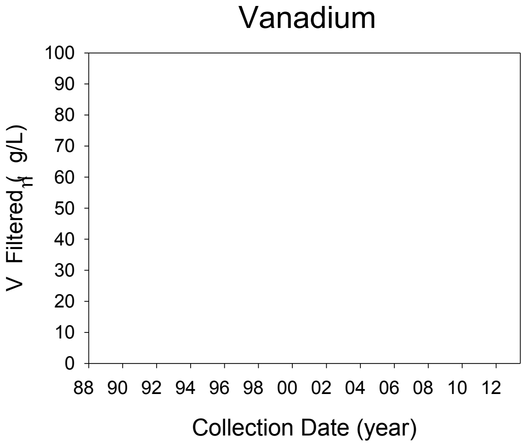

BORE ID - RN23562

Data - U-238, Ra-226, U-234:U-238 & 1/U-238
Uncertainty is 1 standard deviation based on counting statistics only

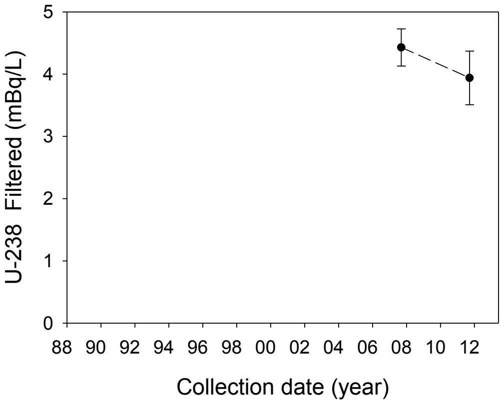
U-238 (alpha spectrometry)

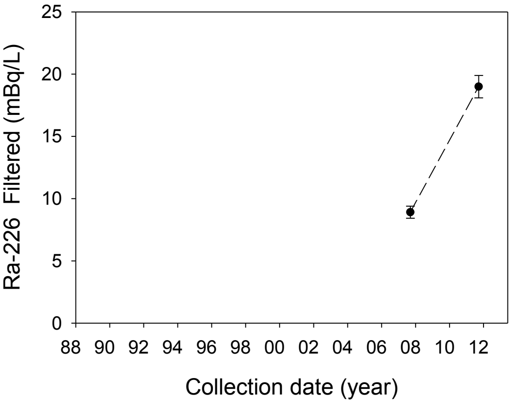
Ra-226 (alpha spectrometry)

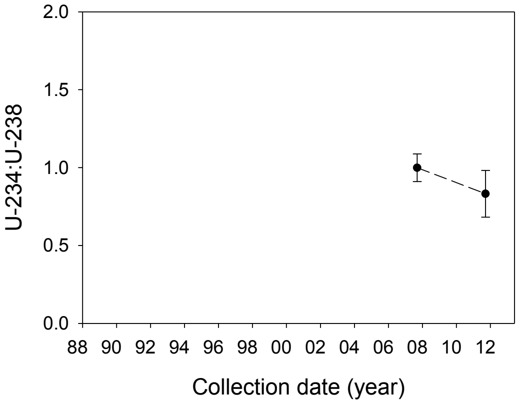
U-234:U-238 (alpha spectrometry)

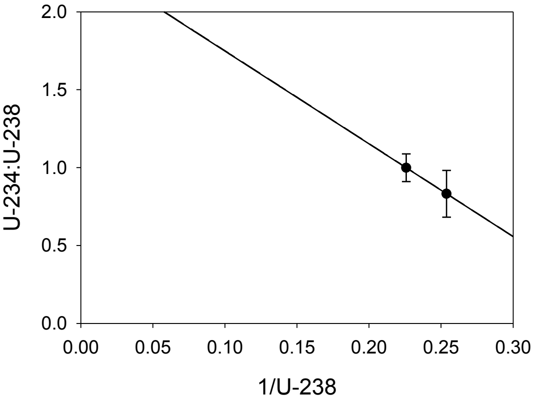
U-234:U-238 vs. 1/U-238

Bore ID – RN23566

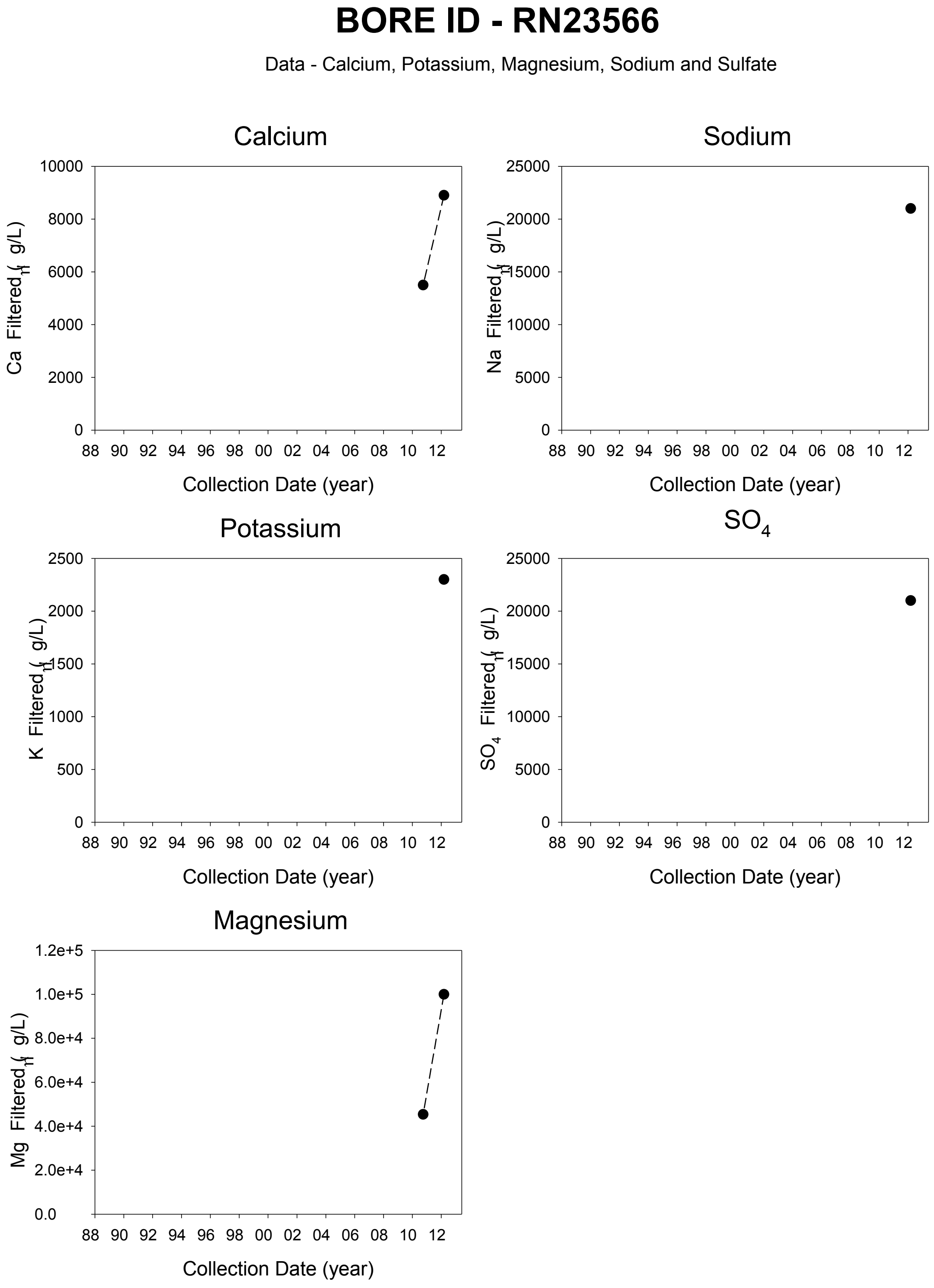

BORE ID - RN23566

Data - Iron, Manganese, Barium, Strontium, Uranium & Vanadium

Iron

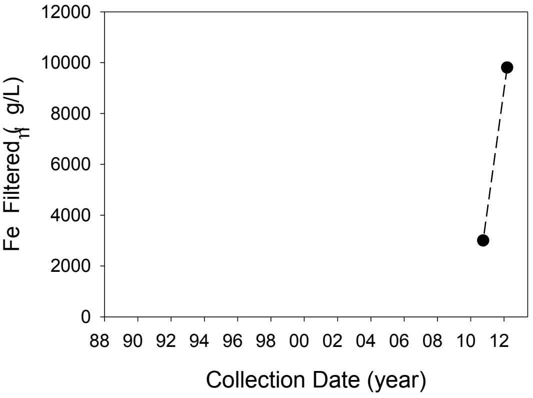

Manganese

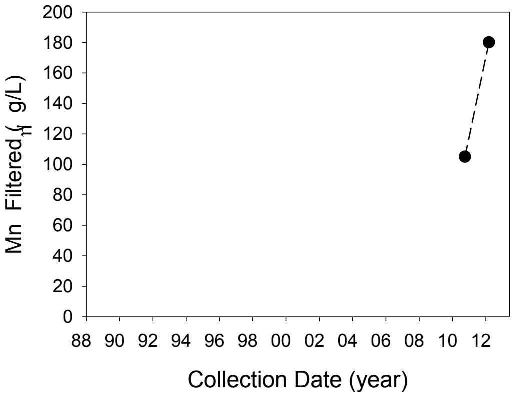

Barium

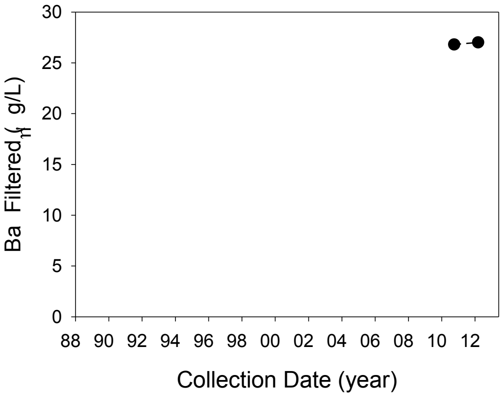

Strontium

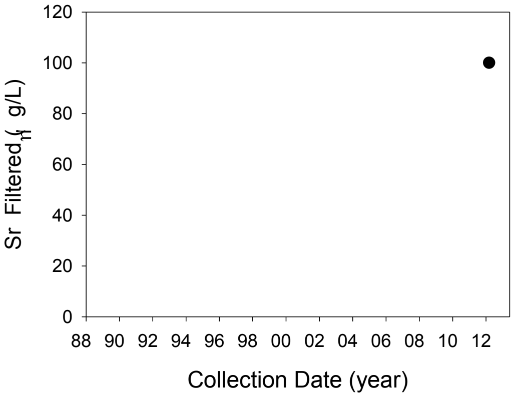

Uranium

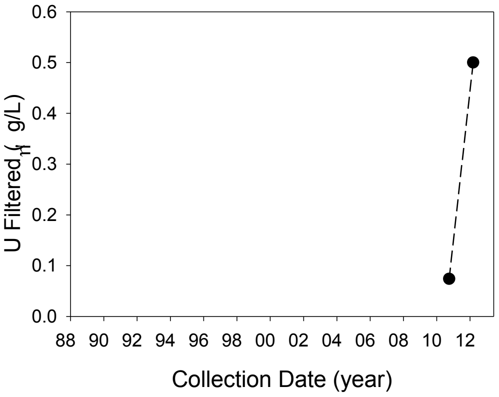

Vanadium

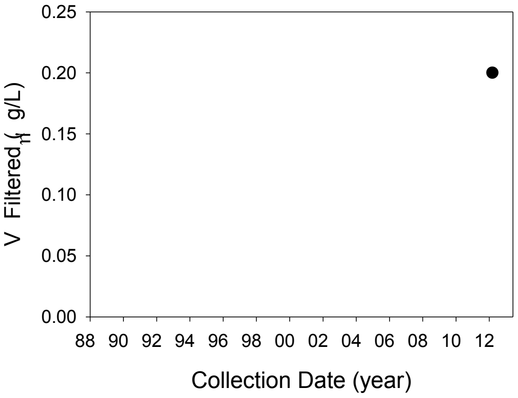

BORE ID - RN23566

Data - U-238, Ra-226, U-234:U-238 & 1/U-238
Uncertainty is 1 standard deviation based on counting statistics only

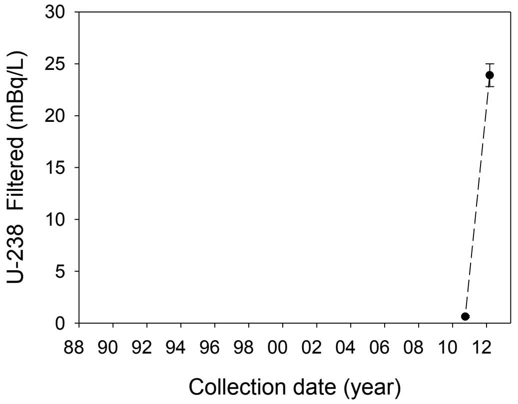
U-238 (alpha spectrometry)

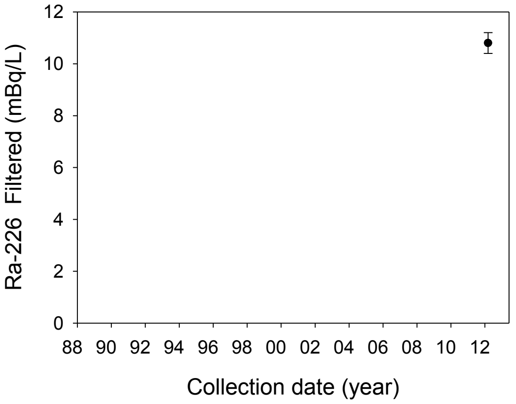
Ra-226 (alpha spectrometry)

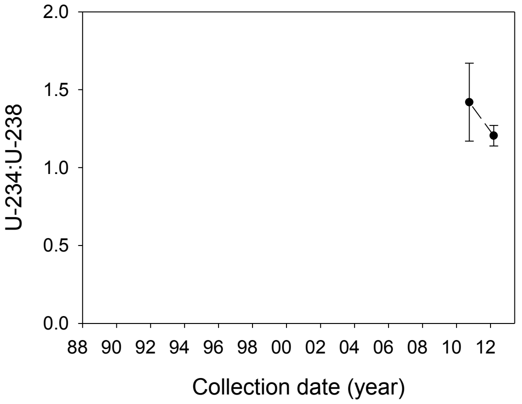
U-234:U-238 (alpha spectrometry)

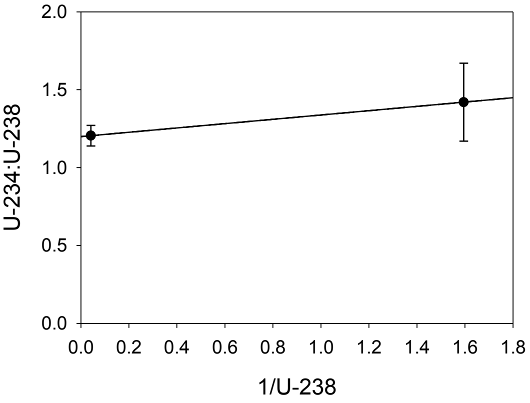
U-234:U-238 vs. 1/U-238

Bore ID – RN23568

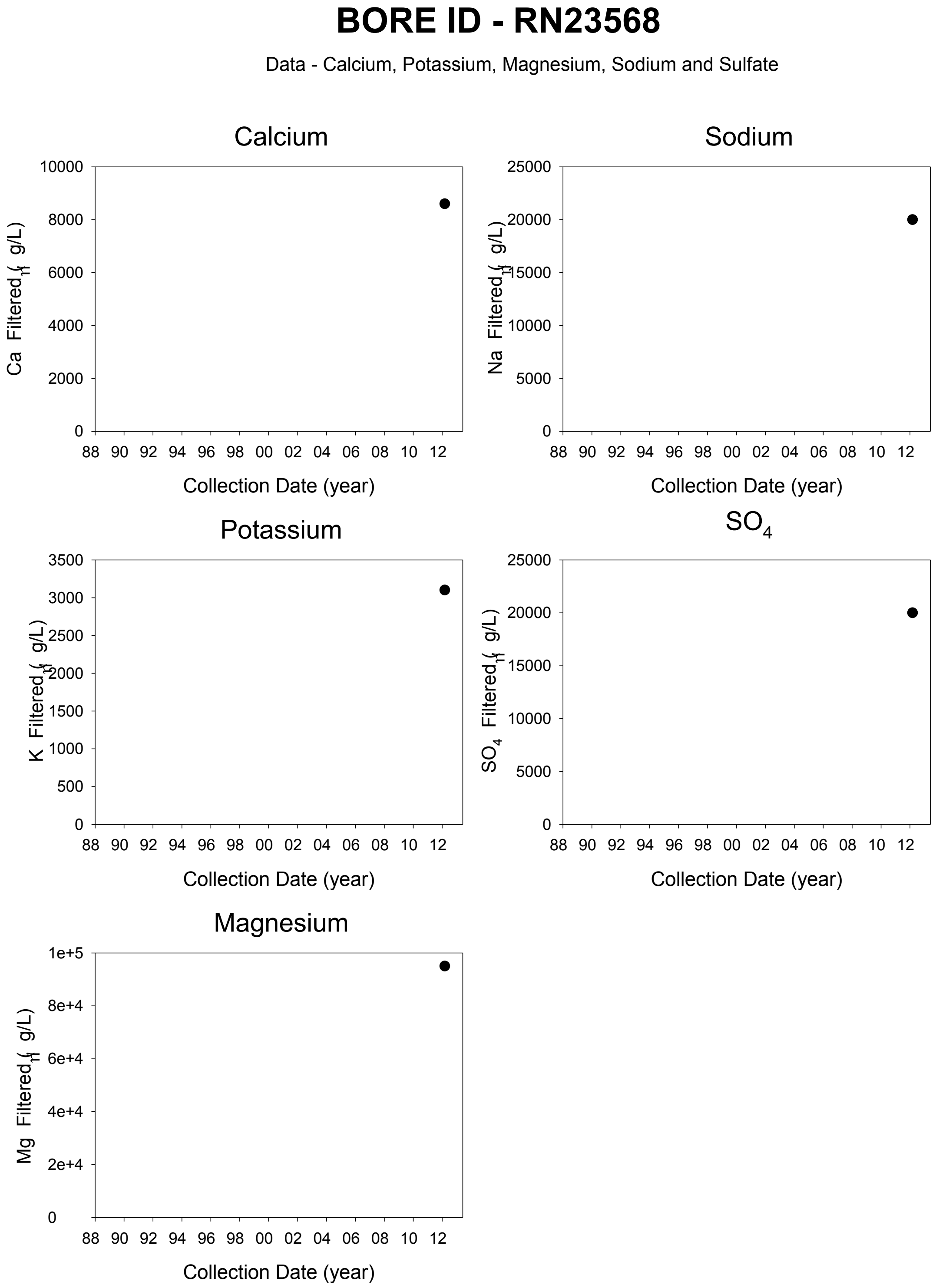

BORE ID - RN23568

Data - Iron, Manganese, Barium, Strontium, Uranium & Vanadium

Iron

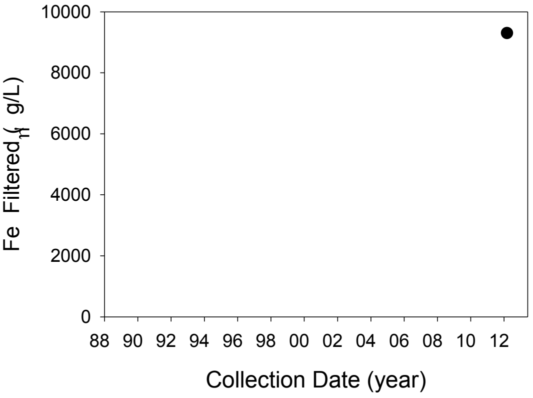

Manganese

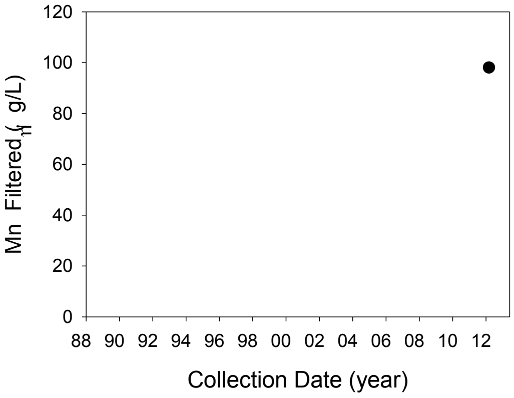

Barium

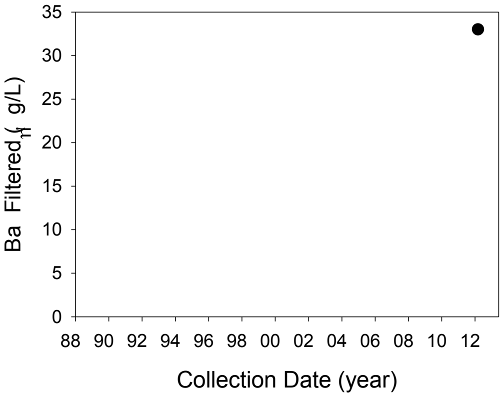

Strontium

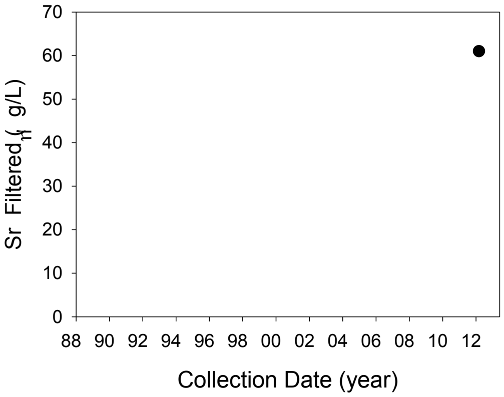

Uranium

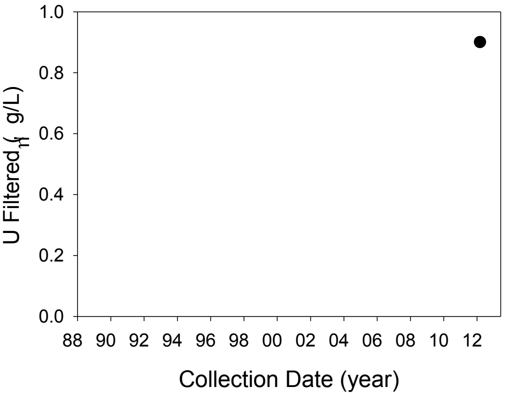

Vanadium

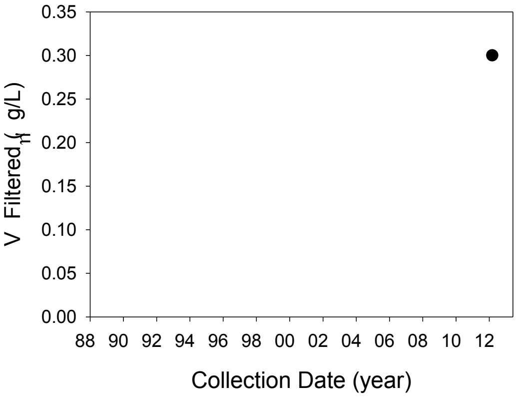

BORE ID - RN23568

Data - U-238, Ra-226, U-234:U-238 & 1/U-238
Uncertainty is 1 standard deviation based on counting statistics only

U-238 (alpha spectrometry)

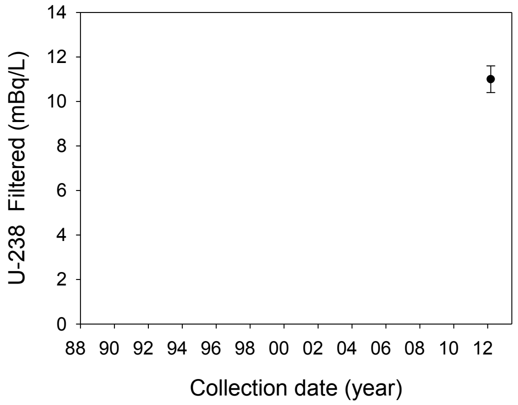

Ra-226 (alpha spectrometry)

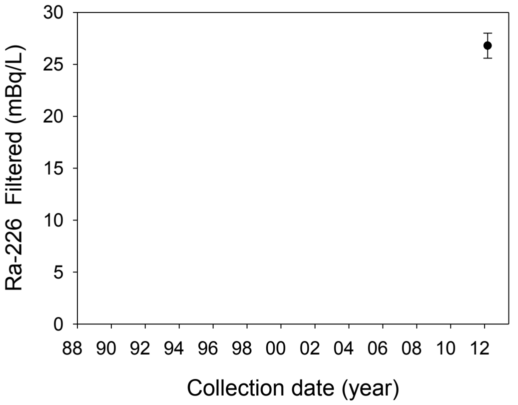

U-234:U-238 (alpha spectrometry)

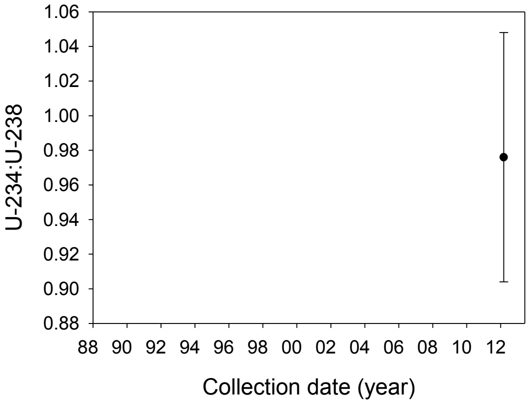

U-234:U-238 vs. 1/U-238

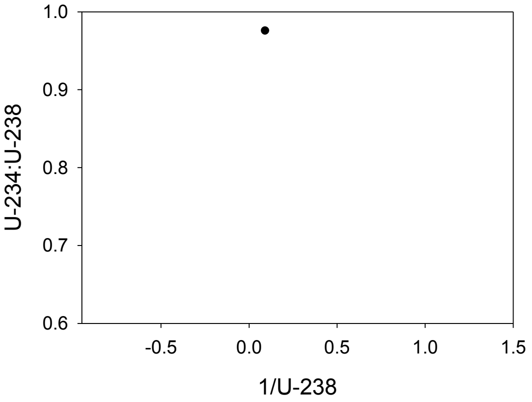

Bore ID – RN8708

BORE ID - RN8708

Data - Calcium, Potassium, Magnesium, Sodium and Sulfate

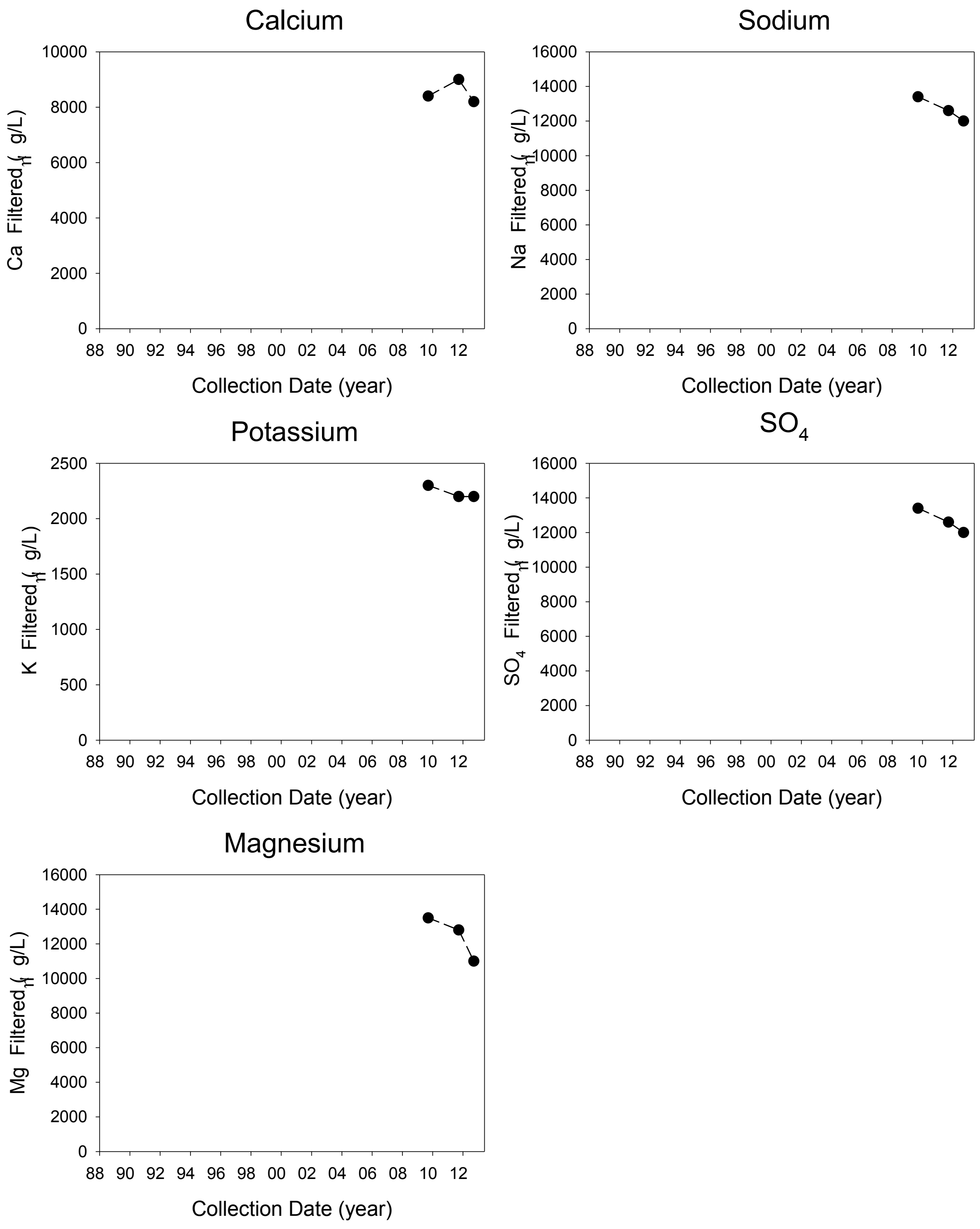

BORE ID - RN8708

Data - Iron, Manganese, Barium, Strontium, Uranium & Vanadium

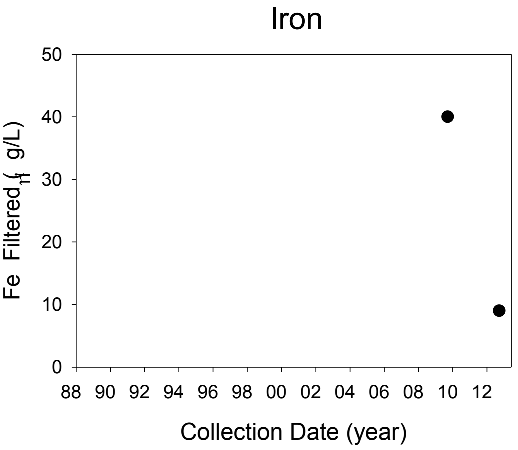

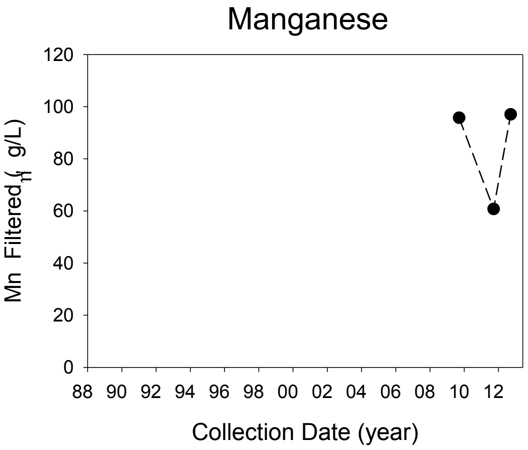

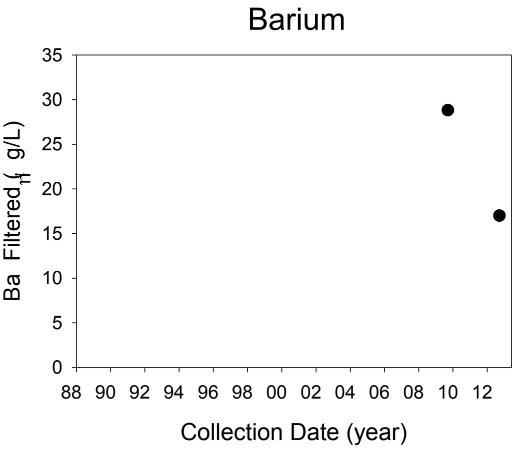

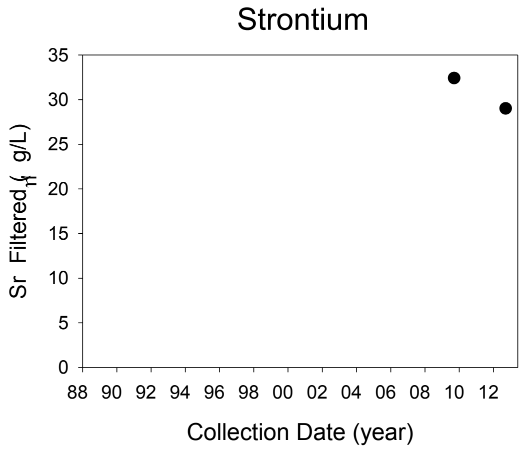

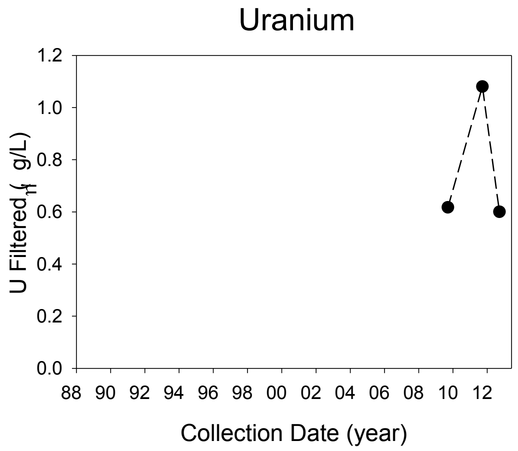

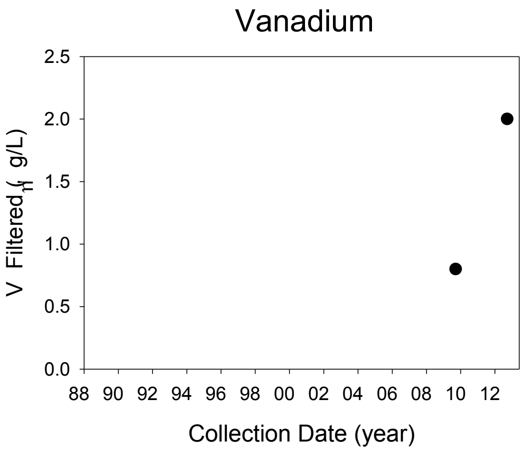

BORE ID - RN8708

Data - U-238, Ra-226, U-234:U-238 & 1/U-238
Uncertainty is 1 standard deviation based on counting statistics only

U-238 (alpha spectrometry)

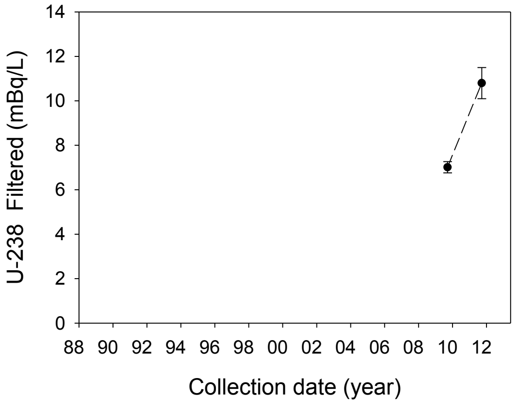

Ra-226 (alpha spectrometry)

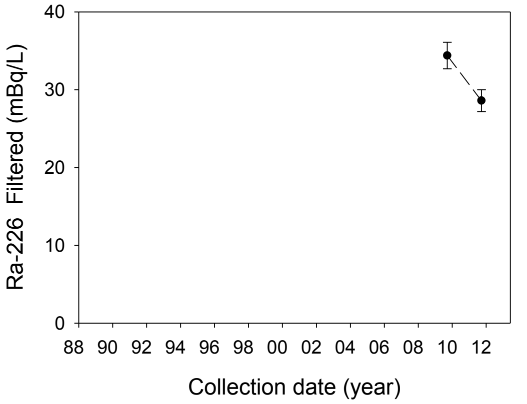

U-234:U-238 (alpha spectrometry)

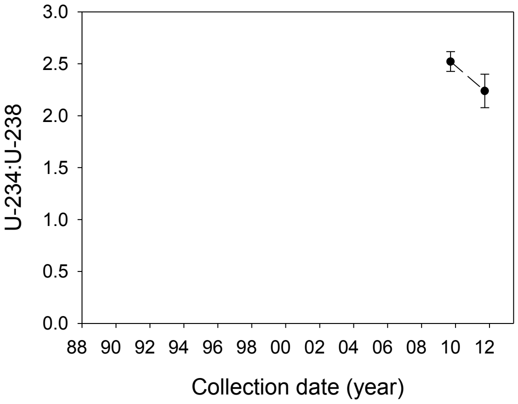

U-234:U-238 vs. 1/U-238

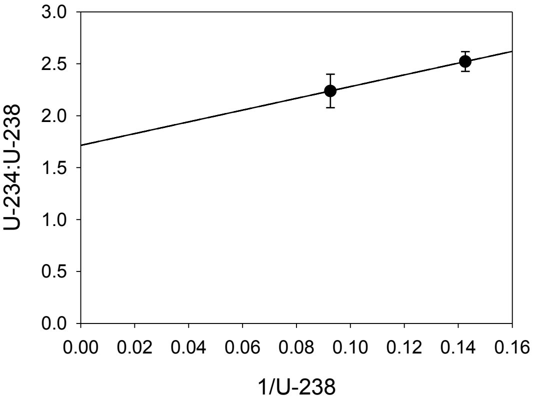

Bore ID – RN9329

BORE ID - RN9329

Data - Calcium, Potassium, Magnesium, Sodium and Sulfate

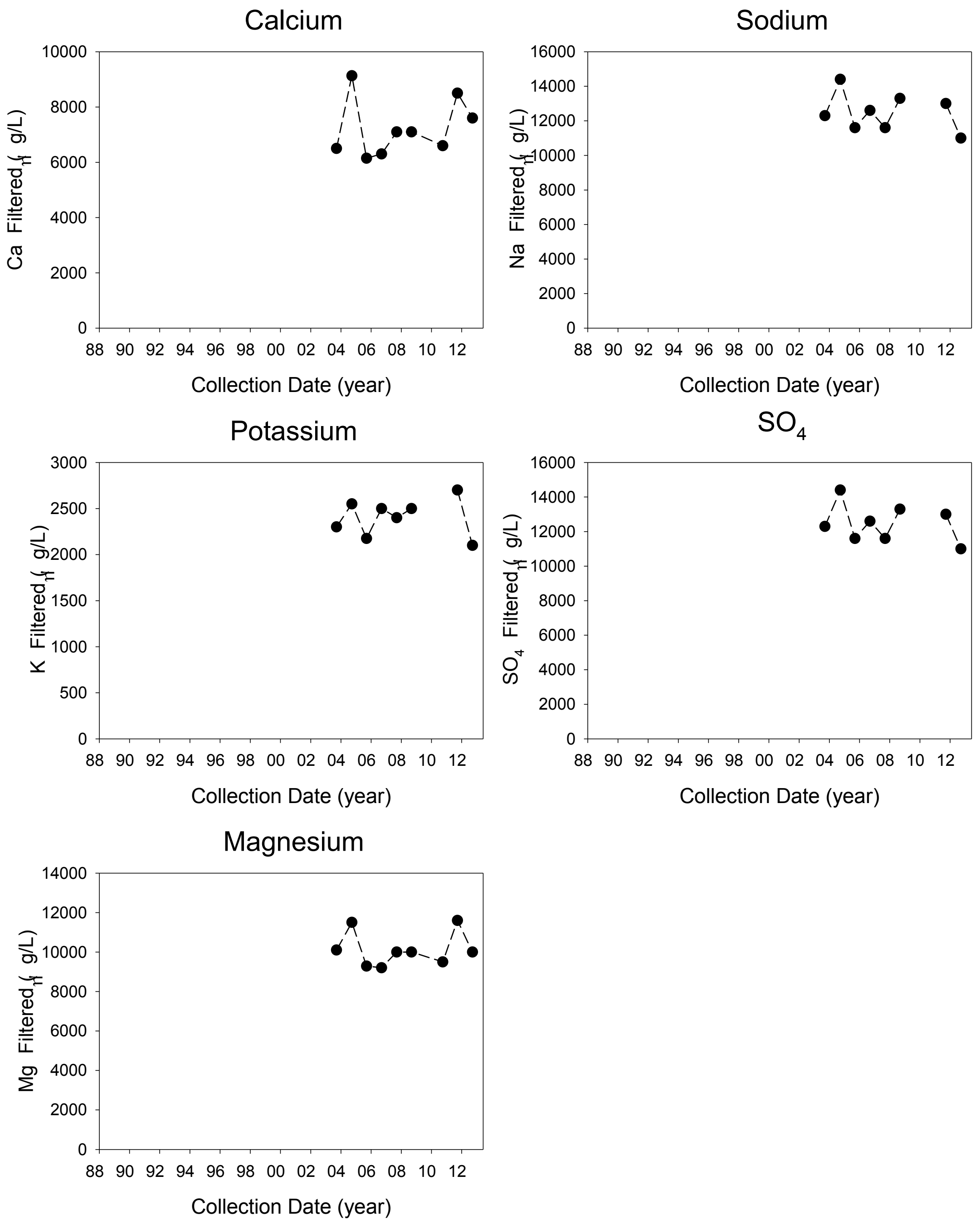

BORE ID - RN9329

Data - Iron, Manganese, Barium, Strontium, Uranium & Vanadium

Iron

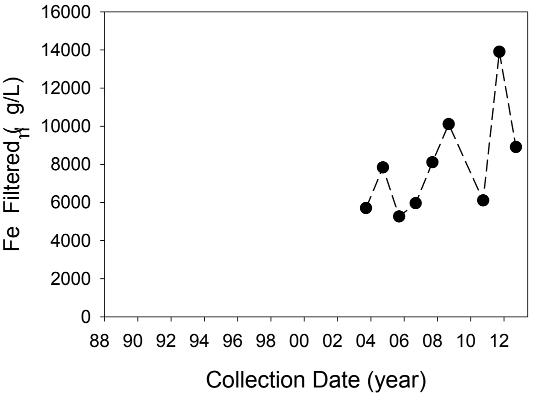

Manganese

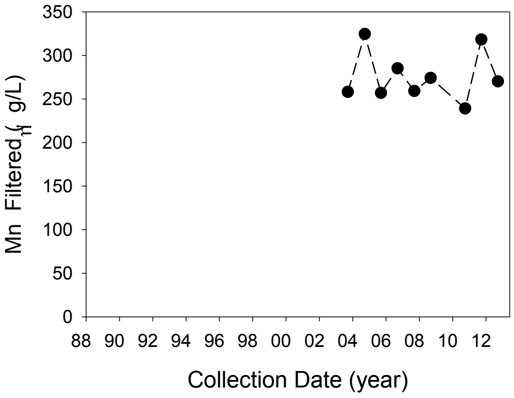

Barium

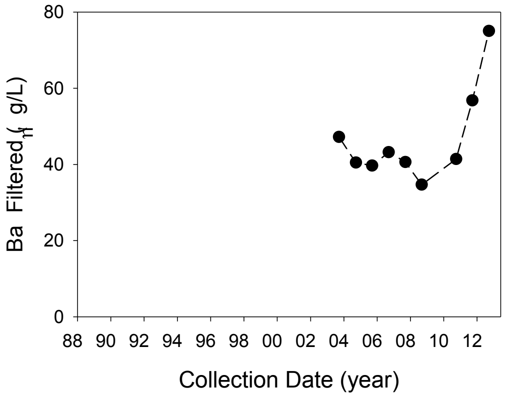

Strontium

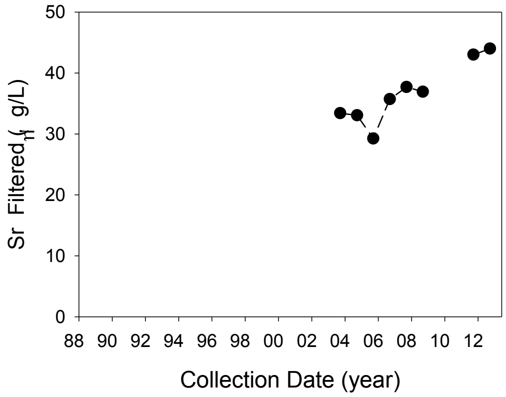

Uranium

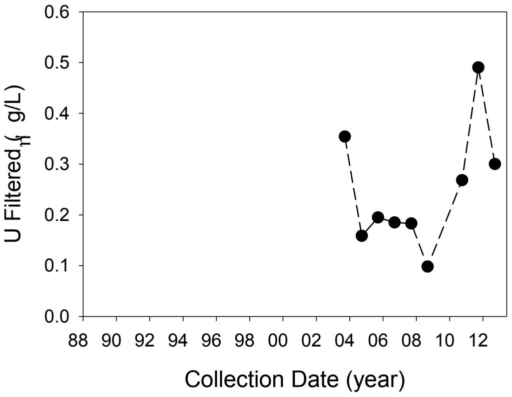

Vanadium

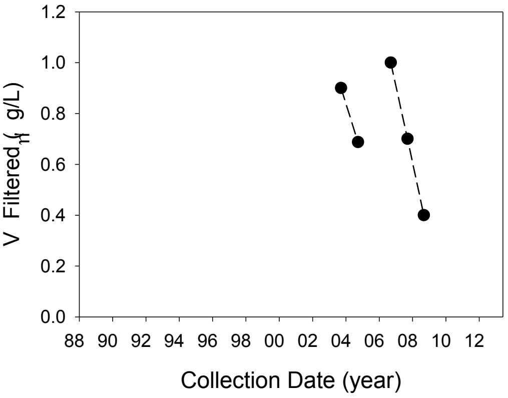

BORE ID - RN9329

Data - U-238, Ra-226, U-234:U-238 & 1/U-238
Uncertainty is 1 standard deviation based on counting statistics only

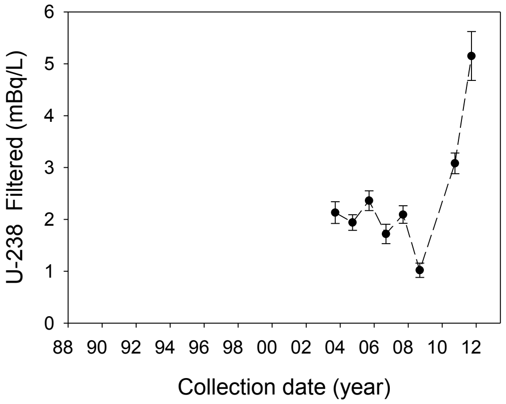
U-238 (alpha spectrometry)

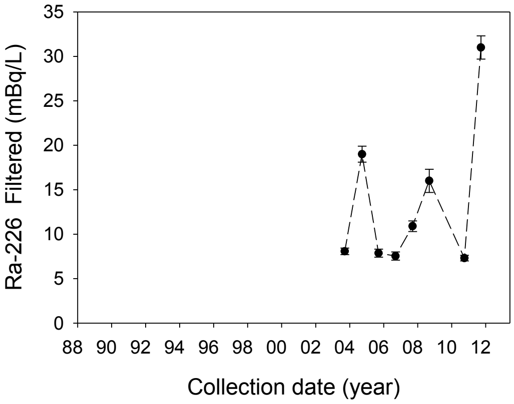
Ra-226 (alpha spectrometry)

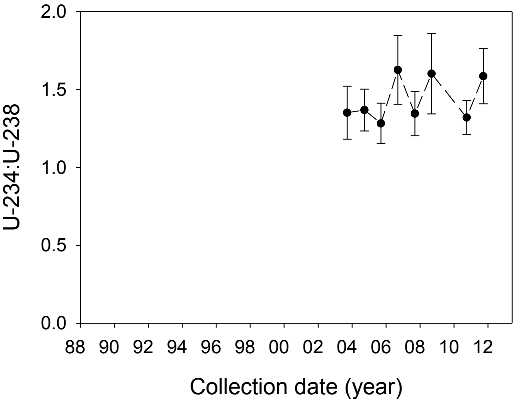
U-234:U-238 (alpha spectrometry)

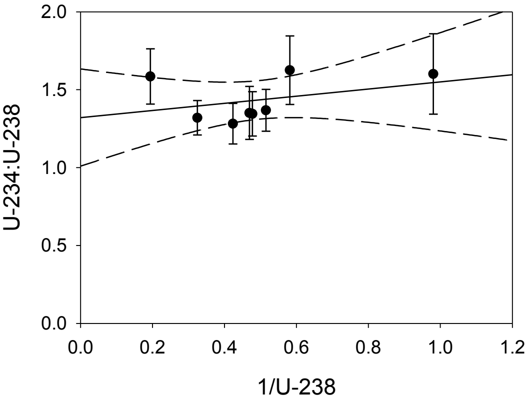
U-234:U-238 vs. 1/U-238

Bore ID – RP1N1 and RP1N2

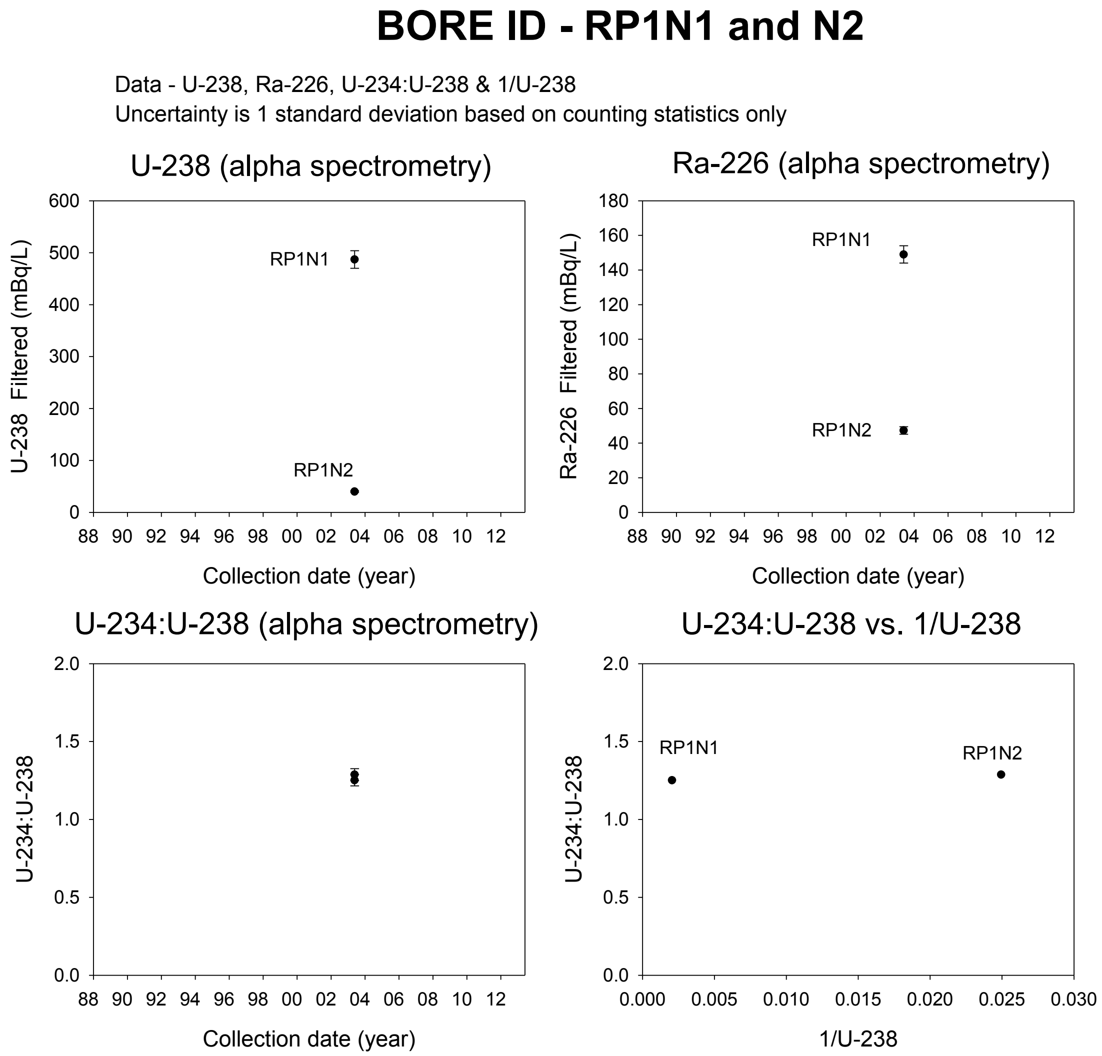

Bore ID – OB79/6A

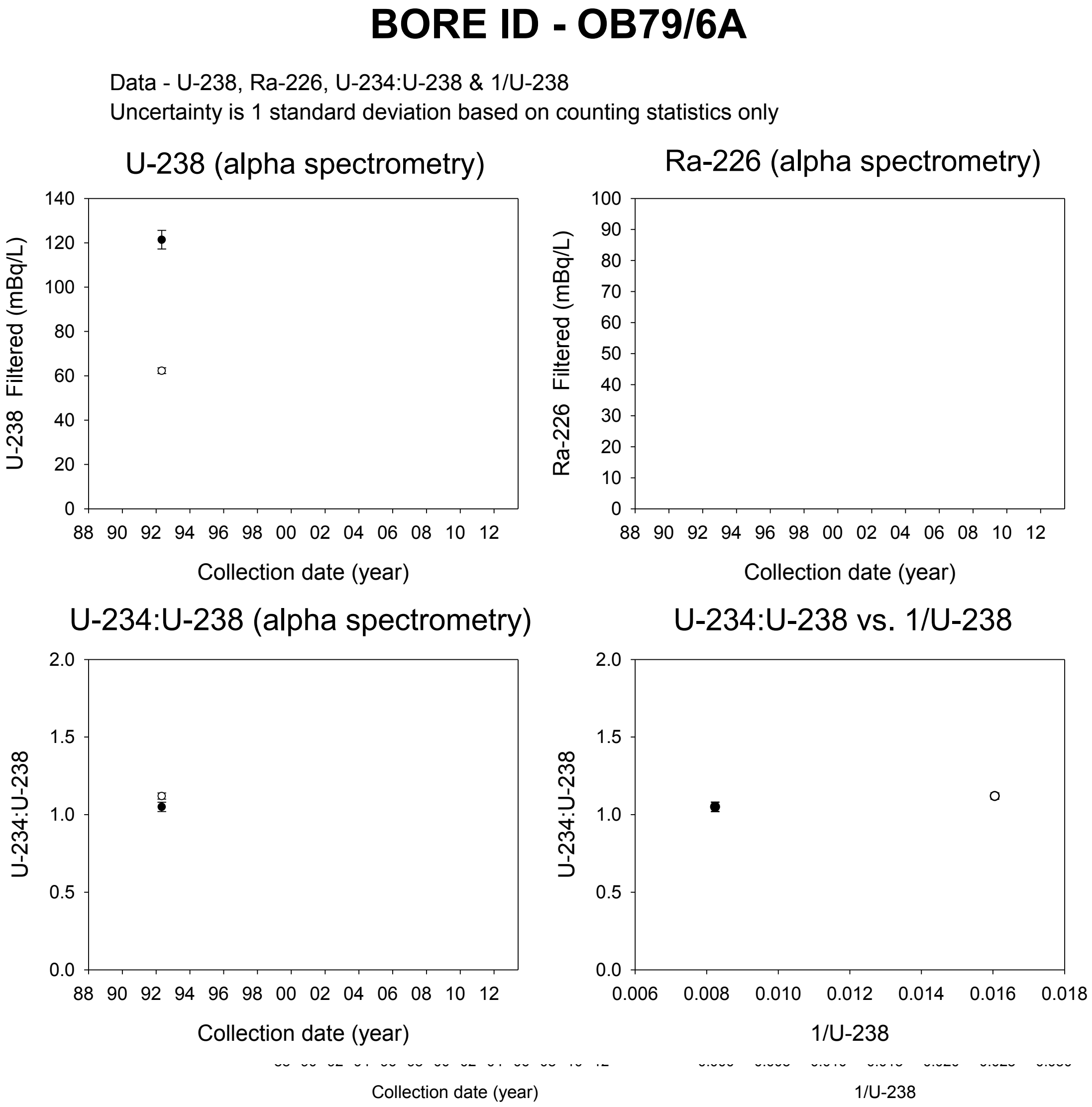

Bore ID – R.P. 79/ 2

BORE ID - R.P. 79/ 2 Ranger

Data - U-238, Ra-226, U-234:U-238 & 1/U-238
Uncertainty is 1 standard deviation based on counting statistics only

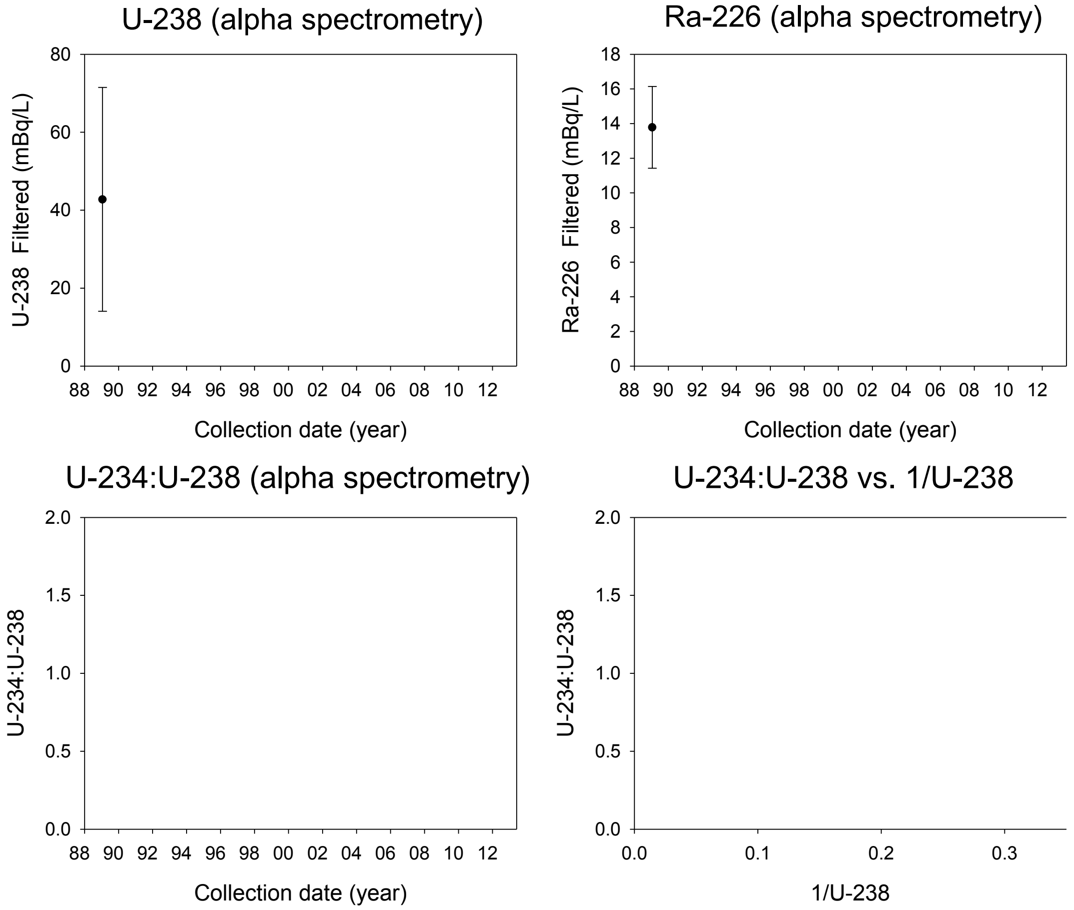

Appendix 2

Bore water metal and radionuclide data

Table A61 Bore water metal and radionuclide activity concentrations. All metal concentrations are given in µg•L-1, radionucIde activity concentrations are given in mBq•L-1.

eriss_ID	Date	Site_ID	RN number	Ba	Ca	Fe	K	Mg	Mn	Na	S	SO4	Sr	U	V	U-238 (1)	234U/238U	U-238 (2)	234U/238U	Ra-226 (1)	Ra-226 (2)
OB11015	22/09/11	23931_DEEP	RN023931	21.4	9800	<20	5200	17400	9.6	13000		900	21.2	1.77	8	21.4 ± 1.1	1.52 ± 0.10			39.9 ± 1.5	
OB12020	19/09/12	23931_DEEP	RN023931	33	8300	31	4700	15000	5	12000			18	1.1	4					25.3 ± 1.3	
	10/11/89	79/6	RN022901																	536.8 ± 4.6	
	12/05/92	79/6A	RN022901																	546 ± 25	
	10/11/89	79/9	RN020098																	174 ± 2.4	
OB9619	1/05/96	79/9	RN020098													6.7 ± 0.3	1.14 ± 0.07				
	21/01/89	R.P. 79/ 2 Ranger	RN020091													43± 29				13.8 ± 2.4	
OB03001	21/05/03	83_1	RN023010													20.1 ± 0.7	1.18 ± 0.043			3.36 ± 0.45	
OB03008	17/09/03	83_1	RN023010	8.38	7100	<20	1000	8000	0.67	8800		900	12.4	1.86	0.2	23.1 ± 1.2	1.008 ± 0.058			3.25 ± 0.33	
OB04008	22/09/04	83_1	RN023010	7.0	6970	<10	1240	7890	44.1	10700	<200		8.6	0.36	1.7	4.38 ± 0.25	1.36 ± 0.093			12.1 ± 0.7	
OB05017	13/09/05	83_1	RN023010	6.2	5220	<20	1080	6490	36.9	9020			7.9	0.27	<10	3.3 ± 0.2	1.424 ± 0.116			4.22 ± 0.27	
RM10037	28/09/10	83_1	RN023010	7.3	5500	<20		6200	35.3			400		0.80		7.42 ± 0.46	1.39 ± 0.11			3.35 ± 0.3	2.71 ± 0.38
OB11002	19/09/11	83_1	RN023010		4600		1000	6000	33.9	8500		1300		0.43		4.73 ± 0.41	1.129 ± 0.13			6.82 ± 0.62	
OB11004	20/09/11	83_1	RN023010		4700		1000	6000	34.8	8500		1500		0.44		5.27 ± 0.56	1.084 ± 0.154			8.57 ± 0.49	
OB06008	12/09/06	83_1	RN023010	7.4	4500	<20	1100	5700	34.4	9300			8.4	0.33	3.7	3.86 ± 0.33	1.335 ± 0.144			1.81 ± 0.3	
OB07006	11/09/07	83_1	RN023010	9.4	4000	<20	1000	5400	25.5	8000			6.9	0.29	2.1	3.06 ± 0.23	1.567 ± 0.144			3.26 ± 0.32	
OB08001	2/09/08	83_1	RN023010	9.9	4100	<50	1000	5100	37.9	8200			7.1	0.28	3.4	3.61 ± 0.24	1.015 ± 0.089			2.08 ± 0.43	
OB09004	15/09/09	83_1	RN023010	9.0	4500	<20	1200	6400	38.4	9600			9	0.39	7.4	4.49 ± 0.21	1.137 ± 0.068			4.06 ± 0.28	
OB12009	19/09/12	83_1	RN023010	21	4500	3	900	5800	42	7800			15	0.3	3						
OB06002	15/09/06	B11	RN007243	8.8	2700	14100	1700	3800	225	11400			11.1	0.46	0.1	5.04 ± 0.28	1.519 ± 0.1			86 ± 2.9	
OB07001	10/09/07	B11	RN007243	13.2	2500	19200	1700	4100	328	10500			12	0.35	0.1	3.50 ± 0.28	1.658 ± 0.159			52.6 ± 2.4	

eriss_ID	Date	Site_ID	RN number	Ba	Ca	Fe	K	Mg	Mn	Na	S	SO4	Sr	U	V	U-238 (1)	234U/238U	U-238 (2)	234U/238U	Ra-226 (1)	Ra-226 (2)
OB08008	5/09/08	B11	RN007243	11.1	2700	18200	1700	4200	312	11400			9.6	0.28	<0.1	3.44 ± 0.33	1.467 ± 0.177			54.5 ± 2.6	
OB09001	14/09/09	B11	RN007243	7.3	2200	9850	1700	3900	163	11400			10.5	0.77	0.2	8.82± 0.37	1.447 ± 0.068			62.4 ± 2.2	
OB07003	11/09/07	C12	NOT FOUND	108	300	40	2800	7800	30.9	7800			6.5	0.12	<0.1	1.53 ± 0.16	1.123 ± 0.16			25.3 ± 1.1	
OB03002	21/05/03	C1SHALLOW	NOT FOUND													9.33 ± 0.45	1.534 ± 0.078			12.5 ± 0.7	
OB07013	18/09/07	Magela Ck 11/80	RN020369	26	700	1350	300	700	48.6	3700			4.3	0.057	0.4	0.81 ± 0.13	1.178 ± 0.248			13.9 ± 0.7	
OB03003	21/05/03	MBH	RN023721													5.36 ± 0.35	1.107 ± 0.089			5.62 ± 0.36	
OB03004	21/05/03	MBL	RN023725													1920 ± 80	0.915 ± 0.038			30.3 ± 1.5	
OB03015	19/09/03	MC24	RN025466	25.4	900	100	<100	79600	10.1	7300		261000	5.8	0.18	2.5	2.17 ± 0.27	1.028 ± 0.176			14 ± 0.7	
OB03014	17/09/03	MC27	RN025469	0.7	7500	<20	4600	21200	5.64	14800		38300	69.8	0.26	0.6	2.7 ± 0.23	1.765 ± 0.174			0.61 ± 0.28	
OB04005	22/09/04	MC27	RN025469	2.2	11300	<10	4460	21700	19.3	17100	15300		59.8	0.13	0.7	2.14 ± 0.14	1.765 ± 0.142			1.91 ± 0.29	
OB06005	14/09/06	MC27DEEP		4	5200	20	2500	13900	11.5	13300			41.8	0.089	0.7	1.25 ± 0.12	1.301 ± 0.175			13.2 ± 0.7	
OB9015	9/05/89	OB10A	RN022920													127 ± 21		136 ± 8		65.6 ± 2.2	
OB9020	6/11/89	OB10A	RN022920													95 ± 16				51 ± 2	
	9/11/90	OB10A	RN022920																	84.9 ± 3.5	
OB1912	14/05/91	OB10A	RN022920													157 ± 6	1.12 ± 0.04			74.5 ± 2.5	
	14/11/91	OB10A	RN022920													130 ± 20				70.6 ± 2.5	
	8/05/92	OB10A	RN022920																	89.5 ± 3.9	
OB9603	1/05/96	OB10A	RN022920													94 ± 4	1.08 ± 0.04				
OB9624	1/11/96	OB10A	RN022920													82 ± 3	1.12 ± 0.04				
OB9707	1/11/97	OB10A	RN022920													126 ± 4	1.34 ± 0.03				
OB9802	1/05/98	OB10A	RN022920													6420 ± 200	1.04 ± 0.01				
OB9914	18/05/99	OB10A	RN022920	48.4	11200	572	4980	188000	18.8	25500	173000		72.8	24.1	<3.0	493 ± 18	1.042 ± 0.035			630 ± 25	
OB02011	31/05/02	OB10A	RN022920	42.6	18400	20500	10600	119000	146	23000		450000	45.1	31.9	0.2	362 ± 9	1.028 ± 0.026			306 ± 13	
OB12002	6/03/12	OB112_DEEP	OB112_DEEP	130	7500	200	7900	6200	460	27000		24000	120	1.8	0.9	22.6 ± 1.2	1.02 ± 0.066			33.7 ± 1.1	
OB12001	6/03/12	OB112_SHALLOW	NOT FOUND	10	100	14	1200	200	3	1900		<1000	0.4	0.1	0.05	0.99 ± 0.12	0.791 ± 0.167			1.66 ± 0.26	
OB13005	15/03/13	OB112_Deep	NOT FOUND																	23.9 ± 1.3	
RM10043	1/10/10	OB116_DEEP	NOT FOUND	154	3900	<20		11600	14.4			4700		3.92		45.8 ± 2.1	1.36 ± 0.06			81.2 ± 2	44.5 ± 2.1
OB12006	8/03/12	OB116_DEEP	NOT FOUND	120	2300	8	2900	9500	2	13000		<1000	28	1.9	2	5.74 ± 0.4	1.04 ± 0.102			50.3 ± 1.1	
OB13003	14/03/13	OB116_Deep	NOT FOUND																	38.3 ± 1.7	
OB12007	8/03/12	OB116_SHALLOW	NOT FOUND	11	<100	62	1400	400	4	1500		<1000	0.8	0.1	0.06	1.1 ± 0.12	1.186 ± 0.168			2.6 ± 0.24	

eriss_ID	Date	Site_ID	RN number	Ba	Ca	Fe	K	Mg	Mn	Na	S	SO4	Sr	U	V	U-238 (1)	234U/238U	U-238 (2)	234U/238U	Ra-226 (1)	Ra-226 (2)
	6/09/88	OB11A	RN022922																	115.7 ± 2.8	115.8 ± 2.6
OB8021	4/11/88	OB11A	RN022922													37.3 ± 7.7				133.7 ± 3.1	140.6 ± 3.1
	16/01/89	OB11A	RN022922																	173 ± 3	
OB9016	9/05/89	OB11A	RN022922													43.0 ± 9.4				172.1 ± 3	
OB9024	7/11/89	OB11A	RN022922													65.2 ± 22.1				143.3 ± 3.1	
	8/11/90	OB11A	RN022922																	192 ± 17	
	8/05/91	OB11A	RN022922																	208 ± 8.6	
	14/11/91	OB11A	RN022922													63 ± 24				177.1 ± 2.7	
	8/05/92	OB11A	RN022922																	189.8 ± 6.2	
	24/11/92	OB11A	RN022922																	168.6 ± 5.4	
	12/05/93	OB11A	RN022922																	309.5 ± 6	
OB9610	1/05/96	OB11A	RN022922													31.4 ± 0.7	1.75 ± 0.04				
OB9626	1/11/96	OB11A	RN022922													70 ± 2	1.3 ± 0.03				
OB9703	1/05/97	OB11A	RN022922													103 ± 4	1.23 ± 0.04				
	6/11/89	OB12A	RN022923													40 ± 6				33 ± 2	
	8/05/91	OB12A	RN022923																	34.79 ± 0.83	
OB9607	1/05/96	OB12A	RN022923													29 ± 1	1.38 ± 0.05				
OB8016	6/09/88	OB13A	RN022924													33.9 ± 0.9	1.57 ± 0.05			64.05 ± 2.44	
OB8025	4/11/88	OB13A	RN022924													31.3 ± 6.8		70 ± 30		66.65 ± 2.23	63.93 ± 2.31
	17/01/89	OB13A	RN022924																	90.04 ± 2.79	
OB9018	9/05/89	OB13A	RN022924													42.9 ± 22.2				81.74 ± 2.71	
OB9025	7/11/89	OB13A	RN022924													71.1 ± 21.2				83.39 ± 2.63	
	9/11/90	OB13A	RN022924																	68.12 ± 3.84	
	8/05/91	OB13A	RN022924													104 ± 4				62.53 ± 2.26	
	8/05/92	OB13A	RN022924																	64.07 ± 1.88	
OB2913	24/11/92	OB13A	RN022924									650000				4920 ± 150	1.1 ± 0.03			55.67 ± 1.98	
OB3903	1/05/93	OB13A	RN022924													369 ± 9	1.13 ± 0.03				
OB3903	12/05/93	OB13A	RN022924													364 ± 6	1.18 ± 0.01			50.1 ± 2.3	
OB9608	1/05/96	OB13A	RN022924													689 ± 20	1.1 ± 0.01				
OB9636	1/11/96	OB13A	RN022924													16300 ± 400	1.09 ± 0.01				

eriss_ID	Date	Site_ID	RN number	Ba	Ca	Fe	K	Mg	Mn	Na	S	SO4	Sr	U	V	U-238 (1)	234U/238U	U-238 (2)	234U/238U	Ra-226 (1)	Ra-226 (2)
OB9701	1/05/97	OB13A	RN022924													818 ± 28	1.12 ± 0.04				
OB9706	1/11/97	OB13A	RN022924													9350 ± 230	1.07 ± 0.01				
OB9803	1/05/98	OB13A	RN022924													4970 ± 170	1.05 ± 0.01				
	4/11/88	OB15	RN022926																	62.16 ± 3.62	71.89 ± 2.8
	18/01/89	OB15	RN022926																	53.51 ± 11.59	
	6/11/89	OB15	RN022926																	53.81 ± 2.41	
	9/11/90	OB15	RN022926																	76.5 ± 4.8	
	14/05/91	OB15	RN022926																	48.8 ± 1.68	
	8/05/92	OB15	RN022926									460000								57.58 ± 1.78	
	25/11/92	OB15	RN022926		43000			120000				580000								47.54 ± 1.7	
	14/05/93	OB15	RN022926																	46.6 ± 1.6	
OB9609	1/05/96	OB15	RN022926													120 ± 4	1.37 ± 0.02				
OB9623	1/11/96	OB15	RN022926													47.9 ± 1.5	1.89 ± 0.05				
OB9704	1/05/97	OB15	RN022926													70 ± 3	1.79 ± 0.06				
	6/09/88	OB16	RN022927													73.2 ± 37.4				76 ± 2	68.65 ± 2.86
	4/11/88	OB16	RN022927													77.1 ± 33.8		38 ± 7		80 ± 2	83.4 ± 2.4
	17/01/89	OB16	RN022927																	103 ± 2.9	
OB9017	9/05/89	OB16	RN022927													46 ± 5		30 ± 12		98 ± 2	98.73 ± 2.26
OB9021	6/11/89	OB16	RN022927													81 ± 20				105 ± 3	
OB0915	9/11/90	OB16	RN022927													699 ± 22	1.06 ± 0.02			211.3 ± 16.1	
OB1904	8/05/91	OB16	RN022927													80 ± 3	1.34 ± 0.05			60.7 ± 1.9	
	14/11/91	OB16	RN022927																	37.3 ± 2.6	
OB2907	8/05/92	OB16	RN022927													129 ± 4	1.34 ± 0.03			38.9 ± 1.5	
	24/11/92	OB16	RN022927		96000			240000				1200000								29.55 ± 1.14	
	12/05/93	OB16	RN022927																	35.4 ± 2.5	
OB9615	1/05/96	OB16	RN022927													174 ± 6	1.27 ± 0.03				
OB9629	1/11/96	OB16	RN022927													416 ± 14	1.18 ± 0.02				
OB9705	1/05/97	OB16	RN022927													213 ± 6	1.2 ± 0.03				
	6/01/89	OB17A	RN026588													61.4 ± 40.9				63.1 ± 3.5	

eriss_ID	Date	Site_ID	RN number	Ba	Ca	Fe	K	Mg	Mn	Na	S	SO4	Sr	U	V	U-238 (1)	234U/238U	U-238 (2)	234U/238U	Ra-226 (1)	Ra-226 (2)
OB9026	7/11/89	OB17A	RN026588													33.2 ± 16.3				64.9 ± 2.1	
	8/05/91	OB17A	RN026588																	123.1 ± 3.7	
OB9912	18/05/99	OB17A	RN026588	60.7	6360	47	2050	7190	6.8	31700	920		64.3	2.27	<3.0	29.7 ± 1.9	1.662 ± 0.103				
OB0006	18/05/00	OB17A	RN026588	24.1	5240.037	25	1730	8820	10.5	36800	1780		29.8	5.26	<3.0	63.6 ± 2.9	1.379 ± 0.055			25.2 ± 1.2	
OB0105	25/05/01	OB17A	RN026588	35.9	5160	32	1800	8440	10.8	35400	1240		33	2.83	<3.0	28.9 ± 1.6	1.736 ± 0.099	28.6 ± 1.3	.829 ± 0.079	20.5 ± 1	
OB02005	28/05/02	OB17A	RN026588	26.8	5200	20	1500	9100	2.55	34700		6500	29.3	7.02	2.1	86.1 ± 3.1	1.347 ± 0.035			23.5 ± 1	
OB8020	7/09/88	OB18A	NOT FOUND													6.3 ± 0.3	1.7 ± 0.09	69 ± 31		74 ± 3	
	19/01/89	OB18A	NOT FOUND																	65 ± 3	
	1/11/89	OB19A	RN026589																	30 ± 2	
	8/11/90	OB19A	RN026589																	200 ± 5	
OB9908	18/05/99	OB19A	RN026589	143	16200	395	4460	20000	285	21600	3580		68.3	0.39	<3.0	16.6 ± 0.8	1.64 ± 0.09	15.3 ± 0.7	.636 ± 0.081	30.0 ± 2.0	
OB0004	18/05/00	OB19A	RN026589	141	16400	15	4490	23000	209	23500	5150		67.6	2.89	<3.0	34 ± 1.5	1.08 ± 0.047			180 ± 7	
OB0102	21/05/01	OB19A	RN026589	143	16100	27	4300	22400	197	22200	5680		70	1.61	<3.0	15.1 ± 0.9	1.139 ± 0.079			145 ± 8	
OB02008	28/05/02	OB19A	RN026589	114	24800	<20	4500	23800	17.1	23400		26400	68	1.56	<0.1	18 ± 0.9	1.083 ± 0.062			79 ± 2.6	
OB1909	7/11/89	OB1A	RN022902																	35.1 ± 2.5	
OB1909	9/05/91	OB1A	RN022902													0.7 ± 0.2	0.9 ± 0.4			38.3 ± 1.4	
OB9605	1/05/96	OB1A	RN022902													4.9 ± 0.2	1.16 ± 0.06				
OB9911	18/05/99	OB1A	RN022902	181	4460	24300	3930	5840	1160	11200	360		49.4	0.58	<3.0	1.35 ± 0.10	1.121 ± 0.115				
OB0007	18/05/00	OB1A	RN022902	163	4160	7230	4050	180.253	1020	11300	<200		45.7	0.77	<3.0	8.79 ± 0.36	0.979 ± 0.046			26.9 ± 1	
OB0104	25/05/01	OB1A	RN022902	175	3540	10000	3750	6000	989	10700	220		44.4	0.15	<3.0	1.1 ± 0.11	1.161 ± 0.163			179 ± 10	
OB02006	28/05/02	OB1A	RN022902	145	3900	10000	3900	6300	1080	11100		200	42.6	1.08	<0.1	9.42 ± 0.78	1.171 ± 0.113			21.8 ± 1	
OB03009	19/09/03	OB1A	RN022902	169	3800	21000	3900	6500	1100	11500		200	45.1	0.15	0.1	0.78 ± 0.12	1.603 ± 0.305			24.2 ± 0.9	
OB04001	22/09/04	OB1A	RN022902	175.0	5310	20500	4020	6720	1160	13200	<200		38.7	0.042	<0.2	0.278 ± 0.073	1.447 ± 0.48			7.67 ± 0.33	
OB05011	13/09/05	OB1A	RN022902	120.9	3170	16600	3205	4740	803	8460			30.3	0.031	<10	0.626 ± 0.11	0.956 ± 0.248			29 ± 1.2	
OB06001	12/09/06	OB1A	RN022902	154	4900	18400	4300	6300	1090	12800			49.9	0.03	<0.1	0.321 ± 0.093	1.358 ± 0.518			26.3 ± 1.5	
OB07007	12/09/07	OB1A	RN022902	122	6900	11300	4300	7000	737	15900			46.3	0.205	0.1	2.25 ± 0.24	1.326 ± 0.181			65.2 ± 3	
OB08007	5/09/08	OB1A	RN022902	150.5	6600	23000	4500	6800	997	14800			48.3	0.089	<1	4.00 ± 0.52	1.076 ± 0.199			47.8 ± 1.7	
OB09010	16/09/09	OB1A	RN022902	193	4800	23300	4500	6500	1240	12900			54.3	0.087	0.2	1.13 ± 0.14	0.978 ± 0.172			41.7 ± 2	
RM10041	30/09/10	OB1A	RN022902	192	4500	23400		6000	1010			<100		0.23		2.33 ± 0.14	1.24 ± 0.1			40.4 ± 1.5	

eriss_ID	Date	Site_ID	RN number	Ba	Ca	Fe	K	Mg	Mn	Na	S	SO4	Sr	U	V	U-238 (1)	234U/238U	U-238 (2)	234U/238U	Ra-226 (1)	Ra-226 (2)
OB11008	20/09/11	OB1A	RN022902		7200		4600	6900	1100	14400		200		0.19						41 ± 1.4	
OB11008	21/09/11	OB1A	RN022902		7300		4500	6900	1120	14400		200		0.18						46.2 ± 2.1	
OB12017	19/09/12	OB1A	RN022902	180	6600	16000	3900	6400	1000	12000			50	0.2	<1						
	9/11/89	OB20	RN022934													17.5 ± 12.6				41.2 ± 1.6	
OB03011	16/09/03	OB20	RN022934	15.2	8600	320	900	15900	21.2	16100		700	40.7	0.17	0.8	1.82 ± 0.15	1.518 ± 0.153			8.39 ± 0.34	
OB04002	22/09/04	OB20	RN022934	15.6	11800	332	1320	18000	26.4	19500	<200		37.7	0.28	1.07	3.61 ± 0.24	1.606 ± 0.124			20.1 ± 1	
OB05012	13/09/05	OB20	RN022934	14.5	9450	245	1210	16100	17.9	16500			37.1	0.25	<10	3.56 ± 0.25	1.644 ± 0.136			8.39 ± 0.33	
OB07010	13/09/07	OB20	RN022934	20.4	8700	40	1100	15200	19.4	13900			39.9	0.5	2	5.77 ± 0.32	1.696 ± 0.108			14.2 ± 0.7	
OB08004	4/09/08	OB20	RN022934	11.9	5000	150	600	8600	10.4	8900			24.0	0.23	1.1	2.90 ± 0.17	1.464 ± 0.105			13.6 ± 1.2	
OB09008	18/09/09	OB20	RN022934	16.8	8900	440	1300	16600	25	16300			46.7	0.29	1.3	3.08 ± 0.19	1.604 ± 0.117			13.3 ± 0.5	
RM10042	30/09/10	OB20	RN022934	16.8	10000	360		16100	20.3			200		0.19		2.18 ± 0.14	1.62 ± 0.13			10.8 ± 0.5	
OB11014	22/09/11	OB20	RN022934		9600		1200	16300	34.4	15200		500		0.60		7.75 ± 0.71	1.353 ± 0.156			35 ± 1.4	
OB12014	19/09/12	OB20	RN022934	19	8800	54	1100	15000	45	14000			37	0.60	2					46.7 ± 2	
	9/11/89	OB21A	RN022935																		
OB03012	16/09/03	OB21A	RN022935	26.4	18600	160	1500	20600	449	16900		500	61.8	0.22	0.1	2.02 ± 0.2	2.504 ± 0.273			94.4 ± 2.5	
OB04003	22/09/04	OB21A	RN022935	25.0	25800	175	2390	22200	352	21100	<200		58.9	0.12	<0.2	1.69 ± 0.15	2.204 ± 0.22			378 ± 15	
OB05013	13/09/05	OB21A	RN022935	24.3	22500	146	2240	19300	298	17500			62.1	0.15	<10	1.94 ± 0.15	2.138 ± 0.196			225 ± 8	
OB06003	13/09/06	OB21A	RN022935	30.2	19900	200	2500	19000	349	18100			67.5	0.085	0.1	1.00 ± 0.11	2.192 ± 0.301			246 ± 5	
OB07008	12/09/07	OB21A	RN022935	30	18400	100	1900	19100	347	15500			59.7	0.46	0.7	5.79 ± 0.38	1.302 ± 0.104			77.7 ± 3.3	
OB08003	3/09/08	OB21A	RN022935	29.5	18500	100	2100	18900	353	17500			60.8	0.47	1	5.44 ± 0.78	1.253 ± 0.242			219 ± 10	
OB09006	16/09/09	OB21A	RN022935	29.8	18200	200	2400	19500	320	18000			66	0.23	0.4	2.24 ± 0.18	2.001 ± 0.189			209 ± 9	
RM10039	28/09/10	OB21A	RN022935	28.6	20600	240		19000	292			<100		0.155		1.62 ± 0.12	1.53 ± 0.14			312 ± 5	
OB11009	21/09/11	OB21A	RN022935		19600		2100	20100	375	16800		3100		0.22						90.6 ± 2.4	
OB12011	19/09/12	OB21A	RN022935	23	16000	29	1700	17000	240	15000			48	1.3	1					68.8 ± 3.7	
	21/11/84	OB22	Not Found																	22.6 ± 0.5	
OB8012	12/07/88	OB22	Not Found													65 ± 3	1.15 ± 0.03				
OB8018	7/09/88	OB22	Not Found													98 ± 32		87 ± 27		131.1 ± 3	
	10/01/89	OB22	Not Found													311 ± 8	1.13 ± 0.02	348 ± 35		196.6 ± 4.6	
	8/11/89	OB23	RN022937													35 ± 18				228.1 ± 2.8	
OB1908	9/05/91	OB23	RN022937													7 ± 0.6	1.13 ± 0.12			102.9 ± 4.7	

eriss_ID	Date	Site_ID	RN number	Ba	Ca	Fe	K	Mg	Mn	Na	S	SO4	Sr	U	V	U-238 (1)	234U/238U	U-238 (2)	234U/238U	Ra-226 (1)	Ra-226 (2)
OB9613	1/05/96	OB23	RN022937													65 ± 3	1.25 ± 0.05				
OB9915	18/05/99	OB23	RN022937	22.6	17200	196	2640	9460.259	151	44600	550		56	1.24	<3.0	18.3 ± 0.9	1.2 ± 0.069				
OB0012	18/05/00	OB23	RN022937	22.9	17000	19	2500	11600	171	45500	220		50.1	1.39	<3.0	16.4 ± 0.9	1.035 ± 0.068			139 ± 5	
OB0106	23/05/01	OB23	RN022937	25.3	17100	24	2660	8700	32.1	48800	300		61.5	3.82	<3.0	41.9 ± 1.8	1.092 ± 0.044	40.7 ± 1.7	1.168 ± 0.053	50.7 ± 1.8	
OB02002	28/05/02	OB23	RN022937	22.8	26000	60	2300	9700	178	49100		300	62.5	0.46	<0.1	5.2 ± 0.3	1.08 ± 0.081			101 ± 4	
OB04004	22/09/04	OB23	RN022937	17.3	29700	167	2670	13500	183.4	45500	<200		40.8	0.080	<0.2	0.74 ± 0.11	3.016 ± 0.499			285 ± 7	
OB05014	13/09/05	OB23	RN022937	17.7	27900	138	2640	12200	175.6	49700			42.2	0.063	<10	0.76 ± 0.12	1.978 ± 0.375			179 ± 5	
OB06004	14/09/06	OB23	RN022937	19.8	24000	160	2700	11200	203	44400			50.3	0.097	<0.1	1.01 ± 0.13	1.805 ± 0.281			179 ± 9	
OB07012	13/09/07	OB23	RN022937	22.6	24400	80	2600	11000	128	40600			49.7	0.23	0.2	2.54 ± 0.20	1.751 ± 0.164			118 ± 3	
OB08005	4/09/08	OB23	RN022937	19.7	23900	250	2700	11200	188	44900			47.8	0.08	<0.1	1.03 ± 0.17	1.948 ± 0.371			172 ± 6	
OB09009	23/09/09	OB23	RN022937	20.8	24100	220	2800	12100	219	44600			53.2	0.084	<0.1	1.12 ± 0.12	1.677 ± 0.233			177 ± 4	
RM10038	28/09/10	OB23	RN022937	20	25200	200		11400	185			300		0.25		2.84 ± 0.18	1.3 ± 0.11			236 ± 11	
OB11005	19/09/11	OB23	RN022937		25300		2800	10700	130	45700		900		3.29		37.9 ± 1.5	1.257 ± 0.056			58.3 ± 2.2	
OB12018	19/09/12	OB23	RN022937	32	22000	61	2600	9300	130	44000			47	1.1	<1					62.1 ± 3.1	
	8/11/89	OB24	RN022938													55 ± 27				9.27 ± 3.76	
	9/05/91	OB24	RN022938																	23.5 ± 1.4	
OB9618	1/05/96	OB24	RN022938													18 ± 1	1.76 ± 0.12				
OB9913	18/05/99	OB24	RN022938	4.0	8310	13	1330	20300	3.7	19400	1480		26.3	0.94	15.5	12.3 ± 0.7	1.827 ± 0.115				
OB0011	18/05/00	OB24	RN022938	14.9	17200	<10	2170	22300	89.3	25000	500		44	3.95	<3.0	44.6 ± 1.5	1.266 ± 0.039			18.6 ± 0.9	
OB0107	23/05/01	OB24	RN022938	20.7	20100	27	2270	20000	188	24400	470		48.4	1.63	<3.0	18.5 ± 1	1.503 ± 0.091			34 ± 1.3	
OB02003	28/05/02	OB24	RN022938	16.6	29500	<20	2100	21900	230	24700		900	46.9	0.52	0.7	5.8 ± 0.3	1.789 ± 0.108			50.5 ± 2.1	
	6/07/88	OB26																		339 ± 11	
OB8017	6/09/88	OB26														527 ± 48		516 ± 44		312.9 ± 4.2	
OB8023	4/11/88	OB26														470 ± 46		469 ± 14		424.1 ± 4.8	410.5 ± 4.8
OB9012	23/01/89	OB26														236 ± 11		207 ± 17		375.6 ± 4.5	375.3 ± 3.9
OB03010	18/09/03	OB27	RN022930	133	7300	360	800	26500	85.9	14800		700	48.6	0.33	0.3	1.49 ± 0.16	1.471 ± 0.204			13.3 ± 0.6	
OB04006	22/09/04	OB27	RN022930	132.6	10700	245	981	33900	141.7	19800	<200		50.1	0.35	1.14	5.03 ± 0.27	1.608 ± 0.097			22.5 ± 1.9	
OB05015	13/09/05	OB27	RN022930	106.5	5640	138	775	23000	58.4	13200			36.6	0.38	<10	4.41 ± 0.28	1.607 ± 0.121			8.99 ± 0.37	
OB06006	11/09/06	OB27	RN022930	122	7000	240	900	24200	84.4	14700			48.2	0.20	0.3	1.79 ± 0.324	2.163 ± 0.453			10.5 ± 0.6	
OB07004	11/09/07	OB27	RN022930	59.6	4000	260	600	10500	56.7	7800			22.6	0.20	0.3	2.473 ± 0.22	1.45 ± 0.159			9.73 ± 0.52	

eriss_ID	Date	Site_ID	RN number	Ba	Ca	Fe	K	Mg	Mn	Na	S	SO4	Sr	U	V	U-238 (1)	234U/238U	U-238 (2)	234U/238U	Ra-226 (1)	Ra-226 (2)
OB09003	15/09/09	OB27	RN022930	66	4700	<20	600	11800	70.9	8000			31.7	0.34	0.5	3.49 ± 0.19	1.229 ± 0.086			10.3 ± 0.5	
RM10036	27/09/10	OB27	RN022930	63.2	4200	200		9600	80.9			36600		0.97		10.3 ± 0.5	1.26 ± 0.08			7.11 ± 0.46	6.18 ± 0.41
OB11012	21/09/11	OB27	RN022930		7500		800	18200	64.7	10000		30100		0.30						72.9 ± 2.3	
OB12010	19/09/12	OB27	RN022930	53	4700	7	600	10000	35	7000			28	0.20	<1						
	10/11/89	OB28	RN023939													39.7 ± 18.4				97.3 ± 2.55	
OB9918	18/05/99	OB28	RN023939	12.8	16500	16	3510	15000	63.1	23500	400		101	0.68	<3.0	9.38 ± 0.87	1.252 ± 0.155				
OB0010	18/05/00	OB28	RN023939	15.6	14000	<10	2780	15800	105	23700	250		88.1	1.47	<3.0	14.6 ± 0.9	1.367 ± 0.095	16.1 ± 1	.103 ± 0.086	18.4 ± 0.8	
OB9010	19/01/89	OB29	RN022940													179 ± 27		165 ± 13		23.04 ± 2.1	
	9/11/89	OB29	RN022940													170 ± 17				84.4 ± 2.3	
OB9614	1/05/96	OB29	RN022940													139 ± 3	1.28 ± 0.02				
OB9712	1/11/97	OB29	RN022940													97 ± 3	1.38 ± 0.04				
OB9917	18/05/99	OB29	RN022940	40.7	10400	15	2410	104000	4.4	7490	82700		77.6	2.30	<3.0	59.9 ± 2.5	1.307 ± 0.051				
OB0013	18/05/00	OB29	RN022940	39	9200	<10	2020	106000	2.5	7010	92000		74.5	1.35	<3.0	59.2 ± 2.9	1.24 ± 0.06			20.9 ± 1	
OB0110	25/05/01	OB29	RN022940	39.7	5880	<10	1930	105000	2.7	5980	99900		69.7	0.60	<3.0	29.8 ± 1.2	1.403 ± 0.063			37 ± 1.6	
OB02012	31/05/02	OB29	RN022940	40.8	11200	120	5000	90300	243	8300		47000	55.6	360	1.7	2860 ± 90	1.113 ± 0.035			406 ± 30	
	7/11/89	OB2A	RN022904													31 ± 17				29.1 ± 1.8	
OB9604	1/05/96	OB2A	RN022904													18.6 ± 0.6	1.28 ± 0.05				
OB9910	18/05/99	OB2A	RN022904	136	5270	491	3950	16400	31.5	15700	17200		46.9	1.05	<3.0	31.6 ± 1.5	1.219 ± 0.056				
OB0008	18/05/00	OB2A	RN022904	181	4830	<10	4160	19600	1.8	20200	18200		48.2	1.90	<3.0	24.6 ± 1.2	1.155 ± 0.057			22.2 ± 0.9	
OB0103	21/05/01	OB2A	RN022904	179	5400	<10	4340	22800	2.1	19200	23500		55.3	1.35	<3.0	19 ± 0.9	1.164 ± 0.059			31.5 ± 1.9	
OB02007	28/05/02	OB2A	RN022904	144	7500	60	4600	28800	3.14	23400		119000	63	2.49	1.8	22.9 ± 1.3	1.311 ± 0.081			17.4 ± 0.5	
	9/11/89	OB30	RN022941													76 ± 12				19.6 ± 1.9	
OB9916	18/05/99	OB30	RN022941	8.5	8680	33	683	47600	<R.L.	2750	2690		16.4	20.6	4.0	305 ± 22	1.070 ± 0.031				
OB0009	18/05/00	OB30	RN022941	10.4	9670	<10	618	49900	<1.0	2660	4050		15.2	22.7	<3.0	257 ± 11	1.102 ± 0.039	280 ± 12	1.05 ± 0.02	6.98 ± 1.3	
OB0108	25/05/01	OB30	RN022941	11.8	7260	24	648	45300	1.9	2610	4840		15.1	17.5	<3.0	198 ± 9	1.100 ± 0.048	228 ± 9	.029 ± 0.044	7.38 ± 1.33	
OB02001	27/05/02	OB30	RN022941	7.3	11200	<20	600	52200	0.44	2800		24900	15	23.6	3.1	264 ± 8	1.054 ± 0.034			1.82 ± 0.72	
OB03005	21/05/03	OB30	RN022941													266 ± 12	1.02 ± 0.056			3.63 ± 0.88	
OB03013	19/09/03	OB30	RN022941	8.32	10900	<20	500	51700	1.2	2700		21600	14.9	20.5	3.4	241 ± 7	1.052 ± 0.03			2.68 ± 0.86	
OB04007	22/09/04	OB30	RN022941	8.9	15000	27	734	62800	2.51	3430	7300		14.9	14.9	3.0	187 ± 7	1.082 ± 0.028			1.76 ± 0.22	
OB05016	13/09/05	OB30	RN022941	8.0	12300	<20	673	55200	4.2	3100			13.8	12.0	<10	150 ± 6	1.05 ± 0.043			2.32 ± 0.19	

eriss_ID	Date	Site_ID	RN number	Ba	Ca	Fe	K	Mg	Mn	Na	S	SO4	Sr	U	V	U-238 (1)	234U/238U	U-238 (2)	234U/238U	Ra-226 (1)	Ra-226 (2)
OB06007	15/09/06	OB30	RN022941	9.8	12900	<20	800	58800	2.58	3300			18.3	18.1	3.5	215 ± 10	1.089 ± 0.026			5 ± 0.4	
OB07009	12/09/07	OB30	RN022941	10.4	13500	<20	700	60800	2.77	3200			19	18	3	207 ± 11	1.093 ± 0.029			3.76 ± 0.36	
OB08002	2/09/08	OB30	RN022941	9.7	12600	<50	800	56700	6.25	3400			17.0	14.8	3.5	192 ± 11	1.1 ± 0.029			2.69 ± 0.48	
OB09002	15/09/09	OB30	RN022941	8.4	11700	<200	800	60400	6.14	3600			17.3	14.9	3.2	152 ± 9	1.093 ± 0.03			4.02 ± 0.31	
RM10040	29/09/10	OB30	RN022941	8.4	12300	<20		55300	6.0			28400		14.2		151 ± 4	1.07 ± 0.02			5.13 ± 0.57	2.43 ± 0.35
OB11011	21/09/11	OB30	RN022941		12400		600	54600	17.7	3200		31300		13.6		165 ± 7	1.115 ± 0.041			22.9 ± 1.1	
OB12013	19/09/12	OB30	RN022941	14	11000	<1	700	50000	36	3200			17	13	2					30.2 ± 1.3	
OB9036	8/11/89	OB44	RN026593													67 ± 19				48.71 ± 2.16	
OB1914	14/05/91	OB44	RN026593													72 ± 3	1.44 ± 0.05			32.92 ± 1.09	
OB2909	12/05/92	OB44	RN026593													69 ± 3	1.49 ± 0.05			49.51 ± 2.15	
OB3906	14/05/93	OB44	RN026593													88 ± 3	1.4 ± 0.04			46 ± 3.07	
OB9622	1/05/96	OB44	RN026593													98 ± 4	1.4 ± 0.05				
OB9625	1/11/96	OB44	RN026593													120 ± 13	1.3 ± 0.09				
OB9702	1/05/97	OB44	RN026593													128 ± 3	1.38 ± 0.03				
OB9711	1/11/97	OB44	RN026593													98 ± 4	1.41 ± 0.04				
OB0111	29/05/01	OB44	RN026593	38.7	72200	67	7030	258000	5.7	60200	301000		224	5.48	3.6	138 ± 6	1.461 ± 0.055			132 ± 5	
OB02004	28/05/02	OB44	RN026593	49.4	154000	60	7800	417000	18.4	77200		1770000	315	13	4.2	150 ± 6	1.441 ± 0.031			134 ± 6	
OB9047	17/11/89	OB46	NOT FOUND													29880±1300		24350 ± 280	1.22 ± 0.01	2930 ± 150	3228 ± 19
OB9048	17/11/89	OB47	NOT FOUND													14 ± 2	1.42 ± 0.26			39.2 ± 5.1	
	1/08/90	OB47	NOT FOUND																	11.1 ± 0.7	
	1/11/90	OB47	NOT FOUND																	18.2 ± 1.9	
OB9049	17/11/89	OB48	NOT FOUND													54 ± 5	1.19 ± 0.13			55.9 ± 5	
	7/08/90	OB48	NOT FOUND																	50.2 ± 2.9	
OB9050	17/11/89	OB49	NOT FOUND													941 ± 50	1.63 ± 0.06	953 ± 50		89 ± 8	
	7/08/90	OB49	NOT FOUND																	112.3 ± 5.4	
OB8007	8/07/88	OB4A	RN22908													12.76 ± 0.52	1.522 ± 0.073			117.9 ± 3.2	
	5/01/89	OB4A	RN22908																	81.54 ± 3.42	
	7/11/89	OB4A	RN22908																	86 ± 2	
	8/11/90	OB4A	RN22908																	75.26 ± 3.67	
	9/05/91	OB4A	RN22908																	82.16 ± 4.18	

eriss_ID	Date	Site_ID	RN number	Ba	Ca	Fe	K	Mg	Mn	Na	S	SO4	Sr	U	V	U-238 (1)	234U/238U	U-238 (2)	234U/238U	Ra-226 (1)	Ra-226 (2)
	13/11/91	OB4A	RN22908																	112.95 ± 3.34	
	6/05/92	OB4A	RN22908																	118.61 ± 4.22	
OB9602	1/05/96	OB4A	RN22908													18.9 ± 1.4	0.97 ± 0.11				
OB9710	1/11/97	OB4A	RN22908													16.2 ± 0.4	1.44 ± 0.04				
OB9804	1/05/98	OB4A	RN22908													408 ± 10	1.07 ± 0.01				
OB9909	18/05/99	OB4A	RN22908	40.3	180000	118000	20100	291000	6070	47600	450000		1500	0.4	<3.0	6.59 ± 0.59	1.009 ± 0.133				
OB0005	18/05/00	OB4A	RN22908	42.8	135000	46300	16400	256000	3480	44200	399000		1150	1.14	<3.0	19.2 ± 0.8	1.017 ± 0.049			63.8 ± 2.6	
OB0112	31/05/01	OB4A	RN22908	49.4	215000	72600	19800	378000	7940	48400	574000		1760	8.28	<3.0	143 ± 6	0.974 ± 0.044			201 ± 10	
OB9051	17/11/89	OB50	NOT FOUND													578 ± 32	1.09 ± 0.05	585 ± 33		213 ± 15	
OB9052	17/11/89	OB51	NOT FOUND													332 ± 21	1.35 ± 0.08	336 ± 21		90.2 ± 7	
	7/08/90	OB51	NOT FOUND																	62.8 ± 2.8	
OB0002	18/05/00	OB6	RN022911	52	43700	122	5870	134000	45.3	49000	156000		53.5	14.7	3.2	170 ± 8	1.546 ± 0.059			183 ± 9	
OB8019	7/09/88	OB6A	RN022912													665 ± 55				368.4 ± 5.2	
OB8027	8/11/88	OB6A	RN022912													418 ± 46				389.8 ± 5	
OB9007	18/01/89	OB6A	RN022912													334 ± 34				303 ± 4	
OB9013	9/05/89	OB6A	RN022912													184 ± 31.2				298.2 ± 4.5	
OB9039	9/11/89	OB6A	RN022912													360 ± 29				414.5 ± 3.9	
OB1911	9/05/91	OB6A	RN022912													222 ± 6	1.74 ± 0.03			281.06 ± 8.06	
	13/11/91	OB6A	RN022912																	341.87 ± 8.94	
	6/05/92	OB6A	RN022912																	307.23 ± 8.07	
	25/11/92	OB6A	RN022912									110000								323.9 ± 10.2	
	13/05/93	OB6A	RN022912																	270.4 ± 9.1	
OB9601	1/05/96	OB6A	RN022912													628 ± 18	1.65 ± 0.01				
OB9628	1/11/96	OB6A	RN022912													468 ± 16	1.75 ± 0.03				
OB9709	1/11/97	OB6A	RN022912													338 ± 12	1.77 ± 0.04				
OB9805	1/05/98	OB6A	RN022912													850 ± 29	1.26 ± 0.02				
OB9907	18/05/99	OB6A	RN022912	77.3	70500	45	8320	105000	578	65700	130000		110	26.6	<3.0	348 ± 12	1.898 ± 0.046				

eriss_ID	Date	Site_ID	RN number	Ba	Ca	Fe	K	Mg	Mn	Na	S	SO4	Sr	U	V	U-238 (1)	234U/238U	U-238 (2)	234U/238U	Ra-226 (1)	Ra-226 (2)
OB0003	18/05/00	OB6A	RN022912	69.1	82300	<10	8780	132000	781	54500	164000		125	26	<3.0	295 ± 14	1.731 ± 0.061			367 ± 18	
OB0109	25/05/01	OB6A	RN022912	52	85800	<10	8260	119000	757	54100	168000		144	23.2	<3.0	284 ± 11	1.986 ± 0.057			1047 ± 29	
OB02010	30/05/02	OB6A	RN022912	43.2	123000	<20	8700	161000	637	62700		786000	124	50.2	3.9	507 ± 22	1.937 ± 0.073			625 ± 29	
OB2910	1/05/92	OB79/6A	NOT FOUND													121.4 ± 4.2	1.05 ± 0.03	62.3 ± 1.3	1.12 ± 0.02		
OB9621	1/05/96	OB79B	NOT FOUND													38 ± 1	1.12 ± 0.03				
OB9038	9/11/89	OB7A	RN022914													35.4 ± 11.2				100 ± 3	
OB9611	1/05/96	OB7A	RN022914													51 ± 1	1.34 ± 0.03				
OB9806	1/05/98	OB7A	RN022914													1410 ± 40	1.07 ± 0.01				
OB9906	18/05/99	OB7A	RN022914	31.5	7740	55	5820	29100	79.0	33600	2170		35.6	6.74	<3.0	83.7 ± 3.7	1.272 ±	84.1 ± 0.4	1.258 ±		
OB0001	18/05/00	OB7A	RN022914	33.4	7590	<10	5440	29800	13.9	33400	2620		34.2	49.2	<3.0	678 ± 37	1.073 ± 0.026	574 ± 24	.138 ± 0.043	232 ± 9	
OB0101	21/05/01	OB7A	RN022914	37.2	7550	<10	4800	30200	32.8	30800	3420		32.4	5.16	<3.0	65.1 ± 3.7	1.444 ± 0.097	55 ± 2	.458 ± 0.055	142 ± 6	
OB02009	30/05/02	OB7A	RN022914	18.4	9300	<20	4600	32400	79.3	32200		16000	33.3	2.69	<0.1	28.3 ± 1.2	1.379 ± 0.063			151 ± 6	
	8/11/88	OB9A	RN022918																	47.76 ± 1.29	
OB9014	9/05/89	OB9A	RN022918													92.5 ± 19.5				63.45 ± 2.23	
OB9019	6/11/89	OB9A	RN022918													78.2 ± 23.6				58.46 ± 2.79	
	8/11/90	OB9A	RN022918																	67.11 ± 3.54	
	9/05/91	OB9A	RN022918													13 ± 1				55.1 ± 1.84	
	14/11/91	OB9A	RN022918													133 ± 18				78.6 ± 1.9	
	6/05/92	OB9A	RN022918																	108.4 ± 3.3	
OB9612	1/05/96	OB9A	RN022918													88 ± 2	1.3 ± 0.02				
OB9630	1/11/96	OB9A	RN022918													130 ± 5	1.32 ± 0.04				
OB9708	1/11/97	OB9A	RN022918													830 ± 20	1.53 ± 0.01				
OB9801	1/05/98	OB9A	RN022918													172000 ± 5000	0.99 ± 0.01				
OB9904	1/03/99	OB9A	RN022918													6860 ± 270	1.05 ± 0.03				
	12/07/88	R.P. 79/ 1 Ranger	RN020090													392 ± 44					
	8/11/89	R.P. 79/ 1 Ranger	RN020090													118.9 ± 30.7		123 ± 29		510.7 ± 4.8	506.2 ± 4.7
OB9620	1/05/96	R.P. 79/ 1 Ranger	RN020098													33 ± 2	1.06 ± 0.08				
OB07014	18/09/07	RN22211	RN022211	83.8	700	260	300	1300	233	3200			6.25	0.038	0.3	0.71 ± 0.10	1.398 ± 0.254			16.9 ± 0.8	
OB09007	17/09/09	RN22211	RN022211	50.6	300	40	100	700	96.7	2900			3.03	0.034	0.3	0.40 ± 0.07	1.039 ± 0.272			11.9 ± 0.4	

eriss_ID	Date	Site_ID	RN number	Ba	Ca	Fe	K	Mg	Mn	Na	S	SO4	Sr	U	V	U-238 (1)	234U/238U	U-238 (2)	234U/238U	Ra-226 (1)	Ra-226 (2)
OB04010	22/09/04	RN23551	RN023551	163.0	2710	34800	1420	184000	96.7	33300	189400		22.1	0.57	0.52	7 ± 0.3	1.573 ± 0.073			33 ± 1.8	
OB05018	13/09/05	RN23551	RN023551	44.1	<200	859	639	10600	10.7	15100			2.7	0.44	<10	5.06 ± 0.29	1.826 ± 0.119			16.2 ± 0.6	
OB07002	10/09/07	RN23551	RN023551	350	4600	10200	1100	124000	95.7	18900			28.6	0.47	0.4	5.82 ± 0.36	1.553 ± 0.112			141 ± 6	
OB11003	19/09/11	RN23551	RN023551		7800		1100	112000	116	16800		428000		0.71		8.65 ± 0.75	1.285 ± 0.144			102 ± 5	
OB12019	19/09/12	RN23551	RN023551	85	2400	110	600	22000	160	15000			14	0.2	<1						
OB12004	7/03/12	RN23556	RN023556	19	<100	1000	200	800	4	7900		19	1.4	0.2	0.1	2.56 ± 0.14	0.986 ± 0.079			3.6 ± 0.32	
OB07005	11/09/07	RN23562	RN023562	33.4	400	220	<100	1000	23.1	1300			2.65	0.38	<0.1	4.43 ± 0.30	0.999 ± 0.089			8.91 ± 0.48	
OB11001	19/09/11	RN23562	RN023562		4100		<100	2000	57.9	2700		3200		0.36		3.94 ± 0.43	0.832 ± 0.15			19 ± 0.9	
OB13001	12/03/13	RN23562	RN023562																	12.4 ± 0.7	
RM10044	1/10/10	RN23566	RN023566	26.8	5500	3000		45400	105			218000		0.074		0.63 ± 0.09	1.42 ± 0.25				
OB12005	8/03/12	RN23566	RN023566	27	8900	9800	2300	100000	180	21000		470000	100	0.5	0.2	23.9 ± 1.1	1.205 ± 0.066			10.8 ± 0.4	
OB12003	6/03/12	RN23568	RN023568	33	8600	9300	3100	95000	98	20000		420	61	0.9	0.3	11 ± 0.6	0.976 ± 0.072			26.8 ± 1.2	
OB09005	16/09/09	RN8708	RN8708	28.8	8400	40	2300	13500	95.7	13400			32.4	0.62	0.8	7.01 ± 0.26	2.521 ± 0.095			34.4 ± 1.7	
OB11013	22/09/11	RN8708	RN8708		9000		2200	12800	60.7	12600		1000		1.08		10.8 ± 0.7	2.238 ± 0.161			28.6 ± 1.4	
OB12012	19/09/12	RN8708	RN8708	17	8200	9	2200	11000	97	12000			29	0.6	2					38.4 ± 2.1	
OB03016	16/09/03	RN9329	RN009329	47.2	6500	5700	2300	10100	258	12300		100	33.4	0.35	0.9	2.13 ± 0.21	1.351 ± 0.17			8.08 ± 0.37	
OB04009	22/09/04	RN9329	RN009329	40.5	9130	7830	2550	11500	324	14400	<200		33.1	0.159	0.7	1.94 ± 0.15	1.368 ± 0.134			19 ± 0.9	
OB05019	13/09/05	RN9329	RN009329	39.7	6145	5255	2175	9285	257	11600			29.2	0.194	<10	2.36 ± 0.19	1.282 ± 0.13			7.87 ± 0.45	
OB06009	13/09/06	RN9329	RN009329	43.2	6300	5950	2500	9200	285	12600			35.7	0.185	1	1.72 ± 0.19	1.625 ± 0.22			7.54 ± 0.46	
OB07011	13/09/07	RN9329	RN009329	40.6	7100	8100	2400	10000	259	11600			37.7	0.183	0.7	2.09 ± 0.17	1.345 ± 0.142			10.9 ± 0.6	
OB08006	4/09/08	RN9329	RN009329	34.7	7100	10100	2500	10000	274	13300			36.9	0.098	0.4	1.02 ± 0.138	1.601 ± 0.258			16 ± 1.3	
RM10045	1/10/10	RN9329	RN009329	41.4	6600	6100		9500	239			100		0.268		3.08 ± 0.2	1.32 ± 0.11			7.31 ± 0.32	
OB11007	20/09/11	RN9329	RN009329	56.8	8500	13900	2700	11600	318	13000		500	43	0.49	<0.5	5.15 ± 0.47	1.585 ± 0.177			31 ± 1.3	
OB12016	19/09/12	RN9329	RN009329	75	7600	8900	2100	10000	270	11000			44	0.3	<1						
OB03006	21/05/03	RP1N1	RN026625													487 ± 17	1.252 ± 0.036			149 ± 5	
OB03007	21/05/03	RP1N2	RN026626													40.1 ± 1.5	1.288 ± 0.038			47.3 ± 2.2	
	6/12/89	TD(EastWall)	NOT FOUND													5230 ± 160	0.96 ± 0.02			23.2 ± 1.1	
RC9003/1	6/12/89	TDSCN	NOT FOUND													1198 ± 43	1.13 ± 0.02	915 ± 22	1.1 ± 0.01	665 ± 25	624 ± 31
OB11006	20/09/11	21030DEEP	RN021030	103	18800	440	3900	12800	45	20800		100	106	1.05	<0.5	10.9 ± 0.8	1.211 ± 0.116			24.2 ± 1.3	
OB12015	19/09/12	21030DEEP	RN021030	66	16000	270	3900	12000	26	20000			94	1.1	<1					42.3 ± 2	

Appendix 3

Bore water electrical conductivity and pH data

Table A62 Bore water electrical conductivity (EC) in μS·cm^{-1} and pH, measured by the Northern Territory Department of Mines and Energy.

Bore OB23

eriss_ID	Date	Site_ID	RN number	EC	pH
OB04004	15/09/2004	OB23	RN022937	394.7	6.91
OB05014	8/09/2005	OB23	RN022937	441.5	7.27
OB06004	14/09/2006	OB23	RN022937	430.3	7.04
OB07012	14/09/2007	OB23	RN022937	479.9	7.16
OB08005	4/09/2008	OB23	RN022937	466.2	7.48
OB09009	23/09/2009	OB23	RN022937	488.4	7.5
RM10038	28/09/2010	OB23	RN022937	446.8	7.18

Bore OB1A

eriss_ID	Date	Site_ID	RN number	EC	pH
OB03009	19/09/2003	OB1A	RN022902	205	6.08
OB04001	22/09/2004	OB1A	RN022902	123.7	5.73
OB05011	7/09/2005	OB1A	RN022902	220.9	5.87
OB06001	12/09/2006	OB1A	RN022902	238.6	6.26
OB07007	12/09/2007	OB1A	RN022902	251.3	6.71
OB08007	5/09/2008	OB1A	RN022902	279.3	6.52
OB09010	16/09/2009	OB1A	RN022902	248.6	6.35
RM10041	30/09/2010	OB1A	RN022902	241	6.15
OB11008	21/09/2011	OB1A	RN022902	282.8	6.4
OB11008	21/09/2011	OB1A	RN022902	282.8	6.4

Bore RN9329

eriss_ID	Date	Site_ID	RN number	EC	pH
OB04009	14/09/2004	RN9329	RN009329	212	6.59
OB05019	6/09/2005	RN9329	RN009329	185	6.15
OB06009	13/09/2005	RN9329	RN009329	193.9	6.25
OB07011	13/09/2007	RN9329	RN009329	222.4	6.41
OB08006	4/09/2008	RN9329	RN009329	222.4	6.79
RM10045	1/10/2010	RN9329	RN009329	177.5	6.38
OB11007	20/09/2011	RN9329	RN009329	256.5	6.79
OB12016	19/09/2011	RN9329	RN009329	243.6	6.65

Bore OB20

eriss_ID	Date	Site_ID	RN number	EC	pH
OB03011	16/09/2003	OB20	RN022934	202	6.52
OB04002	14/09/2004	OB20	RN022934	255.5	6.41
OB05012	6/09/2005	OB20	RN022934	249.5	6.48
OB07010	13/09/2007	OB20	RN022934	295.1	6.63
OB08004	4/09/2008	OB20	RN022934	267.5	6.86
OB09008	18/09/2009	OB20	RN022934	285.1	6.84
RM10042	30/09/2010	OB20	RN022934	276.3	6.65
OB11014	22/09/2011	OB20	RN022934	297.7	6.66
OB12014	19/09/2012	OB20	RN022934	291.3	6.67

Bore OB21A

eriss_ID	Date	Site_ID	RN number	EC	pH
OB03012	16/09/2003	OB21A	RN022935	282	7.01
OB04003	14/09/2004	OB21A	RN022935	358.4	7.42
OB05013	7/09/2005	OB21A	RN022935	357.8	6.92
OB06003	13/09/2006	OB21A	RN022935	376.9	7.05
OB07008	12/09/2007	OB21A	RN022935	401.3	7.54
OB08003	3/09/2008	OB21A	RN022935	382.9	7.48
OB09006	16/09/2009	OB21A	RN022935	387.1	7.58
RM10039	28/09/2010	OB21A	RN022935	363.8	7.24
OB11009	21/09/2011	OB21A	RN022935	387.5	7.17
OB12011	19/09/2012	OB21A	RN022935	360	7.42

Bore OB30

eriss_ID	Date	Site_ID	RN number	EC	pH
OB0108	25/05/2001	OB30	RN022941	398	7.76
OB02001	27/05/2002	OB30	RN022941	409	8.4
OB03005	21/05/2003	OB30	RN022941	391.6	7.72
OB03013	19/09/2003	OB30	RN022941	429	7.33
OB04007	22/09/2004	OB30	RN022941	478.2	6.99
OB05016	7/09/2005	OB30	RN022941	440	7.5
OB06007	15/09/2006	OB30	RN022941	531	7.38
OB07009	12/09/2007	OB30	RN022941	571	7.76
OB08002	2/09/2008	OB30	RN022941	523	7.49
OB09002	15/09/2009	OB30	RN022941	540	7.6
RM10040	29/09/2010	OB30	RN022941	524	7.43
OB11011	21/09/2011	OB30	RN022941	529	7.34
OB12013	19/09/2012	OB30	RN022941	521	7.49

Bore OB27

eriss_ID	Date	Site_ID	RN number	EC	pH
OB03010	18/09/2003	OB27	RN022930	277	6.59
OB04006	17/09/2004	OB27	RN022930	363.3	6.53
OB05015	6/09/2005	OB27	RN022930	270	6.59
OB06006	11/09/2006	OB27	RN022930	322.9	6.45
OB07004	11/09/2007	OB27	RN022930	175.5	6.56
OB09003	15/09/2009	OB27	RN022930	215.4	6.16
RM10036	27/09/2010	OB27	RN022930	167.8	5.75
OB11012	22/09/2011	OB27	RN022930	241.9	6.38
OB12010	18/09/2012	OB27	RN022930	175.3	6.25

Bore 83_1

eriss_ID	Date	Site_ID	RN number	EC	pH
OB03008	17/09/2003	83_1	RN023010	120.8	6.76
OB04008	20/09/2003	83_1	RN023010	139.7	6.89
OB05017	7/09/2005	83_1	RN023010	123.4	6.37
RM10037	28/09/2010	83_1	RN023010	130.8	7.03
OB11002	19/09/2011	83_1	RN023010	110.3	6.77
OB11004	19/09/2011	83_1	RN023010	110.3	6.77
OB06008	12/09/2006	83_1	RN023010	126.8	6.78
OB07006	11/09/2007	83_1	RN023010	122.8	7.31
OB08001	2/09/2008	83_1	RN023010	116.7	6.9
OB09004	15/09/2009	83_1	RN023010	130.4	7.11
OB12009	17/09/2012	83_1	RN023010	123.6	6.71

Bore RN23551

eriss_ID	Date	Site_ID	RN number	EC	pH
OB04010	16/09/2004	RN23551	RN023551	1279	5.58
OB05018	8/09/2005	RN23551	RN023551	1488	5.81
OB07002	10/09/2007	RN23551	RN023551	1299	5.89
OB11003	20/09/2011	RN23551	RN023551	996	6

Bore B11

eriss_ID	Date	Site_ID	RN number	EC	pH
OB06002	15/09/2006	B11	RN007243	147.3	5.91
OB07001	10/09/2007	B11	RN007243	151.7	6.19
OB08008	5/09/2008	B11	RN007243	153.8	6.32
OB09001	14/09/2009	B11	RN007243	146	6.24